

Conservation of Southern California Yellow Pine Mixed Conifer Forests

A Look into the Past, Present, and Future



Figueroa Mountain in 1930 and 2021

Prepared By:

Anne-Marie Parkinson, Hannah Garcia-Wickstrum, Leana Goetze, Jennifer Truong

Prepared For:

U.S. Forest Service

Faculty Advisor:

Dr. Bruce Kendall

Signature Page

As authors of this Group Project report, we archive this report on the Bren School's website such that the results of our research are available for all to read. Our signatures on the document signify our joint responsibility to fulfill the archiving standards set by the Bren School of Environmental Science & Management.

Hannah Garcia-Wickstrum

Leana Goetze

Anne-Marie Parkinson

Jennifer Truong

The Bren School of Environmental Science & Management produces professionals with unrivaled training in environmental science and management who will devote their unique skills to the diagnosis, assessment, mitigation, prevention, and remedy of the environmental problems of today and the future. A guiding principle of the school is that the analysis of environmental problems requires quantitative training in more than one discipline and an awareness of the physical, biological, social, political, and economic consequences that arise from scientific or technological decisions.

The Group Project is required of all students in the Master of Environmental Science and Management (MESM) Program. The project is a year-long activity in which small groups of students conduct focused, interdisciplinary research on the scientific, management, and policy dimensions of a specific environmental issue. This Group Project Final Report is authored by MESM students and has been reviewed and approved by:

Bruce Kendall

Date

Acknowledgements

We would like to express our gratitude towards all those who have supported and helped guide our project:

Faculty Advisor

Dr. Bruce Kendall Bren School of Environmental Science & Management

Clients

Dr. Hugh Safford U.S. Forest Service

Dr. Nicole Molinari U.S. Forest Service

External Advisors

Dr. Frank Davis Bren School of Environmental Science & Management

Gabrielle Bohlman U.S. Forest Service

Guidance

Dr. Ashley Larsen Bren School of Environmental Science & Management

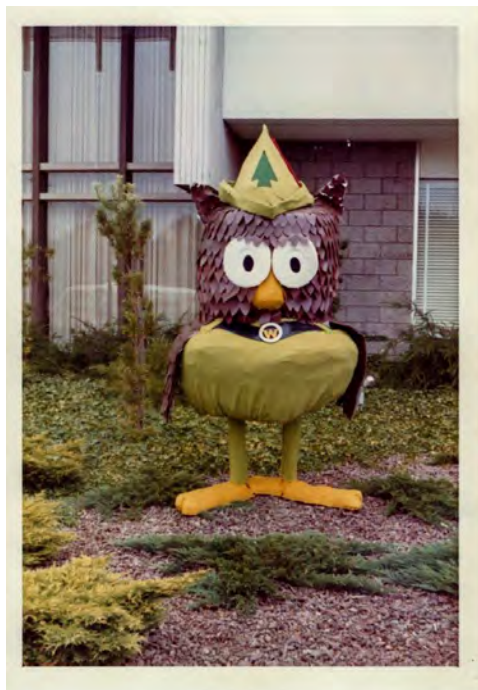
Dr. Allison Horst Bren School of Environmental Science & Management

Dr. Sarah Hennessy U.S. Forest Service

Kama Kennedy U.S. Forest Service

Dr. Peter Alagona University of California, Santa Barbara

Erin McCann University of California, Riverside



Woodsy Owl at LPNF Ranger Station, 1972

Abstract

Fire suppression policies have led to changes in forest structure throughout California, which increases the risk of stand-replacing fires. Additionally, vegetation in California is expected to move towards higher elevations due to climate change. Understanding these shifts in forest structure is important for future resilience. To accomplish this we (1) compared changes in forest structure in yellow pine mixed conifer (YPMC) forests in southern California over the last century and (2) created a MaxEnt model to understand the range shifts of yellow pines in the Transverse Ranges. We found significant increases in tree density, canopy cover, and basal area across southern California YPMC forests. This change is primarily due to an increase in large diameter trees (61-91.3cm) and an increase in shade tolerant trees. *Quercus chrysolepis* has particularly increased at lower elevations, while conifer juveniles have decreased across these elevations. These results indicate a potential composition shift from conifer forests to oak dominated systems. Our MaxEnt model demonstrates that under climate change, suitable habitat for yellow pine saplings is shrinking across the Transverse Ranges. Our project will assist the USFS in creating targeted management goals in selecting high priority areas for the conservation of southern California YPMC forests.

Table of Contents

SIGNATURE PAGE	1
ACKNOWLEDGEMENTS	2
ABSTRACT	3
TABLE OF CONTENTS	4
LIST OF FIGURES	6
LIST OF TABLES	7
LIST OF APPENDIX ITEMS	8
LIST OF ABBREVIATIONS	9
1. SIGNIFICANCE	10
2. OBJECTIVES	11
3. BACKGROUND	12
3.1 NATURAL RANGE OF VARIATION.....	12
3.1.1 Reference sites	13
3.2 YELLOW PINE MIXED CONIFER FORESTS AND SOUTHERN CALIFORNIA NATIONAL FORESTS.....	16
3.3 DISTURBANCE HISTORY	19
3.4 CLIMATE CHANGE	23
4. DATA	24
4.1 HISTORIC DATA - VEGETATION TYPE MAPPING (VTM)	24
4.2 CONTEMPORARY DATA - FOREST INVENTORY ANALYSIS (FIA).....	25
4.3 DATA TIDYING	26
5. 20TH CENTURY SHIFTS IN FOREST COMPOSITION	30
5.1 OVERVIEW	30
5.2 TREE DENSITY	31
5.2.1 Methods.....	31
5.2.2 Results	31
5.2.3 NRV Analysis.....	38
5.3 TREE SIZE CLASS AND SIZE CLASS DISTRIBUTION	46
5.3.1 Methods.....	46
5.3.2 Results	46
5.3.3 NRV Analysis.....	55
5.4 BASAL AREA.....	60
5.4.1 Methods.....	60
5.4.2 Results	62
5.4.3 NRV Analysis.....	66
5.5 CANOPY COVER.....	68
5.5.1 Methods.....	68
5.5.2 Results	68
5.5.3 NRV Analysis.....	72
5.6 SHRUB COVER	73
5.6.1 Methods.....	73

5.6.2 Results	74
5.6.3 NRV Analysis.....	83
5.7 LIMITATIONS.....	85
5.8 CONCLUSIONS AND IMPLICATIONS	87
6. SPECIES DISTRIBUTION MODEL	89
6.1 OVERVIEW	89
6.2 METHODS	90
6.2.1 Study Area	90
6.2.2 Species Selection.....	91
6.2.3 Data.....	91
6.2.5 Final Variable Selection.....	97
6.2.6 Accounting for Sampling Bias.....	97
6.2.7 Analysis.....	99
6.3 RESULTS	101
6.3.1 Current Suitable Habitat of Saplings and Adults	101
6.3.2 Past Suitable Habitat of Saplings.....	103
6.3.3 Future suitable habitat of saplings.....	104
6.4 DISCUSSION.....	110
6.5 LIMITATIONS.....	112
7. PRIORITIZATION.....	114
7.1 METHODS	114
7.2 RESULTS	117
7.3 DISCUSSION.....	119
CITATIONS	121
APPENDIX	135
APPENDIX A: LITERATURE REVIEW.....	135
APPENDIX B: TREE DENSITY CODE EXAMPLE.....	137
APPENDIX C: ADDITIONAL TREE DENSITY ANALYSIS.....	139
APPENDIX D: TREE DENSITY METRICS OF VARIANCE	142
APPENDIX E: ADDITIONAL TREE SIZE CLASS DENSITY ANALYSIS AND METRICS OF VARIANCE.....	145
APPENDIX F: BASAL AREA CODE EXAMPLE.....	152
APPENDIX G: BASAL AREA HISTOGRAMS AND ONE-TO-ONE GRAPHS.....	153
APPENDIX H: ADDITIONAL BASAL AREA ANALYSIS AND METRICS OF VARIANCE.....	156
APPENDIX I: CANOPY COVER FVS EQUATIONS AND CODE EXAMPLE.....	160
APPENDIX J: FIA CANOPY COVER USING D.B.H. MIDPOINTS AND ACTUAL D.B.H. MEASUREMENTS	163
APPENDIX K: CANOPY COVER METRICS OF VARIANCE	164
APPENDIX L: CANOPY COVER HISTOGRAMS	165
APPENDIX M: VTM LOGGING MAP IN SOUTHERN CALIFORNIA.....	166
APPENDIX N: TWI CALCULATIONS	166
APPENDIX O: ENVIRONMENTAL DATA PROCESSING	167
APPENDIX P: MAXENT MODEL PARAMETER SETTINGS	169
APPENDIX Q: ENVIRONMENTAL HISTOGRAMS FOR SDM	173
APPENDIX R: SDM RESULTS - CURRENT SUITABLE HABITAT OF YELLOW PINE SAPLINGS AND ADULTS.....	175
APPENDIX S: SDM RESULTS - PAST SUITABLE HABITAT OF YELLOW PINE SAPLINGS	182
APPENDIX T: SDM RESULTS - FUTURE SUITABLE HABITAT OF YELLOW PINE SAPLINGS.....	186

List of Figures

- Figure 1: Baja reference sites
- Figure 2: CWD in study area and California reference sites
- Figure 3: YPMC forest in the study area
- Figure 4: Logging in Los Angeles and San Bernardino
- Figure 5: VTM and combined FIA plot locations
- Figure 6: Historic and contemporary YPMC tree density
- Figure 7: Historic and contemporary YPMC tree density by species
- Figure 8: Historic and contemporary YPMC tree density of conifers and oaks
- Figure 9: Historic and contemporary YPMC tree density by shade and fire tolerance
- Figure 10: Historic and contemporary YPMC tree density by elevation
- Figure 11: Historic and contemporary YPMC tree density by National Forest
- Figure 12: Historic photo of the San Jacinto Reserve
- Figure 13: Historic photo of the San Bernardino Reserve
- Figure 14: Photos of YPMC forest in SSPM
- Figure 15: Photo of YPMC forest at Mt. Pinos, Los Padres National Forest
- Figure 16: Photo of YPMC forest at Cleveland National Forest
- Figure 17: Historic and contemporary tree density of YPMC forests by size class
- Figure 18: Historic and contemporary tree density of YPMC species by size class
- Figure 19: Historic and contemporary YPMC tree density of conifers and oaks by size class
- Figure 20: Historic and contemporary YPMC tree density by elevation and size class
- Figure 21: Historic and contemporary YPMC tree density of conifers and oaks by size class and elevation
- Figure 22: Historic and contemporary YPMC tree density by size class and National Forest
- Figure 23: Photo of varying size class trees
- Figure 24: Spatial distribution of large diameter trees across plots in the study area
- Figure 25: Basal area comparison using binned and unbinned d.b.h values
- Figure 26: Historic and contemporary distribution of plot basal area in the study area
- Figure 27: Historic and contemporary total, conifer, and oak basal area of YPMC forest
- Figure 28: Historic and contemporary YPMC basal area by species
- Figure 29: Historic and contemporary YPMC basal area by elevation class
- Figure 30: Historic and contemporary YPMC basal area by National Forest
- Figure 31: Historic and contemporary YPMC canopy cover, including oak species
- Figure 32: Historic and contemporary YPMC canopy cover, excluding oak species
- Figure 33: Historic and contemporary YPMC canopy cover by elevation class
- Figure 34: Map of the Transverse Ranges
- Figure 35: Map of Transverse Ranges subdivisions
- Figure 36: Basin Characterization Model climate projections
- Figure 37: Map of contemporary yellow pine presence points
- Figure 38: Summer precipitation distribution comparisons
- Figure 39: Distribution of summer precipitation across the Transverse Ranges
- Figure 40: Current projected yellow pine sapling and adult suitable habitat
- Figure 41: CALVEG YPMC forest and current projected suitable habitat for adults
- Figure 42: Historic postdicted and current projected yellow pine sapling suitable habitat
- Figure 43: Current and future projected yellow pine sapling suitable habitat
- Figure 44: 2010-2039 projected yellow pine sapling suitable habitat
- Figure 45: 2040-2069 projected yellow pine sapling suitable habitat
- Figure 46: Ecosystem services layers in SBNF
- Figure 47: Legal and administrative constraints in southern California YPMC forests in SBNF
- Figure 48: YPMC forests that are a priority for conservation
- Figure 49: Roads buffer
- Figure 50: YPMC forests that are a priority for conservation and feasible to access

List of Tables

- Table 1: YPMC forest acres
Table 2: YPMC species and characteristics
Table 3: Historic logging locations
Table 4: VTM and FIA plot sample sizes
Table 5: Historic and contemporary YPMC tree density statistics by species, classification, and shade/fire tolerance
Table 5a: Historic and YPMC tree density statistics by National Forest and elevation
Table 6: Historic and contemporary YPMC tree densities across southern California and reference sites
Table 7: Historic and contemporary YPMC tree density statistics by size class, functional group, and shade tolerance/fire tolerance
Table 8: Historic and contemporary YPMC tree density statistics by species and size class
Table 9: Historic and contemporary YPMC tree density statistics by elevation and size class
Table 10: Historic and contemporary YPMC tree density statistics of conifers and oaks by elevation and size class
Table 11: Historic and contemporary YPMC tree density statistics by size class, classification, and shade/fire tolerance
Table 12: Largest d.b.h. size class values per species
Table 13: Historic and contemporary YPMC basal area statistics by species, classification, and shade/fire tolerance
Table 14: Historic and contemporary YPMC basal area statistics by National Forest and elevation
Table 15: Historic and contemporary YPMC canopy cover statistics by National Forest, including oak species
Table 16: Historic and contemporary YPMC canopy cover statistics by National Forest, excluding oak species
Table 17: Historic and contemporary YPMC canopy cover statistics by elevation
Table 18: Sample sizes of USFS shrub observations
Table 19: Top 10 shrub species in historic forests
Table 20: Top 10 shrub species in contemporary forests
Table 21: Top 10 shrub genera in historic forests
Table 22: Top 10 shrub genera in contemporary forests
Table 23: Top three shrub species by National Forest in historic forests
Table 24: Top three shrub species by National Forest in contemporary forests
Table 25: Top three shrub species by elevation class in historic forests
Table 26: Top three shrub species by elevation class in contemporary forests
Table 27: Top three shrub genera in historic forests by elevation class
Table 28: Top three shrub genera in contemporary forests by elevation class
Table 29: Shrub cover by National Forest in contemporary forests
Table 30: Preliminary MaxEnt variables
Table 31: Correlation among MaxEnt variables
Table 32: MaxEnt model summaries
Table 33: Current and future projected yellow pine sapling suitable habitat acreage
Table 34: 2010-2039 projected yellow pine sapling suitable habitat acreage by precipitation regime
Table 35: 2040-2069 projected yellow pine sapling suitable habitat acreage by precipitation regime

List of Appendix Items

- Appendix A: Literature review
- Appendix B: Tree density code example
- Appendix C: Additional tree density analysis
- Appendix D: Tree density metrics of variance
- Appendix E: Additional tree size density analysis and metrics of variance
- Appendix F: Basal area code example
- Appendix G: Basal area histograms and one to one graphs
- Appendix H: Additional basal area analysis and metrics of variance
- Appendix I: Canopy cover FVS equations and code example
- Appendix J: FIA canopy cover using d.b.h midpoints and actual d.b.h measurements
- Appendix K: Canopy cover metrics of variance
- Appendix L: Canopy cover histograms
- Appendix M: VTM logging map in southern California
- Appendix N: TWI calculations
- Appendix O: Environmental data processing
- Appendix P: Maxent model parameters settings
- Appendix Q: Environmental histograms for SDM
- Appendix R: SDM results - Current suitable habitat of yellow pine saplings and adults
- Appendix S: SDM results - Past suitable habitat of yellow pine saplings
- Appendix T: SDM results - Future suitable habitat of yellow pine saplings

List of Abbreviations

ABCO - *Abies concolor* (white fir)
ANF - Angeles National Forest
AUC - Area under the ROC curve
BCM - Basin Characterization Model
CADE - *Calocedrus decurrens* (Incense cedar)
CALVEG - Classification and Assessment with Landsat of Visible Ecological Groupings
CNF - Cleveland National Forest
CWD - Climatic Water Deficit
CWHR - California Wildlife Habitat Regions
d.b.h. - Diameter at Breast Height
FIA - Forest Inventory Analysis
FRI - Fire Return Interval
FVS - Forest Vegetation Simulator
LPNF - Los Padres National Forest
MaxEnt - Maximum Entropy
NEPA - National Environmental Policy Act
NF(s) - National Forest(s)
NRCS - Natural Resources Conservation Service
NRV - Natural Range of Variation
PICO - *Pinus coulteri* (Coulter pine)
PILA - *Pinus lambertiana* (Sugar pine)
PIJE - *Pinus jeffreyi* (Jeffrey pine)
PIPO - *Pinus ponderosa* (Ponderosa pine)
PSMA - *Pseudotsuga macrocarpa* (Big cone douglas fir)
QUCH - *Quercus chrysolepis* (Canyon live oak)
QUKE - *Quercus kelloggii* (California black oak)
SBNF - San Bernardino National Forest
SDM - Species Distribution Model
SSPM - Sierra San Pedro Mártir
USFS - U.S. Forest Service
USGS - U.S. Geological Survey
VTM - Vegetation Type Mapping
YPMC - Yellow Pine Mixed Conifer

1. Significance

The U.S. Forest Service's (USFS) mission is to sustain the health and diversity of public lands for present and future generations (USDA, 2019). In southern California, there are four National Forests (NFs): Angeles, Cleveland, Los Padres, and San Bernardino, each of which protects a variety of diverse vegetation communities and wildlife species. Southern California NFs provide habitat for numerous endangered and threatened species including the California condor (*Gymnogyps californianus*), California red-legged frog (*Rana draytonii*), and the California spotted owl (*Strix occidentalis*). Additionally, NFs provide a broad range of ecological, economic, and social services. For example, the NFs in southern California contribute approximately 540 billion gallons of water to downstream watersheds (Brown et al., 2016) and store over 75 million metric tons of carbon (USDA, 2019). In southern California, healthy ecosystems within NFs play an integral role in delivering resources and ecosystem services to over 22 million people (CDF, 2018; Mooney et al., 2009).

In southern California NFs, yellow pine mixed conifer (YPMC) forests are an important vegetation community and make up approximately 70% of conifer forests (Nigro & Molinari, 2019). Southern California YPMC forests are found near the top of their elevation range, which makes them particularly important ecological resources (Minnich, 2007; Stephenson & Calcarone, 1999). These forests face many risks, which threatens the benefits these forests provide. Climate change models predict higher average temperatures, decreased annual snowpack, and variable precipitation (Hayhoe et al., 2004), thereby increasing fuel aridity, length of fire season and the number of high fire danger days (Abatzolou and Williams, 2016). A century of fire suppression policies have resulted in increased forest density, which increases the risk of stand-replacing fires. The long-term anthropogenic impacts experienced by these forests requires management intervention to promote the long-term resilience of YPMC forests to threats like climate change and fire.

The USFS currently uses the Land Management Plan (LMP) (USDA, 2012; amended in April 2012) for forest management guidelines as part of their mission to sustain the health and diversity of public lands. Goal 1.2.1 of the LMP lays out the long-term desired conditions for unburned areas of the forest as:

1. Create forests more resistant to the effects of drought, insect and disease outbreaks and stand-killing crown fires;
2. Encourage tree recruitment that contain a species mix more like pre-settlement composition;
3. Recreate stand densities more like those of the pre-suppression era; and
4. Encourage a stand structure that emphasizes large-diameter trees.

The outlined conditions are largely based on knowledge of forest compositions prior to fire suppression and landscape scale alterations to the natural environment such as logging and grazing. Managers need to know how much contemporary forest conditions deviated from historic conditions in order to plan successful conservation and restoration projects that increase forest resilience.

This project will analyze the changes between historic and contemporary YPMC forest conditions in southern California. Our analysis will contribute to the USFS's work of composing a Natural Range of Variation for southern California YPMC forests, of which there is currently no compiled source on historic conditions. A report on changes in YPMC forest structure and composition over the past century will be an invaluable resource for USFS forest managers to follow and implement management requirements set forth by the LMP. We will also model future suitable habitat for yellow pine saplings in the Transverse Ranges of southern California to determine long-term trends of these important YPMC species. Lastly, we demonstrate one example of how the results of a species distribution model can be used by forest managers.

2. Objectives

The existence and health of southern California YPMC forests are threatened by increasing fire severity, bark beetle mortality, and habitat loss caused by climate change. These forests are “sky islands” that are geographically isolated among many different mountain ranges (McCormack et al., 2009). This makes these forests sensitive to perturbations because there are no nearby seed sources nor can the forests shift upward in latitude to escape or recover from stressors. YPMC forests provide critical ecological services such as watershed stability, hydrological function, biodiversity, and carbon storage (Haffey et al., 2018). Losing these forests means risking a devaluation of these services. Understanding how much forest conditions have changed from a historic baseline is essential information the USFS can utilize to develop management goals that promote resilient forests under a changing climate.

Specific objectives of the project include:

1. **Analyze changes in historic and contemporary YPMC forest in southern California.** Our analysis will focus on five components related to forest structure: tree density, tree size class and class distribution, basal area, canopy cover, and understory shrub cover.
2. **Conduct a natural range of variation** for the topics in Objective 1 by combining our analysis with historic literature review (mid 1800s to early 1900s) and contemporary literature.
3. **Model future habitat suitability for yellow pines** (*P. jeffreyi* and *P. ponderosa*) under various climate scenarios in the Transverse Ranges.
4. **Conduct a case study demonstrating how to prioritize YPMC forests for forest health projects** within SBNF based on feasibility, legal and administrative constraints, ecosystem services, and vulnerability to future threats such as high burn severity and climate change.

3. Background

3.1 Natural Range of Variation

The natural range of variation is defined by Forest Service Handbook 1909-12 Chapter 10 as:

Spatial and temporal variation in ecosystem characteristics under historic disturbance regimes during a reference period... The NRV can help identify key structural, functional, compositional, and connectivity characteristics, for which plan components may be important for either maintenance or restoration of such ecological conditions.

Similarly, Wiens et al. (2012) defines the natural range of variation as:

The variation of ecological characteristics and processes over scales of space and time that are appropriate for management application

There are similar definitions of NRV in the literature (Wiens et al., 2012), but the common themes include a focus on spatial and temporal variability. Historic ecology is a fundamental part in understanding temporal and spatial variability, which serves several purposes to managers including:

- Identifying thresholds and tipping points for shifts in the steady state,
- Quantifying how much contemporary conditions have deviated from a baseline,
- Understanding disturbance history and ecological dynamics such as rates of change, consequences of disturbances, and post-disturbance recovery stages,
- Determining which ecological characteristics contribute to resilience

NRVs have several applications in management planning. NRVs provide valuable information on ecological attributes (Bestelmeyer, 2012) that contribute to resilience so that these attributes can be incorporated into future land management planning and decision making. Additionally, understanding how ecosystems in the past have responded to disturbances is essential when planning for climate change and understanding ecological changes (Veblen et al., 2012). For example, knowing how long it historically took an ecosystem to recover after a disturbance and what those recovery stages looked like can help managers determine if contemporary ecosystems are following those same, natural patterns and determine when management intervention is warranted. NRVs can also be used to determine if there has been a regime shift or shift in the steady state (Bestelmeyer, 2012). NRVs can be applied to correct shifting baseline syndrome, which is when individuals accept contemporary conditions as “normal” (Kirby, 2012). All of these aspects of an NRV can be applied to develop risk management strategies (Safford et al., 2012) and be used as a framework to help establish management goals that sustain the health and diversity of ecosystems (Shedd et al., 2012).

Despite the functionality of NRVs, some question their relevance in management planning. Stephenson et al. (2010) and Landres et al. (1999) argue that human impacts on forests have altered the landscape to the point where restoring historic conditions can be irrelevant or difficult to interpret. Millar et al. (2007) adds that attempts to maintain or restore to historic conditions require more effort from managers, and can create forests ill adapted to contemporary conditions which can cause ecosystems to be more susceptible to undesirable changes. Managers who utilize NRVs reiterate that NRVs do not provide management targets, nor are they trying to restore landscapes back to historic conditions (Wiens et al., 2012). Supporters acknowledge that, in most cases, returning to past conditions will not be sustainable in the long term due to climate change (Romme et al., 2012). Rather, NRVs are used as a framework to better understand ecosystem processes and dynamics to ensure future management actions incorporate features that contribute to resilient forests.

Some also question the relevance of using historic conditions to inform present and future management actions when climate change may result in novel ecosystems and unprecedented, rapid changes in the environment (Hobbs et al., 2010; Stephenson et al., 2010; Williams et al., 2007). Other critics of NRVs question their qualitative nature and emphasize that each point in space and time is unique and changing constantly (Stephenson et al., 2010). However, NRVs are more than a snapshot of the past. Historic conditions provide invaluable insight into how ecosystems and species will respond to differing intensities and frequencies of disturbance events and stressors. Understanding ecological dynamics provides a deeper understanding of ecosystem processes and rates of change that can be applied with some level of predictability into preparing for climate change (Keane et al., 2009; Swetnam et al., 1999). This information is more important now as we enter into an era of unprecedented change (Safford et al. 2012). Understanding how ecosystems and species will react to severe climate events will allow managers to set goals for a dynamic, resilient system that will promote long-term sustainability of the forests. As Safford et al. (2012) stated, “plan for the future, not for the past, but do not forget that the past provides our only empirical glimpse into the likely course of the future” (p. 325).

We used *Natural Range of Variation for Yellow Pine and Mixed-Conifer Forests in the Sierra Nevada, Southern Cascades, and Modoc and Inyo National Forests, California, USA* by Safford and Stevens (2017) as a template for our NRV analysis. Safford and Stevens (2017) conducted a thorough review of ecosystem function, disturbance history, forest structure, and forest composition in YPMC forests in their assessment area. They used a “range of means” approach to conduct their NRV, meaning they compared measures of central tendency between multiple sources. These sources include historic qualitative and quantitative data in addition to contemporary research from the assessment area or reference sites. NRVs often use reference sites with similar climate and species assemblages that have experienced little disturbance to theorize what contemporary conditions should look like if certain anthropogenic activities, such as fire-suppression and logging, had not happened.

We conduct an essential component of a NRV by analyzing changes in historic and contemporary tree density, size class and size class distribution, basal area, canopy cover, and shrub cover (see Section 5). We combine our results with historic and contemporary literature review from our study area and from reference sites (see Section 3.1.1) to conduct a NRV following the range of means approach used by Safford and Stevens (2017). Our NRV will be part of a complete NRV analyzing YPMC forests in southern California that the USFS will complete in the future.

3.1.1 Reference sites

NRVs often utilize data from sources outside of the study area to make comparisons; these are known as reference sites or analog sites. Reference sites have similar climates, vegetation compositions, and disturbance histories to the study area or area of interest which allows for ecological comparisons between the two. We utilized reference sites for our analysis because the historic data (i.e., Vegetation Type Mapping (VTM) surveys, see Section 4.1) used in this study were collected several decades after human influences and approximately 20-30 years after wide-scale fire suppression policies. However, it is unlikely that forest composition changed significantly in those first couple of decades after fire suppression. Unfortunately, the VTM surveys are the only source of historic, quantitative data available for our study area. Our research and other literature in our study area that compare historic and contemporary conditions only use VTM data to represent historic conditions. We acknowledge that only using a single source to represent historic conditions can introduce a potential source of bias. Therefore, utilizing data gathered from reference sites is important to diversify the sources used to draw conclusions about historic conditions.

The Sierra San Pedro Mártir (SSPM) National Park and Sierra Juarez mountain range in Baja California, Mexico (Figure 1) have been identified as the most ideal reference sites for southern California YPMC forests. SSPM and Sierra Juarez are at the southern end of the Peninsular Mountain Ranges, approximately 150km and 50km south of the U.S.-Mexico border, respectively. SSPM and Sierra Juarez fall within the California Floristic Province; they support species also abundant in southern California YPMC forests (e.g., *P. jeffreyi*, *P. lambertiana*, *A. concolor*, *Q. chrysolepis*, and rarely *C. decurrens*).

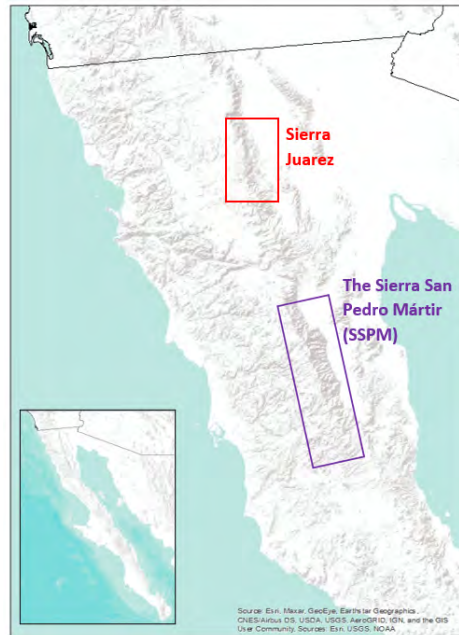


Figure 1. Approximate locations of the Sierra Juarez and the Sierra San Pedro Mártir (SSPM) reference sites in Baja.

Similar to southern California, Baja also has a Mediterranean climate. Temperatures are similar between southern California and Baja, but precipitation varies between these regions (Dunbar-Irwin & Safford, 2016). 14-21% of Baja's annual precipitation falls in summer from monsoons, while southern California weather stations only report 2-7% of annual rain falling in summer (Dunbar-Irwin & Safford, 2016). Additionally, annual precipitation was 33-97% greater in southern California compared to SSPM and Sierra Juarez (Dunbar-Irwin & Safford, 2016). Some question whether using Baja as a reference site is appropriate given the differences in precipitation (Keeley, 2006). The differences in precipitation suggest Baja may not be the best reference site for studies comparing factors strongly influenced by precipitation, such as comparing drought impacts or seedling and sapling survivorship; these comparisons are not done in this study. However, since we are making landscape scale comparisons on vegetation structure, the similarities in temperature, Mediterranean climate regime, fire regime, and vegetation composition indicate that it is still appropriate to make broad scale ecological comparisons with southern California YPMC forests despite the differences in precipitation.

Baja also has a similar fire regime and disturbance history to pre fire suppression southern California (Barbour & Minnich, 2000; Nigro & Molinari, 2019; Rivera-Huerta et al., 2016; Stephens et al., 2003). Additionally, there has been essentially no logging in Baja (Stephens et al., 2003; Dunbar-Irwin & Safford, 2016; Minnich & Vizcaíno, 1998). The main anthropogenic disturbance in SSPM and Sierra Juarez has been grazing. Varying intensities of grazing have been noted in these reference sites for over 200 years, (Minnich et al., 1997; Minnich & Vizcaíno, 1998) including in modern times (Dunbar-Irwin &

Safford, 2016). Thus, Baja provides insight into what southern California's fire regimes and forest densities should be in the absence of logging and over a century of fire suppression.

Estimates of the fire return interval (FRI) in Baja and southern California vary, but are typically similar among the two regions. Dendroecology studies by Burk (unpublished data, cited in Minnich et al., 1995) estimated the mean FRI to be 24 years in SSPM mixed conifer forests, while mean FRI estimates from Stephens et al. (2003) ranged from 6.9-14.5 years. Using aerial photos Minnich et al. (2000) estimated the FRI to be 52 years. The mean historic FRI of 12.7 years estimated by Nigro and Molinari (2019) in southern California align more with Burk and Stephens et al. (2003). The natural fire regime in both SSPM and southern California forests has been described as high frequency, and dominated by low intensity fires (Barbour & Minnich, 2000; Rivera-Huerta et al., 2016; Van de Water & Safford, 2011). Fires in Baja have been largely free burning for most of recorded history, but limited fire-suppression began in the mid 1970s (Stephens et al. 2003). However, researchers have concluded that while a fire suppression policy was enacted, it was not effectively practiced for several decades (Freedman, 1984; Minnich & Bahre, 1995; Minnich & Chou, 1997). Stephens et al. (2007) claimed suppression activities only involved a couple, small hand crews working in the summer and fall. However, there is support that suppression tactics in SSPM are becoming more effective as most fires in YPMC forests are now being extinguished within 24 hours (Dunbar-Irwin & Safford, 2016). Despite the increase in fire suppression, recent research indicates that the fire regime is still dominated by low severity fires (Rivera-Huerta et al., 2016), which indicates it is still appropriate to use modern studies in Baja as a reference site. This may not always be the case as fires within YPMC forests in SSPM may be becoming more severe (Rivera-Huerta et al., 2016).

Though Baja is the most common reference site used in southern California literature (Minnich et al., 1995; Nigro & Molinari, 2019; Chou et al., 1993; Keeley & Fotheringham, 2001), there are other identified reference sites with YPMC forests that we can draw from including: Illiouette Valley in Yosemite National Park, Sugarloaf Valley in Sequoia-Kings Canyon National Park, Grand Canyon National Park, and Gila National Forest (H. Safford, personal communication, 2020). We also compared climatic water deficit (CWD), which is correlated with broad scale vegetation distribution (Stephenson, 1990), from YPMC forests in our study area to CWD across California to identify other potential reference sites (Figure 2). As a result, parts of Sequoia National Forest and Inyo National Forest had the most similar CWD to YPMC forests in our study area and were also included as reference sites if data was available. It is important to note that the identified reference sites in California have experienced over 70 years of fire suppression and forest densification, while reference sites in Arizona experience summer precipitation from monsoons. We address potential limitations associated with these reference sites in the text when making comparisons. Baja was prioritized as a reference site because it has the most similar climate to southern California and has been the least impacted by human disturbances. Other reference sites were used only when we did not have abundant qualitative or quantitative data from our study area or from reference sites in Baja.

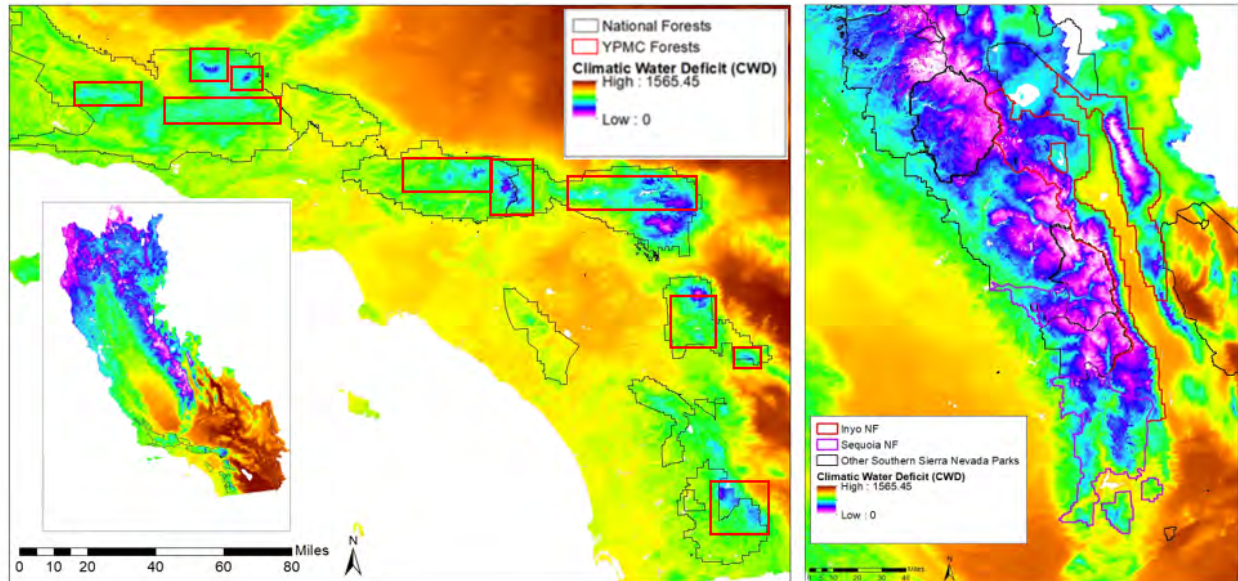


Figure 2. Climatic water deficit (CWD) was used to identify sites in California that could serve as reference ecosystems for southern California. CWD is used because it has been shown to be an indicator for broad vegetation distribution (Stephenson, 1990). General locations of YPMC forests in the study area are outlined in red boxes (left image; CWD ranged 266 - 1064mm; mean 714mm). Parts of Inyo NF and Sequoia NF have the closest CWD to YPMC forests in southern California and were identified as ideal reference sites. CWD layer is available as 30-year climate summaries (1981-2010) from the Basin Characterization Model (Flint & Flint, 2014).

3.2 Yellow Pine Mixed Conifer Forests and Southern California National Forests

Our study area encompasses yellow pine mixed conifer (YPMC) forests within the Transverse and Peninsular Ranges in southern California (Figure 3). This region has a Mediterranean climate characterized by hot, dry summers and warm, wet winters (Minnich & Everett, 2001; Rundel, 2005). Yellow pine mixed conifer forests cover 285,308 acres in southern California, representing 41.3% of all coniferous forests in the study area. 94.3% (269,138.3 acres) of YPMC forests are located within the boundaries of federally managed National Forests (Table 1). These National Forests include the Angeles National Forest (ANF), Cleveland National Forest (CNF), southern Los Padres National Forest (LPNF), and San Bernardino National Forest (SBNF) (Figure 3). The northern portion of LPNF along the central coast has been excluded from this analysis because it is not located within the Transverse or Peninsular Ranges. The southern LPNF, the ANF, and the northern SBNF are all within the Transverse Ranges, while southern SBNF and CNF are within the Peninsular Ranges. Though our analysis of YPMC habitat is not restricted to administrative boundaries, we often break down results by National Forest because most of the YPMC forests are within National Forest boundaries.

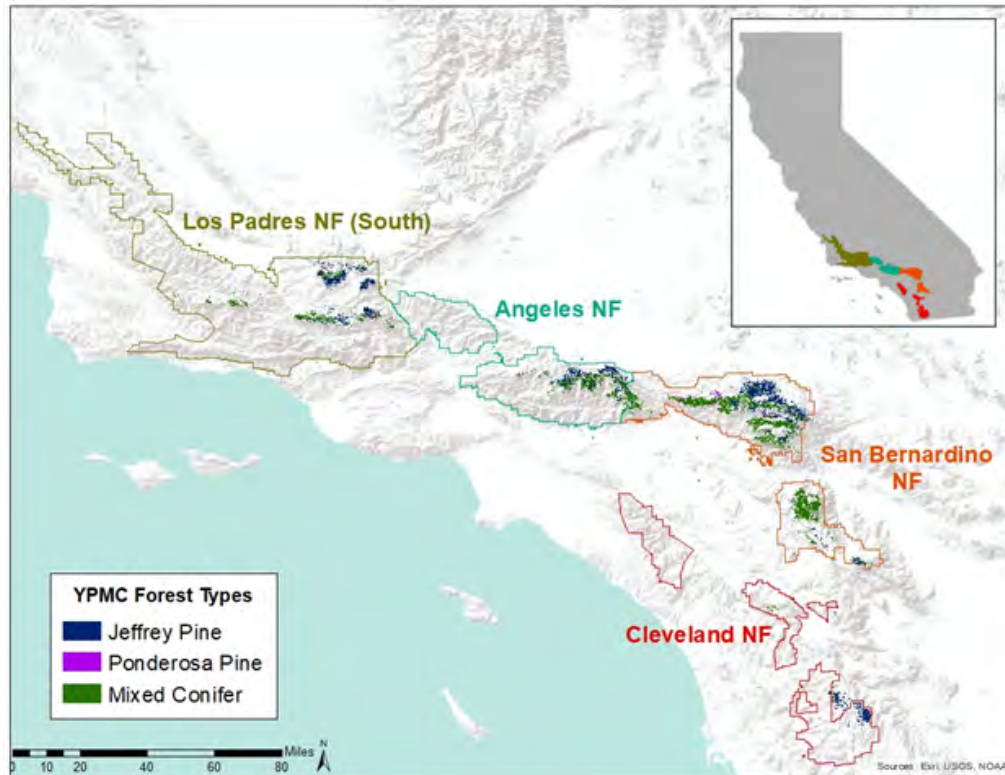


Figure 3. Yellow pine mixed conifer forests in the four southern California National Forests. LPNF, ANF, and northern SBNF fall within the Transverse Ranges. CNF and southern SBNF fall within the Peninsular Ranges. YPMC forests cover 285,309 acres in the study area. Map derived using the Jeffrey Pine, Ponderosa Pine and Mixed Conifer alliances in CALVEG.

Table 1. Acres of YPMC forests in southern California broken down by forest type and administrative boundaries. “Other” indicates forests within State Park boundaries or private land. Acreage was calculated from YPMC CALVEG (Classification and Assessment with Landsat of Visible Ecological Groupings) polygons.

	ANF	CNF	LPNF	SBNF	Other	Total
Total YPMC	89,400	6,262	62,980	113,990	12,674	285,308
Mixed Conifer Forest	51,207	1,900	26,997	75,419	4,682	160,205
Yellow Pine	38,193	4,364	35,983	38,571	7,992	125,103
Jeffrey Pine	34,863	3,913	30,594	35,447	7,640	112,457
Ponderosa Pine	3,330	451	5,389	3,124	352	12,646

Safford and Stevens (2017) used California Wildlife Habitat Regions (CWHR) to identify YPMC forests in Sierra Nevada. After cross referencing [CALVEG](#) (Classification and Assessment with Landsat of Visible Ecological Groupings) and CWHR polygons on Google Earth, we found that CALVEG better classified YPMC while CHWR misclassified a relatively large portion of YPMC in our study area. This was particularly evident in recent fire scars in which forests have been type converted to shrublands. We used vegetation classifications by CALVEG to identify polygons with yellow pine mixed conifers in our study area and to define YPMC species.

We defined YPMC species as *Abies concolor* (White fir), *Calocedrus decurrens* (Incense cedar), *Pinus coulteri* (Coulter pine), *Pinus jeffreyi* (Jeffrey pine), *Pinus lambertiana* (Sugar pine), *Pinus ponderosa* (Ponderosa pine), *Pseudotsuga macrocarpa* (Bigcone Douglas fir), *Quercus chrysolepis* (Canyon live oak), and *Quercus kelloggii* (Black oak) (Table 2). *Abies concolor*, *C. decurrens*, *P. jeffreyi*, *P. lambertiana*, *P. ponderosa*, and *Q. kelloggii* are dominant species in YPMC forests used in Safford & Stevens (2017) and defined by CALVEG. *Pseudotsuga menziesii* is also considered a common YPMC species in Sierra Nevada (Safford & Stevens, 2017), however this species is not found in southern California. We included *P. macrocarpa* in place of *P. menziesii* because they are in the same genus. Additionally, CALVEG listed *P. macrocarpa* as an occurrent in mixed conifer forests. *Pinus coulteri* was also listed as an occurrent in mixed conifer forests, however it was not included in Safford and Stevens (2017) because the species is not found in Sierra Nevada. Safford and Stevens (2017) also did not list *Q. chrysolepis* as a dominant YPMC species despite it being commonly found in Sierra Nevada. A study completed by Dolanc et al. (2014) in central and northern Sierra Nevada found that *Q. chrysolepis* had the largest relative increase in frequency when they compared historic and contemporary surveys. Since *Q. chrysolepis* was listed as a codominant in mixed conifer forests by CALVEG, we decided to include this species in our analysis. Additionally, we were interested to see if these trends in *Q. chrysolepis* observed by Dolanc et al. (2014) also occurred in southern California.

Table 2. Common conifer and oak species observed in YPMC forests in the study area and their general characteristics. Aspects are also listed here: N=north and S=south.

^aSources: Burns and Honkala 1990, Minore 1979, and USDA FS 2013b as cited in Safford and Stevens, 2017; Cope 1993, Howard 1992, and Tollefson 2008, as cited in Fire Effects Information System [Online].

^b Sources: Bonner and Karrfalt 2008, Burns and Honkala 1990, Fowells and Schubert 1956 as cited in Safford and Stevens, 2017; Cope 1993, Howard 1992, and Tollefson 2008, as cited in Fire Effects Information System [Online].

Scientific Name	Common Name	Code	Fire Tolerance ^a	Drought Tolerance ^a	Shade Tolerance ^a	Elevation (m) ^b
Pines						
<i>Abies concolor</i>	White fir	ABCO	Low	Low	High	800 – 2300 N; 1500 – 2500 S
<i>Calocedrus decurrens</i>	Incense cedar	CADE	Moderate	Moderate	Moderate	600 – 2100
<i>Pinus coulteri</i>	Coulter pine	PICO	High	High	Low	200 – 2100
<i>Pinus jeffreyi</i>	Jeffrey pine	PIJE	High	High	Low	1500 – 2400 N; 1700 – 2800 S
<i>Pinus lambertiana</i>	Sugar pine	PILA	Low	Moderate	Moderate	1000 – 2000 N; 1400 – 2700 S
<i>Pseudotsuga macrocarpa</i>	Bigcone Douglas fir	PSMA	Moderate-High	High	Low	600 – 2100
<i>Pinus ponderosa</i>	Ponderosa pine	PIPO	High	High	Low	300 – 1800 N; 1200 – 2100 S
Oaks						
<i>Quercus chrysolepis</i>	Canyon live oak	QUCH	Low	High	High	90–2700
<i>Quercus kelloggii</i>	California black oak	QUKE	High	High	Low	900 – 1500 N; 1400 – 2100 S

To define YPMC forests, we used several CALVEG alliances. Douglas-Fir-Pine, Mixed Conifer-Fir, and Mixed Conifer-Pine CALVEG alliances represent mixed conifer forests. Eastside Pine, Jeffrey Pine, Ponderosa Pine, and Ponderosa Pine-White Fir CALVEG alliances represent yellow pine forests.

Yellow pine forests are dominated by *P. jeffreyi* or *P. ponderosa* and are occasionally intermixed with a few hardwood species like *Q. kelloggii* and *Q. chrysolepis*. Mixed conifer forests are comprised of a mixture of species (Dieterich, 1983) in which no species is dominant. These forests contain species that possess a diverse variety of characteristics (Table 2) which are important for landscape and patch level heterogeneity. For example, yellow pines are some of the most fire-resistant conifers in California (J.K. Brown & Smith, 2000; Foresters, 1980) which has important implications for composition and long-term persistence of conifer forests under a more severe fire regime. However, their non-serotinous cones makes them susceptible to long-term eradication after stand-replacing wildfires (Russell et al., 1998). *Pinus coulteri*, on the other hand, has serotinous cones (Borchert, 1985), which enable this species to resprout vigorously after severe wildfire while other conifer species, such as yellow pines, may struggle to regenerate (Parkinson et al., *in prep.*; Franklin & Bergman, 2011). *Pseudotsuga macrocarpa* is able to regenerate from epicormic buds, which are buds along branches that resprout after a range of fire severities. This is an important adaptation for a moderate-high fire regime (Pausas & Keeley, 2017). *Quercus chrysolepis* and *Q. kelloggii* are obligate resprouters that can resprout from burls after being top killed by wildfires. Oaks tend to resprout vigorously after wildfires due to their established root system (Bowen & Pate, 1993). However, regenerating conifers are dependent on several factors for successful regeneration including post-fire environmental conditions and distance to seed source (Chmura et al., 2011; Crotteau et al., 2013; Donato et al., 2009; Franklin & Bergman, 2011; Tappeiner & Helms, 1971; Welch et al., 2016). These differences in regenerative processes can have long-term impacts on vegetation composition. For example, species composition may shift to more homogenous oak or *P. coulteri* dominant habitats after a severe wildfire, altering contemporary forest structure/composition (Cocking et al., 2014; Franklin & Bergman, 2011; McDonald & Tappeiner, 2002).

Additionally, YPMC species have a range of shade and drought tolerances (Table 2). *Abies concolor*, *C. decurrens*, and *Q. chrysolepis* are all shade tolerant species. In the absence of fire, they grow in the understory and act as ladder fuels. Ladder fuels have the ability to alter fire regimes from low severity, ground fires to high severity, crown fires. Shade intolerant species, such as yellow pines and *P. macrocarpa*, tend to be fire tolerant which enables these species to withstand low to moderate-high fire severity. Yellow pines are also very drought tolerant (J. K. Brown & Smith, 2000; Foresters, 1980), which is an important characteristic to maintain the persistence of conifer forests in the study area as droughts are expected to increase in frequency and intensity under climate change (Diffenbaugh et al., 2015).

In southern California, YPMC forests exist as “sky islands” that are geographically isolated among many different mountain ranges (McCormack et al., 2009). This makes YPMC forests sensitive to perturbations because there are no nearby seed sources to assist in regeneration after a disturbance, nor can the forests shift upward in latitude to escape from stressors. YPMC forests are also limited in their ability to shift upward in elevation, with the exception being the San Gabriel mountains, San Bernardino mountains, and San Jacinto mountains where higher elevations are currently dominated by subalpine species. YPMC species have a variety of adaptations that will be important to maintain the heterogeneity, biodiversity, and persistence of these conifer forests in southern California under increased frequency and intensity of droughts, wildfires, and climate change.

3.3 Disturbance History

When conducting an NRV, it is important to understand how anthropogenic actions have influenced observed changes in forest structure. California has a long history of human caused disturbances

including fire suppression, cessation of Native American burning, logging, and grazing. The cessation of Native American burning and early 20th century implementation of fire suppression has altered the composition and structure of conifer forests across the western United States (Murphy et al., 2007; Safford & Stevens, 2017; Stephens et al., 2007). A century of fire suppression has led to an increase in forest biomass and an abundance of shade tolerant conifers (Safford & Stevens, 2017; Stephens et al., 2018), which enhances the vulnerability of YPMC forests to drought, bark beetle attack, and severe wildfire (Welch et al., 2016; Young et al., 2017). In southern California, half of all YPMC forests have not burned in 109 years, which has resulted in an increase in the proportion of YPMC forests burning at high severity (Nigro & Molinari, 2019). The impacts of logging and grazing on YPMC forests in the study area is less understood. Knowing the locations and intensities of these activities is an important first step in understanding how these activities have impacted YPMC forest structure and composition. Thus, we conducted an extensive, though not complete, literature review of logging and grazing in southern California YPMC forests.

Logging

Though California has a long history of logging, there has been relatively little historic logging in southern California conifer forests (Barbour, 2007; Minnich & Vizcaino, 1998). This is primarily due to the isolated and rugged topography of the mountains in this area, making accessibility difficult (Barbour, 2007; U.S. Geological Survey, 1899; Leiberg, 1898; California State Board Forestry, 1886). Although, the quality of lumber could have also contributed to minimal logging in southern California. Botanist Harvey Monroe Hall referred to timber in San Jacinto as “inferior quality”, while U.S. Geological Survey (1899) reported that lumberman claimed the timber is “less valuable than that found further north.”

Historic logging operations and mills were recorded in all southern California National Forests (Barbour, 2007; USDA, 1905; Stephenson & Calcarone, 1999; Blakley & Barnette, 1985). See Table 3 for logged sites mentioned in the literature. Formal requests for logging in southern California forests date back to 1839 (Blakley & Barnette, 1985). Some of the first reports of logging in the San Bernardino Mountains and the San Jacinto Mountains are estimated around 1865 and the 1880s, respectively (Leiberg, 1898).

In 1902, Harvey Monroe Hall wrote that “the worst enemy the forests have been, not the forest fire, but the sawmill. Many a pine-clad slope has been stripped of its best trees in order that they might be converted into lumber.” Additionally, the California State Board Forestry (1886) described sawmills in San Bernardino and San Jacinto as being “continuously at work.” A few historic sources report that some areas were intensely logged. Walcott (1899) wrote:

“A large quantity of the forest fit for merchantable lumber has been logged off. Sawmills have been in operation for many years. Some of the cutting dates back twenty-five or thirty years. Some is recent, and two sawmills are now running or will soon go into operation. The logged-off areas lie along the main range from Seely Flat to Orchard Canyon. There is also a small tract at the head of City Creek, around the Highland mill, that has been cut over to the extent of 99 percent”.

There were no reports of historic logging in San Gabriel Mountains, which are located in ANF and the western edge of SBNF; the steepness made accessibility too difficult (McKelvey & Johnston, 1992). Plummer and Gowsell (1905) claim approximately 200,000 board meters were logged from 1898 to 1905 in LPNF. They also described some logging in LPNF as “wasteful”, especially on Frazier Mountain. Leiberg (1899) described logging as “extensive” in San Jacinto in comparison to the total amount of merchantable timber. However, Barnard (1900, as cited in McKelvey & Johnston, 1992) offers a conflicting report in which he claimed there was “not more than 1 square mile” logged in San Jacinto by the end of the 1800s. While Leiberg (1899) reported that there were 249,000 acres of merchantable timber

in the San Bernardino Mountains, only around 5,000 acres had been logged “in recent times.” More research is needed to clarify where intense logging operations occurred in these forests as it can have implications when interpreting changes in historic and modern forest structure.

Table 3. Broad and specific locations in southern California that historic sources or modern researchers reported historic logging operations. Locations of sawmills are not included in the table.

National Forest	Logging Location	Source
Cleveland NF	Palomar Mountains	California State Board Forestry, 1886
	Cuyamaca Mountains	California State Board Forestry, 1886
Los Padres NF	Mount Pinos	Plummer & Gowsell, 1905
	Seymour Creek	Plummer & Gowsell, 1905
	Frazier Mountain	Plummer & Gowsell, 1905; Blakley & Barnette, 1985
San Bernardino NF (San Bernardino Mountains)	west San Bernardino Mountains	Barbour 2007
	Fleming Creek	Leiberg 1899
	Strawberry Flat	U.S. Geologic Survey, 1899
	Green Valley	U.S. Geologic Survey, 1899
	Seely Flat	U.S. Geologic Survey, 1899
	Orchard Canyon	U.S. Geologic Survey, 1899
	City Creek	U.S. Geologic Survey, 1899
	Running Springs	Minnich, 1978
	west of Jobs Peak	Minnich, 1978
Lake Arrowhead	Minnich, 1978	
Heap's Peak	Minnich, 1978	
San Bernardino NF (San Jacinto Mountains)	Idyllwild	Barbour, 2007
	Strawberry valley	Hall, 1902
	Fullers Ridge	Hall, 1902

Historic logging in southern California ended in 1910 when the National Forests were established, due to public pressure to maintain the ecosystem services of recreation and watershed protection (Lockmann, 1981, as cited in Barbour, 2007). Logging did resume in SBNF from 1947 and 1990 (Figure 4); approximately 362 million board feet was logged (McKelvey & Johnston, 1992). Stephenson and Calcerone (1999) speculate that some logging occurred in the San Gabriel Mountains in ANF during this time frame, however the amount of logging that occurred in ANF is unknown. There was also a brief revitalization of minor logging in LPNF and CNF in the 1960s-1970s (Stephenson & Calcarone, 1999). In the late 1980s and 1990s, logging in southern California was primarily done to create local firewood, to remove hazard trees, remove burned trees, or for forest health projects (Stephenson & Calcarone, 1999).

In areas where logging did occur, certain conifer species were disproportionately targeted for culling. According to Plummer and Gowsell (1905), *P. jeffreyi* was the most logged timber in LPNF, while *P. lambertiana* and *P. ponderosa* were lightly logged; *A. concolor* and *C. decurrens* were not logged due to inaccessibility. In San Bernardino FR and San Jacinto RF, most (>90%) of the timber logged came from *P. ponderosa* (Leiberg, 1898); only small percentages (<5%) of *P. lambertiana*, *C. decurrens*, and *A. concolor* were logged because they were at high elevations which were mostly inaccessible (Guthrie, 1904) or because they did not provide quality timber. There were reports of logging in CNF (Barbour, 2007; California State Board Forestry, 1886), but no specific details were found on which YPMC species were being logged.

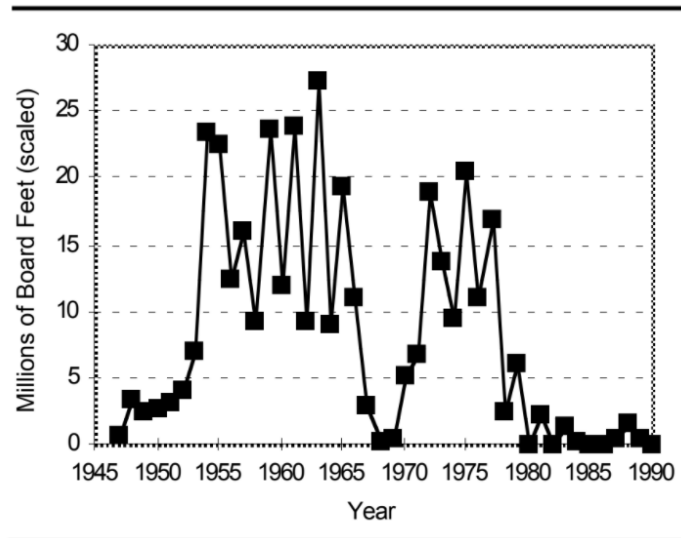


Figure 4. Logged timber in Los Angeles and San Bernardino counties from 1947-1990 (from McKelvey & Johnston, 1992).

The Sierra Nevada have been logged extensively, and as a result, almost all studies comparing historic conditions to modern conditions have found declines in large diameter trees (Safford & Stevens, 2017). Compared to the Sierra Nevada, relatively little logging has occurred in southern California. Most logging occurred in SBNF, with almost no logging in ANF, and very little logging in LPNF and CNF. Additionally, yellow pines were disproportionately logged more than any other YPMC species. Historic disturbances like logging can influence modern day forest structure and will be carefully considered when interpreting our results.

Grazing

Grazing has occurred in the mountains of southern California since the early 1900s (Lockmann, 1981, as cited in Barbour, 2007). Most grazing occurred before the establishment of the National Forests (Barbour, 2007). In his reports, Leiberg (1899a, 1899b) describes grazing in San Bernardino FR and San Jacinto FR, but not in San Gabriel FR (note: Leiberg did not conduct any reports for modern day LPNF and CNF). There was likely no or very little grazing in ANF due to the steep topography (McKelvey & Johnston, 1992; Robinson, 1991).

SBNF was heavily grazed by sheep (Lockmann, 1981, as cited in Stephenson and Calcarone, 1999; Minnich, 1988; McKelvey & Johnston, 1992), resulting in what has been described as “extensive vegetation and erosion damage” in the montane meadows (Minnich, 1988). There was little grazing conducted in Mt. Pinos (Barbour, 2007). Though grazing declined after 1900, grazing still occurs in and adjacent to LPNF and CNF, but reportedly not in YPMC forests (Stephenson & Calcarone, 1999).

Intensive grazing can cause a decline in fire frequency by reducing fine fuels (e.g., grasses and herbs) in the understory which spread fire across the landscape. (Swetnam & Baisan, 1996; Touchan et al., 1995). While historic reports mentioned that grazing was conducted in forests, grazing also occurred in montane meadows and lower elevation foothills, grasslands, and savannas (Guthrie, 1904, as cited in USDA, 1905; Stephenson & Calcarone, 1999). Thus, it is difficult to determine to what extent YPMC forests sustained severe environmental damage due to grazing.

3.4 Climate Change

The Intergovernmental Panel on Climate Change (IPCC) estimates a rise in global temperatures of 2.5 to 10 degrees Fahrenheit over the next century (Shafiel et al., 2021). Throughout California, climate change is expected to increase mean average temperatures and the frequency of extreme temperature events (Hayhoe et al., 2004). Higher elevations in California are expected to be disproportionately affected by the increased temperatures (McCullough et al., 2016). While there is a strong consensus among existing literature that temperatures will increase throughout California under climate change, it is uncertain whether total precipitation will increase or decrease (Bedsworth et al., 2018). However, climate modeling predicts that the precipitation regimes across southern California will be increasingly dominated by rain, rather than snow (Berg et al., 2015; Kapnick & Hall, 2012). As a result, historically snow-dominated sites will experience increased runoff, thereby decreasing plants' abilities to capture water long-term across these sites (Berg et al., 2015). Vegetation in California is expected to move towards higher elevations by the end of the century due to strong climatic influences on vegetation distribution (Davis et al., 2016; Loarie et al., 2008; Staudinger et al., 2013). However, southern California YPMC forests already exist at or near top elevations in relatively isolated sky islands. This puts them at risk of being severely limited or lost indefinitely under climate change as they have limited opportunities to expand to higher elevations.

Severe climatic events, such as drought and wildfire, are increasing under climate change and are further threatening YPMC forests (Diffenbaugh et al., 2015; Fried et al., 2004; Liu et al., 2010). In California, increasing temperatures and changes in precipitation regimes increase the likelihood of drought. Not only is the frequency of droughts expected to increase throughout the state, but drought intensity is expected to increase as well (Cook et al., 2015; Ullrich et al., 2018). Ault et al. (2014) predict an 80% chance of California experiencing a decade long intense drought this century and a 50% chance of a drought lasting as long as 35 years. Prolonged droughts increase susceptibility to bark beetle attacks and result in higher pathogen-related mortality (Hilberg et al., 2016). The 2011-2017 drought alone resulted in the death of over two million trees in southern California (Moore et al., 2019; *Tree Mortality*, n.d.), which altered forest composition and structure and resulted in more hazardous dead fuels across the landscape. Such fuels have been found to increase the burn severity of wildfires throughout the Sierra Nevada (Wayman & Safford, n.d.). Wildfires are now more severe than ever (Nigro & Molinari, 2019) and are more often resulting in larger stand-replaced patches, challenging the persistence of conifer forests (Russell et al., 1998; Parkinson et al., *in prep.*; Franklin & Bergman, 2011).

After stand-replacing disturbance events, environmental conditions are one of the main limitations to conifer regeneration (Davis et al., 2019; Fisichelli et al., 2014). Seedlings are extremely sensitive to environmental conditions, such as near surface temperature (Davis et al., 2019; Fisichelli et al., 2014). Additionally, both precipitation and temperature can affect seedling growth and survival (Brown & Wu, 2005; Chmura et al., 2011; Legras et al., 2010; Savage et al., 2013). Re-establishment will thus be negatively affected by the projected increase in frequency and intensity of droughts (Cook et al., 2015; Ullrich et al., 2018). In southern California, researchers have already noted extremely low conifer regeneration in forests after high severity wildfires, which are now dominated by shrubs (Parkinson et al. *in prep.*; Franklin & Bergman, 2011; Goforth & Minnich, 2008).

Forest management practices will be largely influenced by changes in forest structure and composition caused by climate change (Millar et al., 2007). Therefore, it is necessary to determine the geographic extent and intensity of these structural and compositional shifts to inform management decisions. For plant species, survival of the early life stages is especially critical to both the contemporary persistence and the future expansion of these species (Grubb, 1977; Serra-Diaz et al., 2016; Solbrig & Harper, 1979). Thus, mapping the projected distribution of saplings provides invaluable insight into the future range of long-lived conifer species.

4. Data

4.1 Historic Data - Vegetation Type Mapping (VTM)

From the late 1920's to 1940, forester Albert Everett Wieslander and his team sampled vegetation throughout approximately one-third of California (Thorne et al., 2008). The team of foresters sampled vegetation, took photographs, collected specimens, and drew detailed maps. Surveying focused on documenting California's wild areas, excluding desert, and primarily occurred on USFS land. Although, some surveys were conducted throughout Lassen, Yosemite, and Sequoia/Kings Canyon National Parks, as well as on some private land (Thorne et al., 2008). The data collected by Weislander and his team is called the Vegetation Type Mapping collection, or VTM. Some have referred to the VTM project as "the most important and comprehensive botanical map of a large area ever undertaken anywhere on the earth's surface" (Jepson et al., 2000). In a joint effort, researchers at UC Berkeley, the Marian Koshland Bioscience and Natural Resources Library, and the Information Center for the Environment at UC Davis have compiled all the VTM records and made the data digitally available for download (<http://vtm.berkeley.edu/#/data/>).

The VTM dataset offers the most comprehensive information on historic forest conditions in our study area. To our knowledge, there are no other studies that systematically recorded southern California forest conditions in the early 1900s or before. Starting in the 1800s, General Land Office (GLO) surveys recorded notes on vegetation cover, including tree species and tree diameters, as part of a larger project to document public lands (Bourdo, 1956). While GLO data has been used to analyze temporal changes in forest structure and composition throughout other regions of the country, no such surveys were performed in southern California, making comparisons to historic forest conditions with GLO data impossible for this area.

While the entire project spanned more than ten years, the majority of vegetation plot data was collected between 1929-1935 (Keeley, 2004). This data is available for download from <http://vtm.berkeley.edu/#/data/> and includes general plot information (aspect, slope, elevation, etc.), as well as detailed vegetation measurements. Notable tree data includes information on species composition and diameter at breast height (d.b.h.) measurements, while data collected on brush species includes species composition and percent cover estimates.

While the VTM collection is the earliest and most robust historic dataset available for our study area, there are potential limitations with the dataset. Bouldin (2009) suggested that the VTM collection represents a biased survey of California's vegetation, as the VTM plot selection process is argued to have been highly subjective. Bouldin suggests that foresters preferentially selected sites with mature forest conditions, although there is no explicit mention of this in the field manual (view field manual at https://digitalassets.lib.berkeley.edu/vtm/ucb/text/cubio_vtm_fm.pdf). Bouldin's claims are backed by recent analysis. Unbiased Sierra Nevada plot data from Weeks et al. (1942) was recently compared to VTM plot data across the same assessment area. Results of this comparison indicate that the densities of large trees (>60cm d.b.h.) were 2.6 times greater in the VTM dataset as compared to trees surveyed under Weeks et al. (1942). Similarly, Bouldin found tree densities of large trees from VTM plots to be 2.8 times greater than plots collecting timber inventory roughly at the same time in the same regions of the Sierra Nevada. A conversation between VTM field worker Daniel Axelrod and Jim Bouldin in 1997 suggested that the original intent of the VTM surveys was "not to produce unbiased estimates of landscape scale forest structures" (Bouldin, 2009). We acknowledge that this is a likely limitation to our study and we consider this limitation when drawing final conclusions.

The VTM dataset is further limited by the nature of additional data collection methods. VTM surveyors did not record trees <4in d.b.h. See Section 4.3 and Section 5.7 for details on how we dealt with this in our analysis. Additionally, the precise location of VTM plots were not recorded during the original surveying. However, Keeley (2004) examined the accuracy of inferring historic changes from VTM plot data and concluded that “broad generalizations about historic changes using VTM plots are likely valid.” Therefore, we do not believe the lack of precise plot coordinates are a significant limitation to our study.

Finally, it is worth noting that some records from the VTM collection have been lost due to the historic nature of this dataset, potentially including some data in our study area. Additionally, the digitization of the VTM collection created opportunities for human error (Thorne & Le, 2016). Despite these limitations, the VTM collection has been widely used to assess temporal changes in forest conditions all throughout California and offers important insight into historic forest conditions (Bouldin, 1999; Keeley, 2004; Minnich, 1978; Minnich et al., 1995; Minnich & Dezzani, 1998; Safford & Stevens, 2017).

4.2 Contemporary Data - Forest Inventory Analysis (FIA)

Data used to represent contemporary forest structure were combined from 2 sources:

1. *Forest Inventory and Analysis (FIA) National Program*, which is publicly available (<https://apps.fs.usda.gov/fia/datamart/datamart.html>). We will refer to this data as “**national FIA data**.” This dataset includes plots found within National Forests, state parks, and other areas.
2. USFS data from US Forest Service (USFS) Region 5 Remote Sensing Lab, which is available upon request (kkennedy@fs.fed.us). This dataset contains modified national FIA data found only within USFS boundaries in addition to data from intensified surveys done within USFS boundaries following the protocols established by FIA. We will refer to this data as “**USFS data**.”

The Forest Inventory and Analysis (FIA) National Program conducts randomly placed and spatially unbiased surveys in forests approximately every 6,000 acres across the U.S (O’Connell et al., 2015). The purpose of the program is to inventory and monitor attributes of U.S. forests such as density and composition over time. Several attributes are collected from plots such as species, tree height, tree diameter, slope, elevation, aspect, coarse woody debris, shrub understory, understory percent cover, etc.

The intensified plots within the USFS data are collected following the same sampling protocol as the national FIA program, including random and spatially unbiased plots (K. Kennedy, personal communication, 2020). These surveys were done in order to increase the availability of data on forest conditions in southern California. The most complete record of USFS data was from 2001-2010, which was the time frame selected for our analysis. While national FIA has been collecting data since the 1930s (USDA, 2021), data before the 1990s are very sparse and inaccessible (G. Christensen, personal communication, October 9, 2020). Only data from 1994-2019 national FIA data was available for our study area, however we only used data from 2001-2010 to match with the time frame of the USFS data.

We combined national FIA data and USFS data into a single data frame. It was necessary to combine both datasets to increase the sample size and because the USFS data was only collected inside National Forest boundaries. While only approximately six percent of YPMC forests in southern California exist outside of National Forests, it is important to recognize that forests do not follow human designated jurisdictions. In order to get a complete, representative assessment of contemporary conditions in YPMC forests, all plots in YPMC forests need to be included in the analysis. It was acceptable to combine data from the two sources for our analysis because the data was collected using the same protocol during the same time

frame. For the duration of this report, we will use the phrase “combined FIA data” when referring to the two collective datasets that have been combined into a single dataset.

Since the USFS data contains national FIA data we had to ensure we were not counting the same plot twice during our analysis. We removed the plots from the national FIA dataset that were within the USFS data. We utilized the raw national FIA data because we noticed some minor differences when comparing plot level data between the raw national FIA data to the modified national FIA data included in the USFS dataset. While attributes like slope and aspect were consistently the same between the two sources, occasionally there would be additional trees present in the modified national FIA in the USFS plots not found in the raw national FIA plot. In a couple cases the plot data for a national FIA plot did not match up at all between the datasets. Since we were unable to verify the cause of these discrepancies, we decided to use the original, untouched national FIA data to represent those plots instead of the modified version found in the USFS data.

4.3 Data Tidying

We followed the same methods to get the historic VTM data and the contemporary combined FIA data into a consistent format for analysis. To obtain the final plots used in our analysis we:

- Removed plots that did not contain at least one of the nine YPMC species selected for this analysis (Table 4).
- Removed plots that only contained oaks, *P. macrocarpa*, *P. coulteri*, *P. macrocarpa* and oaks, or *P. coulteri* and oaks. This was done when these were the only YPMC species in the plot. While these are YPMC species, plots with just these vegetation compositions are considered other vegetation types by [CALVEG](#) and do not fit the definition of the alliances we chose to define a yellow pine or mixed conifer forest (see Section 3.2).
- We applied a 750m (~0.5mi) buffer around the CALVEG YPMC forests to capture potential forested areas that may not have been mapped as YPMC. We only included plots that fell within the buffered CALVEG polygons. Occasionally conifer seeds can be transported downstream to lower elevations (USDA, 1905), so the buffer was added so we only analyzed plots that fall within a coniferous ecotone. Plots below the buffered area are located in different habitat types (e.g. scrub oak, chaparral), or represent the species at the extremes of its range limit, which is not within a coniferous ecotone (e.g. a couple *P. ponderosa* plots were in very low elevations below the 750m buffer). A 750m buffer was used because the coordinates of the plots in the national FIA and USFS datasets are altered by about 0.5 miles to protect the rights of private property owners (O’Connell et al., 2015). Additionally, VTM plot coordinates are off by about 200–300m (Kelly & Allen-Diaz, 2009; Thorne et al., 2008).

This resulted in 195 plots from the VTM dataset and 210 plots from the combined FIA dataset (Figure 5). See Table 4 for the number of plots in each National Forest and across elevation bands. Plots were relatively equally distributed across the study area between the two time periods. Within these final plots we conducted some additional tidying:

- Removed any tree that was not one of our nine selected YPMC species (see Table 4).
- Removed trees from the combined FIA data with a d.b.h. less than 4in. VTM surveyors did not record trees with diameters less than 4in, and therefore, we removed trees with diameters less than 4in from the combined FIA data so we could make direct comparisons between the time frames. This is a common practice when making comparisons to VTM data (Bouldin, 1999; Dolanc et al., 2014; McIntyre et al., 2015; Minnich et al., 1995).

- Combined *P. jeffreyi* and *P. ponderosa* into a single class called “yellow pines” because we were unsure if the VTM surveyors correctly classified the two species. When Minnich et al. (1995) compared changes in forest structure between the VTM surveys and contemporary forest structure in SBNF they analyzed the species separately. However, we believed the VTM surveyors incorrectly classified *P. jeffreyi* and *P. ponderosa* since the proportions of these species are not reflected in the VTM and combined FIA datasets (VTM: *P. ponderosa* = 865, *P. ponderosa ssp. jeffreyi* = 444, *P. jeffreyi* = 97; FIA: *P. ponderosa* = 95, *P. jeffreyi* = 1,349). Additionally, we expected the proportion of *P. ponderosa* and *P. jeffreyi* to be relatively unchanged in ANF since this region faced the least amount of impact from human disturbances such as logging and grazing (see Section 3.3). However, this was not the case. In the VTM dataset, 68% of yellow pines in ANF were recorded as *P. ponderosa* and 32% were recorded as *P. ponderosa ssp. jeffreyi*; no trees were recorded as *P. jeffreyi*. While in the combined FIA dataset, 10% of yellow pines in ANF were recorded as *P. ponderosa* and 90% were recorded as *P. jeffreyi*. Additionally, historic reports will often mention *P. jeffreyi*, but then only report data such as logged board feet as *P. ponderosa* yet will not report data for *P. jeffreyi* (Hall, 1902; Leiberg, 1898; U.S. Geological Survey, 1902). Historically, *P. jeffreyi* was considered a variety or subspecies of *P. ponderosa*. The two species are also known to hybridize. Until individuals are cone bearing, these species look very similar (H. Safford, personal communication, 2020; Franklin & Bergman, 2011). Hall (1902) reported that the “difference is sometimes so slight that it is impossible to distinguish them with certainty....young or half- grown specimens are very much like those of the variety.” With this uncertainty, we took a precautionary approach and grouped the two species into a single classification.

Note: these methods only apply to the data used in the NRV analysis. See Section 6.2.3 for tidying methods on the VTM and combined FIA data used for the species distribution model. Additionally, national FIA data records both dead and living trees, but only living trees were included in this analysis.

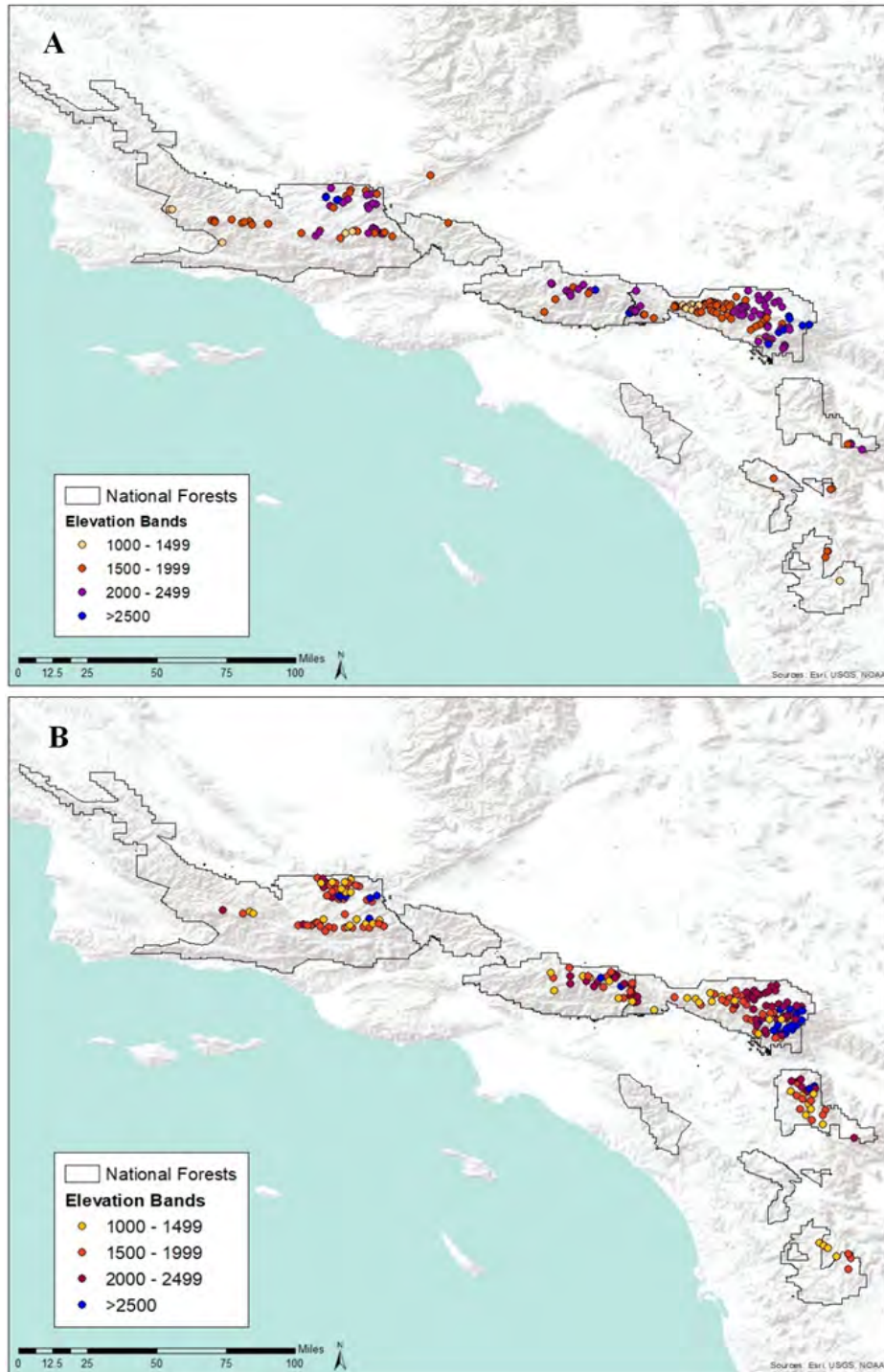


Figure 5. (A) Plot locations of VTM plots (n=195) and (B) combined FIA plots (n=210) used in this analysis. Plots have been grouped by elevation bands.

Table 4. Sample sizes for VTM and FIA plots across elevation bands and in the National Forest jurisdictions.

	VTM Sample Size	Combined FIA Sample Size
Elevation Band (m)*		
1000–1499	20	26
1500–1999	84	80
2000–2499	77	78
>2500	13	26
Jurisdiction		
ANF	20	26
CNF	2	4
LPNF	54	62
SBNF	113	115
Other**	6	3

*: One VTM plot did not have a recorded elevation.

** : Five of the six VTM plots and all three of the combined FIA plots not within federal jurisdictions were near CNF, respectively.

5. 20th Century Shifts in Forest Composition

5.1 Overview

We conduct a landscape-scale analysis investigating structural changes of YPMC forests in southern California over the last century for the following topics: tree density, size class distribution, basal area, canopy cover, and shrub cover. Though a complete NRV comprises of many topics related to forest structure, function, and disturbance, we chose to focus on these five selected topics because they provide valuable information for USFS land managers.

Understanding shifts in tree density and basal area is crucial for limiting high severity wildfires. Increases in tree density, biomass, and ladder fuels are one of the primary drivers for high severity fires (Miller et al., 2009; Miller & Safford, 2012). Fire suppression has caused the mean historic fire return interval (FRI) in southern California to increase from 13 to approximately 78 years (Nigro & Molinari, 2019). With the absence of fire, small trees act as ladder fuels and carry ground fires to the canopy or crown. Crown fires often result in complete mortality even for fire tolerant trees like *P. jeffreyi* and *P. ponderosa* (Barbour & Minnich, 2000; Franklin et al., 2006). Additionally, denser forests experience increased competition for water resources, making them more prone to mortality from bark beetle attacks during droughts (Minnich et al., 2016). Land managers need to examine these changes when making decisions about forest health projects such as thinning and prescribed burning.

Shifts toward increased canopy cover also facilitate spread of fire throughout a landscape (Birch et al., 2015). Closed canopy stands allow fire to travel more easily from crown to crown, increasing tree mortality. Additionally, increased canopy cover provides favorable conditions for shade tolerant species like *A. concolor*, *C. decurrens*, and *Q. chrysolepis*. Though increased canopy cover facilitates wildfires, some wildlife species prefer stands with higher canopy cover or select stands with varying amounts of cover (Stephens et al., 2007). The California spotted owl (*Strix occidentalis*), for example, nest in older stands with moderate to high levels of canopy cover (Gutiérrez et al., 2017; LaHaye et al., 1997; Smith et al., 2002).

Historic forests likely had relatively low, heterogenous shrub cover (Hall, 1902; Leiberg, 1898; USDA, 1905). Forests that have not experienced a recent fire often have higher shrub cover, which is likely less diverse (Safford & Stevens, 2017). Additionally, shrubs promote hotter fires and have more devastating effects on soils (Erickson & White, 2008). In some cases, shrub cover has actually decreased due to large increases in tree density and canopy cover (Knapp et al., 2012). Managers will need to find the right balance of fire, tree density, and shrub cover to ensure optimal forest health.

To date, our analysis is the most in-depth analysis of changes in YPMC forests in southern California. Analyzing compositional shifts allows us to identify how much forests have deviated and in response, land managers can develop management strategies accordingly. In addition to comparing means, which is a single measure of forest conditions, we also calculated medians, standard error, and 25th and 75th quantiles which provide important measures of variability; these tables can be found throughout our Appendix. For our NRV analysis, we combined our structural change results with a literature review of historic sources (mid 1800s-early 1900s) (Appendix A) and contemporary literature. Our NRV analysis will be a subset of a complete NRV that will be published by the USFS in the future.

5.2 Tree Density

5.2.1 Methods

To calculate tree density across the landscape, we summed the number of trees in each plot then divided by the slope corrected area of each plot to get tree density (trees/ha). Tree density is underestimated if plot sizes were not corrected for the slope gradient (Husch et al., 1982 as cited in Abella et al., 2004). We used the equation (original plot size(cosine(arctangent(slope percent as decimal))) from Abella et al. (2004) to calculate the slope corrected area of each plot. The original sizes of the VTM and combined FIA plots were 0.0809ha and 0.067245ha, respectively.

If a YPMC tree species was not present in a plot, it was assigned a 0 for that plot. This was done to ensure we were calculating a landscape average and not just an average of plots where that species was found. See Appendix B for an example of our code. We then calculated the average tree density across southern California YPMC forests. We further investigated drivers of changes in tree density in the study area by analyzing tree density by species, National Forest (including and excluding oaks), shade and fire tolerant species (including and excluding oaks), elevation, and functional group lifeform (conifer vs. oak). We also analyzed tree density by elevation and aspect, elevation and aspect for conifers, elevation and aspect for oaks which are only available in Appendix C.

We performed two significance tests to determine if there was a significant difference between historic and contemporary tree density: two-sample t-test and negative binomial regression. Conducting a two-sample t-test allowed us to perform Cohen's-D (i.e., effect size) to determine how large of a difference exists between the two means. Effect size is an additional valuable measure that can be used in conjunction with p-values to draw conclusions (Sullivan & Feinn, 2012) a). We also performed a negative binomial regression, which is meant for over dispersed count data, using the calculation from Dolanc et al. (2014) who also compared changes in VTM and FIA data: $\text{Stems} \sim \text{Dataset} + \text{offset}(\log(\text{slope corrected area}))$.

If the two tests resulted in different levels of significance (i.e., significant (p-value < 0.05) or not significant (p-value > 0.05)), then we used the results from the negative binomial regression when the data was over dispersed. Otherwise, we used the results from the two-sample t-test because of the added advantage provided by effect sizes in understanding shifts in tree density. We indicate which test was used to draw conclusions from in the results tables. For additional metrics of variance, see Appendix D.

5.2.2 Results

Our analysis comparing tree density between historic and contemporary YPMC forests show that there has been an overall increase in tree density. Tree density in historic plots averaged 242.7 (± 13.7 SE) trees/ha and 414.6 (± 21.5 SE) trees/ha in contemporary plots (Table 5, Figure 6). Overall, tree density has increased by approximately 70% (p<0.001, effect size: medium).

Table 5. Mean tree density by species, classification, and shade/fire tolerance. Means were calculated across the entire landscape (VTM: n = 195; FIA: n = 210), not by the number of plots the species was found in, however this information was included in the table below to provide an idea of the frequency of the species across the landscape. We used a two-sided t-test for all statistical analysis.

	VTM Mean (±SE)	No. of plots observed in	FIA Mean (±SE)	No. of plots observed in	Percent Change	p-value	Effect Size
Total	242.7 (±13.7)	195	414.6 (±21.5)	210	70.8%	< 0.001	medium
Species							
<i>Abies concolor</i>	46.6 (±6.4)	92	87.8 (±10.6)	110	88.4%	< 0.001	small
<i>Calocedrus decurrens</i>	13.9 (±3.3)	37	19.0 (±4.4)	43	36.7%	0.35	--
<i>Pinus coulteri</i>	10.8 (±2.7)	24	8.6 (±2.0)	25	-20.4%	0.52	--
<i>Pinus lambertiana</i>	23.5 (±3.4)	70	24.2 (±3.5)	77	3.0%	0.88	--
<i>Pseudotsuga macrocarpa</i>	4.7 (±1.5)	13	10.0 (±2.5)	24	112.8%	0.07	--
Yellow pine	94.7 (±9.1)	145	107.4 (±8.7)	169	13.4%	0.10	--
<i>Quercus chrysolepis</i>	21.2 (±6.1)	38	129.3 (±17.6)	102	509.9%	< 0.001	medium
<i>Quercus kelloggii</i>	27.4 (±5.2)	54	28.3 (±5.1)	44	3.3%	0.91	--
Classification							
Conifers	194.1 (±12)	195	257.0 (±14.5)	210	32.4%	< 0.001	small
Oaks	48.7 (±7.8)	78	157.6 (±17.8)	125	223.6%	< 0.001	medium
Shade/Fire Tolerant							
Shade Intolerant/Fire Tolerant	133.6 (±9.1)	189	150.2 (±8.9)	201	12.4%	0.22	--
Shade Tolerant/Fire Intolerant	60.5 (±7.3)	128	106.8 (±11.5)	168	76.5%	< 0.001	medium

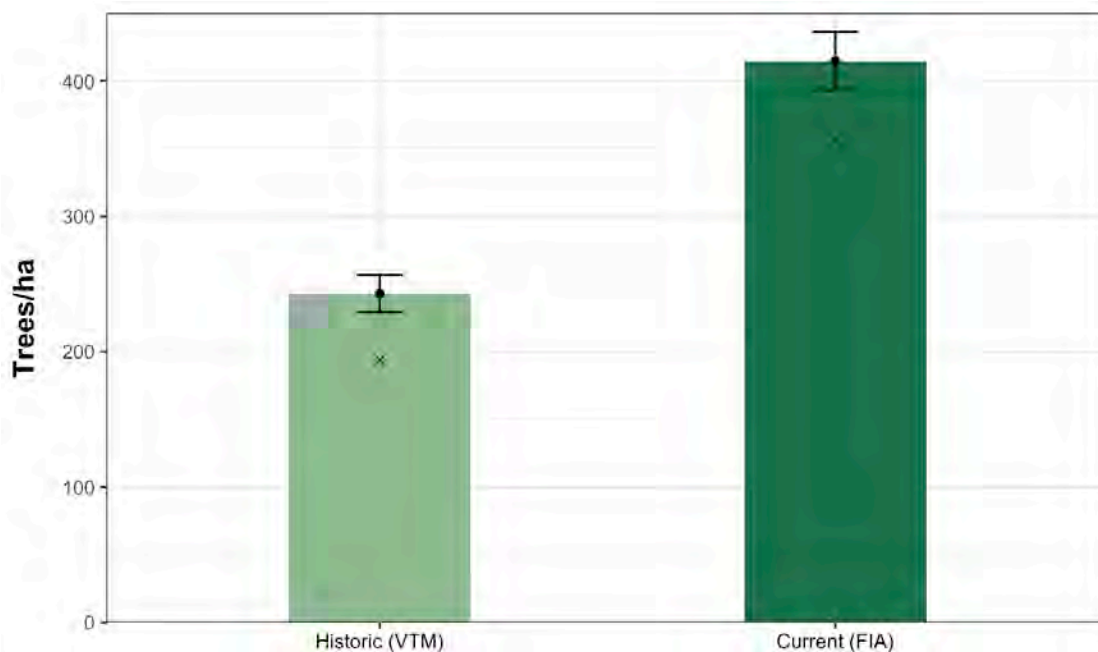


Figure 6. Overall mean tree density in historic (VTM) forests compared to contemporary (FIA) forests. VTM had 195 total plots and FIA had 210 total plots. Xs mark the median, black dots mark the mean, and the bars represent that standard error.

By Species

All conifers, excluding *A. concolor*, either decreased in tree density or did not increase significantly (Table 5, Figures 7). *Pinus coulteri* was the only conifer to experience a decrease in mean density; historic densities averaged 10.2 (± 2.7 SE) trees/ha while contemporary densities averaged 7.9 (± 2.0 SE) trees/ha. Yellow pines increased by 13.4%, though this increase was not statistically significant ($p=0.1$). *Pinus lambertiana*'s average tree density stayed relatively the same (historic mean = 23.5 trees/ha, contemporary mean = 24.2 trees/ha). Of the conifers, *A. concolor* experienced the largest change in density. Historic densities of *A. concolor* averaged 46.6 (± 6.4 SE) trees/ha, but have increased to 87.8 (± 10.6 SE) trees/ha in contemporary forests; a percent change of 88.4% ($p<0.001$). Though *C. decurrens* experienced the second largest percent change (36.7%), the difference between means was not significantly different ($p=0.35$).

Oaks experienced an overall increase of 223.6% (Table 5, Figure 8). *Quercus chrysolepis* increased by 509%, which was the largest percent change/increase in mean density out of all YPMC species (Figure 7). Historic densities of *Q. chrysolepis* averaged 21.2 (± 6.1 SE) trees/ha and contemporary densities averaged 129.3 (± 17.6 SE) trees/ha. The average tree density for *Q. kelloggii* stayed relatively the same between historic and contemporary forests.

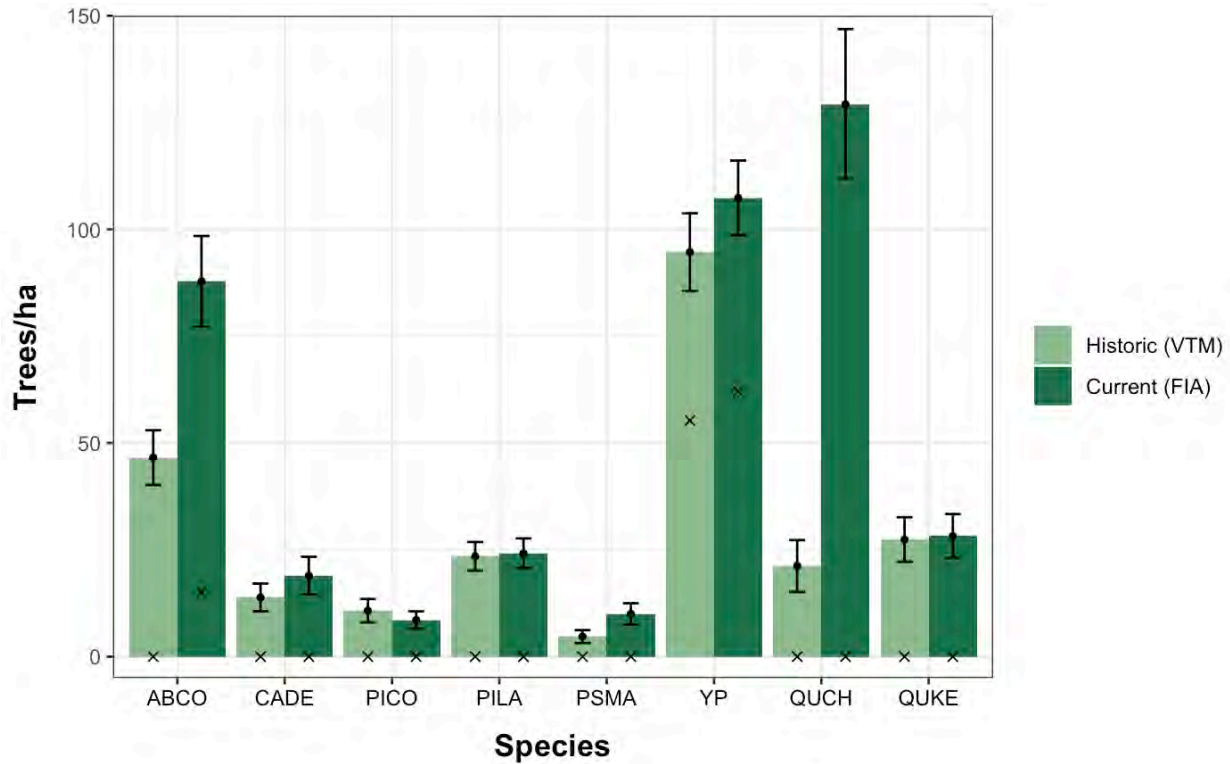


Figure 7. Mean tree density for each YPMC species. Xs mark the median, black dots mark the mean, and the bars represent that standard error.

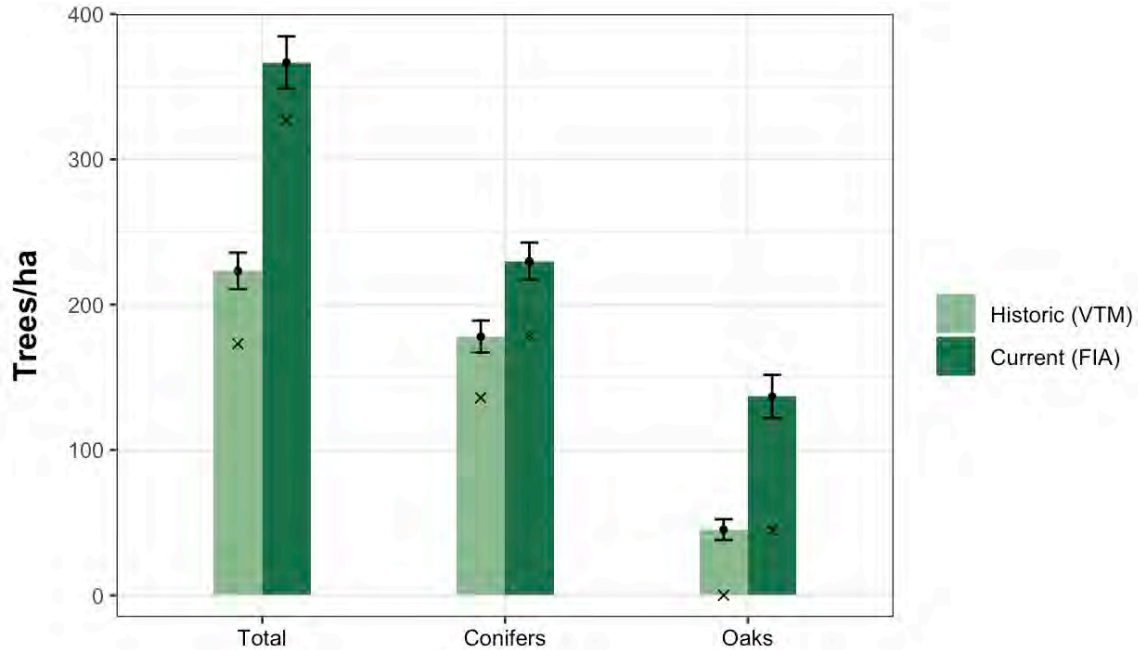


Figure 8. Comparison of mean tree density in functional groups (oaks vs conifers). Xs mark the median, black dots mark the mean, and the bars represent that standard error.

By Shade and Fire Tolerance

Shade tolerant and fire intolerant species include: *A. concolor*, *C. decurrens*, and *Q. chrysolepis*. Two of the YPMC species that experienced the greatest increases in tree density, *A. concolor* and *Q. chrysolepis*, are shade tolerant and fire intolerant (Table 5, Figure 9). Overall, shade tolerant and fire intolerant YPMC species increased by approximately 76% ($p < 0.001$, effect size: medium). On the contrary, shade intolerant and fire tolerant species did not experience a significant increase tree density ($p = 0.22$)

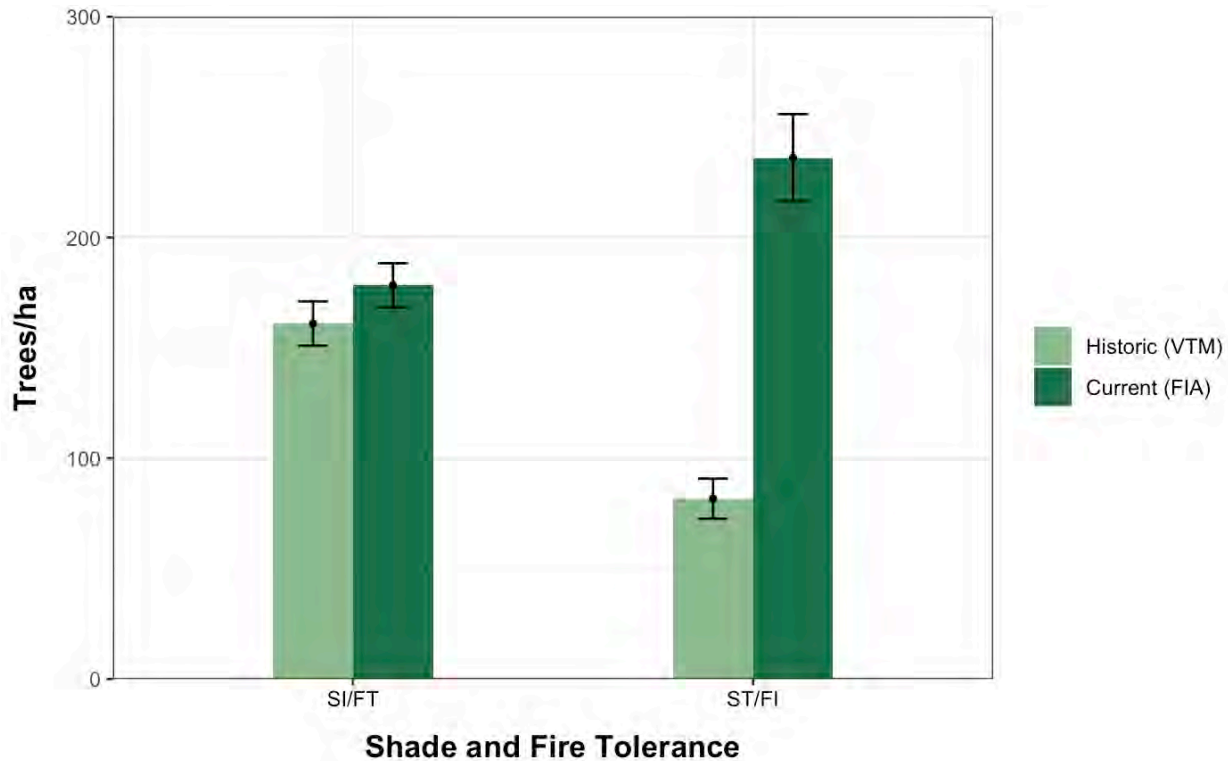


Figure 9. Mean tree density by shade and fire tolerance. Shade intolerant/fire tolerant species include yellow pines (*P. jeffreyi* and *P. ponderosa*), *P. coulteri*, *P. lambertiana*, *P. macrocarpa*, and *Q. kelloggii*. Shade tolerant/fire intolerant species include *A. concolor*, *C. decurrens*, and *Q. chrysolepis*. Black dots mark the mean and the bars represent that standard error.

By Elevation

Tree density increased significantly across all elevation bands except 1000–1499m (Table 5a, Figure 10). Between 1500–1999m, historic density increased from 264.3 (± 19.0 SE) trees/ha to 407.8 (± 28.7 SE) trees/ha; an increase of approximately 54.3% ($p < 0.001$, effect size: medium). Tree density between 2000–2499m experienced the largest increase out of all elevation bands; historic densities averaged 199.7 (± 16.9 SE) trees/ha while contemporary forests averaged 465.4 (± 40.8 SE) trees/ha. Density more than doubled and increased by 133%. At elevations greater than 2500m, historic densities averaged 198.8 (± 40.9 SE) trees/ha and increased by 59% to 316.1 (± 49.4 SE) trees/ha.

Table 5a. Mean tree density by National Forest and elevation. Sample size represents the number of plots found in each National Forest and elevation band. We used a two-sided t-test for all statistical analysis.

	VTM Mean (±SE)	VTM Sample Size	FIA Mean (±SE)	FIA Sample Size	Percent Change	p-value	Effect Size
National Forest							
ANF	222.4 (±17.0)	20	351.4 (±52.7)	26	58.0%	0.027	medium
LPNF	243.4 (±19.8)	54	380.0 (±32.8)	62	56.1%	< 0.001	medium
SBNF	245.1 (±20.9)	113	451.5 (±31.4)	107	84.2%	< 0.001	medium
Elevation (m)							
1000–1499	372.7 (±72.8)	20	381.3 (±68.0)	26	2.3%	0.93	--
1500–1999	264.3 (±19.0)	84	407.8 (±28.7)	80	54.3%	< 0.001	medium
2000–2499	199.7 (±16.9)	77	465.4 (±40.8)	78	133.0%	< 0.001	large
>2500	198.8 (±40.9)	13	316.1 (±49.4)	26	59.0%	0.028	medium

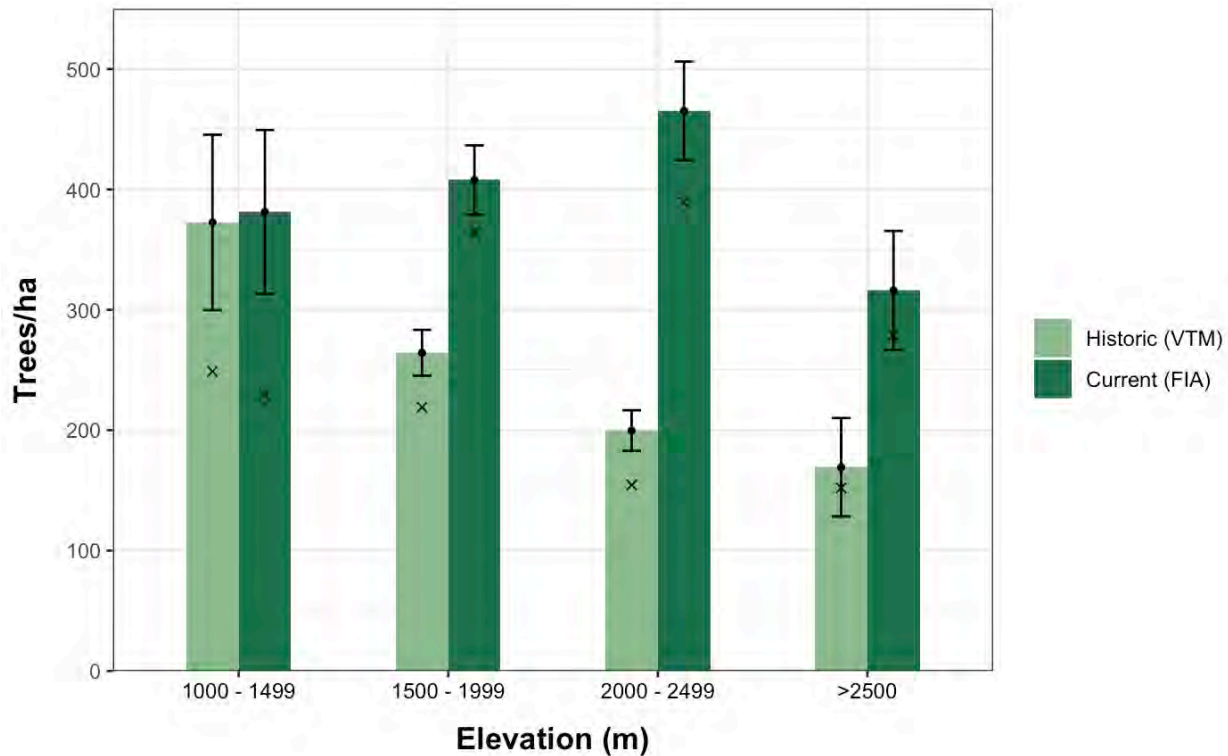


Figure 10. Mean tree density by elevation. Note, VTM data only had 13 plots in the >2500m elevation band while FIA data had 26 plots. Xs mark the median, black dots mark the mean, and the bars represent that standard error.

By National Forest

All southern California National Forests experienced a significant increase in tree density (Table 5a, Figure 11A). SBNF experienced the greatest increases in tree density; historic forests averaged 245.1 (±20.9 SE) trees/ha and contemporary forests averaged 451.5 (±31.4 SE) trees/ha. SBNF increased in tree density by approximately 84.2% (p<0.001, effect size: medium). ANF and LPNF experienced similar increases in tree density; 58% and 56%, respectively. When oaks were excluded from our analysis, average tree density between historic and contemporary forests were less variable (Figure 11B). Out of

the three National Forests, only SBNF experienced an increase in tree density; historic forests averaged 182.2 trees/ha and contemporary forests averaged 294.3 trees/ha.

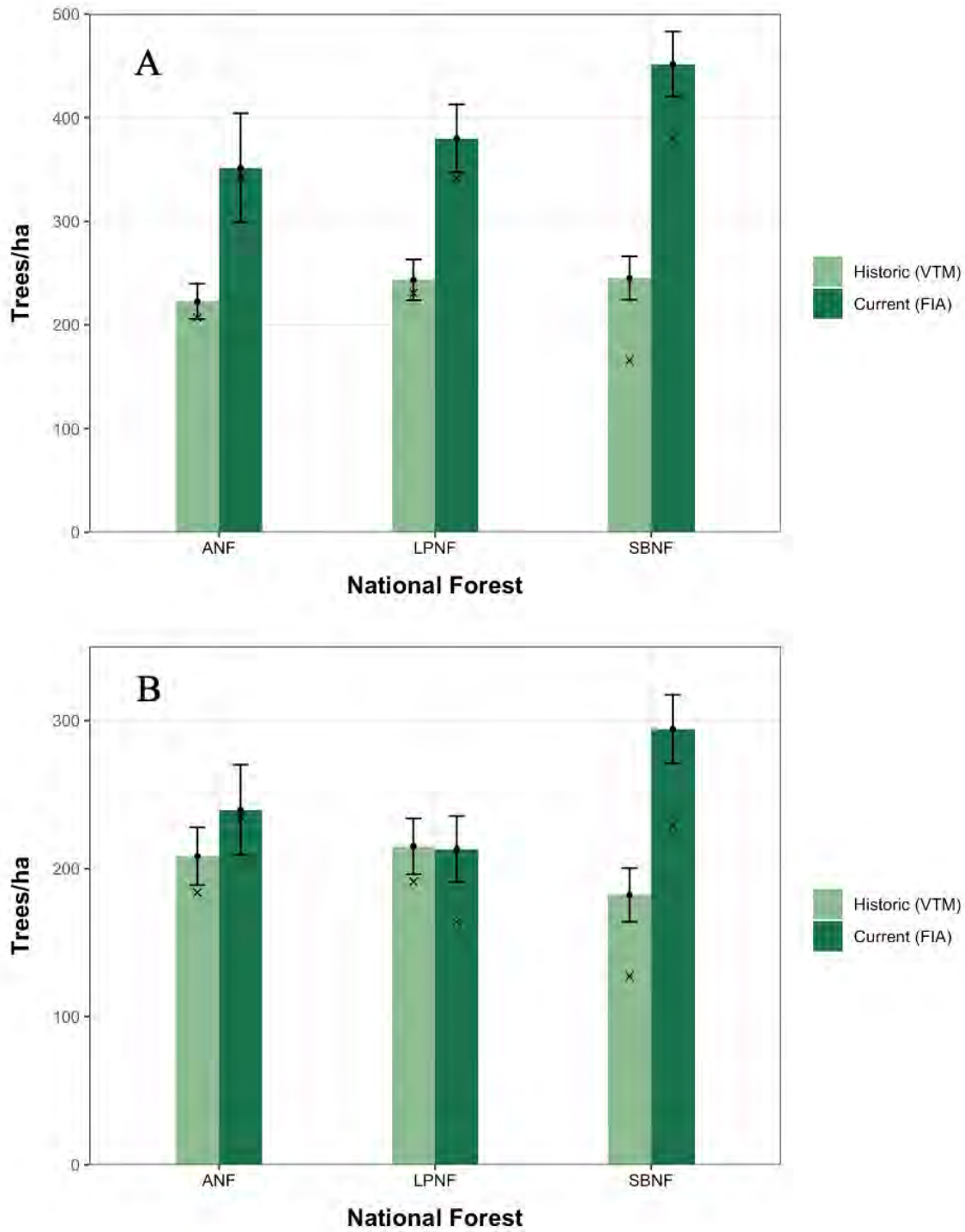


Figure 11. Mean tree density by National Forest including oaks (A) and without oaks (B). Xs mark the median, black dots mark the mean, and the bars represent that standard error.

5.2.3 NRV Analysis

Historic Observations: Southern California and Sierra San Pedro Mártir (SSPM)

Historic surveys in southern California and SSPM have been used to describe pre-suppression conditions of YPMC forests. Numerous historic observations from the early 1900's describe southern California YPMC forests as thin, open, and park-like (Leiberg, 1898; Minnich et al., 2000; Minnich, 1988; Minnich & Vizcaino, 1998; Passini et al., 1989; Rundel et al., 1988; Saunders, 1923; USDA, 1905; Wright & Bailey, 1982) (Figures 12 & 13). Though most reports describe southern California YPMC forests as open and park-like, forests were still spatially heterogeneous. In a collection of field reports from the USFS, observers described a stand on Big Pine Mountain in SBNF as “fairly dense, but with openings” (USDA, 1905).

Several Spanish Expeditions provide observations of SSPM YPMC forests and describe what forest conditions looked like in the mid to late 18th century. The Longinos-Martinez and Arrillaga expeditions, for example, noted dominant stands of *P. jeffreyi* with mixtures of different species (*A. concolor*, *C. decurrens*, and *P. lambertiana*), and wrote about the relative openness of the forest (Minnich and Vizcaino, 1998). Colonel D.K. Allen, a land inspector for the International Colonization Company, performed extensive surveys of SSPM in 1888 (Minnich and Vizcaino, 1998). Allen's records provide insight on historic SSPM tree densities and overall forest composition. Allen noted there were approximately 87 trees/ha in Jeffrey pine dominated forests (62 large and 25 small). Additionally, John Leiberg, a timber surveyor with the U.S. Geological Service (USGS), wrote descriptions of the San Bernardino, the San Gabriel, and San Jacinto Mountains between 1897 and 1899. Leiberg's survey records provide insights into historic YPMC forest densities. At all three mountain ranges, Leiberg noted that forests were usually “open” indicating that stands of trees were widely spaced. We can use these various historic observations of southern California and SSPM YPMC forests as a baseline for historic forest densities and to compare how much today's forests have deviated (Figure 14).

Comparing Contemporary Conditions and Sierra San Pedro Mártir

There have been several studies that have investigated historic and contemporary SSPM forest densities. Minnich et al. (2000) reconstructed fire regimes in SSPM by investigating relationships between fires and changes in forest composition and structure between 1925 and 1991. Minnich et al. analyzed 256 stands in SSPM through aerial photographs of SSPM taken in 1991. Their team also sampled 24 contemporary plots in SSPM in which all trees with a d.b.h. of 3cm or greater were recorded. Analyses for both the aerial analysis and field sampling were separated into three forest types: Jeffrey pine, mixed Jeffrey pine, and mixed white fir. Aerial photographs revealed that tree density was approximately 80 trees/ha across all three forest types (Table 6). Field samples found a slightly higher average of approximately 105 trees/ha across all three forest types. Mixed white fir (*A. concolor*) forests were the densest in both the aerial photographs and ground sampling: 126 trees/ha and 156 trees/ha, respectively. From Minnich et al.'s (2000) field sampling in SSPM, they found that Jeffrey pine forest densities averaged 78 trees/ha and mixed Jeffrey pine forest densities averaged 82 trees/ha.

A more recent study by Stephens and Gill (2005) set out to quantify forest structure of contemporary SSPM YPMC forests that have not been logged and have only experienced a few decades of fire suppression. Stephens and Gill (2005) randomly sampled 49 plots in SSPM mixed Jeffrey pine forests on a 200m grid. They then compared their results to Minnich et al. (1995), who compared changes in density in SBNF between 1930 and 1990. Stephens and Gill recorded trees with a d.b.h. >2.5cm, which is a lower threshold than Minnich et al. (1995) who only recorded trees with a d.b.h. \geq 12cm. Stephens and Gill found that average tree densities in SSPM mixed Jeffrey pine forests were approximately 145.3 trees/ha (\pm 10.4 SE, range 30-320 trees/ha). When Stephens and Gill adjusted their minimum d.b.h. value (>12cm),

average tree density was 108 trees/ha. When using a similar minimum d.b.h., Stephens and Gill's results are similar to average density observed in historic SBNF mixed Jeffrey pine forests (93 trees/ha) (Minnich et al., 1995) and also similar to SSPM estimates by Minnich et al. (2000) (105 trees/ha) (Table 6). The results from these two studies are an example of how historic southern California YPMC tree densities are similar to contemporary SSPM tree density and how SSPM can serve as a reference site for historical conditions in southern California.

Dunbar-Irwin and Safford (2016), also sampled plots in contemporary SSPM forests to determine reference conditions for California YPMC forest restoration. Their study measured all trees with a d.b.h. ≥ 7.6 cm, which is closer to the d.b.h. cut-off used by Minnich et al. (1995). Dunbar-Irwin and Safford found that mean tree density in SSPM was 187.9 trees/ha (± 15.1 SE) (Table 6). They suggested that the higher densities they encountered were the result of the high dispersion of their plots around SSPM National Park and the inclusion of white fir dominated stands in the sample. Stephens and Gill, however, sampled from a much smaller area of relatively homogeneous Jeffrey pine-mixed conifer forest. The average tree density reported by Dunbar-Irwin and Safford is similar to the average tree density found by Minnich et al. (1995) in mixed white fir forests in historic SBNF plots (174 trees/ha).

Comparing Historic and Contemporary Conditions: Southern California

Overall, our results show an increase in tree density between the early 1900s and 2010. Other contemporary studies have also found increases in tree density in southern California (McIntyre et al., 2015; Minnich et al., 1995; Nigro & Molinari, 2019; Stephenson & Calcarone, 1999) (Table 6).

Minnich et al. (1995) directly measured changes in tree density between historic and contemporary YPMC forests by revisiting 68 VTM plots in SBNF approximately 60 years after the VTM surveys were conducted. Similarly to Minnich et al. (2000), Minnich et al.'s (1995) study was subdivided by forest type (Table 6). The 1932 combined average of all VTM plots was approximately 115 trees/ha (Minnich et al., 1995). Overall mean tree densities in 1992 were 79% higher, approximately 207 trees/ha (Minnich et al., 1995). This is due to a 10-fold increase of small and medium *A. concolor* and *C. decurrens* (d.b.h. < 33 cm). Mixed white fir forests had the highest density in 1932 (174 trees/ha), and had the second highest density in 1992 (246 trees/ha); an increase of approximately 41%. Historic densities in the SBNF were lowest in Jeffrey pine forests at 79 trees/ha, which is almost the same density found in contemporary SSPM Jeffrey pine stands (78 trees/ha) (Minnich et al., 2000). Both our historic and contemporary tree density estimates in SBNF are higher than those calculated by Minnich et al. (1995); 245.1 trees/ha and 451.5 trees/ha, respectively. This could be due to the fact that Minnich et al. (1995) did not include oak species in their analysis. However, when we excluded oaks in our analysis of SBNF tree density, historic densities were 182.2 trees/ha and contemporary densities were 294.3 trees/ha; an approximate increase of 63% (Appendix D). It is likely that our estimated densities would be lower if we separated our analysis by forest type like Minnich et al. did. However, similar to Minnich et al. (1995), our analysis did find significant increases in shade tolerant *A. concolor* (88%). *Abies concolor* is likely experiencing such large increases in density because canopy cover has also increased since the early 1900s (see Section 5.5). In mixed white fir forests surveyed by Wieslander in the early 1900s ($n=16$), species were mostly evenly distributed; *A. concolor* was present in this forest type but not as an overwhelmingly dominant species. Similar to what our analysis has revealed, Minnich et al. (1995) now considers white fir as the dominant species in this forest type.

McIntyre et al. (2015) analyzed the changes in tree density across all of California by comparing the VTM dataset from the 1930s with contemporary FIA data from 2001-2010. In the Transverse Ranges, McIntyre documented an increase in tree density of approximately 79%, which is similar to our finding of a 70% increase in overall tree density. Additionally, McIntyre et al. investigated changes in density of *Pinus* and *Quercus* species and noted that forests are exhibiting an increased dominance of oaks over

pinus. This can also be seen in our analysis where we found that average *Quercus* densities increased by 223.6% due to a 509.9% increase in *Q. chrysolepis* (Table 5). *Pinus* species (*P. ponderosa*, *P. jeffreyi*, *P. lambertiana*, *P. macrocarpa*, and *P. coulteri*), however, either decreased or showed no statistically significant increase in our analysis. These trends demonstrate that YPMC forests in California support higher densities of oaks today than at the beginning of the 20th century, and also support the general idea that California forests are likely to become more oak dominated as climates continue to warm (Lenihan et al., 2008; Safford et al., 2012; McIntyre et al., 2015; Stocker et al., 2013).

Nigro and Molinari (2019) compared historic and contemporary tree densities in Los Padres NF at Frazier Mountain by resurveying 4 VTM plots with contemporary plots. Nigro and Molinari found historic densities averaged 160.6 trees/ha, and contemporary densities (n=41) averaged 393 trees/ha; a percent change of approximately 144%. Though Nigro and Molinari's historic tree density average for LPNF was less than our calculated average (243.4 trees/ha; n=62), we found similar contemporary densities (380.9 trees/ha; n=62). The difference in our historic estimates is likely due to Nigro and Molinari's small sample size, which may have also resulted in their percent change to be about three times bigger than ours (56.1%) (Figure 15). Nigro and Molinari's findings were also due to an increase in conifer species while our analysis revealed that *Q. chrysolepis* was the primary driver for increases in tree density. Additionally, Nigro and Molinari (2019) looked at one location in LPNF while our analysis encompassed all of LPNF. It is possible that there is sub-regional heterogeneity within LPNF and the VTM plots on Frazier Mountain captured a denser area of the forest, and that the density increases are being driven by different species in different areas of the forest. Furthermore, some historic sources reported logging on Frazier Mountain in the late 1800s to early 1900s, before VTM surveys occurred (Blakley & Barnette, 1985). It is possible that the VTM surveyors had plots in or around these logged areas, which could account for the low average tree density captured in Nigro and Molinari's study.

Stephenson and Calcerone (1999) compared historic and contemporary mixed conifer forest conditions throughout LPNF, ANF, and the San Diego County mountains. Similar to Minnich et al. (1995), Stephenson and Calcerone used VTM data (n=32) and resurveyed those plots to estimate changes in density. Stephenson and Calcerone's historic densities were approximately 150 trees/ha and contemporary densities averaged 350 trees/ha (Table 6). Though Stephenson and Calcerone also had a relatively small sample size, their contemporary averages are similar to our findings; we found that contemporary tree densities in ANF (n=26) and LPNF (n=62) were between 351 to 380 trees/ha (Table 5a). However, their historic average tree densities were lower than our historic average densities for ANF (222.4 trees/ha) and LPNF (243.4 trees/ha).

Summary

The observed compositional shifts in YPMC forests is being driven by an increase in density of shade tolerant and fire intolerant species. *Abies concolor* and *Q. chrysolepis* experienced a significant increase in density (88.4% and 509.9%, respectively). *Calocedrus decurrens*, also a shade tolerant and fire intolerant species, was the only one to not have a significant change in density despite its rather high percent change (+36.7%). This non-significant change could be due to us filtering out all trees with a d.b.h. <10.2cm (see Section 4.3) (Figure 16). It is likely that if all trees were included in our analysis, that *C. decurrens* would have experienced a significant change in density.

Shade intolerant and fire tolerant species have not experienced the same increase in density. The absence of fire in most of these forests for the last century (Nigro & Molinari, 2019) has allowed these species to flourish in the understory. Additionally, recruitment of shade tolerant species is likely enhanced by increasing canopy cover (Section 5.5) that leads to more forest floor shading, providing optimal habitat. Stephenson and Calcerone (1999) also cited that past timber harvesting events could be responsible for the increased dominance of *A. concolor* due to the logging of large yellow pines.



A. FOREST GROWTH OF SECOND CLASS, COMPOSED OF YELLOW PINE, SAN JACINTO RESERVE.

Figure 12. Historic YPMC forest structure and density in the San Jacinto Reserve (now known as San Bernardino National Forest). Photo taken by John Leiberg in 1897-1899.



B COMMERCIALY VALUABLE TIMBER OF FIRST CLASS, SAN BERNARDINO RESERVE.

Figure 13. Historic YPMC forest structure and density in the San Bernardino Reserve (now known as San Bernardino National Forest). Photo taken by John Leiberg in 1897-1899.



Figure 14. Contemporary image of YPMC forest in SSPM. Top photo source: [MSJ Images](#). Bottom two photos source: [Scott Stephens](#).

Table 6. Average tree densities for YPMC forests across southern California and reference sites in Baja, Mexico. MPP = Mixed Ponderosa Pine, MJP = Mixed Jeffrey Pine, MWF = Mixed White Fir, JP = Jeffrey Pine, MC = Mixed Conifer, and YPMC = Yellow Pine Mixed Conifer.

Study Area	Time Period	n	Forest Type	Minimum d.b.h. Recorded (cm)	Average Density (trees/ha)	Study
San Bernardino Mountains	1920-1930	--	MPP	12	144	Minnich et al. (1995)
		--	MJP	12	93	
		--	MWF	12	174	
		--	JP	12	79	
Mount Pinos, San Gabriels, & San Diego Mountains	1920-1930	32	MC	10	~150	Stephenson and Calcarone (1999)
Los Padres National Forest	1920-1930	4	Conifer Forest	10.2	160.6	Nigro and Molinari (2019)
Transverse & Peninsular Ranges	1920-1930	--	All Forests	10.2	266.1	McIntyre et al. (2015)
Transverse & Peninsular Ranges	1920-1930	195	YPMC	10.2	242.7 (± 13.7)	GotF Bren Analysis (2021)
Baja/SSPM	1991	256				Minnich et al. (2000) Aerial photographs
			JP	--	51	
			MJP	--	63	
			MWF	--	126	
Baja/SSPM	1990s	24				Minnich et al. (2000) Field sampling
			JP	3	78	
			MJP	3	82	
			MWF	3	156	
Baja/SSPM	2000s	49	MJP	2.5	145.3 (± 10.4)	Stephens and Gill (2005)
		49	MJP	12	108	
Baja/SSPM	2012-2013	86	YPMC	7.6	187.9 (± 15.1)	Dunbar-Irwin and Safford (2016)
San Bernardino Mountains	1990s	5	MPP	12	250	Minnich et al. (1995)
		11	MJP	12	167	
		16	MWF	12	246	
		9	JP	12	169.1	
Mount Pinos, San Gabriels, & San Diego Mountains	1990s	32	MC	10	~350	Stephenson and Calcarone (1999)
Transverse & Peninsular Ranges	2000s	--	All Forests	10.2	364.8	McIntyre et al. (2015)
Los Padres National Forest	2016	41	Conifer Forest	10	393	Nigro and Molinari (2019)
Transverse & Peninsular Ranges	2001-2010	210	YPMC	10.2	414.6 (± 21.5)	GotF Bren Analysis (2021)



Figure 15. Current photo of YPMC forest at Mt. Pinos, Los Padres National Forest. Photo courtesy of Nicole Molinari, USFS.



Figure 16. Current photo of YPMC forest at Cleveland National Forest showing the recruitment of small-diameter *C. decurrens* in the forest understory. These small-diameter trees were likely missed in our analysis because we removed trees from our analysis that were less than 10.2cm in diameter. Photo courtesy of Anne-Marie Parkinson.

5.3 Tree Size Class and Size Class Distribution

5.3.1 Methods

We calculated tree density across the landscape (see Section 5.2.1) by size class. Size classes are defined by the diameter of the tree measured at breast height (i.e., diameter at breast height (d.b.h.)). The VTM surveyors did not record the actual d.b.h. of each tree. Instead, they recorded d.b.h. into four size classes: 4–12in, 12–24in, 24–36in, and greater than 36in. In contrast, the true d.b.h. of trees is recorded in the combined FIA data. We used the following size classes from Dolanc et al. (2014), to group the combined FIA data into size classes and standardize the size class bins between the two datasets:

- o 10.2–30.4 cm (4–12 in) (also referred to as juveniles)
- o 30.5–60.9 cm (12–24 in)
- o 61.0–91.3 cm (24–36 in)
- o >91.4 cm (>36 in)

We investigated drivers of change in tree density for each size class by analyzing tree density by species, National Forest (including and excluding oaks), shade and fire tolerant species (including and excluding oaks), elevation, elevation of oaks, elevation of conifers, and functional group (conifer vs. oak). We did not analyze change by elevation and aspect as sample sizes were too small.

We performed three significance tests to determine if there was a significant difference between historic and contemporary tree density: two-sample t-test, bootstrapped t-test, and negative binomial regression. A bootstrapped t-test was used in place of the two-sample t-test if the assumption of normality could not be met using the central limit theorem. We used Cohen's-D (i.e., effect size) in conjunction with two-sample t-tests and bootstrapped t-test to determine how large of a difference exists between the two means. Effect size is an additional valuable measure that can be used in conjunction with p-values to draw conclusions (Sullivan & Feinn, 2012). We also performed a negative binomial regression, which is meant for over dispersed count data, using the calculation from Dolanc et al. (2014) who also compared changes in VTM and FIA data: $\text{Stems} \sim \text{Dataset} + \text{offset}(\log(\text{slope corrected area}))$.

If the p-values from the two-sample t-tests or bootstrapped t-tests resulted in different levels of significance (i.e., significant or not significant) compared to the negative binomial regression, then we used the results from the negative binomial regression when the data was over dispersed. Otherwise, we used the results from the two-sample t-test or bootstrapped t-test because of the added advantage provided by effect sizes in understanding shifts in tree density. We indicate which test was used to draw conclusions from in the results tables. For additional metrics of variance, see Appendix E.

5.3.2 Results

Tree density in all size classes has increased in southern California YPMC forests since the early 1930s (Figure 17). However, not all observed changes were significant (Table 7). Overall, changes in mean density were greatest in juveniles (10.2-30.4cm d.b.h. class), which were driven by oaks, and 61-91.3cm diameter trees, which were primarily driven by conifers. Historic density of juveniles averaged 110.4 (± 11.1 SE), which significantly increased by 82.8% ($p < 0.001$), although the effect size was small, to 201.9 (± 17.1 SE) by 2010. Likewise, density of 61-91.3cm trees more than almost tripled ($p < 0.001$, effect size: large) from 42.9 (± 3.1 SE) to 103.6 (± 6.2 SE) trees/ha in 80 years. 30.5-60.9cm trees had a modest 24% increase, which was significant ($p = 0.02$) although it had a small effect size. Density of trees over 91.4cm increased by 17.3%, but did not increase significantly ($p = 0.18$).

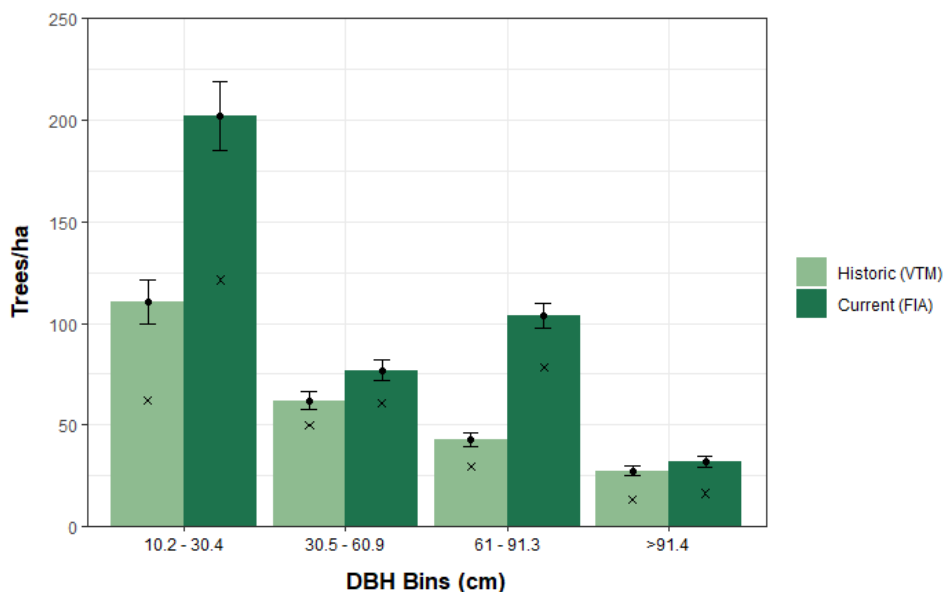


Figure 17. Comparison of the average tree density by size class across all southern California plots using VTM and FIA data. Xs mark the median, black dots mark the mean, and the bars represent that standard error.

Table 7. Mean tree density by size class by species, functional group, and shade/fire tolerance. Means were calculated across the entire landscape, not by the number of plots the species was found in. We used a two-sided t-test for all statistical analysis.

	Tree Size Class (cm)	VTM Mean (\pm SE)	No. of plots observed in	FIA Mean (\pm SE)	No. of plots observed in	Percent Change	p-value	Effect Size
Total	10.2 – 30.4	110.4 (\pm 11.1)	175	201.9 (\pm 17.1)	187	82.8%	< 0.001	small
	30.5 – 60.9	62.1 (\pm 4.4)	165	76.9 (\pm 4.9)	183	24.0%	0.02	small
	61.0 – 91.3	42.9 (\pm 3.1)	148	103.6 (\pm 6.2)	198	141.8%	< 0.001	large
	>91.4	27.4 (\pm 2.3)	118	32.1 (\pm 2.7)	134	17.3%	0.18	--
Functional Group								
Conifers	10.2 – 30.4	73.9 (\pm 8.8)	159	68.2 (\pm 5.9)	159	-7.8%	0.59	--
	30.5 – 60.9	54.3 (\pm 4.1)	159	59.5 (\pm 4.1)	170	9.7%	0.37	--
	61.0 – 91.3	39.9 (\pm 3.1)	141	97.8 (\pm 6.0)	198	144.8%	< 0.001	large
	>91.4	25.9 (\pm 2.3)	113	31.5 (\pm 2.7)	131	21.4%	0.11	--
Oaks	10.2 – 30.4	36.5 (\pm 7.0)	64	133.7 (\pm 16.8)	116	266.3%	0.03	medium
	30.5 – 60.9	7.8 (\pm 1.6)	42	17.4 (\pm 2.6)	71	123.2%	0.0002	small
	61.0 – 91.3	2.9 (\pm 0.7)	23	5.9 (\pm 1.2)	32	103.4%	< 0.001	small
Shade/Fire Tolerant								
Shade Intolerant/Fire Tolerant	10.2 – 30.4	64.5 (\pm 7.4)	106	54.7 (\pm 5.6)	150	-15.3%	0.29	--
	30.5 – 60.9	43.5 (\pm 3.7)	89	39.6 (\pm 2.9)	115	-9.0%	0.40	--
	61.0 – 91.3	31.6 (\pm 2.7)	61	64.4 (\pm 4.4)	110	103.7%	< 0.001	medium
	>91.4	21.4 (\pm 2.0)	43	19.8 (\pm 1.9)	71	-7.5%	0.55	--
Shade Tolerant/Fire Intolerant	10.2 – 30.4	45.9 (\pm 7.1)	145	147.2 (\pm 16.6)	140	220.9%	< 0.001	medium
	30.5 – 60.9	18.6 (\pm 2.2)	144	37.3 (\pm 3.8)	158	101.2%	< 0.001	small
	61.0 – 91.3	11.2 (\pm 1.6)	136	39.2 (\pm 4.2)	181	249.0%	< 0.001	medium
	>91.4	6.0 (\pm 1.0)	109	12.4 (\pm 1.8)	104	106.7%	0.002	small

By Species

Density of large diameter (61-91.3cm) conifers increased significantly across all conifer species (Figure 18, Table 8) with an overall increase of 144.8%. *Calocedrus decurrens* experienced the largest increase (313.1%) in density of large diameter (61-91.3cm) conifers; historic density averaged 1.7 (± 0.6 SE) trees/ha and contemporary density averaged 6.9 (± 1.6 SE) trees/ha. *Abies concolor* and yellow pines had the second and third largest increases in 61-91.3cm diameter trees; 233.9% and 120.1% respectively. While all conifers increased in density of 61-91.3cm diameter trees, all conifers but *A. concolor* decreased in density of juveniles by 19.7% to 46%. Although, none of these declines were significant (p-value range: 0.055 to 0.39) (Figure 18, Table 8); there were not enough PSMA juveniles to draw robust conclusions. This resulted in an overall 7.8% decline in density of juvenile conifers.

Oak density more than doubled in all size classes, excluding the greater than 91.4cm class as there was not enough data to draw robust conclusions (Figure 19). *Quercus chrysolepis* was the oak species responsible for this large increase; juveniles increased by 575.2% and the 30.5-60.9cm diameter trees increased by 249.9%. Historic density of *Q. chrysolepis* juveniles and 30.5-60.9cm diameter trees increased from 16.8 (± 5.6 SE) trees/ha to 113.5 (± 16.5 SE) trees/ha and 3.4 (± 1.2 SE) to 11.9 (± 2.3 SE). Comparatively, density of *Q. kelloggii* juveniles was relatively constant over time (historic: 19.7 (± 4.5 SE) trees/ha, contemporary: 20.1 (± 4.3 SE) trees/ha).

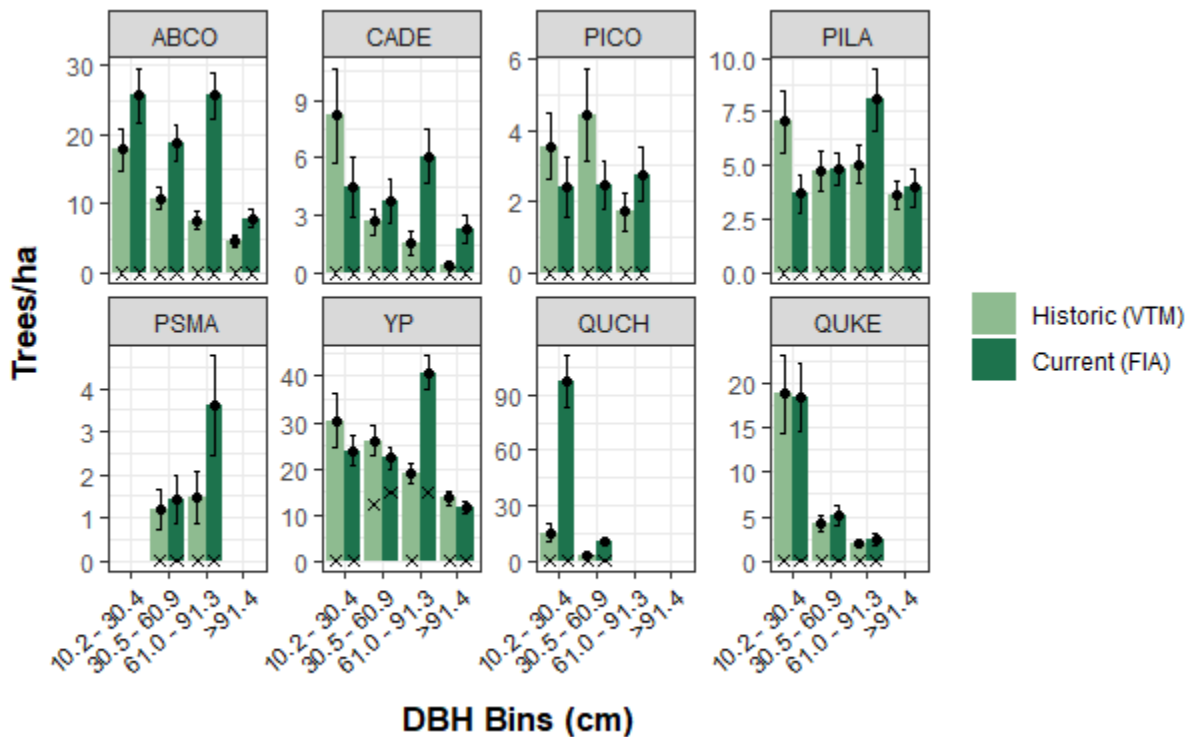


Figure 18. Comparison of the average tree density of each YPMC species by size class across all southern California plots using VTM and FIA data. Groupings were removed from analysis when the number of plots observed in was less than 10. Xs mark the median, black dots mark the mean, and the bars represent that standard error.

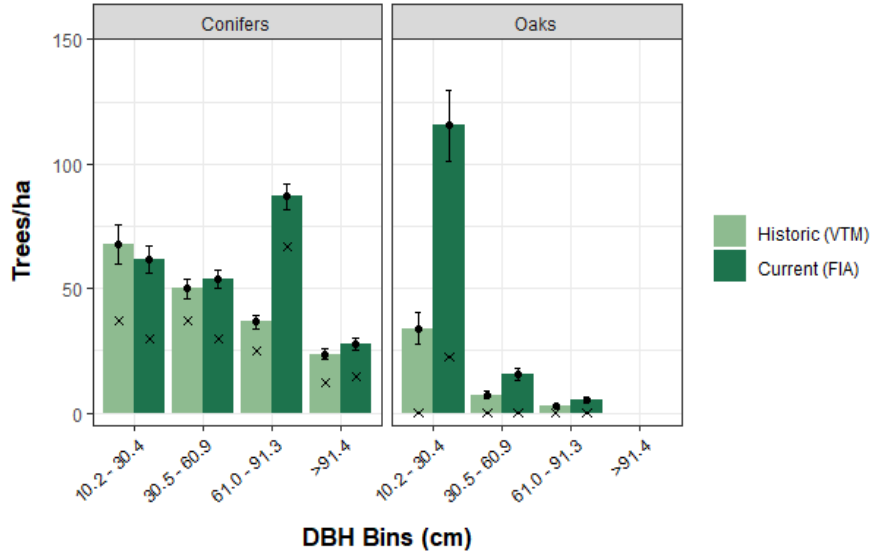


Figure 19. Comparison of the average tree density of conifers and oaks by size class across all southern California plots using VTM and FIA data. Oaks with d.b.h. >91.4cm did not have a large enough sample size to make statistical comparisons (VTM: n=21, FIA: n=8). Xs mark the median, black dots mark the mean, and the bars represent that standard error.

Table 8. Mean tree density of each YPMC species by size class. Means were calculated across the entire landscape, not by the number of plots the species was found in. Significance values from two-sample t-tests are reported below unless otherwise noted. Some size classes do not have significance values as the same size was too small to make robust comparisons.

Species	Tree Size Class (cm)	VTM Mean (± SE)	No. of plots observed in	FIA Mean (± SE)	No. of plots observed in	Percent Change	p-value	Effect Size
<i>Abies concolor</i> ^b	10.2 – 30.4	20.2 (± 3.4)	67	28.7 (± 4.4)	74	42.3%	0.13	--
	30.5 – 60.9	12.3 (± 1.8)	63	21.2 (± 3.0)	72	71.9%	0.012	small
	61.0 – 91.3	8.7 (± 1.4)	49	29.0 (± 3.7)	88	233.9%	< 0.001	small
	>91.4	5.4 (± 1.0)	38	8.9 (± 1.4)	56	65.7%	0.04	small
<i>Calocedrus decurrens</i> ^b	10.2 – 30.4	8.9 (± 2.7)	27	5.0 (± 1.7)	18	-43.9%	0.22	--
	30.5 – 60.9	2.8 (± 0.7)	22	4.2 (± 1.3)	22	49.6%	0.34	--
	61.0 – 91.3	1.7 (± 0.6)	14	6.9 (± 1.6)	32	313.1%	0.002	small
<i>Pinus coulteri</i> ^b	10.2 – 30.4	3.8 (± 1.0)	18	2.6 (± 0.9)	14	-30.6%	0.39	--
	30.5 – 60.9	4.7 (± 1.4)	19	2.7 (± 0.7)	17	-42.8%	0.20	--
	61.0 – 91.3	1.8 (± 0.6)	13	3.1 (± 0.8)	15	69.6%	0.21	--
<i>Pinus lambertiana</i> ^b	10.2 – 30.4	8.0 (± 1.6)	40	4.3 (± 1.1)	27	-46.0%	0.38	--
	30.5 – 60.9	5.58 (± 1.2)	34	5.60 (± 0.9)	47	0.3%	0.64	--
	61.0 – 91.3	5.8 (± 1.1)	41	9.6 (± 1.8)	48	65.6%	0.08	--
	>91.4	4.1 (± 0.8)	37	4.6 (± 1.0)	26	13.6%	0.07	--
Yellow Pine	10.2 – 30.4	32.2 (± 6.1)	90	25.9 (± 3.4)	92	-19.7%	0.37	--
	30.5 – 60.9	27.6 (± 3.3)	99	24.1 (± 2.5)	111	-12.4%	0.40	--
	61.0 – 91.3	20.3 (± 2.3)	94	44.8 (± 4.0)	144	120.1%	< 0.001	medium
	>91.4	14.6 (± 1.7)	84	12.6 (± 1.5)	77	-13.5%	0.38	--
<i>Quercus chrysolepis</i> ^b	10.2 – 30.4	16.8 (± 5.6)	33	113.5 (± 16.5)	95	575.2%	< 0.001	medium
	30.5 – 60.9	3.4 (± 1.2)	17	11.9 (± 2.3)	46	249.9%	0.001	small
<i>Quercus kelloggii</i> ^b	10.2 – 30.4	19.7 (± 4.5)	42	20.1 (± 4.3)	39	2.5%	0.94	--
	30.5 – 60.9	4.4 (± 0.9)	30	5.5 (± 1.2)	32	24.8%	0.49	--
	61.0 – 91.3	2.1 (± 0.5)	18	2.6 (± 0.8)	15	25.6%	0.58	--

^b P-value is obtained through boot strapped t-test.

By Elevation

Density of YPMC juveniles increased across all elevations except at the lowest elevation (1000–1499m), in which density decreased by 1.8% (Figure 20, Table 9). Density significantly increased 61.8% from 1500–1999m ($p=0.007$, effect size: small) and 2000–2499m ($p<0.001$, effect size: medium). Juvenile density increased 82.9% above 2500m from 62.7 (± 19.6 SE) to 114.6 (± 33.6 SE), but this was not significant ($p=0.19$). Density for 30.5–60.9cm and over 91.4cm trees decreased from 10001–499m. Large diameter trees increased across all elevation bands; increases were significant in all but the lowest elevation band.

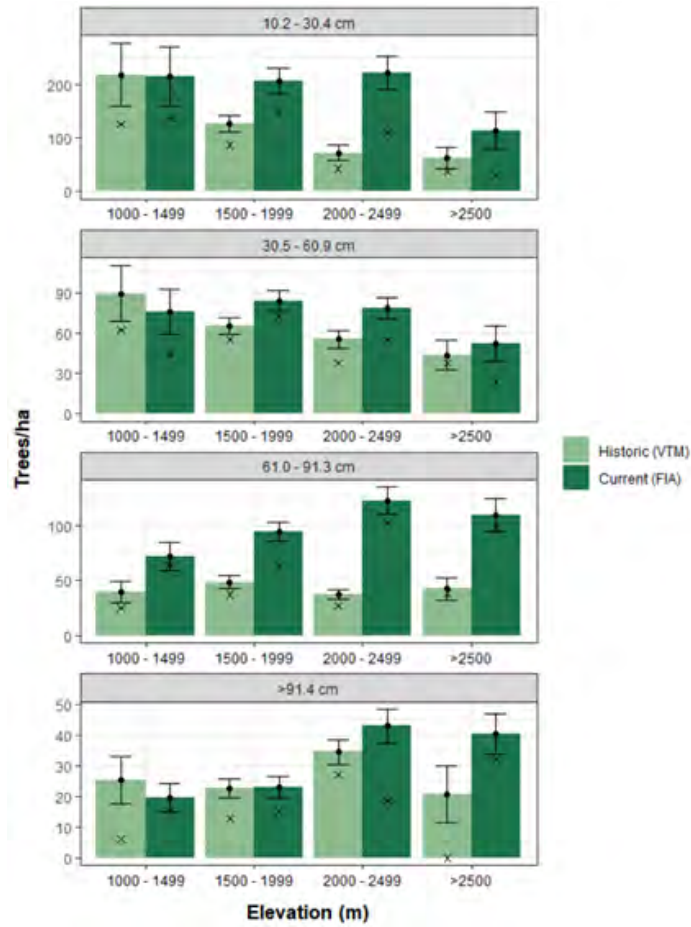


Figure 20. Mean tree density by size class and elevation. Xs mark the median, black dots mark the mean, and the bars represent that standard error.

Table 9. Mean tree density by size class by elevation. Means were calculated across the entire landscape, not by the number of plots the species was found in. Significance values from two-sample t-tests are reported below unless otherwise noted.

Elevation (m)	Tree Size Class (cm)	VTM Mean (\pm SE)	No. of plots observed in	FIA Mean (\pm SE)	No. of plots observed in	Percent Change	p-value	Effect Size
1000 – 1499	10.2 – 30.4	218.4 (\pm 59.0)	19	214.4 (\pm 55.2)	22	-1.8%	0.96	--
	30.5 – 60.9	89.3 (\pm 21.0)	18	75.8 (\pm 16.9)	23	-15.1%	0.62	--
	61.0 – 91.3 ^a	39.7 (\pm 9.8)	15	71.5 (\pm 12.7)	24	80.3%	0.29	--
	>91.4	25.4 (\pm 7.8)	10	19.6 (\pm 4.6)	15	-22.8%	0.53	--
1500 – 1999	10.2 – 30.4	127.8 (\pm 15.4)	82	206.8 (\pm 24.5)	73	61.8%	0.007	small
	30.5 – 60.9	65.0 (\pm 6.2)	71	83.8 (\pm 7.4)	71	28.9%	0.055	--
	61.0 – 91.3	48.7 (\pm 5.4)	63	94.0 (\pm 8.9)	75	92.9%	< 0.001	medium
	>91.4	22.7 (\pm 3.1)	49	23.2 (\pm 3.5)	43	1.9%	0.93	--
2000 – 2499	10.2 – 30.4	72.3 (\pm 14.2)	58	221.8 (\pm 31.9)	74	207.0%	< 0.001	medium
	30.5 – 60.9	55.2 (\pm 6.6)	65	78.4 (\pm 7.8)	72	42.0%	0.03	small
	61.0 – 91.3	37.7 (\pm 4.3)	59	122.3 (\pm 11.9)	73	224.2%	< 0.001	large
	>91.4	34.5 (\pm 4.0)	53	42.8 (\pm 5.4)	55	24.1%	0.22	--
> 2500	10.2 – 30.4 ^a	62.7 (\pm 19.6)	11	114.6 (\pm 33.6)	18	82.9%	0.19	--
	30.5 – 60.9	43.5 (\pm 11.1)	10	52.3 (\pm 13.1)	17	20.3%	0.61	--
	61.0 – 91.3	42.4 (\pm 10.3)	10	109.0 (\pm 14.8)	26	157.0%	< 0.001	large
	>91.4	20.7 (\pm 9.1)	6	40.2 (\pm 6.5)	21	94.1%	0.096	--

^a P-value is obtained through negative binomial regression.

By Elevation and Functional Group (Oaks vs Conifers)

Many of these changes in density across elevations are further explained by analyzing changes by functional group. Oaks increased across all elevations up to 2500m (Figure 21A, Table 10). Some of the largest increases were observed in juveniles across all elevations (1000–1499m: +135.4%, $p=0.002$; 1500–1999m: 164.4%, $p<0.001$; 2000–2499m: +66%, $p<0.001$). On the other hand, density of conifer juveniles has significantly declined from 1000–1499m (historic: 155.5 (\pm 60.1 SE), contemporary: 53 (\pm 15.3 SE), $p=0.002$) and 1500–1999m (78.9 (\pm 12.3 SE), contemporary: 48.3 (\pm 6.4 SE), $p=0.03$). Comparatively, mean conifer density has increased in all size classes above 2000m (Figure 21B, Table 10), however median density of conifer juveniles at elevations over 2500m has decreased. Density of large diameter trees (61-91.3cm) has significantly increased across all elevations; increased density ranged from 67% to 223.1%. The largest increase in density occurred from 2000–2499m where density increased from a historic average density of 37.4 (\pm 4.3 SE) to a contemporary average density of 120.7 (\pm 11.6 SE).

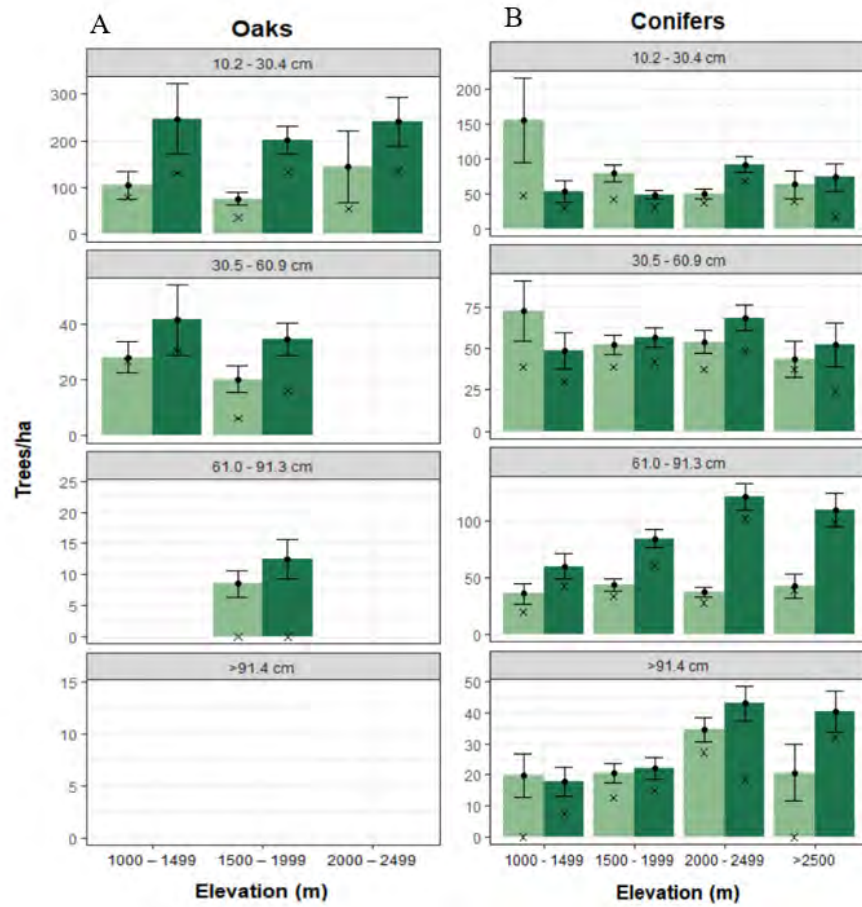


Figure 21. Mean tree density by size class, functional group ((A) oaks and (B) conifers), and elevation. There was not sufficient sample size ($n < 10$) on certain groupings of oaks (e.g., oaks with >91.4 cm diameter or oaks above 2500 m in elevation), so they were excluded from the graph. Xs mark the median, black dots mark the mean, and the bars represent that standard error.

Table 10. Mean tree density by size class, elevation, and functional group. Means were calculated across the entire landscape, not by the number of plots the species was found in. Significance values from two-sample t-tests are reported below unless otherwise noted. Some size groupings do not have significance values as the same size was too small ($n < 10$) to make robust comparisons, so they were excluded from the table.

	Elevation (m)	Tree Size Class (cm)	VTM Mean (\pm SE)	No. of plots observed in	FIA Mean (\pm SE)	No. of plots observed in	Percent Change	p-value	Effect Size
Oaks	1000 – 1499	10.2 – 30.4 ^a	104.8 (\pm 29.0)	10	246.8 (\pm 75.9)	15	135.4%	0.002	--
		30.5 – 60.9	28.1 (\pm 5.7)	11	41.5 (\pm 12.6)	13	47.6%	0.34	--
	1500 – 1999	10.2 – 30.4	76.1 (\pm 13.7)	43	201.3 (\pm 29.3)	58	164.4%	< 0.001	medium
		30.5 – 60.9	20.1 (\pm 4.8)	27	34.5 (\pm 5.8)	41	71.6%	0.06	--
		61.0 – 91.3 ^a	8.5 (\pm 2.1)	18	12.5 (\pm 3.2)	19	46.6%	< 0.001	--
	2000 – 2499	10.2 – 30.4 ^a	145.2 (\pm 77.3)	11	241.1 (\pm 51.3)	40	66.0%	< 0.001	--
Conifers	1000 - 1499	10.2 – 30.4 ^a	155.5 (\pm 60.1)	17	53.0 (\pm 15.3)	16	-65.9%	0.11	--
		30.5 – 60.9	72.4 (\pm 18.2)	18	48.7 (\pm 11.0)	20	-32.8%	0.27	--
		61.0 – 91.3 ^a	35.6 (\pm 9.4)	13	59.5 (\pm 11.2)	24	67.0%	0.11	--
		>91.4	19.8 (\pm 7.0)	9	17.8 (\pm 4.7)	13	-10.2%	0.81	--
	1500 - 1999	10.2 – 30.4	78.9 (\pm 12.3)	73	48.3 (\pm 6.4)	60	-38.8%	0.03	--
		30.5 – 60.9	52.1 (\pm 5.8)	66	56.7 (\pm 5.7)	63	8.8%	0.57	--
		61.0 – 91.3	43.3 (\pm 5.3)	58	84.2 (\pm 8.2)	75	94.6%	< 0.001	medium
		>91.4	20.7 (\pm 3.0)	45	22.1 (\pm 3.3)	42	6.8%	0.76	--
		2000 - 2499	10.2 – 30.4	49.6 (\pm 6.5)	57	92.0 (\pm 11.5)	65	85.3%	0.002
		30.5 – 60.9	53.9 (\pm 6.6)	64	68.4 (\pm 7.4)	70	26.8%	0.15	--
		61.0 – 91.3	37.4 (\pm 4.3)	59	120.7 (\pm 11.6)	73	223.1%	< 0.001	large
		>91.4	34.5 (\pm 4.0)	53	42.8 (\pm 5.4)	55	24.1%	0.22	--
	> 2500	10.2 – 30.4	62.7 (\pm 19.6)	11	73.4 (\pm 19.5)	18	17.1%	0.70	--
		30.5 – 60.9	43.5 (\pm 11.1)	10	52.3 (\pm 13.1)	17	20.3%	0.61	--
		61.0 – 91.3	42.4 (\pm 10.3)	10	109.0 (\pm 14.8)	26	157.0%	< 0.001	large

^a P-value is obtained through negative binomial regression.

By National Forest

Changes in size class distribution were relatively consistent across all southern California National Forests (Figure 22, Table 11). Mean tree density of juveniles has increased in all three National Forests. However, the median density of trees in the smallest size experienced a slight decrease in ANF. Juvenile density increased the most in LPNF (128.6%, $p < 0.001$), however the observed increase was primarily due to an increased density of juvenile oaks (Figure 22B). Density of juvenile conifers experienced a decline in LPNF and ANF. In SBNF, the overall mean density of juveniles significantly increased by 79.5% ($p < 0.001$, effect size: small). SBNF was the only National Forest to have an overall increase in density of juveniles when excluding oaks.

Mean density of 61-91.3cm diameter trees significantly increased in all three National Forests (Table 11). The largest increase was observed in ANF where mean density increased by 252.6% from 35.2 (\pm 6.1 SE) trees/ha to 124.2 (\pm 15.5 SE) trees/ha. SBNF had the second largest increase (179.5%) followed by LPNF (53.3%).

Changes in mean density of trees with a diameter greater than 91.4cm differed between the National Forests. Density increased significantly ($p < 0.001$, effect size: large) in ANF; historic density averaged 5.5 (± 1.9 SE) trees/ha and increased by 558.5% to 36 (± 7.5 SE) trees/ha. Mean density increased in SBNF by 25.9% from 26.8 (± 3.0 SE) trees/ha to 33.7 (± 4.51 SE) trees/ha, although this was not significant ($p = 0.17$). In LPNF, mean density decreased by 22.3% from 37.6 (± 5.0 SE) trees/ha to 29.2 (± 4.4 SE) trees/ha.

Table 11. Mean tree density by National Forest. Significance values from two-sample t-tests are reported below unless otherwise noted.

National Forest	Tree Size Class (cm)	VTM Mean (\pm SE)	No. of plots observed in	FIA Mean (\pm SE)	No. of plots observed in	Percent Change	p-value	Effect Size
ANF	10.2 – 30.4	78.3 (\pm 12.6)	19	130.8 (\pm 37.3)	22	67.1%	0.19	--
	30.5 – 60.9	103.6 (\pm 17.3)	19	60.4 (\pm 12.1)	21	-41.7%	0.047	--
	61.0 – 91.3	35.2 (\pm 6.1)	17	124.2 (\pm 15.5)	25	252.6%	< 0.001	large
	>91.4	5.5 (\pm 1.9)	7	36.0 (\pm 7.5)	18	558.5%	< 0.001	large
LPNF	10.2 – 30.4	85.2 (\pm 10.5)	51	194.8 (\pm 27.7)	54	128.6%	< 0.001	medium
	30.5 – 60.9	66.3 (\pm 7.2)	47	72.6 (\pm 8.0)	52	9.6%	0.56	--
	61.0 – 91.3 ^a	54.4 (\pm 6.8)	41	83.3 (\pm 9.5)	57	53.3%	0.33	--
	>91.4	37.6 (\pm 5.0)	37	29.2 (\pm 4.4)	38	-22.3%	0.21	--
SBNF	10.2 – 30.4	124.1 (\pm 17.5)	93	222.7 (\pm 22.4)	98	79.5%	< 0.001	small
	30.5 – 60.9 ^a	54.7 (\pm 5.8)	92	84.4 (\pm 7.5)	96	54.4%	0.66	--
	61.0 – 91.3	39.6 (\pm 4.1)	84	110.7 (\pm 9.7)	101	179.5%	< 0.001	large
	>91.4	26.8 (\pm 3.0)	67	33.7 (\pm 4.51)	68	25.9%	0.17	--

^a P-value is obtained through negative binomial regression.

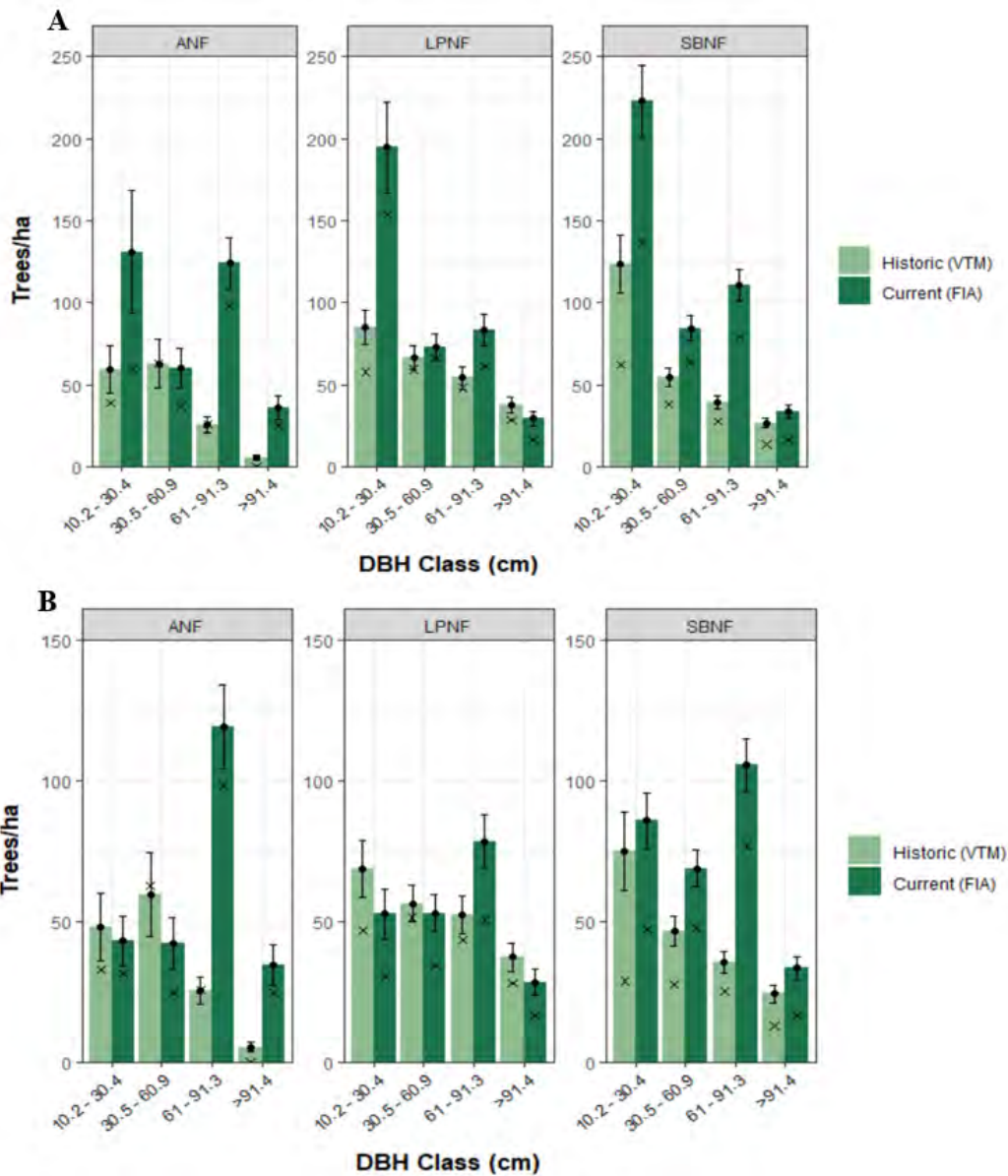


Figure 22. Change in size class distribution of YPMC species in three of the southern California National Forests with oaks (A) and without oaks (B). Size class data from CNF was not included due small sample sizes ($n < 10$). Xs mark the median, black dots mark the mean, and the bars represent that standard error.

5.3.3 NRV Analysis

Historic Observations: Southern California and Sierra San Pedro Mártir

Early explorers in the mid to late 19th century often noted the grand size of mature conifers in southern California forests. Many of these explorers and researchers assessed the largest pines and firs to be greater

than 42.7m in height and 152.4 to 182.9cm in diameter. Diaries from lumbermen revealed that old-growth forests in western SBNF “consisted of large individuals (2-3m d.b.h.) of all species” (La Fuz, 1971, as cited in Minnich et al., 1995). The widest tree recorded in the early 1900s was a *C. decurrens* in SBNF that was a 1.2m high stump over 300 years old with a 213.4cm diameter (Allen Peck, 1904, as cited in USDA, 1905).

In 1888, British land inspector Colonel D.K. Allen surveyed 22ha across mixed conifer forests in SSPM. He found that forests were very open with a 0.4ha area of forest containing an average of 62 “large” trees/ha and 25 “small” trees/ha. There was an average of 42 “large” *P. jeffreyi*, 10 “large” *P. lambertiana*, 7 “large” *A. concolor*, and 3 “large” *C. decurrens* per hectare. Unfortunately, Allen did not report quantitative thresholds to define “large” and “small” trees. Diameters for trees in three plots surveyed by Allen were provided by Minnich and Vizcaíno (1998). The average d.b.h. of trees in these plots ranged from 87.3-92cm. The smallest diameter tree recorded in the data provided by Minnich and Vizcaíno (1998) was 12.7cm, which was the only tree to fall in the smallest VTM d.b.h. size class (10.2-30.4cm). Overall, the distribution was heavily skewed towards larger diameter trees. Since Allen was surveying the land for lumbering potential, it is possible that he ignored measuring small trees. However, Minnich et al. (1995) claimed there were few trees with diameters less than 33cm in pre-suppression mixed conifer forests in SBNF. Minnich et al. (2000) concluded that surface fires removed sapling and pole-size trees from the understory, leaving the surviving saplings scattered across the landscape. Therefore, it is likely that of the data shown from a small sample of just three of D.K. Allen’s surveys, the plots truly contained few or no pole-sized trees. However, these plots may not be representative of all of his surveyed plots, or SSPM YPMC forests in general.

Several sources have alluded to the heterogeneity of tree size classes in historic southern California forests and modern forests in Baja. In 1796, Spanish explorer Arrillaga noted “pine trees of all sizes” during a trip into the southern Sierra Juarez (Minnich & Vizcaíno, 1998). Arrillaga documented “the increasing size of pine forests from Santa Catarina northward to Laguna Hanson.”

Comparing Contemporary Conditions and Sierra San Pedro Mártir

Contemporary researchers, Minnich and Vizcaíno (1998), Minnich et al. (1995), and Stephens and Gill (2005), have all described the modern size class distribution in SSPM YPMC forests as highly variable with a heterogeneous, multi-size structure. Minnich et al. (1995) also refer to historic southern California forests as having a heterogeneous age-structure prior to fire-suppression, which others have attributed to frequent forest fires (Wright & Bailey, 1982; Rundel et al., 1988).

In SSPM, Stephens and Gill (2005) surveyed 49 Jeffrey pine mixed conifer plots in a 0.1ha area. They recorded trees greater than 2.5cm diameter and 1.37cm in height. All trees had an average d.b.h. of 32.6cm (range 2.5-112cm). Results from Stephens and Gill (2005) align more with the findings of Dunbar-Irwin and Safford (2016), who found a mean d.b.h. of trees in SSPM to be 39.1cm when excluding trees with diameter less than 7.5cm, than with D.K. Allen. Mean d.b.h. of trees in our assessment area was 43.9cm, but when excluding oaks, the mean d.b.h. was 53.6cm.

Stephens and Gill reported the number of trees in their plots. We used their total plot size (4.9ha) to convert tree count to tree density per hectare. They found that the average tree density was approximately 71.4 trees/ha in the 10-30cm size class, approximately 49 trees/ha in the 30-60cm size class, and approximately 24.5 trees/ha in the 60-90cm size class. Dunbar-Irwin and Safford had very similar results. They recorded approximately a mean density of 62 trees/ha, 56 trees/ha, and 29 trees/ha in the same size classes, respectively. Our estimates of historic tree density of 10.2-30.4cm diameter trees (110.4 trees/ha) in southern California were much higher than Stephens and Gill and Dunbar-Irwin and Safford estimates in SSPM. Density of trees in the 61-91.3cm size classes (42.9 tree/ha) were also larger in our study area, but density of 30.5-60.9cm diameter trees (42.9 trees/ha) were more similar to SSPM. Density of these

three size classes has significantly increased in southern California indicating a large deviation from reference site conditions. Oaks were recorded in studies by Stephens and Gill and Dunbar-Irwin and Safford, however oaks are not common in SSPM; thus their estimates of density by size class more closely align with our historic estimates when excluding oaks (Appendix E).

Comparing Historic and Contemporary Conditions: Southern California

Several studies have compared the changes in forest size class distributions across southern California (Minnich et al., 1995; McIntyre et al., 2015; Stephenson & Calcarone, 1999; Nigro & Molinari, 2019). Minnich et al. (1995) compared changes in forest structure in SBNF 60 years after the VTM surveys were conducted by resurveying the approximate locations of 68 VTM plots. Minnich et al. split their results up by forest type: mixed conifer (n=16), Jeffrey pine (n=9), and mixed Jeffrey pine (n=11).

In mixed Jeffrey pine forests, Minnich et al. (1995) found an overall decline of trees >67cm, mostly due to decline in *P. jeffreyi*, and increases in juvenile (d.b.h. <33cm) *P. jeffreyi*, *C. decurrens*, *A. concolor*, and *P. lambertiana*. In Jeffrey pine dominated forests, *P. jeffreyi* in the largest size class (>100cm) decreased in abundance by 66.7% from 30 trees/ha to 10 trees/ha, but density of *P. jeffreyi* juveniles more than tripled from approximately 20 trees/ha to approximately 75 trees/ha. In mixed Jeffrey pine and Jeffrey pine dominated forests, Minnich et al. (1995) found declines in density of large (68-100cm) trees. In mixed white fir forests, density of *A. concolor* increased by 70% due to a 300% increase in trees <67cm. Overall, trees in the smallest d.b.h. size class (12-33cm) in white fir forests nearly tripled from 54 to 140 trees/ha, but the density of trees >67cm (26.4in) decreased by half from 76 to 38 trees/ha (Minnich et al., 1995). Within mixed white fir forests, density of *P. jeffreyi* and *P. lambertiana* only increased in the juvenile size class (approximately 25 to 55 trees/ha and 25 to 48 trees/ha, respectively), while density declined in the other three size classes. *Calocedrus decurrens*, another shade tolerant species, declined in density across all size classes in white fir forests, except for the 68-100cm size class. We only found a slight, non-significant decrease (14.9%) of yellow pines in the largest diameter size class (d.b.h. >91.4cm) across all of southern California. Additionally, across the study area we found a decrease in density of all conifer species, but the density of large diameter trees (61-91.3cm) in all conifer species significantly increased.

Stephenson and Calcarone (1999) revisited 32 mixed conifer VTM plots in Mount Pinos/Mount Abel (LPNF), the San Gabriel Mountains (ANF), and CNF. Nigro and Molinari (2019) resurveyed 4 VTM plots in LPNF on Frazier Mountain. Stephenson and Calcarone (1999) and Nigro and Molinari (2019) found significant or substantial increases in the average density of trees from the two smallest d.b.h. classes (10-29cm and 30-59cm) in their respective study areas. Nigro and Molinari found that increases in smaller diameter trees were primarily responsible for the 144% increase in average tree density. Nigro and Molinari (2019) and Stephenson and Calcarone (1999) also found no significant change in average density of trees in the two largest d.b.h size classes (60-89cm and >91cm), which could be due to their small sample sizes.

McIntyre et al. (2015) compared changes in size class distributions across the Transverse and Peninsular Ranges using VTM and 2001-2010 FIA data. McIntyre et al. also found an increase (+82.4%) in density of small diameter trees (10.2-30.4cm) (VTM: 165 trees/ha, FIA: 301 trees/ha). Unlike Nigro and Molinari (2019) and Stephenson and Calcarone (1999), McIntyre et al. found a slight, but non-significant decline in trees in the second smallest d.b.h. class (30.5-60.9; VTM: 60.1 trees/ha, FIA: 52.8 trees/ha) and a significant 73.4% decline in trees >61cm (VTM: 40.9 trees/ha, FIA: 10.7 trees/ha).

While our overall tree density calculations show an increase in density of juveniles, which aligns with results from other researchers (Nigro & Molinari, 2019; Stephenson & Calcarone, 1999; McIntyre et al., 2015; Minnich et al., 1995), a deeper analysis of the data revealed that this is primarily due to a significant increase in small diameter oaks. The large increase in juvenile oaks can primarily be attributed

to a 541% increase in juvenile *Q. chrysolepis*; density increased from 15.2 trees/ha to 97.1 trees/ha. Density of all juvenile conifers declined except for shade tolerant *A. concolor*.

Summary

Tree density has increased in all size classes since the early 1930s. The most significant changes occurred in trees with the smallest diameter (10.2-30.4cm) (Figure 23) and the second largest diameter (61-91.3cm) size classes. Across the National Forests, density of juveniles has increased but when excluding oaks from the analysis juveniles have actually increased in ANF and LPNF. This demonstrates that overall, density of conifer juveniles has decreased and increases in oak juveniles were driving the increased density of juvenile trees in the assessment area.

Increases in oak densities were greatest at elevations between 1000–1999m and were primarily due to an increase in oak trees with diameters less than 30cm. Conifers with diameters less than 30cm in this same elevation band were decreasing. We believe that the large increase of small diameter oaks and the large decrease of small diameter conifers are keeping the overall tree density relatively the same at low elevations (see Section 5.2). As the climate warms and oak ranges expand, YPMC forests, especially at lower elevations, will likely experience further changes in composition (Fellows & Goulden, 2012).

Our results showing significant increases in density of all conifers in large diameter trees (61-91.3cm), which is evenly distributed across the study area (Figure 24), contrasts with the other researchers (Minnich et al., 1995; McIntyre et al., 2015; Stephenson & Calcarone, 1999; Nigro & Molinari, 2019). The decline in large diameter trees has been observed in other conifer forests in California (Dolanc et al., 2014; Dolph et al., 1995; Lutz et al., 2009; Ritchie et al., 2008; Smith et al., 2005; van Mantgem et al., 2009), except for Collins et al. (2011), yet this is the first reported case of increases in large diameter trees in southern California mixed conifer forests. This could be due to the lack of logging that took place in the study area compared to other forested regions (e.g., Sierra Nevada) and long (approximately 80-109+ year) absence of fire in YPMC forests (Stephenson & Calcarone, 1999; Nigro & Molinari, 2019), which could have allowed smaller diameter trees to graduate to the larger class sizes.



Figure 23. Variety of size class trees. Increased density of small diameter shade tolerant species in the understory. Photo courtesy of Nicole Molinari, USFS.

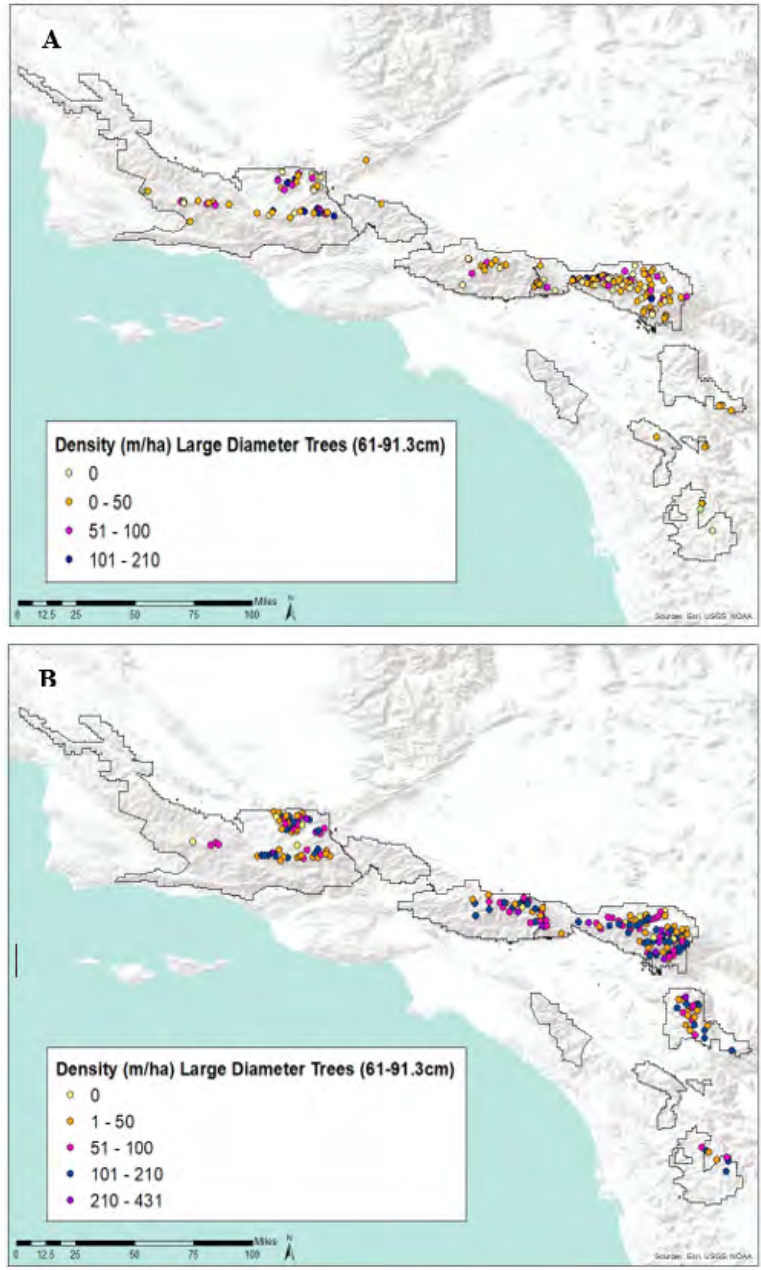


Figure 24. Spatial distribution of large diameter trees in 1930s (A) and 2001-2010 (B).

5.4 Basal Area

5.4.1 Methods

Typical basal area calculations are relatively straightforward (see http://www.ruraltech.org/virtual_cruiser/lessons/lesson_10/Lesson_10_PDF.pdf). Note, slope corrected plot size was used to calculate basal area (see Section 5.2.1). For an example of our code, see Appendix F. However, because Wieslander (1935) recorded trees into size class bins instead of recording the true d.b.h, modifications were made to the general basal area calculations in order to make direct comparisons between historic and modern basal area. While there are different methods to calculate basal area for binned data (Bouldin, 1999; Fellows & Goulden, 2008; Hagmann et al., 2013; McIntyre et al., 2015), our approach was most similar to Bouldin (1999).

D.b.h.'s for trees in the combined FIA dataset were converted to inches and classified into the same bins as the VTM dataset (4-11in, 12-23in, 24-36in, and >36in). We then used the midpoint (i.e., mean) of the three smallest d.b.h. bins to calculate basal area (Bouldin, 1999; Hagmann et al., 2013). For example, 7.5in was used to calculate the basal area for all trees in the 4-11in size class. We then followed the equations outlined by [RuralTech](#) to calculate basal area for trees below 36in in the VTM and FIA data. However, an issue arises when selecting the value to represent the midpoint of the largest size class (>36in) as there is no upper limit for the bin like with the other d.b.h. size classes. At this step, we took a slightly different approach from Bouldin (1999) when determining the value to represent the end of the d.b.h. range for trees in the largest size class.

Bouldin (1999) used literature and the FIA dataset to determine the maximum d.b.h. for each species. He then fit the basal area of the cumulative diameters in a plot using five linear and nonlinear equations. In our approach, we only used diameters from trees in the combined FIA plots to determine the maximum d.b.h. (Appendix G). The second largest diameter tree for *C. decurrens* was used to represent the maximum d.b.h. of the species since the largest d.b.h. was over 60 inches larger than the tree with the second largest d.b.h., which could result in a large source of error (Bouldin, 1999). We then compared several different metrics to determine the best value to represent the end range of the largest class size of each species before calculating the midpoint. The metrics we assessed were the maximum, maximum - 10% (Bouldin, 1999), mean + 1 standard deviation, and mean.

To determine the best metric for each species we plotted the total basal area per plot using the true, unbinned FIA d.b.h. of trees over 36in and the total basal area per plot for binned FIA d.b.h. of trees over 36in (Appendix G). This was done because using midpoints could result in the true basal area being under or overrepresented depending on the distribution of trees within the bins. For example, a left skewed distribution in which most of the trees are near the high end of the range will result in the basal area being underestimated. A one-to-one line was added to each graph to help visually assess bias for each species and determine the best metric to represent the end range for each species in the largest d.b.h. size class (Appendix G). Visual analysis included selecting the metric that resulted in the basal area estimated being closest to the one-to-one line. We used a conservative approach when selecting the best metric, meaning we selected the metric that slightly underestimated rather than slightly overestimated basal area if no metric best fit the one-to-one line.

Different metrics provided better fits depending on the species (Appendix G). A conservative approach was also taken when selecting the metric for species that had too small of a sample to accurately assess for bias: (*P. coulteri*, *Q. chrysolepis*, and *Q. kelloggii*). In this case we selected the mean plus one standard deviation. The values used to best represent the midpoint of the largest size class are available in Table 12. The values used to represent the end of the range for large diameter trees (>91.4cm), which was determined using FIA data, were then applied and used to calculate the basal area of large trees in the

VTM data. This assumes the large diameter trees in the VTM data have a similar distribution to the FIA data.

Table 12. The different values used to represent the end range of the largest d.b.h class size by species. These values were also applied to species in the VTM data.

Species	End Range (cm)	End Range Metric	Midpoint
ABCO	131	Max - 10%	111.2
CADE	145	Max - 10%	118.2
PICO*	104	Max - 10%	97.7
PILA	123	Mean + 1SD	107.2
PSMA	126	Max - 10%	108.7
Yellow Pine	117	Mean + 1SD	104.2
QUCH*	98	Max - 10%	94.7
QUKE*	93	Max - 10%	92.2

*: Denotes species with a sample size too small (n=1 or n=2) to compare across the different metrics. A conservative approach was taken by using the maximum - 10% to represent the end range for the species.

We also compared the total basal area of plots in the combined FIA dataset using the true, unbinned d.b.h. and the binned d.b.h to check for bias in all plots (Figure 25). Though little bias was observed, bias did increase as d.b.h increased. Larger diameter trees will have more variance when using the midpoint than smaller diameter trees since basal area calculations require squaring the diameter. Overall, there is little to no bias which indicates using binned d.b.h.s is a representative alternative of using the true, unbinned d.b.h.s.

We performed a two-sample t-test to determine if there was a significant change between historic and contemporary basal area. We also calculated Cohen’s-D (i.e., effect size) to determine the magnitude of the difference between two means when the p-value was less than the chosen significance level ($\alpha < 0.05$). When the assumption of normality could not be met using the central limit theorem, we used a bootstrapped t-test. We indicate which test was used to draw conclusions from in the results tables. For additional metrics of variance, see Appendix H.

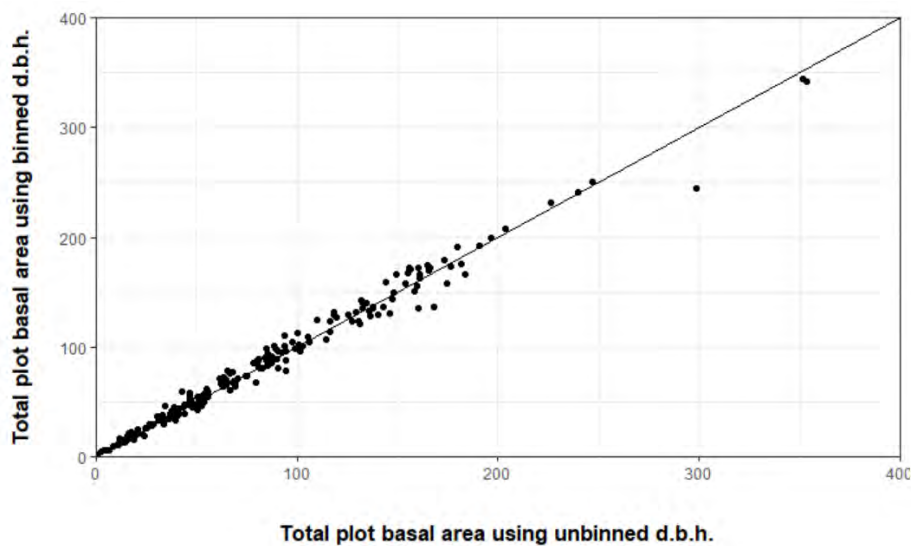


Figure 25. Comparison of total plot basal area using binned and unbinned d.b.h to calculate basal area.

5.4.2 Results

Our analysis shows that the overall mean basal area increased between historic and contemporary conditions. Basal area in historic plots averaged $55.7 (\pm 3.0 \text{ SE}) \text{ m}^2/\text{ha}$ and $92.8 (\pm 5.0 \text{ SE}) \text{ m}^2/\text{ha}$ in contemporary plots. Overall, the mean basal area throughout the study area increased significantly by 66.5% ($p < 0.001$; effect size: medium) (Table 13). There are a variety of basal area ranges across VTM plots in ANF, LPNF, and SBNF (Figure 26). Contrastingly, a majority of FIA plots with high basal area is clustered in northern SBNF (dark blue). For additional graphs and analyses, see Appendix H.

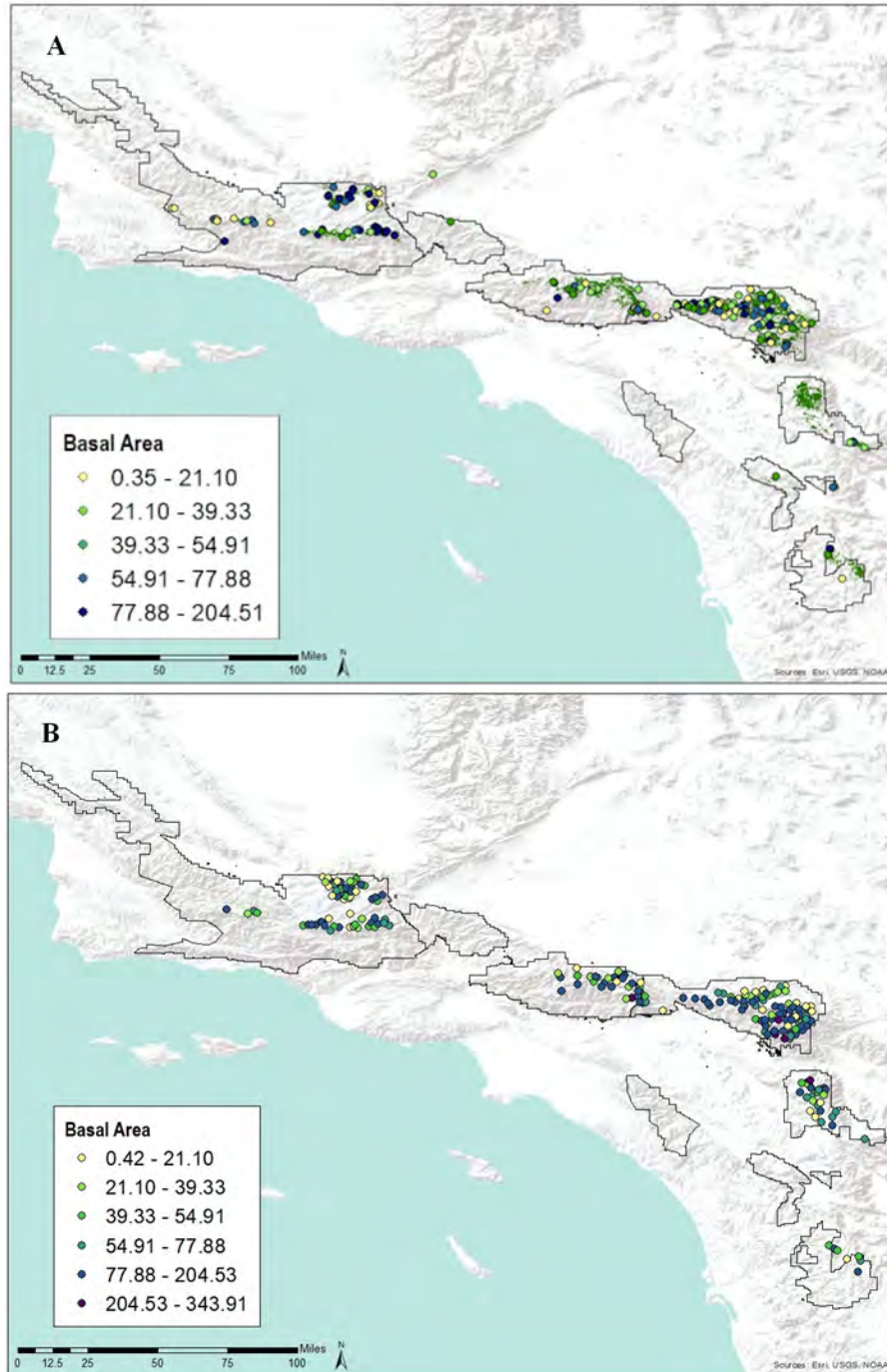


Figure 26. Locations of VTM (A) and combined FIA (B) plots classified by mean basal area.

By Functional Group (Oak vs Conifer)

Mean basal area of oaks increased significantly from 4.5 (± 0.7 SE) m²/ha in historic forests to 9.5 (± 1.0 SE) m²/ha in contemporary forests ($p < 0.001$). While historic oak basal area increased more than doubled (111.1% increase), the effect size was small (Figure 27, Table 13). Mean basal area of conifers also increased significantly from historic to contemporary forests with a greater effect size, although they had a smaller increase of 62.6% ($p < 0.001$; effect size: medium) (Table 13).

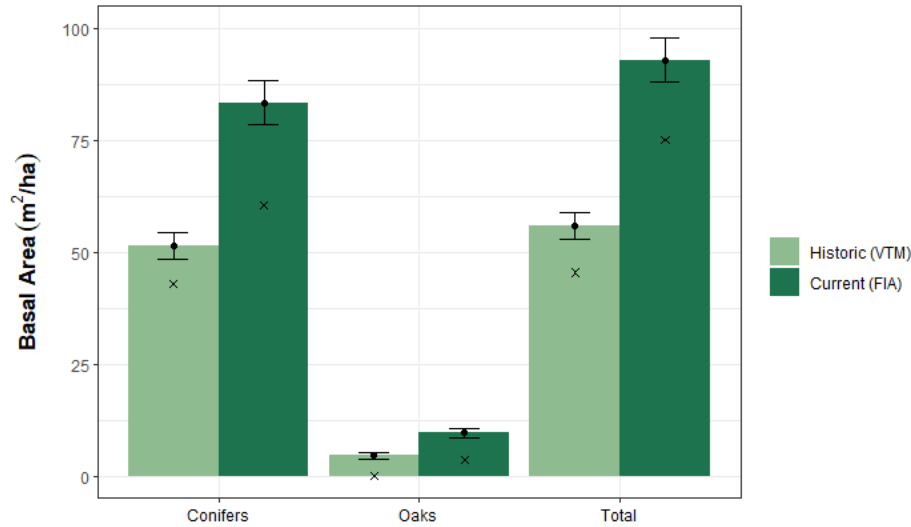


Figure 27. Average basal area for the conifer and oak functional groups plus the overall basal area. Sample sizes were $n = 195$ for historic data and $n = 210$ for current data. Xs mark the median, black dots mark the mean, and the bars represent that standard error.

Table 13. Change in basal area (m²/ha) by total number of plots, species, classification, and shade/fire tolerance. Means were calculated across the entire landscape, not the number of plots the species was found in. Significance values from two-sample t-tests are reported below unless otherwise noted.

	VTM Mean (± SE)	No. of plots observed in	FIA Mean (± SE)	No. of plots observed in	Percent Change	p-value	Effect Size
Total	55.7 (± 3.0)	195	92.8 (± 5.0)	210	66.5%	< 0.001	medium
Species							
<i>Abies concolor</i> ^b	11.6 (± 1.6)	90	25.6 (± 3.0)	110	121.2%	< 0.001	--
<i>Calocedrus decurrens</i> ^b	2.0 (± 0.5)	36	7.0 (± 1.6)	43	254.9%	0.003	--
<i>Pinus coulteri</i> ^b	2.03 (± 0.6)	23	2.01 (± 0.5)	25	-1.0%	0.98	--
<i>Pinus lambertiana</i> ^b	7.3 (± 1.1)	69	9.4 (± 1.6)	77	28.4%	0.30	--
Yellow Pine	26.6 (± 2.2)	145	35.0 (± 2.8)	169	31.5%	0.02	small
<i>Quercus chrysolepis</i> ^b	1.5 (± 0.5)	38	6.9 (± 0.9)	102	364.9%	< 0.001	--
<i>Quercus kelloggii</i> ^b	3.0 (± 0.5)	54	2.6 (± 0.5)	44	-13.9%	0.57	--
Functional Group							
Conifers	51.2 (± 3.0)	195	83.3 (± 4.9)	210	62.6%	< 0.001	medium
Oaks	4.5 (± 0.7)	78	9.5 (± 1.0)	125	111.1%	< 0.001	small
Shade/Fire Tolerant							
Shade Intolerant/Fire Tolerant	40.7 (± 2.5)	189	53.3 (± 3.1)	201	30.9%	0.002	small
Shade Tolerant/Fire Intolerant	15.0 (± 1.7)	126	39.5 (± 3.7)	163	162.9%	< 0.001	medium

^b P-value is obtained through boot strapped t-test.

By Species

Quercus chrysolepis experienced the greatest increase in mean basal area compared to any other YPMC species (364.9%). (Table 13). Historic basal area of *Q. chrysolepis* averaged 1.5 (± 0.5 SE) m²/ha while the contemporary basal area averaged 6.9 (± 0.9 SE) m²/ha (Table 13). Contrastingly, mean basal area of *Q. kelloggii* experienced a decline (historic mean = 3.0 (± 0.5 SE) m²/ha, contemporary mean = 2.6 (± 0.5 SE) m²/ha) (Table 13).

All conifers, excluding *P. coulteri*, increased in mean basal area (Figure 28). Of the conifers, *A. concolor* and *C. decurrens* experienced the largest increases in mean basal area. Mean basal area of *A. concolor* and *C. decurrens* increased significantly by 121.2% ($p < 0.001$) and 254.9% ($p = 0.003$), respectively. Yellow pines increased slightly in basal area (31.5% percent change; $p = 0.02$); historic basal area averaged 26.2 (± 2.2 SE) m²/ha while contemporary basal area averaged 35.0 (± 2.8 SE) m²/ha (Table 13). *Pinus lambertiana* experienced a similar increase in basal area by 28.4%, although the increase was not statistically significant ($p = 0.30$) (Table 13). The only conifer species to experience a decline in basal area was *P. coulteri*, which decreased by -1.0%.

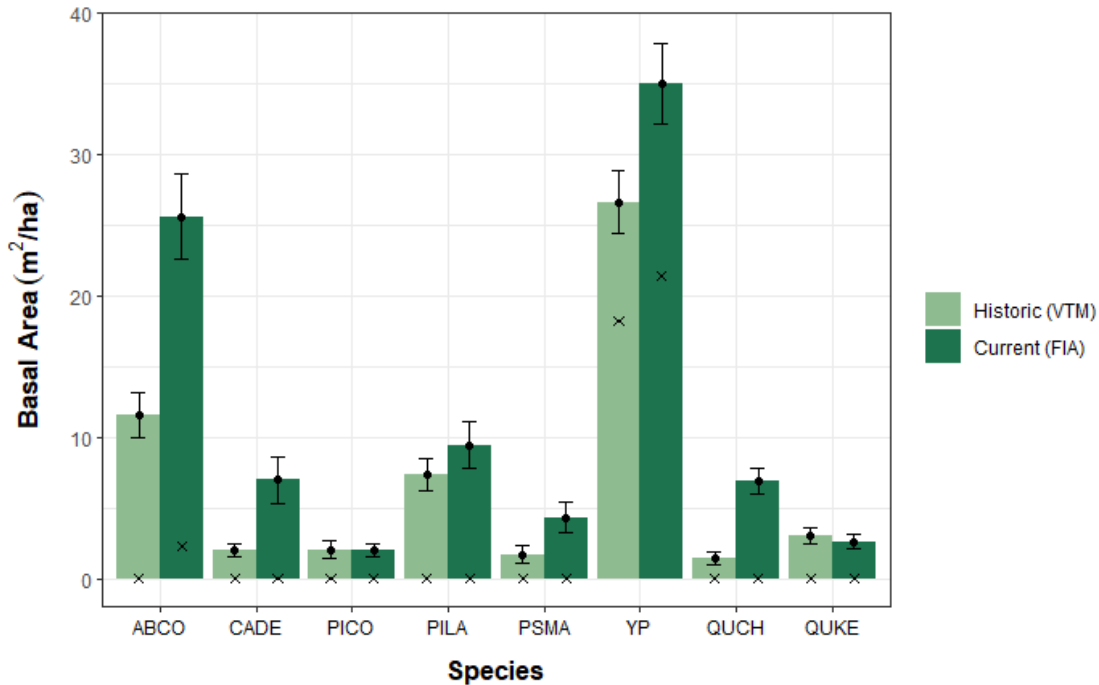


Figure 28. Average basal area for each YPMC species. Sample sizes were $n=195$ for historic data and $n=210$ for contemporary data. Xs mark the median, black dots mark the mean, and the bars represent that standard error.

By Shade and Fire Tolerance

Mean basal area of shade tolerant/fire intolerant species in our study area increased significantly by 162.9% ($p < 0.001$; effect size: medium); historic basal area averaged 15.0 (± 1.7 SE) m²/ha and contemporary basal area averaged 39.5 (± 3.7 SE) m²/ha (Table 13). *Abies concolor*, *C. decurrens*, and *Q. chrysolepis*, are categorized as shade tolerant/fire intolerant species. Mean basal area of shade intolerant/fire tolerant species increased slightly by 30.9% (Table 13).

By Elevation

Mean basal area increased across all elevation bands (Figure 29). Mean basal area at elevations greater than 2500m increased significantly by 107.2% ($p=0.004$; effect size: large); historic basal area averaged 46.2 (± 13.2 SE) m^2/ha and contemporary basal area averaged 95.7 (± 11.0 SE) m^2/ha (Figure 29; Table 14). Mean basal area also increased significantly by 48.0% at elevations between 1500–1999m and by 93.2% at between 2000–2499m ($p<0.001$; effect size: medium). While mean basal area increased between 1000–1499m, this was the only elevation band to not increase significantly; historic basal area averaged 58.1 (± 9.9 SE) m^2/ha and contemporary basal area averaged 66.8 (± 9.4 SE) m^2/ha (Table 14).

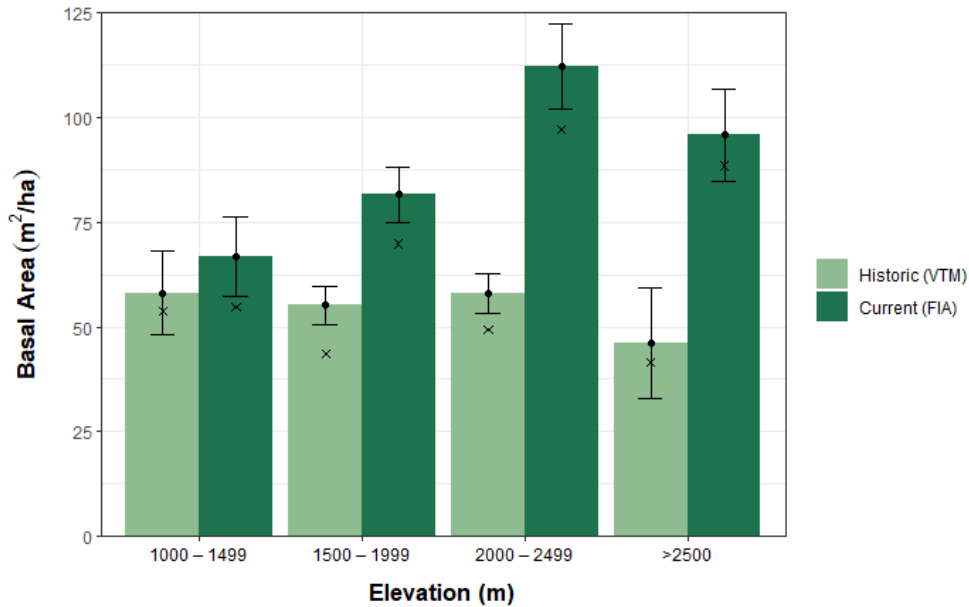


Figure 29. Average basal area by elevation class for all YPMC species (including oaks). Xs mark the median, black dots mark the mean, and the bars represent that standard error.

Table 14. Change in basal area (m^2/ha) by National Forest and elevation classes. Means were calculated across the entire landscape, not the number of plots the species was found in.

	VTM Mean (\pm SE)	VTM Sample Size	FIA Mean (\pm SE)	FIA Sample Size	Percent Change	p-value	Effect Size
National Forest							
ANF	38.7 (± 4.2)	20	100.6 (± 13.3)	26	160.0%	< 0.001	large
LPNF	69.8 (± 6.9)	54	79.6 (± 7.2)	62	14.1%	0.33	--
SBNF	52.9 (± 3.8)	113	99.8 (± 8.0)	107	88.6%	< 0.001	medium
Elevation (m)							
1000 – 1499	58.1 (± 9.9)	20	66.8 (± 9.4)	26	15.0%	0.53	--
1500 – 1999	55.1 (± 4.6)	84	81.6 (± 6.6)	80	48.0%	0.0012	medium
2000 – 2499	58.0 (± 4.7)	77	112.0 (± 10.1)	78	93.2%	< 0.001	medium
> 2500	46.2 (± 13.2)	13	95.7 (± 11.0)	26	107.2%	0.007	large

By National Forest

Out of the three National Forests we analyzed, ANF had the largest (160.0% percent change) increase in mean basal area between historic and contemporary conditions, which was also found to be significant ($p < 0.001$; effect size: large) (Table 14, Figure 30). Historic basal area in ANF averaged $38.7 (\pm 4.2 \text{ SE}) \text{ m}^2/\text{ha}$ and contemporary basal area averaged $100.6 (\pm 13.3 \text{ SE}) \text{ m}^2/\text{ha}$. Mean basal area in SBNF increased significantly by 88.6% ($p < 0.001$; effect size: medium); historic basal area averaged $59.2 (\pm 3.8 \text{ SE}) \text{ m}^2/\text{ha}$ and contemporary basal area averaged $99.8 (\pm 8.0 \text{ SE}) \text{ m}^2/\text{ha}$. (Table 14). In contrast, LPNF increased in basal area by 14.1%, however this increase was not statistically significant ($p = 0.16$) (Table 14).

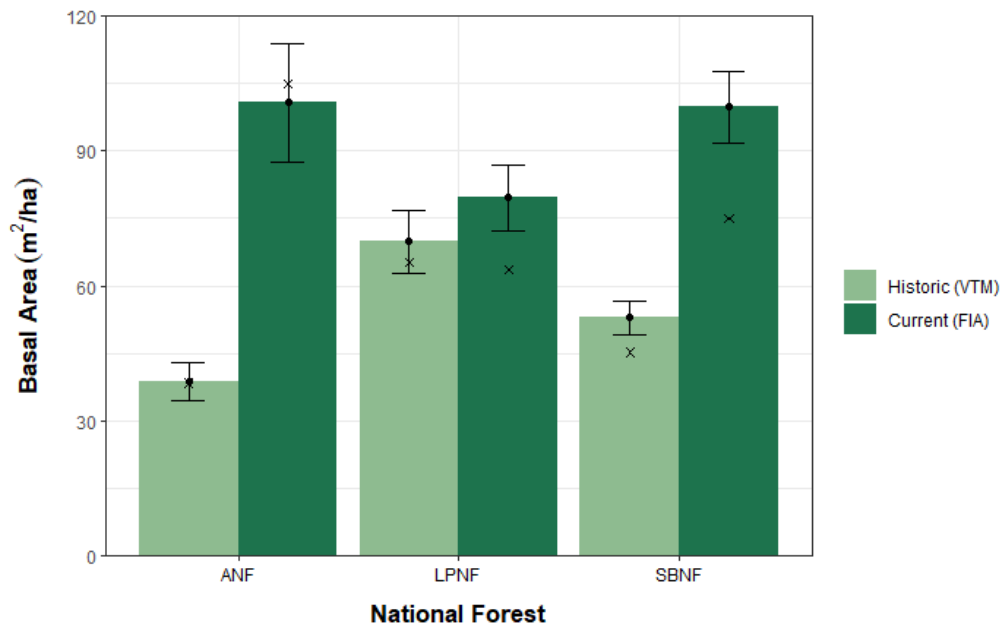


Figure 30. Average basal area by National Forest. Xs mark the median, black dots mark the mean, and the bars represent that standard error.

5.4.3 NRV Analysis

Contemporary Observations: Sierra San Pedro Mártir

There is limited qualitative and quantitative data describing the historic basal area (forest biomass) of southern California YPMC forests. To address this, we used contemporary data from SSPM as a reference for historic conditions. SSPM provides sufficient data on basal area for researchers to simulate historic conditions in southern California prior to fire-suppression. Through field sampling, Minnich et al. (2000) recorded mean basal areas of $21 \text{ m}^2/\text{ha}$, $27 \text{ m}^2/\text{ha}$, and $34 \text{ m}^2/\text{ha}$ in Jeffrey pine, mixed Jeffrey pine, and mixed white fir forests, respectively, in a total of 24 plots. Minnich et al. (2000) also recorded higher tree density among large diameter (60.1-80cm) trees (~ 20 trees/ha for Jeffrey pine forests, ~ 10 trees/ha for mixed Jeffrey pine forests, and ~ 25 trees/ha for mixed white fir forests) compared to the smaller size class trees, which led Minnich et al. to conclude that “high basal area reflected high tree density.” Stephens and Gill (2005) surveyed 49 plots in SSPM, which consisted of Jeffrey pine mixed conifer forests between elevations of 2400 and 2500m, and reported a mean basal area $19.9 \text{ m}^2/\text{ha}$. From the VTM data, we found a mean basal area of $58 \text{ m}^2/\text{ha}$ from 2000–2499m. Similar to Stephens and Gill, Dunbar-Irwin and Safford (2016) surveyed 70 plots of dry YPMC forests in SSPM and found a mean basal area of $22.5 \text{ m}^2/\text{ha} (\pm 1.5 \text{ SE})$.

The average basal area found in these studies is lower than the average basal area we calculated from the VTM dataset. One possible cause may be that we found higher overall tree densities and higher densities of large diameter trees (d.b.h. 61.0-91.3cm) compared to the other studies (see Section 5.3.2). Our overall historic tree density is 39.9 trees/ha for large diameter trees and 27.4 trees/ha for the largest (d.b.h. >91.4cm) size class, which is greater than the tree densities Minnich et al. (2000) reported in their size classes. Additionally, Stephens and Gill and Dunbar-Irwin and Safford found lower tree density in SSPM than we observed from the historic VTM dataset in southern California.

Comparing Historic and Contemporary Conditions

Overall, our results show an increase in mean basal area between the early 1900s and 2010. Many of the trends we saw in our basal area results correlated with the patterns we saw in tree density (see Section 5.2.2) and tree size class distribution (see Section 5.3.2).

McIntyre et al. (2015) found basal area declines of up to 40% in the Transverse and Peninsular Ranges when comparing VTM to FIA data. In their study, basal area of conifers and oaks declined; conifer basal area declined by 50%. In our assessment area, McIntyre et al. found that large (>61cm d.b.h.) tree density decreased by 30% (40.8 trees/ha to 10.6 trees/ha), while small tree density (10.2-30.4cm d.b.h.) increased by over 50% (165 trees/ha to 301 trees/ha). Thus, the significant decline McIntyre et al. found in large diameter trees may explain why they did not have an increase in basal area despite an overall increase in tree density. In contrast to McIntyre et al., our basal area results increased overall and increased in each functional group. This is likely due to a 141.8% increase in density of large diameter (61.0-91.3cm) trees and a 500% increase of *Q. chrysolepis*.

Previous research did not investigate basal area changes by individual YPMC species as we did in our analysis. However, Stephens and Gill (2005) did calculate the overall mean basal area for the whole landscape and listed the composition of the total mean basal area by species. They found that *P. jeffreyi* comprised most of the basal area within a plot (67.1%), followed by *A. concolor* (23.1%), and *C. decurrens* (8.4%). Comparatively, within our study area, *P. jeffreyi*, *A. concolor*, and *P. lambertiana* consistently had the highest basal area in the early 1900s and 2000s.

Summary

Shade tolerant species *Q. chrysolepis*, *A. concolor*, and *C. decurrens* had the largest increase in mean basal area between historic and contemporary forests. Density of *C. decurrens* did not significantly increase, but basal area of the species did. This is likely due to the large increase in *C. decurrens* with a diameter over 91.4cm.

When comparing National Forests, basal area only significantly increased in ANF and SBNF. On average, basal area slightly increased in LPNF, but the median basal area in LPNF decreased. This is despite the significant increase in tree density in LPNF. This could be because LPNF was the only National Forest to have a decrease in density of trees >91.4cm.

5.5 Canopy Cover

5.5.1 Methods

Canopy cover is a measure of the percentage of the ground surface that is shaded by overstory trees (Safford & Stevens, 2017). A canopy, which is assumed to be whole, is the perimeter of the edge of the foliage. We followed methods outlined in Safford and Stevens (2017), which have been followed by many other researchers (Collins et al., 2011; Dolanc et al., 2014; North et al., 2007; Scholl & Taylor, 2010; Stephens et al., 2015; Taylor, 2004; Taylor et al., 2014; Taylor, 2010). This approach results in estimates of relative canopy cover, meaning overlapping canopies are not double counted. This ensures that the maximum canopy cover in a plot is 100%. Calculating canopy cover involves applying the d.b.h. of each tree in a species-specific equation from the forest vegetation simulator (FVS); species-specific constants are provided in table 4.4.2.1 by Keyser and Dixon (2012). Constants and equations used in the analysis can be found in Appendix I.

VTM data recorded d.b.h. values into bins instead of recording the actual d.b.h. measurement. Combined FIA data does have actual d.b.h. measurements recorded; however, we binned the FIA d.b.h. so that we could directly compare our canopy cover estimates to the VTM canopy cover estimates. Therefore, we assigned each tree the midpoint value of their d.b.h. class (see Section 5.4.1 for midpoint values). For the d.b.h. size class of over 36in, we assigned the minimum size of 36in. Though 36in is not a true midpoint value, the greater than 36in size class is open ended and therefore, there is no true midpoint. Though this is a different approach taken for our basal area analysis, this method of using 36in as the midpoint was used by Safford and Stevens (2017). To check whether or not using binned d.b.h.s over or underrepresented true canopy cover within a plot, we compared canopy cover results using actual measurements for d.b.h. and midpoint d.b.h. values for combined FIA data (Appendix J). There was no significant difference of the calculated average canopy cover between the two methods ($p=0.94$).

Next, we applied the FVS species-specific equations outlined in Keyser (2010) to calculate the crown-width. Methods for our calculations can be seen in Appendix I. This gave us the absolute canopy cover. Absolute canopy cover does not account for overlapping canopies and can therefore be over 100%.

Lastly, To find the relative canopy cover for each plot, we applied the Crookston and Stage (1999) equation to account for overlapping canopies: $(C = 100 [1 - \exp(-.01 C')])$, where C' is the percent canopy cover without accounting for overlap. We then found the average relative canopy cover across all plots. We also calculated the average canopy cover by National Forest and by elevation. Additionally, we calculated the canopy cover of conifers by excluding oaks. We were interested to see how results varied due to the large increase in density of *Q. chrysolepis* (see Section 5.2.2). We performed two-sided t-tests to determine whether or not there was a significant difference between the average percent canopy cover between historic and contemporary forests. For additional metrics of variance, see Appendix K.

5.5.2 Results

By National Forest

Canopy cover has increased in all three southern California National Forests between the early 1900s and 2000s. The first part of our analysis of canopy cover included all YPMC species, which includes oak species. When oaks were included in our analysis, total canopy cover increased from approximately 53.4% (± 1.7 SE) to 70.2% (± 1.7 SE) (Table 15, Figure 31). Increases in canopy cover between all three National Forests were relatively similar and ranged between 22% to 52%, though ANF experienced the

greatest change between historic and contemporary conditions. All changes in canopy cover were statistically significant (Table 15). Average canopy cover for contemporary forests were all relatively similar across National Forests (Figure 31) and were between 68–70%. The median canopy cover for all three National Forests for contemporary estimates was higher than the mean canopy cover. This is due to the FIA data being left skewed toward large d.b.h. trees and therefore, resulting in higher percent canopy cover (Appendix L).

Table 15. Total percent change in canopy cover by National Forest between historic (VTM) and contemporary (FIA) data when oaks were included in the analysis.

National Forest	VTM Mean (±SE)	FIA Mean (±SE)	Percent Change	p value	Effect Size
Total	53.4 (±1.7)	70.2 (±1.7)	31.49%	< 0.001	medium
ANF	46.3 (±3.4)	70.7 (±4.8)	52.69%	< 0.001	large
LPNF	56.0 (±3.6)	68.7 (±3.2)	22.52%	0.0104	small
SBNF	53.6 (±2.1)	70.1 (±2.4)	30.78%	< 0.001	medium

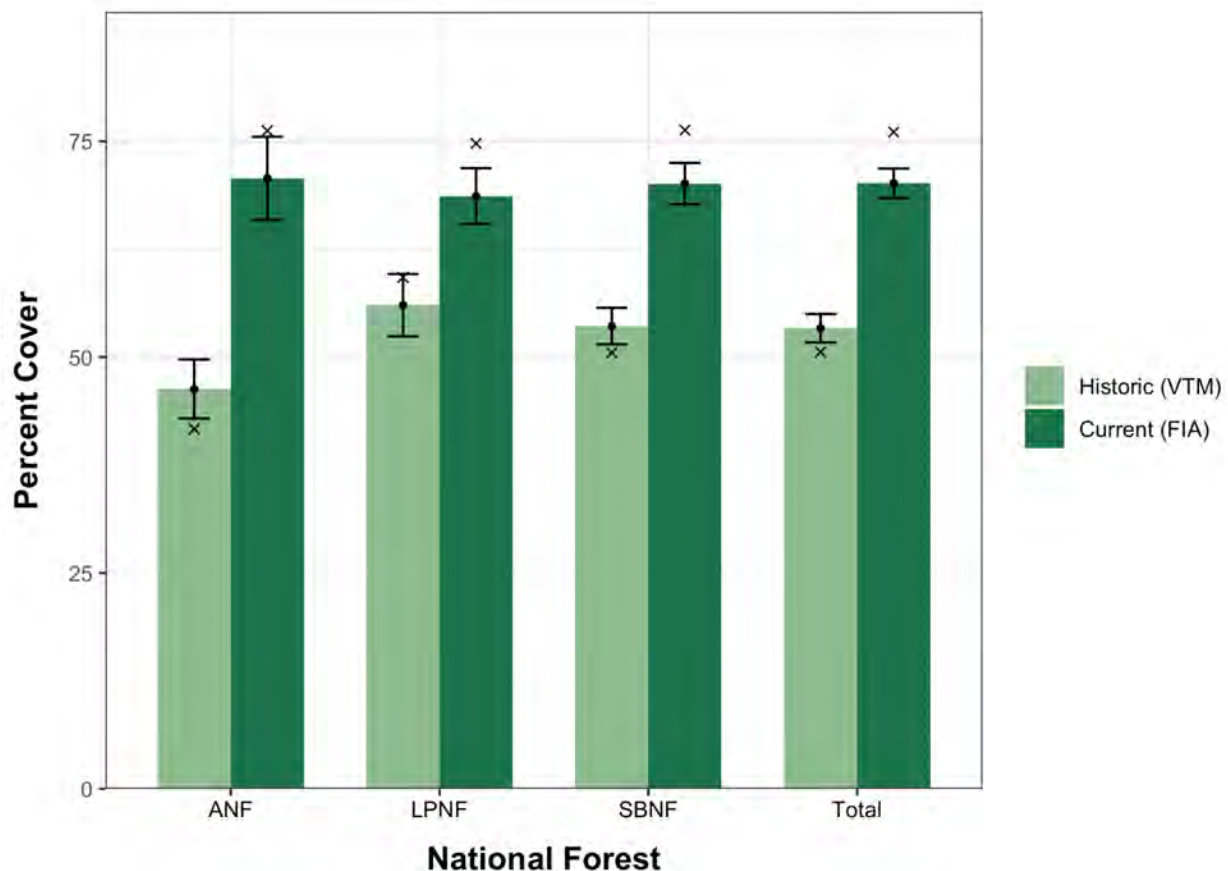


Figure 31. Percent canopy cover including oak species (*Q. chrysolepis* and *Q. kelloggii*). CNF was excluded from the analysis due to small sample sizes. Xs mark the median, black dots mark the mean, and the bars represent that standard error.

We conducted an additional analysis of canopy cover by excluding oaks from our estimates and only included conifer contributions to canopy cover. This allowed us to better estimate how density and distribution of conifers has affected canopy cover without these estimates being skewed by these large

changes in oak density. Because *Q. chrysolepis* density increased significantly more than any other species, we were concerned that the increase in *Q. chrysolepis* may be one of the sole drivers behind the observed increases in canopy cover estimates. When oaks were excluded, total canopy cover increased from 45.2% (± 1.7 SE) to 57.1% (± 1.9 SE) resulting in a percent increase of 26.3% (Table 16, Figure 32). ANF still experienced the largest increase in canopy cover; historic estimates were 43.8% (± 3.4 SE) and current estimates are 62.5% (± 5.8 SE). This represents a percent increase of approximately 43% ($p < 0.01$). SBNF also experienced a significant increase (37.7%, $p < 0.001$) in canopy cover but LPNF did not ($p=0.85$).

Table 16. Total percent change in canopy cover and National Forest between historic (VTM) and contemporary (FIA) data when oaks were excluded in the analysis.

National Forest	VTM Mean (\pm SE)	FIA Mean (\pm SE)	Percent Change	p value	Effect Size
Total	45.2 (± 1.7)	57.1 (± 1.9)	26.27%	< 0.001	small
ANF	43.8 (± 3.4)	62.5 (± 5.8)	42.7%	0.008	medium
LPNF	52.8 (± 3.5)	53.8 (± 3.6)	1.84%	0.85	--
SBNF	42.4 (± 2.2)	58.3 (± 2.5)	37.65%	< 0.001	medium

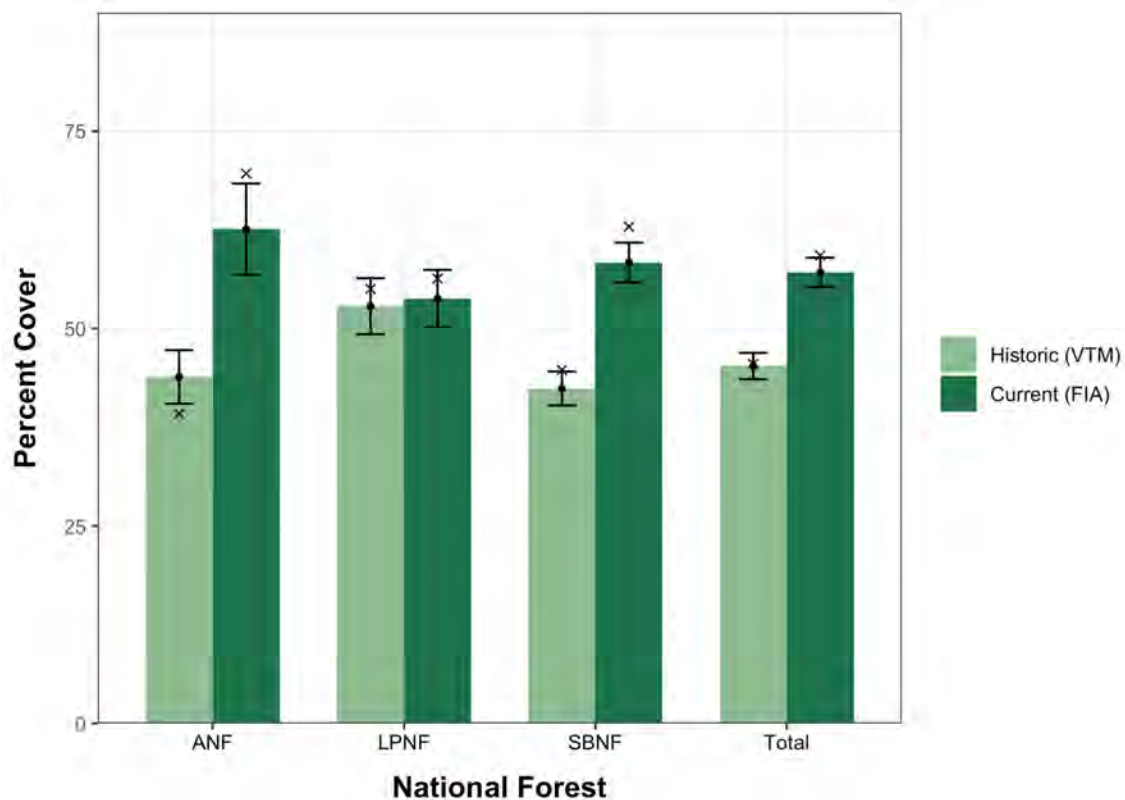


Figure 32. Percent canopy cover excluding oak species (*Q. chrysolepis* and *Q. kelloggii*). CNF was excluded from the analysis because there were only 2 VTM plots and 4 FIA plots. Xs mark the median, black dots mark the mean, and the bars represent that standard error.

By Elevation

All elevations classes except the lowest elevation (1000–1499m) experienced a significant increase in canopy cover (Table 17, Figure 33). Higher elevations (2000–2500+m) experienced greater changes in canopy cover than lower elevations (1000–1999m). The greatest increase in canopy cover occurred at elevations greater than 2500m. Historic canopy cover estimates averaged 35.8% (± 6.8 SE) while contemporary canopy cover estimates averaged 61.4% (± 5.0 SE). This resulted in an increase of approximately 72%. Though elevations greater than 2500m experienced the greatest increase, this elevation class also had the smallest sample size with only 13 plots in the VTM dataset.

Table 17. Average canopy cover by elevation band.

Elevation band (m)	VTM Mean (\pm SE)	FIA Mean (\pm SE)	Percent Change	p value	Effect Size
1000–1499	63.0 (± 6.5)	67.7 (± 5.3)	7.45%	0.58	--
1500–1999	58.4 (± 2.4)	74.1 (± 2.7)	26.62%	< 0.001	medium
2000–2499	48.7 (± 2.4)	69.9 (± 2.7)	43.39%	< 0.001	medium
>2500	35.8 (± 6.8)	61.4 (± 5.0)	71.79%	0.005	large

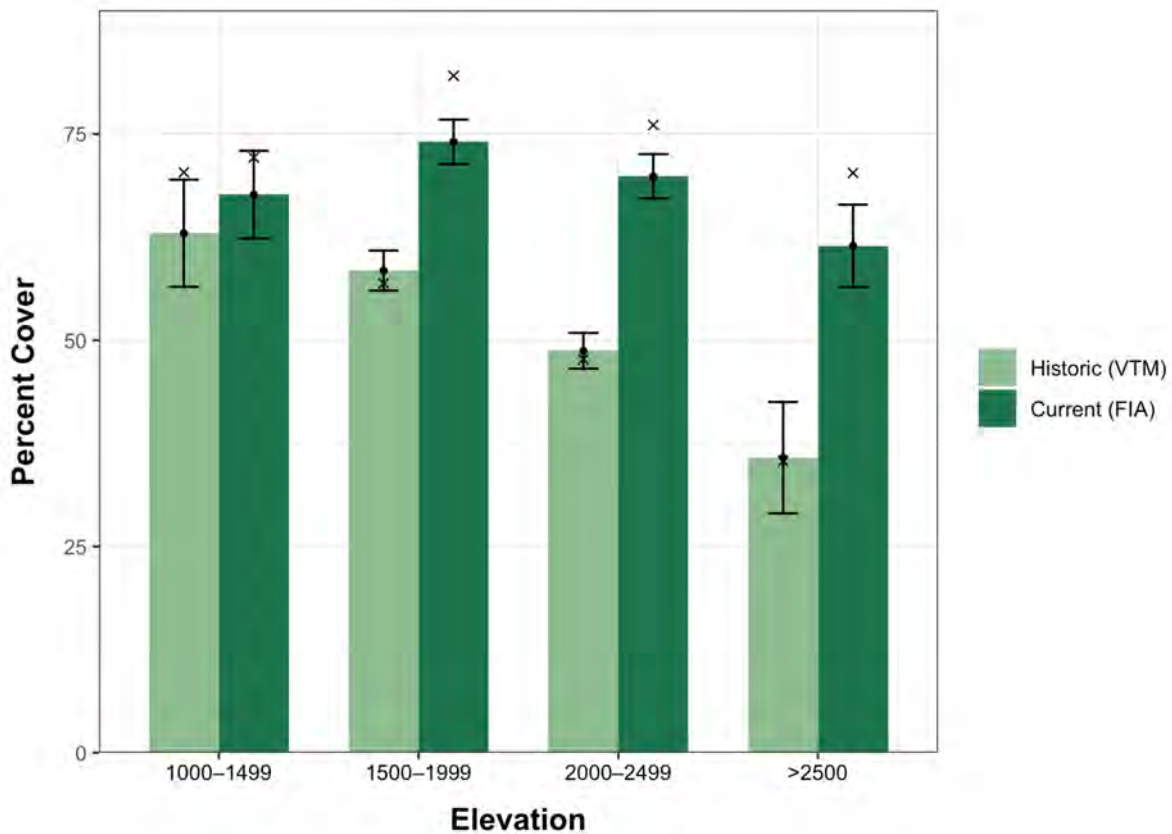


Figure 33. Historic and current canopy cover averages by elevation band. Xs mark the median, black dots mark the mean, and the bars represent that standard error.

5.5.3 NRV Analysis

We were unable to find any studies that calculated percent canopy cover using FVS methods for historic or contemporary southern California YPMC forests. However, there are studies that have calculated percent canopy cover in SSPM using field methods, including ocular estimates (Dunbar-Irwin and Safford, 2016; Safford, *in prep.* as cited in Safford & Stevens, 2017) and site tubes (Stephens et al., 2007).

Stephens et al. (2007) sampled 121 plots in SSPM and recorded canopy cover using two methods: a sight tube and a spherical densiometer. Plots were spaced 5m apart and at each plot, percent canopy cover was estimated. With the sight tube, surveyors counted the total number of points under the canopy and divided by the total number of points sampled. Stephens et al. (2007) found an average canopy cover of 26.8% (± 1.1 SE) across all sampled SSPM plots using the sight tube. With the densiometer, measurements of canopy cover at each plot center were tallied in each cardinal direction. With this method, the percent canopy cover was estimated at 40.1% (± 1.6 SE). Our canopy cover estimates using the FVS method resulted in estimates that more closely match Stephens et al.'s densiometer results, although our historic estimates of canopy cover, with oaks included in the calculations, are still 10 percentage points larger. Our historic estimates of canopy cover, excluding oaks from the calculations, is only 5 percentage points larger than Stephen et al.'s densiometer results. This suggests that historic canopy cover, both as estimated from the VTM dataset (with and without oaks) and estimates from SSPM as a reference site, was approximately 41%. Dunbar-Irwin and Safford (2016) found a similar canopy cover estimate to Stephens et al.'s (2007) sight tube method. Using an ocular estimate for 86 plots, Dunbar-Irwin and Safford found that the average canopy cover in SSPM was 24.9% (± 2.4 SE). Our combined historic averages for canopy cover – including and excluding oaks – were approximately 23 percentage points larger than Stephens et al.'s sight tube estimates and Dunbar-Irwin and Safford's ocular estimate.

Safford (*in prep.*) estimated canopy cover in contemporary Jeffrey pine forests in Sierra Juarez, another reference site in Baja California. Using an ocular estimate, Safford found an average canopy cover of approximately 35.8% (± 7.6 SE). In this case, Safford's results are more similar to Stephens et al.'s densiometer method. Though we did not break down our analysis by sub-forests within YPMC, our canopy cover estimates of just conifer species was 10 percentage points greater than Safford's. As shown by Stephens et al. (2007), Dunbar-Irwin and Safford (2016), and Safford (*in prep.*, as cited in Safford & Stevens, 2017), using different methods to calculate canopy cover can result in very different estimates. Different instruments will evaluate different characteristics of canopy cover. Using a variety of methods to estimate canopy cover can enhance an NRV by producing multiple average measurements.

Though we are unable to compare our contemporary canopy cover estimates with other studies, we believe our contemporary estimates could be underestimating true canopy cover, due to non-YPMC species being excluded from our analysis. On average, there were approximately four non-YPMC tree species per plot that were not included in our canopy cover analysis. Our results reveal that canopy cover is increasing significantly in all National Forests (when oaks are included) and at all elevation bands except 1000–1499m. With the increasing threat of more frequent wildfires, southern California YPMC are at risk of experiencing stand-replacing crown fires (Weatherspoon et al., 1992). As canopy cover in southern California YPMC forests continue to increase, these forests are at risk of being lost indefinitely.

5.6 Shrub Cover

5.6.1 Methods

We explored two datasets for gathering historic shrub data, both obtained from the Wieslander VTM project: 1) vegetation maps and 2) plot data. VTM vegetation maps were created in the field by direct observation and depicted forest types and associated dominant plant species across the surveyed landscape (Kelly et al., 2016; Kelly & Allen-Diaz, 2009). While Thorne et al. (2008) found vegetation maps useful to analyze more general patterns in land cover change, we concluded that the VTM vegetation maps do not accurately capture historic shrub cover in YPMC forests, and therefore would be of little value to the NRV shrub analysis (Section 5.6.3). A consultation with Dr. Frank Davis confirmed that these vegetation maps would likely not be the best measure of understory species composition or abundance. Shrubs that were not directly exposed to the sky would not have been accounted for due to being blocked by taller vegetation. Vegetation surveying for the mapping project took place from vantage points at the tops of ridges and peaks, rather than at ground level. Surveyors were only concerned with “the dominant vegetation visible externally” (Wieslander, 1935) and understory vegetation was not recorded.

In contrast to the vegetation maps, VTM plot data provides us with more robust information on historic YPMC shrub composition. Brush and ground cover data at the plot level was collected by recording the dominant shrub species present in each of the 100 equal subplots comprising each plot. VTM forested plots were roughly 800m², therefore each subplot was approximately 8m². A shrub species was recorded as dominant for any given subplot if the species covered over 50% of the subplot. The final percent shrub cover recorded for each species was the percentage of subplots in which it was dominant. Therefore, 100% shrub cover in a given plot means that shrub cover was >50% in each of the 100 subplots (Keeley, 2004). This approximation allows for a significant amount of true bare ground and other vegetation to be classified as shrub cover (Keeley, 2004). VTM shrub cover can also be an overestimation. For example, a shrub species could have covered only 60% of a subplot but recorded as 100%. Therefore, we concluded that the quantitative shrub cover estimates would not be useful to compare shrub cover estimates with contemporary shrub cover. Instead, we reported the most dominant shrubs as well as provide the relative dominance of that shrub. This was calculated by dividing the total number of subplots dominated by a single shrub species by the total number of subplots marked by shrub presence (see Supplemental Appendix A).

We obtained information on contemporary shrub cover from the USFS dataset. The FSVEG_VXPT_V datasheets provided by the USFS Region 5 Remote Sensing Lab recorded shrub cover to the nearest 1%. Shrub cover is defined as the percent of the area occupied by the plant or ground surface cover (O’Connell et al., 2015). Shrub cover was recorded as absolute cover and did not account for overlapping shrubs, which means a plot could have over 100% cover (Safford & Stevens, 2017). We only used shrub data from the USFS dataset instead of from the combined FIA dataset. Shrub records in the national FIA data were still in their raw form and we were unable to replicate the methods used by the Remote Sensing Lab to calculate shrub cover. Therefore, our sample size for the shrub analysis is smaller than previous analyses (Table 18). We summed the total shrub cover by species or genus across the entire YPMC landscape, by National Forest, and elevation band. We then divided by the total number of plots (either all plots, plots in each NF, and plots per elevation band) to find the average absolute percent cover. Shrub species and genera with the highest average absolute cover were generated into a table. The relative dominance calculated in the VTM data measures the sum of recorded cover for dominant shrubs, while USFS data calculates average shrub cover. Though these results cannot be directly compared between one another, they can be used to estimate shrub dominance between the historic VTM data and USFS contemporary data.

Making statistical comparisons between shrub cover from the VTM and combined FIA datasets was not possible due to shrub cover being recorded differently between the two datasets. Instead, we made qualitative comparisons on the dominant shrubs over time. Analysis of both historic and contemporary shrub cover focused on the overall dominant YPMC shrub species, as well as dominant YPMC shrub species by genus, National Forest, and elevation bands. This analysis demonstrates the most dominant species and genus across the landscape both in the early 1900s and 2000s.

Table 18. Only the USFS data had recorded shrub data and therefore, not all plots analyzed in Sections 3.1-3.4 were analyzed for shrubs. The number of plots in the USFS data represents the number of plots with recorded shrub observations.

National Forest	No. of Plots in USFS data	Total Plots in FIA + USFS data
All	124	210
ANF	12	26
CNF	2	4
LPNF	41	62
SBNF	69	107

5.6.2 Results

By Species

In historic YPMC forests, *Artemisia tridentata* (sagebrush) was the most dominant shrub species followed by *Ceanothus cordulatus* (mountain whitethorn) and *Quercus chrysolepis* (Canyon live oak) (Table 19). Though *Q. chrysolepis* is also considered a tree and was used in our previous analyses, it can often grow as a shrub (Tollefson, 2008), especially after wildfires. *Quercus chrysolepis* was recorded in both the shrub and tree datasheets in the VTM and USFS dataset, however, *Q. chrysolepis* may have been recorded more often as a tree than a shrub in the USFS dataset. In contemporary forests, *C. cordulatus*, *Cercocarpus ledifolius* (curl-leaf mountain mahogany), and *Arctostaphylos patula* (greenleaf manzanita) were the three most dominant shrub species (Table 20). *Artemisia tridentata* was the fourth most dominant shrub species. Both datasets recorded *A. tridentata* and *C. cordulatus* as two of the top four most dominant shrub species.

Table 19. Relative dominance of the top 10 shrub species in historic forests.

Common Name	Scientific Name	No. of plots observed in	Relative Dominance
big sagebrush	<i>Artemisia tridentata</i>	20	15.72%
mountain whitethorn	<i>Ceanothus cordulatus</i>	27	13.65%
canyon live oak	<i>Quercus chrysolepis</i>	50	10.86%
bush chinquapin	<i>Chrysolepis sempervirens</i>	19	10.08%
deer brush	<i>Ceanothus integerrimus</i>	19	5.41%
Eastwood manzanita	<i>Arctostaphylos glandulosa</i>	4	4.27%
interior live oak	<i>Quercus wislizenii</i>	10	3.97%
curl-leaf mountain mahogany	<i>Cercocarpus ledifolius</i>	8	3.53%
pinkbracted manzanita	<i>Arctostaphylos drupacea</i>	12	3.17%
chamise	<i>Adenostoma fasciculatum</i>	2	2.21%

Table 20. Average percent cover of the top 10 shrub species in contemporary forests. Percent cover is the cover across all plots (n=124).

Common Name	Scientific Name	No. of plots observed in	Percent Cover
whitethorn ceanothus	<i>Ceanothus cordulatus</i>	25	6.58%
curl-leaf mountain mahogany	<i>Cercocarpus ledifolius</i>	21	5.97%
greenleaf manzanita	<i>Arctostaphylos patula</i>	20	4.07%
big sagebrush	<i>Artemisia tridentata</i>	22	3.91%
bush chinquapin	<i>Chrysolepis sempervirens</i>	7	3.08%
deerbrush	<i>Ceanothus integerrimus</i>	19	2.31%
Tucker's oak	<i>Quercus john-tuckeri</i>	11	2.04%
buckbrush	<i>Ceanothus cuneatus</i>	5	1.99%
Eastwood's manzanita	<i>Arctostaphylos glandulosa</i>	7	1.83%
creeping snowberry	<i>Symphoricarpos mollis</i>	16	1.49%

By Genus

When we analyzed the most dominant shrub genera, we found that *Ceanothus* had the highest percent cover in both time frames. In historic forests (n=195), *Ceanothus* was recorded in 62 plots and had approximately 24.22% relative dominance (Table 21). In contemporary forests (n=124), *Ceanothus* was recorded in 56 plots and averaged approximately 11.4% cover (Table 22). *Arctostaphylos* was also among one of the most dominant shrub genera in both time frames; approximately 7% of the landscape in contemporary forests and had a relative dominance of 16.5% in historic forests. This does not mean that *Arctostaphylos* or *Ceanothus* are decreasing; historic shrub cover records are likely overestimates. *Artemisia* and *Quercus* were also two genera that were dominant between both time frames.

Table 21. Relative dominance of the top 10 shrub genera in historic forests (n=195).

Genus	No. of plots observed in	Relative Dominance
<i>Ceanothus</i>	62	24.22%
<i>Quercus</i>	58	16.64%
<i>Arctostaphylos</i>	37	16.49%
<i>Artemisia</i>	20	15.72%
<i>Chrysolepis</i>	19	10.08%
<i>Cercocarpus</i>	20	5.52%
<i>Adenostoma</i>	2	2.21%
<i>Symphoricarpos</i>	6	1.80%
<i>Ribes</i>	12	1.32%
<i>Amorpha</i>	37	1.25%

Table 22. Average percent cover for the top 10 shrub genera in contemporary forests (n=124).

Genus	No. of plots observed	Percent cover
<i>Ceanothus</i>	56	11.40%
<i>Arctostaphylos</i>	36	7.00%
<i>Cercocarpus</i>	32	6.69%
<i>Artemisia</i>	26	4.82%
<i>Quercus</i>	16	3.67%
<i>Chrysopsis</i>	7	3.08%
<i>Symphoricarpos</i>	28	2.41%
<i>Eriogonum</i>	15	1.48%
<i>Ericameria</i>	11	1.35%
<i>Fremontodendrom</i>	5	1.05%

By National Forest

Though *Arctostaphylos* and *Ceanothus* are some of the most dominant shrub genera across the entire study area, there was variation in dominant shrub species when we separated the analysis by National Forest. In ANF, *Chrysolepis sempervirens* (bush chinquapin) was the most dominant shrub species in both historic and contemporary forests. In historic forests, *C. sempervirens* had a relative dominance of approximately 33% (Table 23) and had an average shrub cover of 10% in contemporary forests (Table 24). In CNF, both time frames had *Eriogonum fasciculatum* (California buckwheat) as one of the three most dominant shrub species; historic forests had a relative dominance of 4.4% and contemporary forests average 18% cover. It is important to note that there were only 2 plots within CNF in both the VTM and USFS dataset so the reported measures may be biased. *Artemisia tridentata* was again one of the most dominant shrub species in both historic and contemporary forests in LPNF; historic relative dominance was 33.6% and contemporary average shrub cover was 8.63%. *Ceanothus cordulatus* and *A. patula* continued to be two of the most dominant shrub species in SBNF in both historic and contemporary forests.

Table 23. Relative dominance for the top three shrub species by National Forest in historic forests. ANF has 20 plots, CNF has 2 plots, LPNF has 54 plots, and SBNF has 113 plots.

National Forest	Common Name	Scientific Name	No. of plots observed in	Relative Dominance
ANF	bush chinquapin	<i>Chrysolepis sempervirens</i>	3	32.97%
ANF	prostrate ceanothus	<i>Ceanothus prostratus</i>	1	24.18%
ANF	bigberry manzanita	<i>Arctostaphylos glauca</i>	3	19.78%
CNF	big sagebrush	<i>Artemisia tridentata</i>	1	52.94%
CNF	pointleaf manzanita	<i>Arctostaphylos pungens</i>	1	38.24%
CNF	California buckwheat	<i>Eriogonum fasciculatum</i>	1	4.41%
LPNF	big sagebrush	<i>Artemisia tridentata</i>	12	33.64%
LPNF	Eastwood manzanita	<i>Arctostaphylos glandulosa</i>	3	11.04%
LPNF	canyon live oak	<i>Quercus chrysolepis</i>	25	8.08%
SBNF	mountain whitethorn	<i>Ceanothus cordulatus</i>	2	22.38%
SBNF	bush chinquapin	<i>Chrysolepis sempervirens</i>	16	15.51%
SBNF	canyon live oak	<i>Quercus chyrsolepis</i>	25	13.41%

Table 24. Average percent cover for the top three shrub species by National Forest in contemporary forests. ANF had a total of 12 plots, CNF had 2 plots, LPNF had 41 plots, and SBNF had 69 plots. The percent cover represents the cover of the shrub only in the corresponding National Forest.

National Forest	Common Name	Scientific Name	No. of plots observed in	Percent Cover
ANF	bush chinquapin	<i>Chrysolepis sempervirens</i>	2	10.33%
ANF	curl-leaf mountain mahogany	<i>Cercocarpus ledifolius</i>	2	6.83%
ANF	Eastwood's manzanita	<i>Arctostaphylos glandulosa</i>	1	4.75%
CNF	California buckwheat	<i>Eriogonum fasciculatum</i>	2	18.00%
CNF	Palmer ceanothus	<i>Ceanothus palmeri</i>	1	3.50%
CNF	birchleaf mountain mahogany	<i>Cercocarpus montanus var. glaber</i>	1	3.00%
LPNF	big sagebrush	<i>Artemisia tridentata</i>	8	8.63%
LPNF	whitethorn ceanothus	<i>Ceanothus cordulatus</i>	6	6.63%
LPNF	Tucker's oak	<i>Quercus john-tuckeri</i>	11	6.17%
SBNF	curl-leaf mountain mahogany	<i>Cercocarpus ledifolius</i>	18	9.43%
SBNF	whitethorn ceanothus	<i>Ceanothus cordulatus</i>	19	7.88%
SBNF	greenleaf manzanita	<i>Arctostaphylos patula</i>	18	6.45%

By Elevation

Similarly, when analyzing shrub cover by elevation, *Arctostaphylos* and *Ceanothus* species remained the most dominant. In historic forests, *C. cordulatus* was one of the top three most dominant shrub species in elevations between 2000–2499m and greater than 2500m (Table 25). *Ceanothus cordulatus* was one of the top three most dominant shrub species in every elevation class in contemporary forests (Table 26). The most dominant shrub genera across each elevation class were largely comprised of *Arctostaphylos*, *Ceanothus*, *Quercus*, *Artemisia*, and *Chrysolepis* in both historic and contemporary forests (Table 27 and Table 28).

Table 25. Relative dominance of the top three species by elevation class in historic forests. 1000–1499m has 20 plots, 1500–1999m has 84 plots, 2000–2499m has 77 plots, and greater than 2500m has 13 plots.

Elevation (m)	Common Name	Scientific Name	No. of plots observed in	Relative Dominance
1000–1499	big sagebrush	<i>Artemisia tridentata</i>	4	35.06%
1000–1499	deer brush	<i>Ceanothus integerrimus</i>	8	18.83%
1000–1499	woolly leaf manzanita	<i>Arctostaphylos tomentosa</i>	2	12.55%
1500–1999	canyon live oak	<i>Quercus chrysolepis</i>	30	14.55%
1500–1999	Eastwood manzanita	<i>Arctostaphylos glandulosa</i>	4	11.89%
1500–1999	pinkbracted manzanita	<i>Arctostaphylos drupacea</i>	11	8.61%
2000–2499	mountain whitethorn	<i>Ceanothus cordulatus</i>	26	30.26%
2000–2499	big sagebrush	<i>Artemisia tridentata</i>	12	19.79%
2000–2499	bush chinquapin	<i>Chrysolepis sempervirens</i>	15	18.82%
>2500	bush chinquapin	<i>Chrysolepis sempervirens</i>	4	44.78%
>2500	mountain whitethorn	<i>Ceanothus cordulatus</i>	1	20.15%
>2500	curl-leaf mountain mahogany	<i>Cercocarpus ledifolius</i>	2	12.69%

Table 26. Average percent cover for the top three shrub species by elevation class in contemporary forests. 1000–1499m has 12 plots, 1500–1999m has 51 plots, 2000–2500m has 48 plots, and >2500m has 13 plots. Percent cover reflects the cover within each elevation class.

Elevation (m)	Common Name	Scientific Name	No. of plots observed in	Percent Cover
1000–1499	whitethorn ceanothus	<i>Ceanothus cordulatus</i>	3	12.25%
1000–1499	Tucker’s oak	<i>Quercus john-tuckeri</i>	3	10.17%
1000–1499	scrub oak	<i>Quercus berberidifolia</i>	1	6.25%
1500–1999	whitethorn ceanothus	<i>Ceanothus cordulatus</i>	6	4.86%
1500–1999	big sagebrush	<i>Artemisia tridentata</i>	9	4.82%
1500–1999	deerbrush	<i>Ceanothus integerrimus</i>	14	4.71%
2000–2499	curl-leaf mountain mahogany	<i>Cercocarpus ledifolius</i>	15	13.63%
2000–2499	whitethorn ceanothus	<i>Ceanothus cordulatus</i>	12	7.40%
2000–2499	greenleaf manzanita	<i>Arctostaphylos patula</i>	12	6.29%
>2500	bush chinquapin	<i>Chrysolepis sempervirens</i>	5	25.31%
>2500	greenleaf manzanita	<i>Arctostaphylos patula</i>	4	15.15%
>2500	big sagebrush	<i>Artemisia tridentata</i>	1	7.00%

Table 27. Relative dominance for the top three genera in historic forests by elevation class. 1000–1499m has 20 plots, 1500–1999m has 84 plots, 2000–2499m has 77 plots, and >2500m has 13 plots.

Elevation (m)	Genus	No. of plots observed in	Relative Dominance
1000–1499	<i>Artemisia</i>	4	35.06%
1000–1499	<i>Quercus</i>	9	21.86%
1000–1499	<i>Ceanothus</i>	8	19.05%
1500–1999	<i>Arctostaphylos</i>	21	29.92%
1500–1999	<i>Quercus</i>	35	24.18%
1500–1999	<i>Ceanothus</i>	23	14.55%
2000–2499	<i>Ceanothus</i>	30	35.27%
2000–2499	<i>Artemisia</i>	12	19.79%
2000–2499	<i>Chrysolepis</i>	15	18.82%
>2500	<i>Chrysolepis</i>	4	44.78%
>2500	<i>Ceanothus</i>	1	20.15%
>2500	<i>Cercocarpus</i>	2	12.69%

Table 28. Average percent cover for the top three genera in contemporary forests by elevation class. 1000–1499m has 12 plots, 1500–1999m has 51 plots, 2000–2500m has 48 plots, and >2500m has 13 plots.

Elevation (m)	Genus	No. of plots observed in	Percent cover
1000–1499	<i>Ceanothus</i>	8	1.77%
1000–1499	<i>Ericameria</i>	5	0.83%
1000–1499	<i>Artemisia</i>	4	0.58%
1000–1499	<i>Quercus</i>	4	0.58%
1500–1999	<i>Ceanothus</i>	25	1.18%
1500–1999	<i>Arctostaphylos</i>	16	0.55%
1500–1999	<i>Artemisia</i>	11	0.55%
2000–2499	<i>Cercocarpus</i>	16	13.79%
2000–2499	<i>Ceanothus</i>	18	12.35%
2000–2499	<i>Arctostaphylos</i>	13	6.38%
>2500	<i>Chrysolepis</i>	5	25.31%
>2500	<i>Arctostaphylos</i>	5	15.69%
>2500	<i>Artemisia</i>	1	7.00%

5.6.3 NRV Analysis

Historic observations of shrubs in YPMC forests reveal that the composition was relatively open and heterogeneous. According to Leiberg (1898), shrub cover was inverse to tree density; areas with greater tree density had less shrub cover, and areas with lower tree density had higher shrub cover (Minnich, 1988). Additionally, lower elevations of YPMC forests had higher shrub cover compared to high elevations. At lower elevations of the San Gabriels, Leiberg recorded moderate quantities of scrub oak (*Quercus berberidifolia*), manzanita (*Arctostaphylos sp.*), mountain mahogany (*Cercocarpus sp.*), and ceanothus. We found similar dominant genera of shrubs at lower elevations in our analysis of historic and contemporary forests (Table 27). However, Leiberg reported significantly less, and oftentimes, no shrubs at all at higher elevations.

While surveying within SBNF, Leiberg (1898) recorded that brush was “mostly low and scattered.” Early 1900s observations from Charles Francis Saunders and Harvey Monroe Hall in other National Forests were similar. Saunders (1923) noted that LPNF was clear of underbrush. In ANF, Saunders recorded that the forest floor was “open to the sun that wild grasses were abundant.” In CNF, the higher elevations were generally clear of brush but with annual blooms of violets and buttercups. In a botanical survey of San Jacinto Mountain, Hall (1902) noted that shrubs were not of great importance due to forests being largely free of underbrush. A compilation of surveys and reports from 1902-1906 (USDA, 1905) yields similar observations from Leiberg, Saunders, and Hall. In SBNF, ground cover is described as scant, thin, and scattered (USDA, 1905). However, there were observations of abundant patches of sagebrush (*A. tridentata*), ceanothus, mountain mahogany, and manzanitas, suggesting heterogeneity across the landscape (USDA, 1905).

Many observations noted that areas with the greatest shrub cover were areas that recently experienced fire (Blakley & Barnette, 1985; Leiberg, 1898). When looking at VTM maps and 1938 photographs, Minnich (1988) was able to confirm Leiberg’s observations that chaparral understory was most dense in recent burn areas. Chaparral shrubs, like ceanothus, generally respond well to fire as they are obligate and facultative resprouters (League, 2005; Meyer, 2011), and produce seeds that germinate after fires (Cornwell et al., 2012). Additionally, with less canopy cover in historic forests, light was able to reach the forest floor and support the regeneration of shrub species.

Analysis of SSPM shrub cover provides an example of what shrub cover looks like in a landscape that has experienced a more natural fire regime than southern California. SSPM has been described to have open shrub cover (Minnich et al., 2000; Passini et al., 1989). Dunbar-Irwin and Safford (2016) surveyed understory shrubs in SSPM in 86 of plots and found that the average percent cover was approximately 17%. This is considerably lower than what we found in contemporary southern California YPMC forests (Table 29). Average shrub cover in our analysis ranged from 40% to 56%. Though CNF had an average percent cover of 29%, there were only 2 plots with shrub data. Therefore, our CNF shrub cover results are unlikely to be representative of true shrub cover. Additionally, Barbour and Minnich (2000) reported that shrub and herb cover in SSPM Ponderosa pine forests was only around 5-10%, even lower than what was reported by Dunbar-Irwin and Safford. The lack of frequent fires in southern California YPMC forests could be contributing to higher shrub cover and litter accumulation (Minnich et al., 2000).

Table 29. Average shrub cover by National Forest in contemporary southern California YPMC forests.

National Forest	Average Percent Cover
All	52.4%
ANF	40.6%
CNF	29.0%
LPNF	50.8%
SBNF	56.1%

Our qualitative analysis of shrub composition in both historic and contemporary southern California forests reveals similarities between shrub composition in SSPM. Minnich et al. (2000) noted that SSPM mixed Jeffrey pine and white fir forests had *Quercus chrysolepis*, *Arctostaphylos patula*, and *Ceanothus cordulatus*, which are all common species in current and historic southern California YPMC forests. Additionally, the dominant genera found in SSPM are similar to those found in southern California: *Ceanothus*, *Arctostaphylos*, *Artemisia*, *Ericameria*, and *Salvia* (Dunbar-Irwin & Safford, 2016).

There is limited literature available on recent shrub cover estimates in southern California. However, it is likely that there are areas in contemporary forests with low shrub cover even in the absence of regular fire. A somewhat recent phytogeography of SBNF in 1994 noted that Jeffrey pine forests had an open understory, and that understory species were relatively diverse (Krantz, 1994). Shrubs often grow in scattered patterns due to their high light requirement (Conrad et al., 1985; Cronemiller, 1959). Areas with a heterogenous stand structure and high canopy cover will likely have lower cover of understory shrubs because of the limited amount of light able to reach the understory. Conversations with the USFS revealed that managers are primarily concerned about increases in shrub cover and their potential to drive high severity fires. Though shrub cover may not be high in all areas of contemporary forests, shrubs play an integral role in forest health and too much shrub cover can prevent tree regeneration and increase fire severity (Knapp et al., 2012).

Due to the large differences in how data was collected, our analysis does not reveal with certainty whether average shrub cover has increased significantly between the early 1900s and 2000s. It does appear that species composition has remained relatively consistent, and there are clearly some shrub genera and species that are more dominant than others throughout both time periods. Some of the most dominant shrub species we noted were: *Arctostaphylos patula*, *Ceanothus cordulatus*, *Artemisia tridentata*, *Amelanchier utahensis*, and *Cercocarpus ledifolius*.

5.7 Limitations

There are several limitations to our analysis that are important to address. While VTM data is the only set of robust, quantitative data available to represent historic conditions for our study area, there are several issues that reveal some shortcomings when using the data to compare to contemporary conditions. The main issue is the speculation that surveyors preferentially placed plots in forests that were less dense but contained more mature trees (Bouldin, 2009). This suggests that the VTM data will have lower mean density than the actual historic density. However, basal area depends on the number of trees and the size of the trees, so basal area calculated from the VTM dataset may be larger or smaller than true historic conditions depending on these factors. Using data from the mid-1900s, Bouldin (2009) and Weeks (1942) found that the density of large trees (>60cm d.b.h.) were 2.8 and 2.6 times greater than estimates found in the VTM data, respectively. This indicates that the basal area calculated from the VTM dataset overestimated the true landscape scale basal area. Thus, our findings of significant increases in basal area and significant increases in large diameter trees are likely larger than observed. Contrastingly, the increases in overall tree density and density of trees <61cm is likely lower than we observed.

While we found over a 500% increase in oak density, it is currently unknown if this significant increase is completely the result of increased *Q. chrysolepis* density or if it is partially the result of differing sampling methodologies between the VTM and FIA datasets. It is common for *Q. chrysolepis* to split into more than one branch below diameter at breast height. In this case, it is highly likely that FIA surveyors recorded multiple branching stems from one tree as multiple trees instead of as a single tree. While the FIA data collection protocol does not explicitly state that this process occurred, other federal surveying protocols use this approach (e.g., Common Stand Exams). The VTM data collection protocol also does not state how surveyors recorded multiple *Q. chrysolepis* branches, however we believe that they recorded them as a single tree because there were no many *Q. chrysolepis* individuals in a plot. Other researchers in California have found increases in *Q. chrysolepis* (Dolanc et al., 2013; Dolanc et al., 2014, Lutz et al., 2009), but they did not address this surveying bias in their methods. This discrepancy in methodologies likely resulted in the dramatic increase in *Q. chrysolepis*. While our understanding of ecological systems reinforces that there has likely been a large increase in oak density in southern California, especially as the climate warms (Adam & West, 1983; Heusser, 1992), land managers need to know the true extent of this change in vegetation composition and structure to make informed management decisions. Future research should look into how FIA and VTM surveys recorded *Q. chrysolepis* to determine the true change in density of *Q. chrysolepis*.

Additionally, there were some discrepancies between how VTM and FIA surveyors recorded oaks in the shrub cover analysis. According to the Natural Resources Conservation Service (NRCS), *Q. chrysolepis* can be classified as both a tree and a shrub. *Quercus chrysolepis* was frequently recorded by VTM surveyors as a shrub although there was no indication into the distinction the surveyors used to classify *Q. chrysolepis*. It may be safe to assume they used 4in. d.b.h. as their threshold, however, there were some *Q. chrysolepis* recorded as shrubs with a height over 10ft and a maximum of 30ft. While *Q. chrysolepis* was also recorded as a shrub by FIA surveyors, we believe surveyors recorded *Q. chrysolepis* primarily as a tree since FIA is a tree inventory program and because *Q. chrysolepis* was not one of the top 10 dominant shrub species (see Section 5.6.2) despite a greater than 500% increase in contemporary *Q. chrysolepis* density. We did not remove *Q. chrysolepis* from the VTM shrub data nor did we count *Q. chrysolepis* in the shrub data above a certain height threshold as a tree when calculating tree density because there was no way to verify these assumptions. If *Q. chrysolepis* was being recorded as a shrub in the VTM dataset instead of a tree this also would have underestimated true *Q. chrysolepis* abundance and could have contributed to the large increase in *Q. chrysolepis* density. Future analysis of shrub cover should consider removing *Q. chrysolepis* from the VTM data when performing a comparative analysis with FIA shrub data.

Regarding our shrub cover analysis (Section 5.5), we were limited due to the way VTM surveyors collected data, which resulted in historic estimates being over or underestimated relative to modern shrub cover measurements. VTM surveyors broke down each plot into 100 subplots and only recorded a shrub species if it covered 50% or more of that subplot. If a shrub species did cover 50% or more of a subplot, it was recorded as having 100% cover for that subplot, or 1% cover of that plot. Recorded shrub cover can be overestimated because VTM surveyors recorded a shrub as having 100% cover in a subplot even if the shrub only covered 60% of the subplot. Similarly, recorded shrub cover could have been underestimated. For example, if a shrub only had 20% cover in a subplot, then it was not recorded at all. Due to this limitation, we were unable to conduct a reliable quantitative analysis to determine how much shrub cover has changed between historic and contemporary forests. While our analysis captures qualitative information on general changes in species composition in the understory, an analysis on quantitative changes would have been a more useful analysis for managers.

In regards to our estimates for density, basal area, and canopy cover analysis, only the nine defined YPMC species were used. The purpose of our analysis was to capture YPMC forest density and structure and not total forest density. Any tree that was not identified as a YPMC species, as defined by CALVEG (see Section 3.2), was removed from the analysis. This method was applied to both datasets so that comparisons could still be made between historic and contemporary forests. We calculated the total number of non-YPMC tree species in the plots used in our analysis. On average, there were approximately four non-YPMC tree species (range 0-49 trees) per plot that were not included in our density, basal area, and canopy cover analysis. Therefore, our analysis underestimates the true density, basal area, and canopy cover of these areas. Future research should investigate changes in forest structure and composition considering all tree species.

The approach used to calculate basal area of trees binned in the greater than 91.4cm d.b.h. size class could have impacted basal area estimates. The values used to represent the end range for trees with a d.b.h. greater than 91.4cm was determined from the FIA data, then applied and used to calculate the basal area of large trees in the VTM data (see Section 5.4.1). This assumes that large diameter trees in the VTM dataset have a similar distribution to those in the FIA data. Since basal area calculations require squaring the diameter, large diameter trees affected basal area estimates more than small diameter trees. If the distribution of trees in the VTM data is different from the distribution observed in the combined FIA data, then the historic basal area could be over or underestimated.

Lastly, due to data availability, our contemporary conditions were based on data collected between 2001 and 2010. Forest conditions may have changed substantially in the subsequent decade for several reasons. Numerous disturbances could have impacted landscape scale forest structure after 2010. Several large fires, which likely had large proportions of area burning at high severity (Nigro & Molinari, 2019), occurred in YPMC forests in SBNF (e.g., Cranston, Mountain, and Lake Fires). Additionally, the 2011-2018 drought resulted in the mortality of over 2 million trees in southern California (Moore et al., 2019); LPNF was the most affected in the study area. Mature trees were particularly impacted by the drought (Young et al., 2019). Future analyses should use more current data and should analyze plots based on the number of times burned (e.g., Dolanc et al., 2014) or burn severity to distinguish between trends that could be impacted by different disturbance histories.

5.8 Conclusions and Implications

Southern California YPMC forests have increased in tree density, basal area, and canopy cover since the early 1900s. Increases in shade tolerant and fire intolerant species, like *A. concolor* and *Q. chrysolepis*, are largely driving the increase in tree density. With climate change models predicting more frequent and severe drought (Berg & Hall, 2017; Diffenbaugh et al., 2015; Hayhoe et al., 2004), more destructive wildfires are likely to occur. Increases in tree density and drought can have disastrous consequences as denser and drier forests facilitate the spread and severity of wildfire (Miller et al., 2009; Miller & Safford, 2012). Additionally, a higher density of trees results in an increase in competition for water, and with climate change predicting more variable rainfall (Hayhoe et al., 2004), this competition will only be exacerbated. Increases in canopy cover have similar consequences; areas with larger canopies can facilitate the spread of crown fires (Birch et al., 2015). Crown fires often result in higher tree mortality and can devastate the habitat of California spotted owls who seek old-growth stands with moderate to high levels of canopy cover for nesting sites (Gutiérrez et al., 2017; LaHaye et al., 1997; Smith et al., 2002).

The observed increases in tree density, basal area, and canopy cover varied across the assessment area. Mean basal area significantly increased in ANF and SBNF, but median basal area declined in LPNF. Differences in logging intensity among the National Forests likely had an impact on these structural changes. ANF, which was the least impacted by logging (see Section 3.3), had the largest percent increase in the density of trees over 61cm. As a result, ANF had the largest increase in basal area. Conversely, while SBNF was the most impacted by logging, density of 61-91.3cm diameter trees more than doubled, although there was relatively no change in the density of trees >91.4cm. LPNF had moderate logging compared to SBNF, but had the smallest increase in 61-91.3cm diameter trees and was the only National Forest to have a decline in trees greater than 91.4cm. Climate change may be driving this trend in LPNF more than disturbance history, although more research is needed to verify this as this trend could also be the result of several compounding factors such as climate change, drought, fire, and bark beetles mortality.

YPMC forests in LPNF have some of the highest climatic water deficits (CWD) in the assessment area (see Section 3.1.1, Figure 2). LPNF also had a decline in median basal area, likely as a result of a net loss of the largest diameter trees which contribute the most to basal area. LPNF experienced some of the largest increases in CWD in southern California (McIntyre et al., 2015, Figure 3C). McIntyre et al. (2015) found a significant correlation ($p < 0.0001$, $R^2 = 0.11$) between CWD and changes between historic (VTM) and contemporary (FIA) density of large (>61cm) trees across California. However, the low R^2 value indicates that there are still other factors that are contributing more to declines in large diameter trees.

Climate may also be contributing to a more oak dominated forest at lower elevations. We found a significant decline in density of juvenile conifers at lower elevations (<1999m), yet density on average increased at higher elevations (>2000m). This suggests that when large diameter conifers die at lower elevations there will not be sufficient juveniles to replace them. Conversely, the density of oaks has increased in all size classes across all elevations where oaks are present, particularly below 1499m. More generally, increased dominance of oaks in California is expected (Lenihan et al., 2008; Safford et al., 2012; McIntyre et al., 2015; Stocker et al., 2013). Palynological records showed that oak and pine dominance has historically shifted with climatic changes in the past 150,000 years (Adam & West, 1983; Heusser, 1992); oak abundance increased during warmer, drier periods. Thus, our results indicate that there will likely be a compositional shift from conifer forests to oak woodlands that will be occurring at lower elevations (<1999m) as a result of climate change.

Fire will likely be the catalyst for this compositional shift because adult conifers can continue to persist for a long time in climates no longer suitable for seedlings (Bell et al., 2014). However, severe wildfire,

which has become common in southern California (Nigro & Molinari, 2019), has the ability to remove all or most of the adult conifers from large patches across the landscape. Non-serotinous conifers, like yellow pines, have shown to have poor regeneration after severe wildfires (Franklin & Bergman 2011; Parkinson et al., *in prep.*). Oaks, however, can resprout after their aboveground biomass is killed by fire, thus their abundance is reinforced by high severity fire in comparison to conifers (Cocking et al., 2014).

In addition to a compositional shift from conifer forests to oak woodlands, a compositional shift in southern California has also been observed in the density of shade tolerant and fire intolerant species. Minnich et al. (1995) noted a compositional shift occurring in SBNF when comparing VTM data to contemporary field surveys. In Jeffrey pine dominated forests, Minnich et al. found *P. jeffreyi* mixed with *C. decurrens* and some *A. concolor*. However, VTM surveyors only encountered *P. jeffreyi* in this forest type, demonstrating a shift in species composition to now include shade tolerant species in the understory. While we did not analyze our data by forest type, we did find a significant increase in density of shade tolerant/fire intolerant species. This was primarily due to *A. concolor* and *Q. chrysolepis*. It is possible that these shade tolerant species are thriving because of increases in large diameter (61-91.3cm) trees that likely resulted in a more closed canopy that favored shade tolerant species.

Another unique observation from our study is the significant increase in large diameter (61-91.3cm) trees. We believe these increases in large diameter conifer occurred for two reasons. Firstly, while logging has occurred in southern California it was not done nearly as intensely as seen in other parts of the state, particularly in Sierra Nevada. In our study area, most logging occurred in SBNF (see Section 3.3), while very little occurred in the other National Forests. We also checked VTM surveyors' records on disturbances in the plots they surveyed. Only 13 of the 195 plots used in our analysis were recorded as having been influenced by logging, and all 13 plots were in SBNF (Appendix M). However, historical literature review revealed that Frazier Mountain was heavily logged (Blakley & Barnette, 1985; Plummer & Gowsell, 1905), but there was no mention of logging in VTM plot notes in this area. This suggests that the VTM surveys may not have been diligent about recording disturbances in every plot. This could explain why Nigro & Molinari (2019) did not find a significant increase in large diameter trees (61-91.3cm) trees in their study area, which was confined to Frazier Mountain. Yellow pines were the most heavily logged conifer in the assessment area. Despite this, we still found a significant increase in density of yellow pines in the 61-91.3cm size class. This change could have occurred because these yellow pines were too small for harvesting in the early 1900s, but have now graduated to a larger size class. However, large diameter trees were disproportionately logged (Stephens et al. 2007), and we did observe a slight decline in density of yellow pines with diameters over 91.4cm. There are conflicting reports on the extent of historic logging that occurred in the National Forests, especially in SBNF which had the highest density of logging. So it is difficult to determine how logging could have impacted modern day forest structure. Logging may have occurred in discrete areas across the assessment area, and thus just small patches would be influenced by logging. Further research is needed to verify the extent of logging in southern California. Secondly, wildfires have been largely absent from interior forests since the early 1900s to the 2000s (Stephenson & Calcarone, 1999; Nigro & Molinari, 2019). Collins et al. (2011) found an increase in density of large diameter (>61.1cm) trees in Yosemite National Park as result of fire suppression. Thus, the approximately 80 to 100+ year absence of fire could have been sufficient time for small diameter trees to graduate to the larger size class.

In conclusion, we found significant changes in forest structure over the past century. These changes have important consequences for forest resilience, ecosystem services, and fire regimes. Our qualitative and quantitative analysis will be a valuable contribution to the USFS' NRV of southern California YPMC. The USFS will be able to integrate our analysis of historic conditions and shifts of forest structure over the last century into their forest health planning, as mandated by the LMP. Our analysis will provide a framework when making decisions about YPMC forest conservation.

6. Species Distribution Model

6.1 Overview

We used the maximum entropy model (MaxEnt) version 3.3.3k (Phillips et al., 2006; Phillips & Dudík, 2008) species distribution model (SDM) to model the historic, current, and projected habitat suitability of *P. jeffreyi* and *P. ponderosa* (yellow pines) across the Transverse Ranges. MaxEnt is a popular SDM used to estimate the probability of suitable habitat and future species distributions. MaxEnt has been found to outperform comparative SDMs on several occasions (Aguirre-Gutiérrez et al., 2013; Elith et al., 2006; Giovanelli et al., 2010; Merckx et al., 2011; Wisz et al., 2008).

Researchers have used MaxEnt to estimate suitable habitat for adult conifers (Franklin et al., 2013; McKenzie et al., 2003; Qin et al., 2017), but predicting future ranges based on current adult conifer distributions has drawbacks. This is an inappropriate approach since the conditions in which adult conifers germinated hundreds of years ago are not indicative of today's climate. Adult conifers can persist in areas no longer suitable for new recruits (Bell et al., 2014; Serra-Diaz et al., 2015). Therefore, the earlier and more climatically sensitive life stage of a conifer, i.e. seedlings and saplings (Ropert-Coudert et al., 2015), should be used as indicators of range shifts for long-lived, sessile species or as indicators for more general changes in forest conditions. Current researchers have already found range shifts between the ranges of adult and juveniles of the same species using species distribution models (Lenoir et al., 2009; Monleon & Lintz, 2015; Serra-Diaz et al., 2016; Zhu et al., 2012, 2014) and common garden experiments have also highlighted these shifts (Dingman et al., 2013; Fisichelli et al., 2014). Thus, we projected future distributions of yellow pines using presence data of saplings, rather than adults. Modeling sapling distributions is a more practical approach since saplings are more representative of how current climatic conditions impact landscape scale distribution of a species. To our knowledge, only one other researcher has created a SDM or MaxEnt model using only data on conifer saplings. McCann & Spasojevic (2020) compared the current distribution of saplings and adults from over two dozen tree species. Shirk et al. (2018) modeled Southwestern white pine using all life stages of the species, including seedlings and saplings, as presence points, but did not model based on sapling presences separately.

While seedling germination and survival in the first few years is a critical bottleneck period (Walck et al., 2011), we instead decided to focus on the continued survival of saplings, which is the next step of conifer recruitment after seedling establishment. Researchers have found that 30-year climate averages are poor predictors of seedling establishment (Serra-Diaz et al., 2016). 30-year intervals are marked by high annual variability. Seedlings tend to recruit during periods of above average rainfall, which are masked by 30-year climate averages. While we considered using annual weather data of the year a seedling or sapling germinated as climate inputs into our model, this was not feasible for two reasons. One, neither the year of germination nor tree age was provided in the presence data. There are no studies linking d.b.h. or height of yellow pines, or conifers in general, to an exact or approximate age since growth is highly dependent on environmental conditions (Hallin, 1957). However, some researchers have approximated *P. jeffreyi* age from d.b.h., but estimates vary between studies. Minnich et al. (2000) approximated that it took around 10 years for a sapling to reach a d.b.h. of 1.2in Jenkinson (1990) noted that it took 11 years for *P. jeffreyi* in plantations, which are managed to have ideal growing conditions, to reach a d.b.h. of 1.7in and 20 years to reach a d.b.h. of 6.4in, while Oliver (1972) noted it took these trees 30 years to reach an average d.b.h. of 6in on another plantation. These studies illustrate strong variation in *P. jeffreyi* growth rates, and therefore, we could not reliably link d.b.h. measurements to age in our data. Second, using annual weather data in our model was not feasible because weather data was only available at 4-km resolution, which is too coarse for our study area. Overall, we conclude that it is appropriate to model habitat suitability for saplings because yellow pines can persist in the sapling life stage (<5in d.b.h.) for several decades and the presence of yellow pine saplings indicate areas where yellow pines can not only

germinate and survive the critical first few years, but also where individuals can continue to persist for several years or decades.

Our analysis was split into three parts to compare habitat suitability of yellow pines saplings in the past, present, and future. First, we compared current (1981-2010) habitat suitability for yellow pine saplings and adults. Second, we modeled historic (1921-1950) yellow pine sapling distributions using current sapling presence points to postdict suitable habitat under a historic climate. Third, we projected future suitable habitat of yellow pine saplings in 2010-2039 and 2040-2069 under a range of eight likely climate change scenarios. Analyzing historic, current, and future suitable habitat of saplings allowed us to compare changes in yellow pine distributions across time, while comparing current sapling and adult suitable habitat assessed for potential modern-day range mismatches between the two conifer life stages.

6.2 Methods

6.2.1 Study Area

We narrowed the geographic extent of our analysis to just the Transverse Ranges, rather than modeling suitable habitat of yellow pines across all of southern California. The Transverse Ranges include southern LPNF, ANF, and northern SBNF (Figure 34). We chose to model the entirety of the Transverse Ranges as this area had the most available data and had the same geographic orientation (east-west). Local species adaptations, which may be influenced by geographic orientation, often affect species distributions (W T Adams et al., n.d.). Modeling across the same geographic orientation helped ensure that we were modeling trees with similar genotypes. In contrast, CNF and southern SBNF, which are located in the Peninsular Range, have a north-south orientation, and were lacking presence points. We further subdivided the Transverse Ranges into three regions: western, central, and eastern (Figure 35). These three regions consist of unique mountain ranges and climates. Comparing trends in habitat suitability across these regions may provide insight into how yellow pine saplings will fare under various environments.

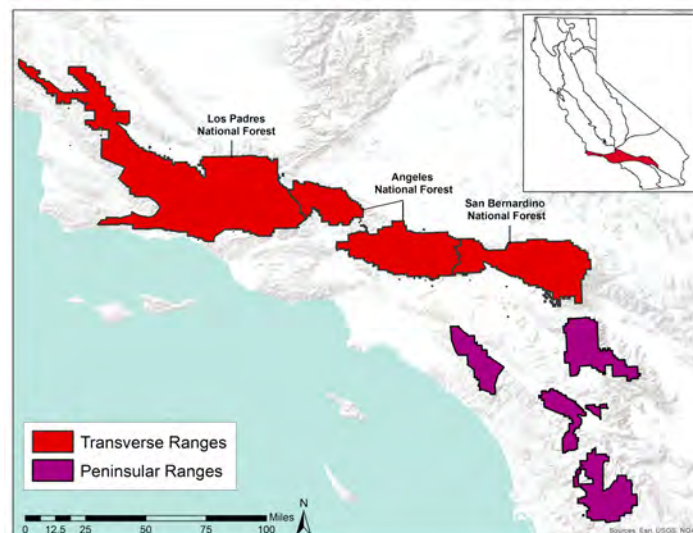


Figure 34. We analyzed suitable habitat of yellow pines in the Transverse Ranges, which includes the southern LPNF, ANF, and northern SBNF.

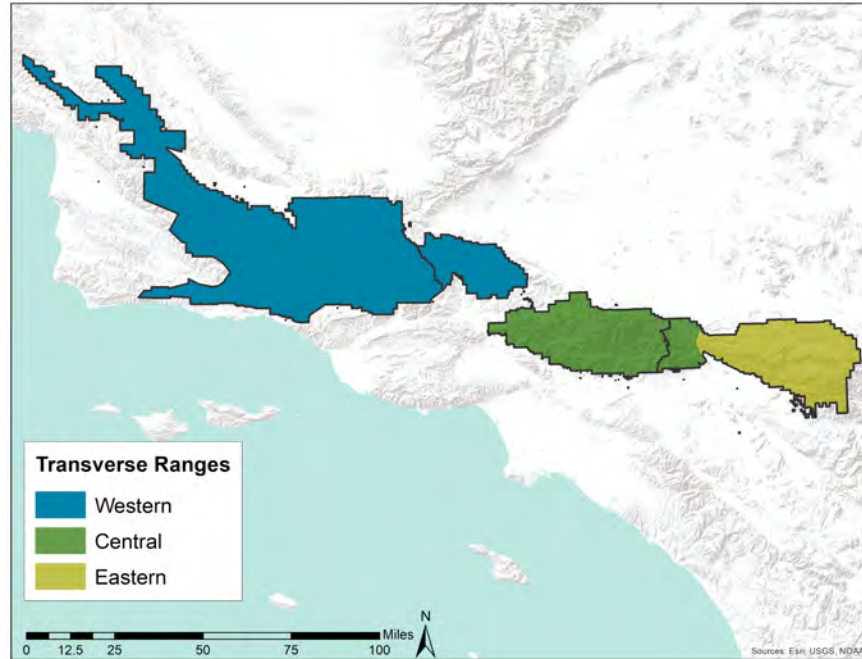


Figure 35. Subdivisions of the Transverse Ranges. The western Transverse Ranges includes LPNF and western ANF. The central Transverse Ranges includes eastern ANF, and western SBNF. The eastern Transverse Ranges includes central and eastern SBNF.

6.2.2 Species Selection

We focus our model on yellow pines as they are well adapted to drought (Hilberg et al., 2016) and fire (U.S. Forest Service, 2019). These important adaptations make yellow pines critical to the long-term persistence of conifer forests under climate change. Additionally, with *P. jeffreyi* covering over 112,000 acres (Table 1) it is one of the most abundant conifers in southern California. *Pinus ponderosa* only occupies approximately 12,000 acres (Table 1). While we would have preferred to model *P. jeffreyi* and *P. ponderosa* separately, these species look very similar at the sapling stage before they are cone bearing (H. Safford, personal communication, 2020; Franklin & Bergman, 2011). Since they also occupy the same geographic range, modern-day surveyors could have accidentally mistaken the species for one another. We thus modelled the joint distributions of these species to account for this potential source of bias.

6.2.3 Data

6.2.3.1 Environmental Data

A literature review was conducted to determine which environmental variables influence overall vegetation distribution and contribute to the survival and germination of yellow pine seedlings and saplings. While we do not model seedlings, saplings first need to germinate and survive the seedling stage before becoming a sapling. Thus, it is important to consider factors that can influence seedling germination and survival. See Table A for a final list of preliminary variables.

Climate data:

Literature review revealed that summer drought stress and soil water moisture were the biggest factors affecting establishment of *P. jeffreyi* (Alpert & Loik, 2013; Davis et al., 2019; Gucker, n.d.; Haller, 1959). Near surface temperature (<0.5cm from the soil surface) was also an important factor (Dingman et al., 2013). Similarly, *P. ponderosa* establishment is also largely affected by moisture stress (Davis et al., 2019). Unfortunately, near surface air temperature layers from NASA Earth Exchange (NEX) Downscaled Climate Projections (NEX-DCP30) (Thrasher et al., 2013) are only available at 1km resolution. 1km was too coarse to provide reliable estimates in mountainous terrain as local topography influences microclimates at scales much smaller than 1km; 270m was deemed a more appropriate scale (Franklin et al., 2013). Soil water moisture was also not available at a high enough resolution, nor was it available projected under future climate scenarios. However, climatic water deficit (CWD) data were available at relatively high resolutions (270m) and also projected under future climate scenarios. This single variable is commonly used as an estimate for drought stress on plants as it integrates several relevant factors such as solar radiation, evapotranspiration, precipitation, and soil water storage (McCullough et al., 2016). CWD is also an indicator for broad vegetation distribution (Stephenson, 1990).

Historic, current, and projected climate data was obtained as 30-year averages from the Basin Characterization Model (BCM) (Flint & Flint, 2014). While we explored other sources of climate data, including Cal-Adapt and NASA NEX, the finest resolution climate data for our study area was provided by BCM at 270 m resolution. 270 m resolution climate data has been deemed an appropriate resolution to provide valid, interpretable results from SDMs (Franklin et al., 2013).

We obtained several climate variables from BCM (version 2014) that were deemed to be important for the germination and survival of yellow pines (Table 30). Summer CWD was manually calculated by summing 30-year averages of June, July, and August CWD in ArcGIS. We included the maximum temperature of the hottest month. July was found to have the highest average maximum monthly temperature when compared against June, August, and September temperatures.

1921-1950 climate data from the BCM was used to model suitable habitat under a historic climate. Current suitable habitat was modeled using 1981-2010 climate data. Future suitable habitat was modeled using climate projections from two future time periods: 2010-2039 and 2040 -2069. We do not model future suitable habitat under 2070-2099 projected climates as the uncertainty associated with climate modeling increases with time (Littell et al., 2011); estimates of future climate in 2070-2099 may not be reliable (F. Davis, personal communication, May 19, 2020).

While BCM includes 18 total climate change projections, we selected a representative sample of projections to model: MRI-CGCM3 RCP26, MPI-ESM-LR RCP45, CCSM4 RCP85, CNRM-CM5 RCP85, MIROC5 RCP26, MIROC-ESM RCP45, MIROC-ESM RCP60, MIROC-ESM RCP85 (Figure 36). The majority of these projections are well represented in California SDM literature (Davis et al., 2016; Riordan et al., 2018; Stewart et al., 2016), while MRI-CGCM3 was selected to diversify the range of emission scenarios modeled. These projections represent a range of emission scenarios and future climatic conditions. We selected four wet (MIROC5 RCP26, MIROC-ESM RCP45, MIROC-ESM RCP60, MIROC-ESM RCP85) and four dry (MRI-CGCM3 RCP26, MPI-ESM-LR RCP45, CCSM4 RCP85, CNRM-CM5 RCP85) climate projections, because it is uncertain whether total precipitation will increase or decrease in the future (Bedsworth et al., 2018). In contrast, there is a strong consensus among existing literature that temperature will continue to increase throughout California (Bedsworth et al., 2018). Therefore, while the selected climate projections display variability in future precipitation, temperature is expected to increase under all scenarios (Figure 36).

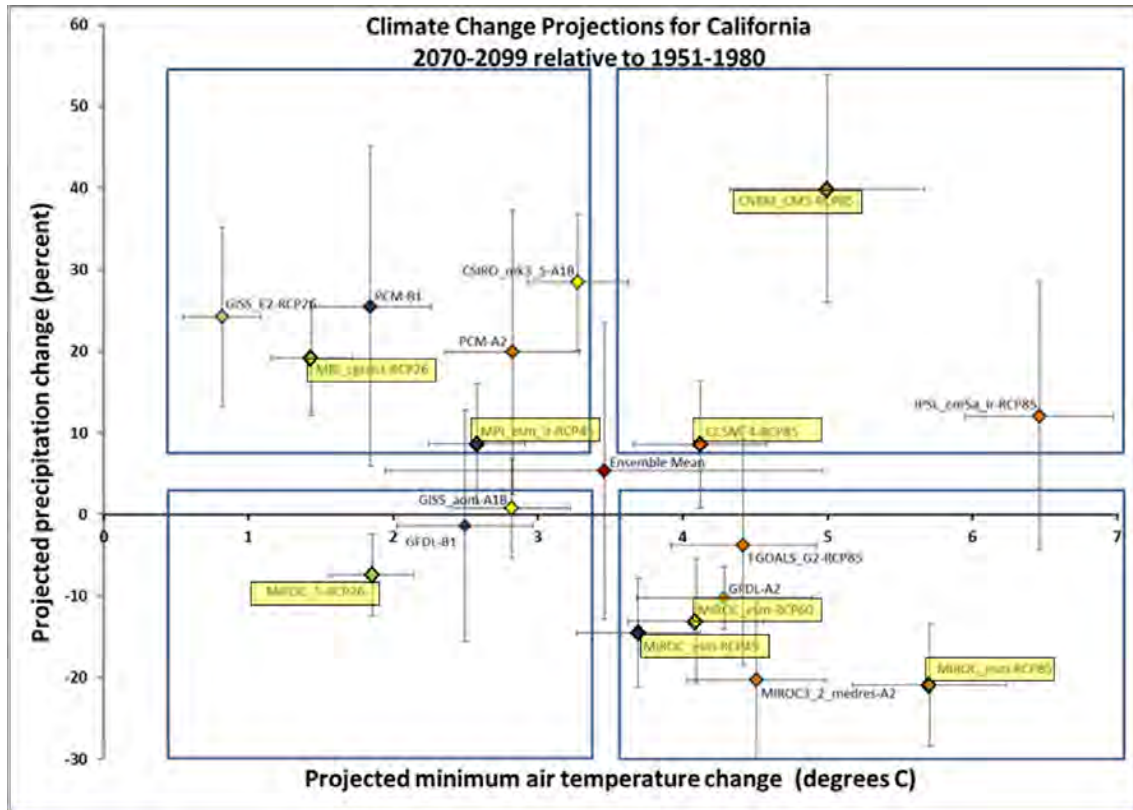


Figure 36. Expected changes in precipitation and temperature from 18 climate projections available from the Basin Characterization Model. Climate projections selected for use in our model are highlighted in yellow. Average temperatures are expected to increase under all selected climate projections, while projected precipitation is variable.

Topography:

A 30m (1 arc second) digital elevation model (DEM) was extracted from USGS Earth Explorer (USGS 2017). The DEM was used to calculate topographic wetness index (TWI) and topographic position Index (TPI). TWI is used to estimate soil moisture (Beven & Kirby, 1979). TWI values are determined by the slope of a pixel and the upslope area that drains through the pixel (Grabs et al., 2009). TPI represents the difference in elevation between a pixel and the surrounding pixels in a predetermined neighborhood (Guisan et al., 1999; Jenness 2011).

We used Topography Tools for ArcGIS 10.3 (Dilts, 2015) to calculate TPI. TPI is scale-dependent and determined by a user-defined neighborhood. We chose a neighborhood of 5, 7, 10, and 20 cells to cover a range of TPI that still represent topographic variation without over or under-representing topographic complexity. We decided to let MaxEnt choose the best predictive TPI layer during preliminary model runs. ArcGIS hydrology tools and raster calculator were used to calculate TWI. See Appendix N for how TWI was calculated.

Typically, we would want fine-scale TPI and TWI since topography influences microclimates (Opedal et al., 2015) which can affect seedling germination and survival (Dingman et al., 2013). However, MaxEnt requires all layers to be in the same resolution, so the 30m TPI was upscaled to the same resolution of the climate data, which has 270m resolution. This resulted in missing fine-scale spatial variability, but was unavoidable.

Soil:

The success of yellow pine establishment is partially influenced by soil characteristics, (Gucker, n.d.; Moore, 2006) and therefore, the preliminary soil variables we selected were soil temperature, texture and pH. Soil data was obtained from the Soil Survey Geographic Database (SSURGO). SSURGO is the most thorough and complete soils database for our study area and has been incorporated into similar habitat suitability studies (Hohmann & Wall, 2016; McComb et al., 2019). Downloaded data included both tabular and spatial data files. Tabular attribute data was related to spatial data using the ArcGIS Soil Data Viewer Toolbar. SSURGO data is available as polygons, but was converted to rasters with the same spatial resolution as the 270m BCM climate data.

Table 30. Preliminary variables included in the initial model runs. Summer is defined as June, July, and August (JJA). Original soil variables were available as polygons and thus did not have a resolution. Variables selected for inclusion in the final models are highlighted in green.

Environmental Variable	Source	Resolution (m)
<i>Climate</i>		
April Snowpack	BCM	270
Annual Climatic Water Deficit (CWD)	BCM	270
Annual Precipitation	BCM	270
Maximum July Temperature	BCM	270
Summer Climatic Water Deficit	BCM	270
Summer Precipitation	BCM	270
<i>Soil</i>		
Soil Temperature	SSURGO	--
pH	SSURGO	--
Texture	SSURGO	--
<i>Topography</i>		
Elevation	USGS DEM	30
Topographic Position Index (TPI) – 5x5	USGS DEM	30
Topographic Position Index (TPI) – 7x7	USGS DEM	30
Topographic Position Index (TPI) – 10x10	USGS DEM	30
Topographic Position Index (TPI) – 20x20	USGS DEM	30
Topographic Wetness Index (TWI)	USGS DEM	30

Appendix O details how we transformed raw climate and soil data layers into finalized ASCII files for input into MaxEnt.

Variable Correlation:

All climate variables and elevation were checked for correlation in R using `corrtest()` (Table 31). With the exception of annual average precipitation, all variables exhibited strong correlation ($r > 0.7$) with at least one other variable. In contrast, annual average precipitation exhibited very weak ($r < 0.3$), weak ($0.3 < r < 0.5$) and moderate ($0.5 < r < 0.7$) correlations to all other variables (Moore et al., 2013). When selecting for the final variables in our models (Section 6.2.5), we reduced the amount of correlated variables as much as possible. For instance, elevation was removed from the final model as it was moderately to strongly correlated with five out of the six additional variables.

Table 31. Correlation of the preliminary climate variables and elevation.

	April Snowpack	Annual CWD	Summer CWD	Annual Precipitation	Summer Precipitation	Max July Temperature	Elevation
April Snowpack	1	-0.76	-0.7	0.38	0.60	-0.65	0.67
Annual CWD		1	0.88	-0.53	-0.62	0.78	-0.78
Summer CWD			1	-0.38	-0.70	0.83	-0.80
Annual Precipitation				1	0.15	-0.41	0.19
Summer Precipitation					1	-0.54	0.67
Max July Temperature						1	-0.70
Elevation							1

6.2.3.2 Presence Data

Modern data was obtained from three sources: FIA (2001-2010), USFS Region 5 Remote Sensing Lab (2001-2010), and Field Sampled Vegetation (FSVeg) (2008-2020) (Figure 37). While FIA and USFS plots were only included in the NRV analysis when they fell within a 750m buffer around YPMC polygons from CALVEG, all plots within the Transverse Ranges were used for analysis in the SDM.

FIA conducts randomly placed and spatially unbiased surveys approximately every 6,000 acres across the United States (O’Connell et al., 2015). FIA provides ideal data for use in MaxEnt since MaxEnt can be sensitive to sampling bias (Elith et al., 2011). The data from the USFS is collected using the same protocols as the FIA data, including spatially unbiased samples, making it an acceptable dataset to use in addition to the FIA data. FSVeg surveys were unfortunately both biased and spatially clustered (Figure 37). These surveys typically occurred in forest health projects or in fire scars (N. Molinari, personal communication, 2021). While it would have been ideal to only use spatially unbiased data from one or two sources, the sample size from using FIA and USFS data was too small for a robust model. Thus, it was necessary to seek additional presence data. We address how we accounted for this bias in Section 6.2.6.

According to the FIA metadata, a seedling is defined as having d.b.h. <1in, while saplings are defined as having d.b.h. >1in and <5in (O’Connell et al., 2015). Adults are considered trees with d.b.h. >5in (O’Connell et al., 2015). Some plots from the FSVeg dataset were surveyed after 2010. Since these plots were surveyed after the time frame of the climate data used in the model (1971-2010), we took a conservative approach and only considered saplings to be trees in surveys conducted after 2010 if the d.b.h. was 5-7in. We used a slightly higher d.b.h. threshold to account for the surveys occurring outside of the time frame of the data. Setting a higher threshold ensured that we did not accidentally classify trees that germinated after 2010 as saplings. After combining all three current datasets, there were 1779 adult presence points and 377 sapling presence points in our study area. After removing duplicate points per lifeform within the same pixel, approximately 1133 adult present points and approximately 374 sapling presence points remained as inputs for our models.

The true coordinates of the FIA plots and the USFS plots are altered by a couple hundred meters to up to a half mile to protect the plot’s location (O’Connell et al., 2015). Plot locations are altered along a horizontal axis, not a vertical axis. This makes the data suitable to be used in a SDM since environmental

variables have a strong correlation with elevation. Gibson et al. (2014) did not find a significant difference in SDM results when using the altered FIA plot coordinates compared to the true plot coordinates. Additionally, FIA and USFS data only comprises a small fraction of our total presence points, so they should not significantly affect our MaxEnt results. Thus, we deemed it appropriate to also use data with altered coordinates.

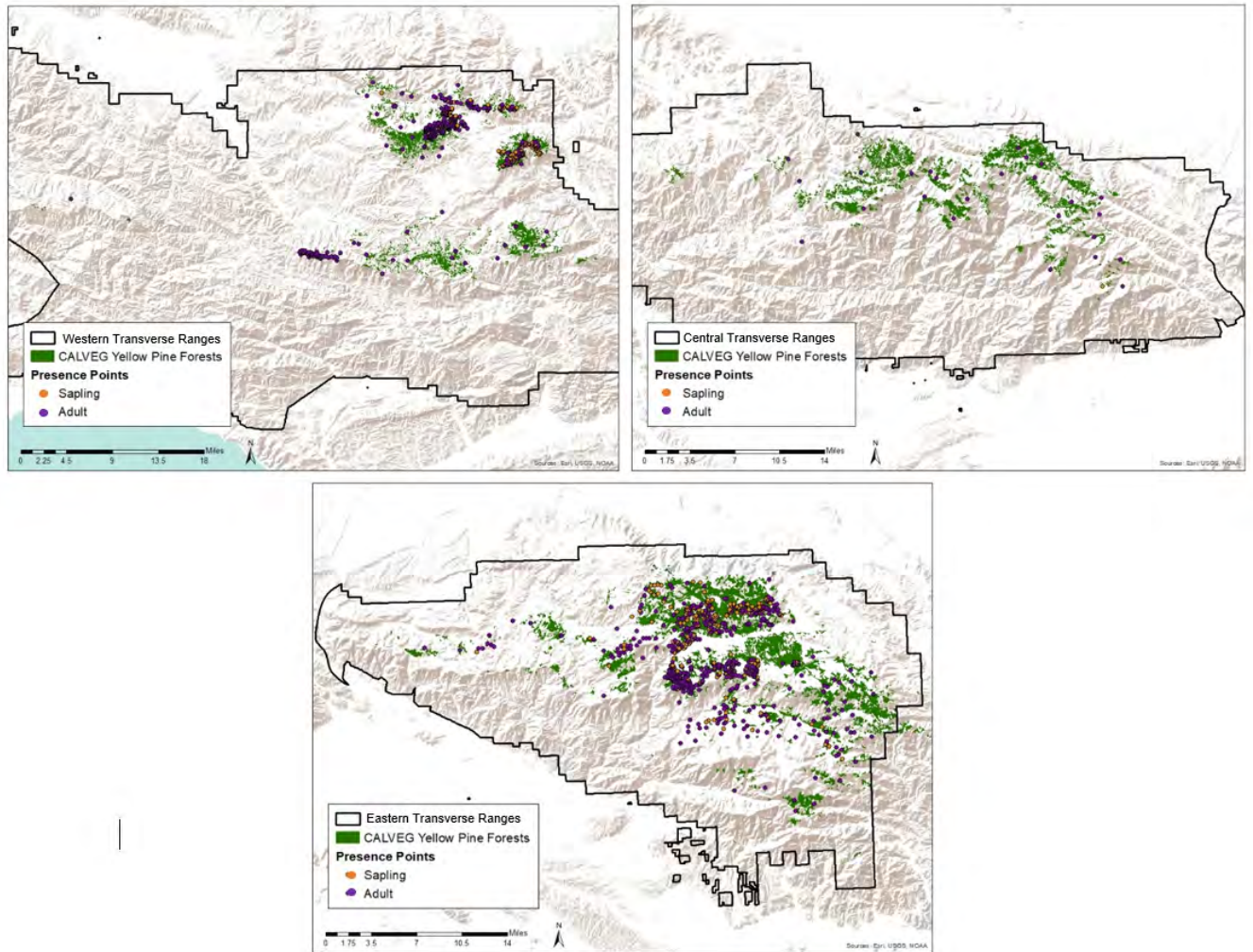


Figure 37. Yellow pine presence points from the three contemporary datasets.

6.2.4 MaxEnt Parameters

Feature types: MaxEnt allows users to choose between five different methods (threshold, hinge, linear, quadratic, and product) of modeling features. Our model consisted of linear and quadratic features only. Threshold features are valuable in a MaxEnt model when known environmental thresholds exist for the establishment and survival of a species (Merow et al., 2013). Literature review did not reveal any evidence for the existence of environmental thresholds specific to the survival of yellow pine saplings, and therefore we disabled threshold features from our model. Furthermore, thresholds can often be problematic and hard to accurately define (Merow et al., 2013), while quadratic features are considered appropriate for modeling a species response to predictors (Austin, 2007; Merow et al., 2013). While we

considered enabling product features, we had concerns about overfitting our model. Simpler models with fewer feature classes can reduce overfitting of the model (Merow et al., 2013). Similarly, threshold and hinge features greatly increase model complexity, which can lead to overfitting (Elith et al., 2011; Radosavljevic & Anderson, 2014).

Replication: Replication allows for multiple model runs of the data for consistency and MaxEnt allows for three possible resampling methods (cross-validation, subsampling, and bootstrapping). We used the K-fold cross-validation resampling method, as this is the most popular method for resampling in MaxEnt models (Merow et al., 2013). Using 5-fold cross-validation (k=5) allowed for all presence data to contribute to both model training and validation. During cross-validation, presence data is divided into five equal subsets. Then, the model is run five times, each time leaving out one of the subsets to be used for validation. Finally, results from all five runs were used to create the final probability model (Merow et al., 2013; Stohlgren et al., 2015).

See Appendix P to view MaxEnt model parameter settings in more detail.

6.2.5 Final Variable Selection

We define the most parsimonious model as one with the fewest correlated variables with the highest AUC (Qin et al., 2017). We had 15 preliminary variables (Table 30); 6 were highly correlated. We performed several preliminary model runs for both models (current sapling suitable habitat and current adult suitable habitat) to systematically remove variables that contributed little towards predicting habitat suitability. This allowed us to minimize the number of correlated variables. We further reduced correlation by selecting the variable with the most consistent highest permutation importance from a group of similar variables (e.g. annual CWD or summer CWD). We used knowledge of ecological systems (Yiwen et al., 2016), jackknifing (Qin et al., 2017), permutation importance, response curves, and AUC (Qin et al., 2017) to select the final variables. The area under the receiver operating characteristic curve (AUC) is a commonly used measure of MaxEnt model fit. AUC values above 0.50 indicate that the model is better than random at distinguishing true presence points from background points. Therefore, models with high predictive accuracy have AUC values close to 1.0 (R. Pearson, 2010).

The final variables used in both models included: April snowpack, annual CWD, summer precipitation, maximum July temperature, and TPI with a user defined grid of 20 cells (Table 30). These variables were selected as final variables from both the models.

6.2.6 Accounting for Sampling Bias

The majority of current presence data was collected from non-randomly placed FSVeg surveys. While FIA and USFS surveys were spatially unbiased, they contributed very little to the total number of presence points. To determine if this biased sampling of the FSVeg surveys would affect the model results, we compared the distribution of climate across sampled sites to the distribution of climate across 20,000 random points from YPMC forests in our study area. We did so by comparing the distributions of all final variables across these two regions.

With the exception of summer precipitation (Figure 38), the distribution of these variables across sampled plots is generally representative of the distribution of these variables across the background of interest (see Appendix Q). Sampled plots generally fell within areas experiencing either low (<5mm) or high (>8.5mm) amounts of summer precipitation. Very few current plots (adults: n=35, saplings: n=2) were located in areas experiencing intermediate (5-8.5mm) amounts of summer precipitation. However, much of the YPMC forest across our study area does receive intermediate amounts of summer precipitation

(Figure 39). These areas mainly occur across ANF and western SBNF (Figure 39). We believe areas with intermediate precipitation are underrepresented by the plot data because ANF and western SBNF were under sampled compared to LPNF and eastern SBNF.

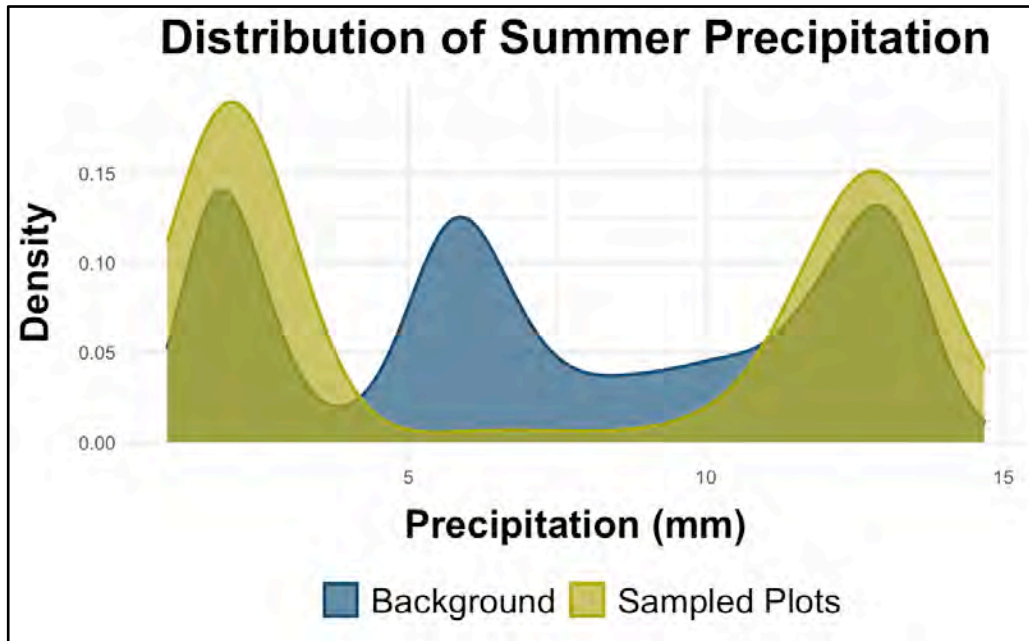


Figure 38. Distribution of summer precipitation. The distribution of summer precipitation (mm) at sampled plots is displayed in yellow and is compared to the distribution of summer precipitation across a random background sample taken from YPMC forest in the sample area, as displayed in blue.

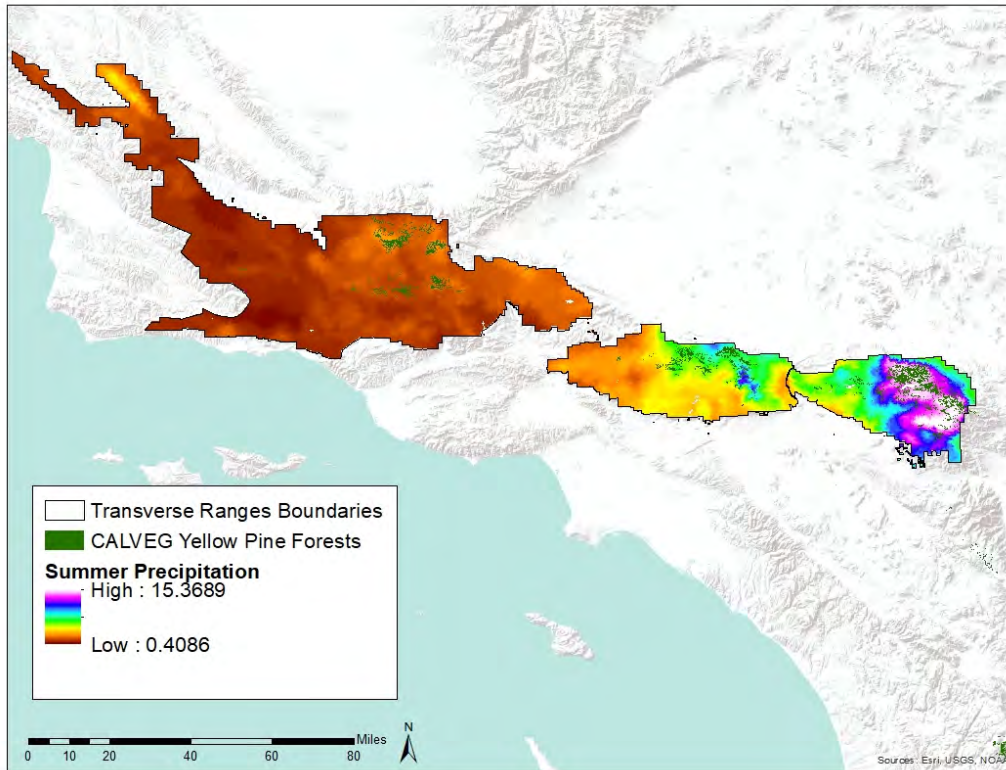


Figure 39. Distribution of summer precipitation across the Transverse Ranges. Regions with mid-precipitation mainly occur across the Central Transverse Range.

Out of all variables explored, summer precipitation had the greatest relative contribution to our MaxEnt models, and therefore, we felt strongly about including summer precipitation as a predictor variable in our models. However, by retaining this variable in our models, we had different levels of confidence in projections across different regions of the study area. We account for differences in the model’s reliability by classifying the entire study area into two regions: high confidence areas and low confidence areas.

High confidence areas are regions where we have high confidence in the abilities of our models to project habitat suitability. These are typically heavily surveyed areas in LPNF and eastern SBNF where the sampled plots represent the distribution of low and high amounts of summer precipitation. **Low confidence areas** are regions with projected intermediate amounts of summer precipitation. We have less confidence in the ability of our models to accurately predict suitable habitat in these areas because the sampled plots do not accurately represent the true distribution of summer precipitation across these areas. Conclusions drawn from low confidence areas should be used with caution. Results are reported for high and low confidence areas separately.

6.2.7 Analysis

We used the maximum training sensitivity plus specificity logistic threshold (maxSSS) values as the threshold values for suitability across our models. Threshold selection based on maxSSS has proven effective (C. Liu et al., 2005, 2015) and has been used in similar studies (McComb et al., 2019; Riordan et al., 2018). Doing so allowed us to transform outputs from continuous values to binary values by designating pixels as either suitable or unsuitable depending on whether they fell above or below the threshold maxSSS value. The maxSSS value is unique to each model and works by maximizing the sum of the true positive rate and the true negative rate. The true positive rate is the probability that suitable

habitat is detected as suitable and the true negative rate is the probability that unsuitable habitat is detected as unsuitable.

In the third part of our analysis, we used an integrated outlook approach (McComb et al., 2019), also known as an ensemble, by summing habitat suitability under multiple future climate projections to obtain final measures of suitability. This is a more desirable and conservative approach that ensures that we do not rely on any single projection to draw conclusions since future climate scenarios are so variable. We summed habitat suitability across all eight 2010-2039 climate projections to obtain a final measure of 2010-2039 habitat suitability, which we refer to as the **2010-2039 summed scenario**. Similarly, the **2040-2069 summed scenario** represents 2040-2069 habitat suitability across all eight climate projections.

Furthermore, we explored the effect of two different precipitation regimes on estimates of habitat suitability. The eight selected climate projections were subdivided into two groups: wet projections and dry projections (see Section 6.2.3.1). For each future time period, suitable habitat under all four wet projections was summed in ArcGIS to obtain a joint measure of habitat suitability under a wet future. We will refer to the summed measures of habitat suitability under the wet futures as the **2010-2039 summed wet scenario** and the **2040-2069 summed wet scenario**.

While we modeled habitat suitability across the entirety of the Transverse Ranges, we believe our models performed more reliably across certain areas. We took a conservative approach and analyzed high confidence areas and low confidence areas separately (see Section 6.2.6). Regions classified as low and high confidence changed depending on which climate projection was utilized in the model. Low confidence areas under the current sapling and current adult habitat suitability projections were designated as such because these areas experienced intermediate amounts of summer precipitation under the *current* climate. In part three of our analysis, future habitat suitability projections were summed to create final summed scenarios. Low confidence areas under the final summed scenarios were designated as such if they were projected to have intermediate amounts of summer precipitation under any of the *future* climate projections used to create the given summed scenario.

Each of the three parts of our analysis involved comparing two or more final habitat suitability layers (final habitat suitability layers used in analysis included the following: current sapling, current adult, 2010-2039 summed scenario, 2040-2069 summed scenario, 2010-2039 summed wet scenario, 2010-2039 summed dry scenario, 2040-2069 summed wet scenario, and 2040-2069 summed dry scenario). For comparison purposes, areas were analyzed as low confidence areas if they were projected to have intermediate amounts of summer precipitation under any of the layers being compared. For instance, when comparing suitable habitat between the current sapling, 2010-2039 summed scenario, and 2040-2069 summed scenario, cells were assigned as low confidence areas if they had intermediate amounts of precipitation under any of the three layers. This may cause some high confidence areas from certain layers to be re-classified as low confidence areas for analysis purposes. For this reason, the amount of current suitable sapling habitat reported across high confidence areas will vary depending on which layers are being compared. We acknowledge that this is a conservative approach towards determining low and high confidence areas for analysis. However, doing so allows us to more reliably compare across various climate scenarios with high confidence.

6.3 Results

All final model AUC and maxSSS values are displayed below in Table 32.

Table 32. MaxEnt model summaries. Model AUC and MaxSSS values were consistent across all historic, current, and future sapling projections, as all projections were built from the current sapling model.

Time Period Modelled	Presence Points Utilized	Model AUC	MaxSSS	Date of Climate Data	Scenario	Section of analysis
Historic	Current saplings	0.953	0.1144	1921-1950	N/A	II
Current	Current saplings	0.953	0.1144	1981-2010	N/A	I, II, III
Current	Current adults	0.915	0.1913	1981-2010	N/A	I
Future	Current saplings	0.953	0.1144	2010-2039	2010-2039 summed scenario	III
Future	Current saplings	0.953	0.1144	2040-2069	2040-2069 summed scenario	III
Future	Current saplings	0.953	0.1144	2010-2039	2010-2039 summed dry scenario	III
Future	Current saplings	0.953	0.1144	2010-2039	2010-2039 summed wet scenario	III
Future	Current saplings	0.953	0.1144	2040-2069	2040-2069 summed dry scenario	III
Future	Current saplings	0.953	0.1144	2040-2069	2040-2069 summed wet scenario	III

6.3.1 Current Suitable Habitat of Saplings and Adults

Current suitable habitat for both saplings (AUC=0.953) and adults (AUC=0.915) was concentrated in eastern SBNF and central LPNF; notably less suitable habitat was found in ANF (Figure 40). Our models predicted a 10.4% decrease in suitable habitat for saplings as compared to adults across high confidence areas (363,324 vs. 405,675 acres). Across low confidence areas, we expect a 30.6% decrease in suitable habitat for saplings as compared to adults (56,222 vs. 81,045 acres).

Of the total 405,675 acres of projected adult suitable habitat across high confidence areas, 55,249 acres were found to be uniquely suitable for just adults. Across low confidence areas, 24,841 out of the 81,045 total acres of projected adult suitable habitat were found to be uniquely suitable for just adults. In comparison, only 12,898 acres of habitat projected across high confidence areas and no habitat projected across low confidence areas were uniquely suitable for saplings. The remaining suitable habitat is suitable for both saplings and adults. See Appendix R for detailed maps and analysis comparing current sapling and adult suitable habitat in the three portions of the study area.

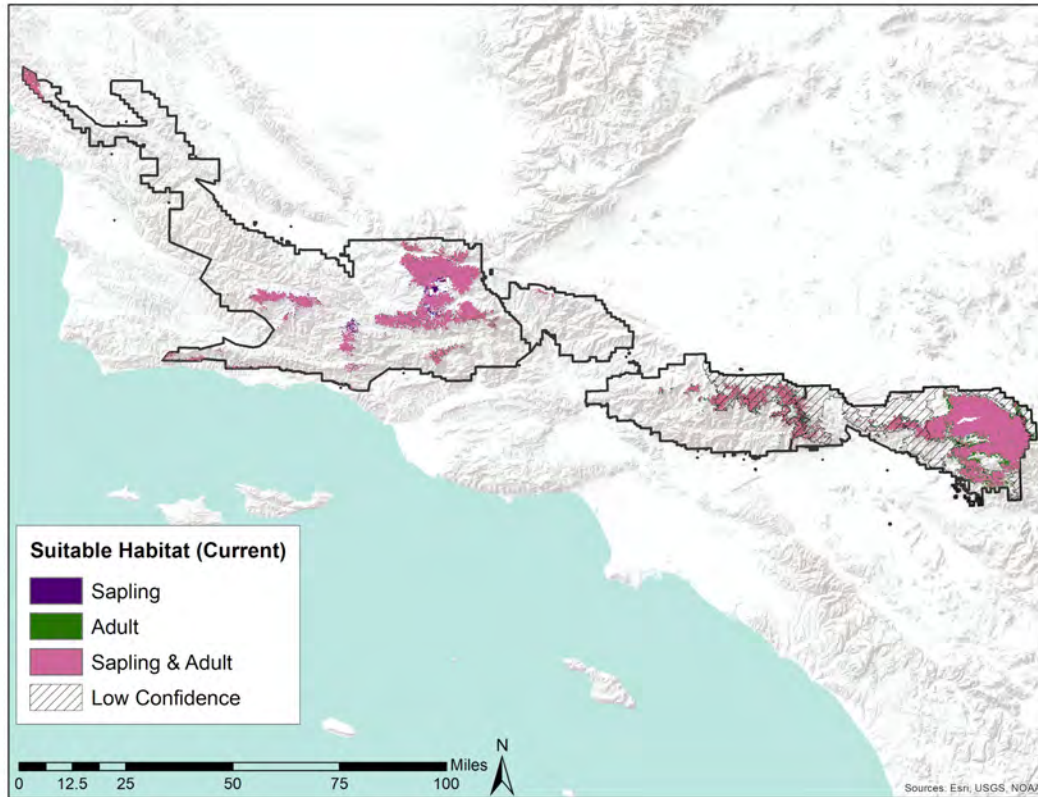


Figure 40. Current (1981-2010) projected yellow pine sapling and adult suitable habitat. Pink regions depict habitat projected to be suitable for both saplings and adults, while purple regions depict habitat projected to be suitable for only saplings and green regions depict habitat projected to be suitable for only adults. Low confidence areas are represented by hash marks.

Forests currently dominated by Ponderosa pine, Jeffrey pine, and mixed conifers (YPMC forest), as classified by CALVEG, generally overlap with projected suitable habitat of adult yellow pines (Figure 41). Only a small proportion of the study area that currently has YPMC forests was not predicted to be suitable for adult yellow pines. See Appendix R for detailed maps of current CALVEG YPMC forest distributions as compared to projected suitable habitat of yellow pines in the three portions of the study area.

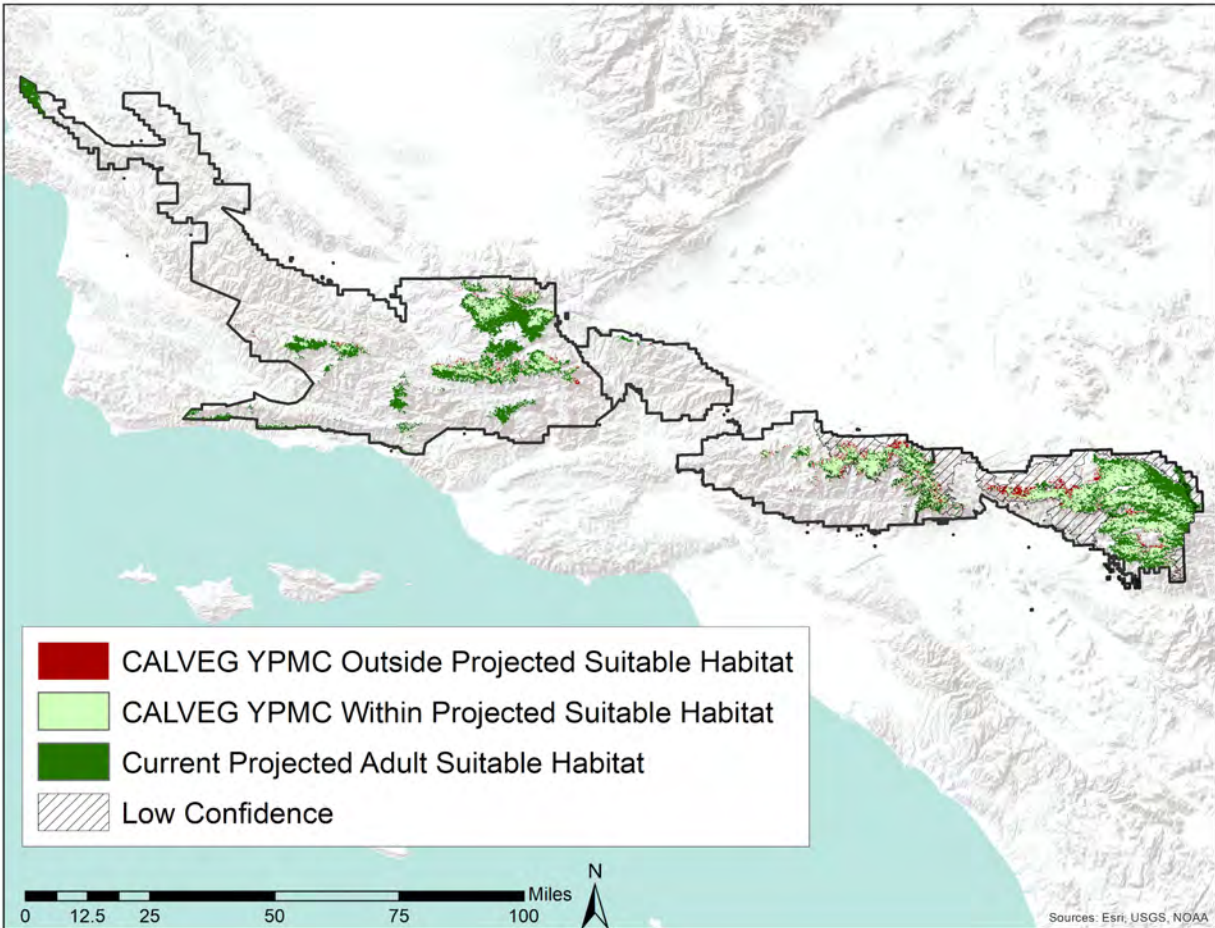


Figure 41. Current habitat classified by CALVEG as YPMC forest compared to current projected suitable habitat for adults. Light green regions represent regions where current YPMC forests overlap with projected suitable habitat for adult yellow pines, while red regions represent regions where current YPMC forests do not fall within regions of projected suitable habitat. Dark green regions depict projected suitable habitat not currently dominated by YPMC forest. Low confidence areas are represented by hash marks.

6.3.2 Past Suitable Habitat of Saplings

Our models predict a 0.3% increase in suitable habitat across high confidence areas and a 16.4% decrease in suitable habitat across low confidence areas for yellow pine saplings under current climate conditions (AUC=0.953) as compared to historic climate conditions (AUC=0.953). This corresponds to a gain of approximately 1,243 acres (from 362,081 to 363,324) and a loss of approximately 11,024 acres (from 67,246 to 56,222) of suitable sapling habitat across these respective areas. While we observe an overall negligible increase in suitable habitat across high confidence areas, trends differ across different portions of the study area. The western Transverse Ranges experienced a net gain in suitable sapling habitat (27,219 acres), while the central and eastern Transverse Ranges experienced net decreases in suitable sapling habitat (11,511 and 14,465 acres, respectively) (Figure 42). See Appendix S for detailed maps and

analysis comparing historic and current projected yellow pine sapling suitable habitat in each of the three portions of the study area.

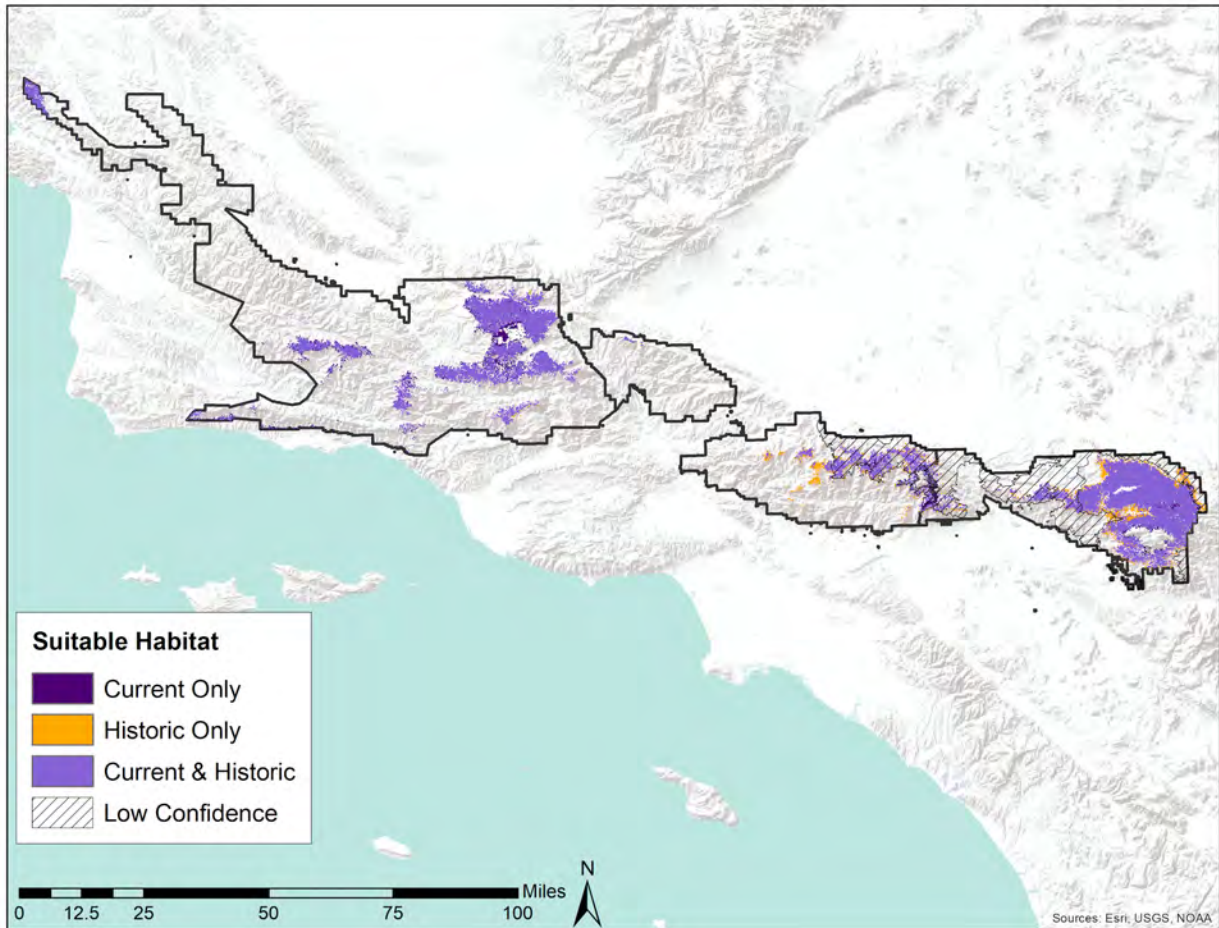


Figure 42. Historic (1921-1950) postdicted and current (1981-2010) projected yellow pine sapling suitable habitat. Light purple regions depict habitat that is predicted to be suitable under both time periods. Orange regions depict habitat only predicted to be suitable under historic climate conditions, while dark purple regions depict habitat only predicted to be suitable under current climate conditions. Low confidence areas are represented by hash marks.

6.3.3 Future suitable habitat of saplings

Comparing projected suitable habitat from high confidence areas under the 2010-2039 summed scenario and current sapling projection, we found a 50.4% decrease (from 304,328 to 150,867 acres) in projected sapling suitable habitat by 2010-2039. Analysis of the low confidence areas revealed a 64.8% decrease (from 115,217 to 40,531 acres) in sapling suitable habitat by 2010-2039. Furthermore, our models predicted even larger decreases in sapling suitable habitat by 2040-2069, as compared to present-day. Our models predicted a 67.1% decrease in suitable habitat (from 304,328 to 100,086 acres) across high confidence areas, and a 79.5% decrease (from 115,217 to 23,670 acres) across low confidence areas (Figure 43, Table 33). See Appendix T for detailed maps and analysis of current, 2010-2039, and 2040-2069 projected suitable habitat in the three portions of the study area.

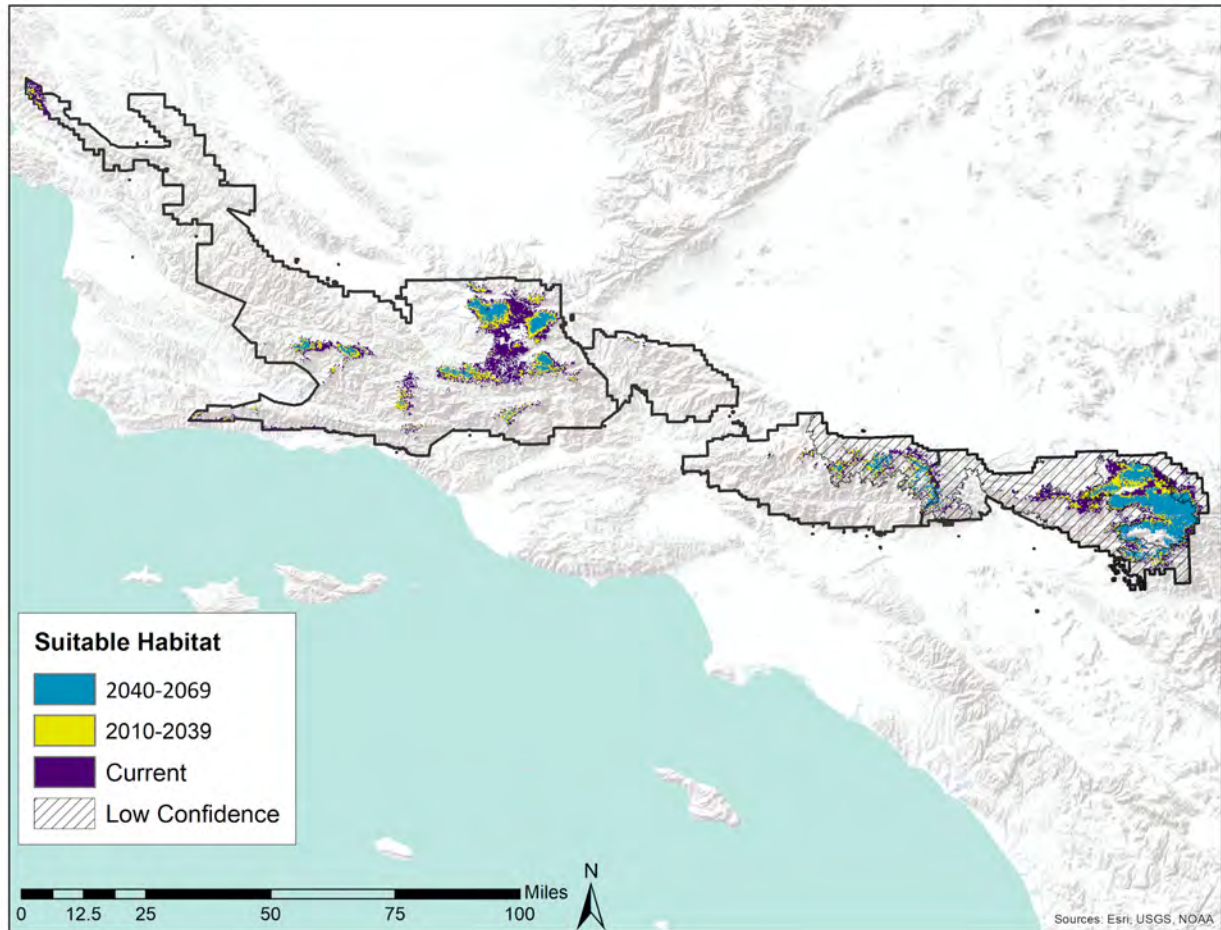


Figure 43. Current and future projected yellow pine sapling suitable habitat. Dark purple regions depict projected suitable habitat under current climate. Yellow regions represent projected suitable habitat under the 2010-2039 summed scenario, while blue regions represent projected suitable habitat under the 2040-2069 summed scenario. Low confidence areas are represented by hash marks.

Table 33. Projected yellow pine sapling suitable habitat under current, 2010-2039, and 2040-2069 climates.

Entire Study Area				
Time Period	Acres Suitable Habitat <i>High Confidence</i>	Percent Change in Suitable Habitat <i>High Confidence</i>	Acres Suitable Habitat <i>Low Confidence</i>	Percent Change in Suitable Habitat <i>Low Confidence</i>
Current	304,328.21	N/A	115,217.43	N/A
2010-2039 <i>Summed Scenario</i>	150,867.10	-50.43%	40,531.46	-64.82%
2040-2069 <i>Summed Scenario</i>	100,085.68	-67.11%	23,670.37	-79.46%

Under dry future climates, our models projected a 44.6% decline in suitable habitat (from 340,590 to 188,751 acres) across high confidence areas by 2010-2039 as compared to present-day. Low confidence areas are expected to experience a decrease of 54.8% in suitable habitat (from 78,955 to 35,704 acres) across the same time frame and conditions (Figure 44, Table 34). Gaps in current and projected suitable habitat under a dry future widen under the 2040-2069 projections. Our models predicted a 64.3% decrease (from 304,328 to 108,714 acres) in sapling suitable habitat across high confidence areas under dry future climates, and a 72.7% decrease (from 115,217 to 31,470 acres) across low confidence areas (Figure 45, Table 35).

Under wet future climates, suitable habitat is projected to decrease 40.7% (from 340,590 to 202,045 acres) across high confidence areas and 49.4% (from 78,955 to 39,973 acres) across low confidence areas by 2010-2039 (Figure 44, Table 34). Similarly to trends observed under a dry future, suitable habitat is expected to continue decreasing as we project under a wet future into 2040-2069. Under wet future climates, our models predicted a 62.4% decrease (from 304,328 to 114,533 acres) across high confidence areas and a 78.4% decrease (115,217 to 24,931 acres) across low confidence areas by 2040-2069 (Figure 45, Table 35).

See Appendix T for detailed maps and analysis of 2010-2039 and 2040-2069 dry and wet habitat suitability projections in the three portions of the study area. The model AUC was consistent across all current sapling and future sapling projections (AUC=0.953), as all projections were built from the current sapling model.

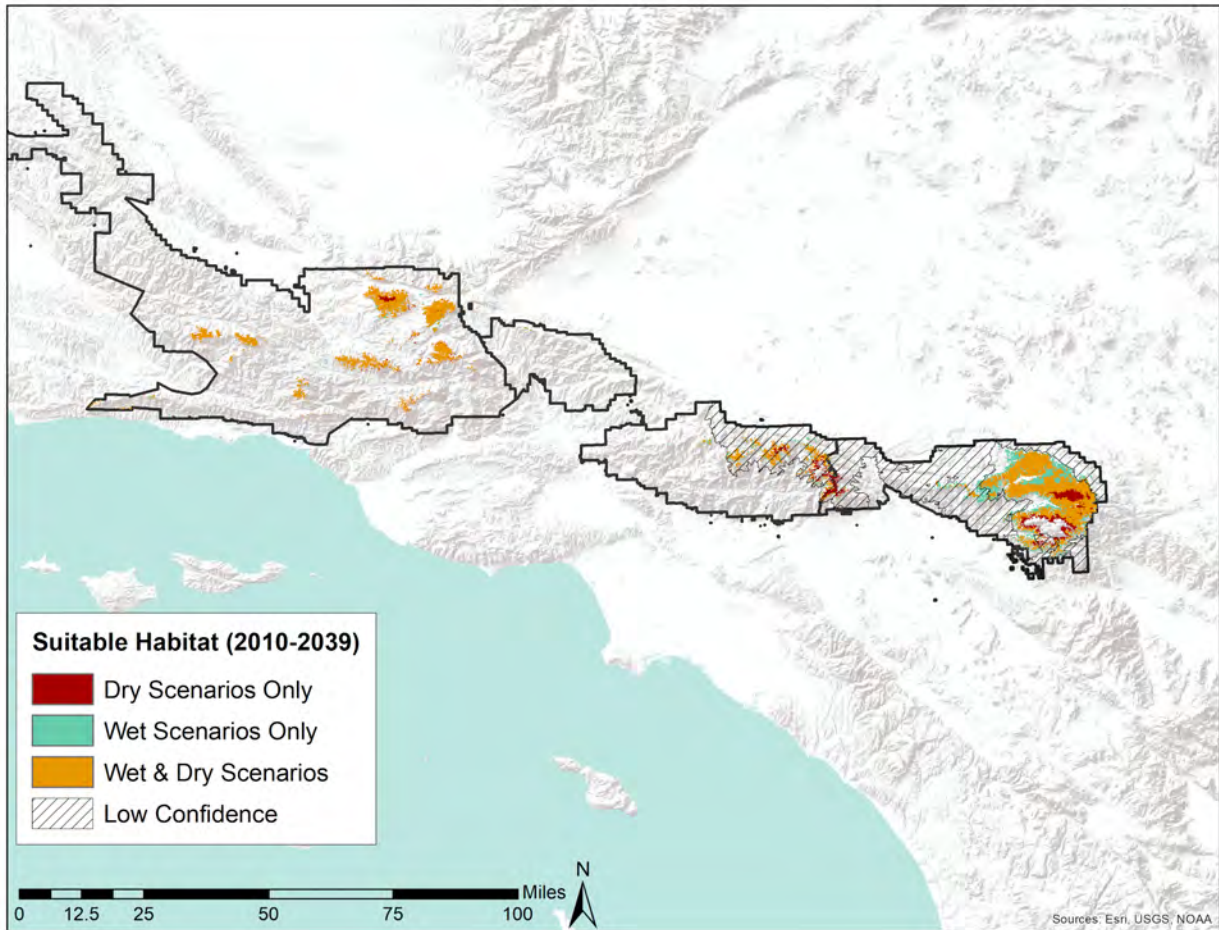


Figure 44. 2010-2039 projected yellow pine sapling suitable habitat. Orange regions depict habitat projected to be suitable under both the 2010-2039 summed dry scenario and the 2010-2039 summed wet scenario. Aqua regions represent habitat projected to be suitable only under the summed wet scenario, and red regions represent habitat projected to be suitable only under the summed dry scenario. Low confidence areas are represented by hash marks.

Table 34. Projected yellow pine sapling suitable habitat under 2010-2039 wet and dry futures.

Entire Study Area				
Time Period	Acres Suitable Habitat <i>High confidence</i>	Percent Change in Suitable Habitat <i>High Confidence</i>	Acres Suitable Habitat <i>Low confidence</i>	Percent Change in Suitable Habitat <i>Low Confidence</i>
Current	340,590.36	NA	78,955.28	NA
2010-2039 <i>Summed Dry Scenarios</i>	188,750.50	-44.58%	35,703.71	-54.78%
2010-2039 <i>Summed Wet Scenario</i>	202,044.82	-40.68%	39,973.03	-49.37%

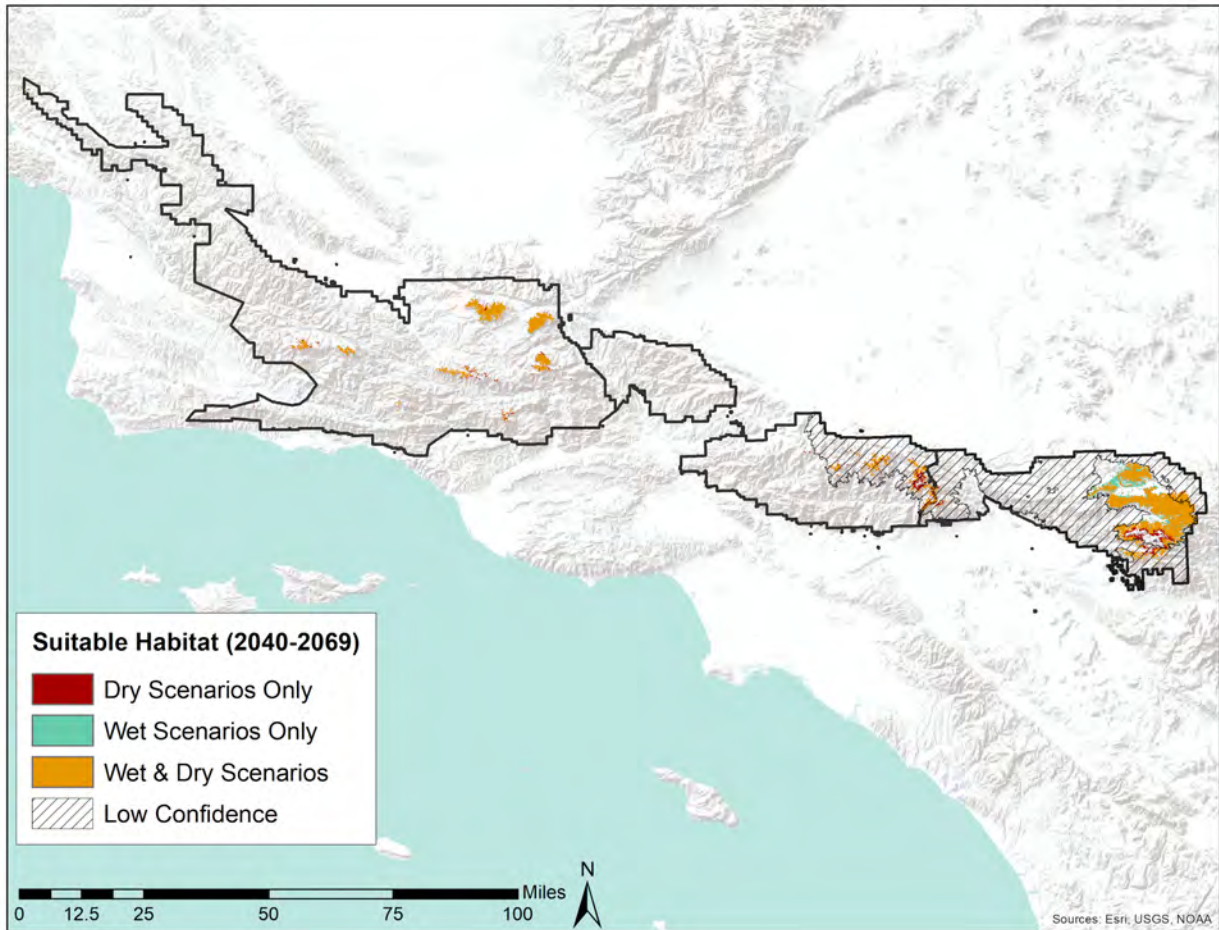


Figure 45. 2040-2069 projected yellow pine sapling suitable habitat. Orange regions depict habitat projected to be suitable under both the 2040-2069 summed dry scenario and the 2040-2069 summed wet scenario. Aqua regions represent habitat projected to be suitable only under the summed wet scenario, and red regions represent habitat projected to be suitable only under the summed dry scenario. Low confidence areas are represented by hash marks.

Table 35. Projected yellow pine sapling suitable habitat under 2040-2069 wet and dry futures.

Entire Study Area				
Time Period	Acres Suitable Habitat <i>High confidence</i>	Percent Change in Suitable Habitat <i>High Confidence</i>	Acres Suitable Habitat <i>Low confidence</i>	Percent Change in Suitable Habitat <i>Low Confidence</i>
Current	304,328.21	NA	115,217.43	NA
2040-2639 <i>Summed Dry Scenario</i>	108,714.38	-64.28%	31,470.43	-72.69%
2040-2069 <i>Summed Wet Scenario</i>	114,532.90	-62.37%	24,931.35	-78.36%

6.4 Discussion

Our models indicate that there is a small range mismatch between the current distribution of yellow pine saplings and adults across both low and high confidence areas. Literature supports our findings that less current habitat may be suitable for conifer saplings as compared to adults (McCann *in prep.*), as young yellow pines are especially vulnerable to environmental conditions (Hilberg et al., 2016). Slight changes in climate, such as increases in temperature or decreases in precipitation, are likely to disproportionately affect saplings. For instance, saplings may struggle with accessing deep soil water reserves due to their shallow root systems, and therefore, will fare worse under drought conditions than adults (Niinemets, 2010; Wright et al., 2013). With climate change already at play, we expect to see a reduction in the potential range of saplings as compared to adults as supported by our model results. Thus, we expect to see smaller distributions of yellow pines in the future, as these trees will not be able to regenerate across their entire contemporary range following mortality events. Throughout California, the frequency and intensity of severe climatic events, such as wildlife and drought, are increasing under climate change (Diffenbaugh et al., 2015; Fried et al., 2004; Liu et al., 2010). Such events will likely result in the die-off of adult trees, including die-off from areas that are unsuitable for yellow pines saplings in the future. While yellow pines may currently occupy these areas, they will not be able to successfully re-populate these areas under future conditions, and therefore, the species will no longer be able to persist in these areas following die-off events.

Comparing projections of the current suitable habitat of adults to areas currently mapped as YPMC forest gives insight into the accuracy of our models. YPMC forests include mixed conifer forests, Ponderosa pine, and Jeffrey pine forests. Mixed conifer forests are dominated by a variety of conifers, including *P. jeffreyi* and *P. ponderosa* as classified by CALVEG. The accuracy of our model results are supported by the fact that regions projected to be suitable yellow pine habitat overlap with the majority of YPMC forested areas mapped by CALVEG. The main exception to this is projected habitat at the top right of

CALVEG mapped YPMC forests in SBNF and in LPNF. In both cases, our model overestimates habitat suitability in these areas. This suggests that the loss of suitable habitat in the future is overestimated, particularly in LPNF.

Projections of suitable habitat reveal a negligible change in the amount of sapling suitable habitat under historic and current climates across high confidence areas. However, our models' projections indicate notable decreases in sapling suitable habitat across high confidence areas under expected 2040-2069 future climates. Across low confidence areas, results illustrate a loss in suitable sapling habitat under both historic and current comparisons and current and future comparisons. However, the loss in sapling suitable habitat is much greater when comparing current and future projections as compared to past and current projections (79.5% vs. 16.4%). Although climate change was already at play in the early 20th century, the rate of warming quickly accelerated in the 1970s and is expected to continue accelerating (*Indicators of Climate Change in California*, 2018). Between 1880-1980, global temperatures have increased at an average rate of 0.07°C per decade, while global temperatures have increased at a much faster rate of 0.18°C per decade since 1981 (*State of the Climate: Global Climate Report for Annual 2019*, 2020). Therefore, comparisons of historic and current climates will be more similar than comparisons of current and future climates across the same time period, resulting in greater similarities in habitat suitability across historic and current models as compared to current and future models. In fact, comparisons of projected suitable sapling habitat under current and 2010-2039 climates reveal notably greater changes across both low and high confidence areas in 30 years than changes observed across the past 60 years. Due to the accelerating rate of climate change, we can expect to see disproportionately greater losses in sapling suitable habitat beyond our 2040-2069 projections.

The projected losses of suitable habitat for yellow pine saplings by 2010-2039 and 2040-2069 does not necessarily mean that the overall range of yellow pines will also contract by these time frames. Yellow pine adults are very drought tolerant (Hilberg et al., 2016) and therefore, can continue to persist in areas that are not suitable for saplings for several decades, if not centuries. Rather, disturbance events, such as severe wildfire, drought, or bark beetle attack, will likely be the catalyst for shifting ranges of yellow pines (Davis et al., 2019). Wildfires and droughts are predicted to become more frequent and severe (Diffenbaugh et al., 2015; Williams et al., 2019), which will contribute to the mortality of adult yellow pines across the landscape. The loss of adult yellow pines from areas unsuitable for saplings will lead to areas where yellow pines will likely not re-establish, as future climates across these areas are predicted to no longer support sapling regeneration. This trend has already been observed with oak species, *Q. douglasii* and *Q. kelloggi*, in the southern Sierra Nevada and western Tehachapi Mountains (Davis et al., 2016). However, bark beetles tend to avoid pole-sized trees (H. Safford, personal communication December 1, 2020), so it's possible that some younger yellow pines will be spared from such attacks and continue to persist across these areas.

Despite our predictions of future losses in yellow pine suitable habitat, Serra-Diaz et al. (2016) suggest that areas suitable for seedling establishment are likely larger than predicted by species distribution models. Seedling establishment is strongly influenced by annual climate variability and often occurs in pulses during favorable climatic conditions (Jackson et al., 2009). However, these periods of favorable weather are masked by 30-year climate averages. We used 30-year climate averages in the present study, so it's possible that our results underestimate true suitable habitat. Given the general consensus in literature that climate change is threatening conifer forests (Diffenbaugh et al., 2015; Fried et al., 2004; Liu et al., 2010), we believe that our results illustrating future losses in yellow pine suitable habitat are accurate. However, results from Serra-Diaz et al. (2016) suggest that the magnitude of these predicted losses may be overrepresented.

Habitat suitability projections may be used to help in the prioritization of specific areas for conservation, by illustrating habitat that will likely be critical to the long-term survival of a species of interest (Elith & Leathwick, 2009; Wiens et al., 2009). Funds and resources for conservation activities are often limited,

and therefore, conservation efforts should focus on areas that have a high likelihood of contributing to the long-term success of the project. MaxEnt models of future plant distributions have been considered in various land use planning projects. The results of Qin et al.'s (2017) study mapping future distributions of an endangered conifer species were intended to be used in the selection of priority areas for the introduction of the species. Similarly, Saarimaa et al. (2019) argue for the results of their MaxEnt model to be used to prioritize areas for restoration, thereby benefiting threatened wetland plants. Our analysis illustrates areas where yellow pine forests will likely thrive under future climates, as well as where these forests are at risk of being lost indefinitely in the event of a stand-replacing disturbance. Conservation projects may choose to prioritize one or both of these areas depending on project goals and feasibility, among other considerations. Section 7 provides an example of how the results of our SDM may be used to help determine high priority conservation areas in YPMC forests throughout southern California.

6.5 Limitations

While MaxEnt has been used to model habitat suitability across wide ranges (Hu et al., 2015; McKenzie et al., 2003; Qin et al., 2017), local genotypes can affect species distributions (Valladares et al., 2014). While the Transverse Ranges have the same geographic orientation (east-west) and can be considered the same “geographic extent”, this area experiences variation in such factors as topography and rainfall. All of these factors can affect local species adaptations, and thus species distributions (Valladares et al., 2014; Vizcaíno Palomar, 2016). A MaxEnt model of habitat suitability for oaks on the California Channel Islands found that model results changed depending on whether the geographic extent of their model included all the Channel Islands or each island individually (McComb et al., 2019). This implies that our results may vary if we were to model each portion of the Transverse Ranges as their own geographic extent. However, the lack of presence data across specific regions of our study area, mainly ANF, prevented us from modeling the eastern, western, and central Transverse Ranges separately. General trends in future yellow pine distributions can still be drawn from our analysis.

We acknowledge that it would have been more representative to model the distribution of *P. jeffreyi* and *P. ponderosa* separately. Although both species are tolerant to drought and cold, *P. ponderosa* is thought to be less drought and cold tolerant than *P. jeffreyi* and has a smaller distribution throughout southern California (Comer et al., n.d.). Young seedlings and saplings are disproportionately affected by drought and cold as compared to adult trees, and therefore, such variables are especially important to capture when modeling sapling distributions (Gucker, n.d.). The species' differing tolerances to these environmental conditions suggests that projections of these species' future distributions will vary under certain climates, including drought conditions which are expected to increase in the future (Williams et al., 2015). By modeling the joint distribution of these species, we may be biasing our models and masking the species' true distributions. However, given that there is a high chance that surveyors are misidentifying and mistaking these trees for one another (Section 6.2.2), it is likely that we would to some extent unwillingly be mapping their joint distributions even if we chose to model *P. jeffreyi* and *P. ponderosa* presence points separately. Additionally, although these species may have slightly different habitat responses, they are generally believed to occupy similar habitats (Hallin, 1957). Again, our models were designed to illustrate general trends in future yellow pine distributions, rather than precise, fine scales estimates of habitat suitability.

We also acknowledge that incorporating annual climate data, rather than 30-year climate summaries into our MaxEnt models would likely have more accurately captured suitable sapling habitat across the time frame(s) of interest. Annual climate variability strongly affects the germination and survival of young trees, and in turn, seedling establishment often occurs in pulses of favorable climatic conditions which are masked under 30-year climate summaries (Serra-Diaz et al., 2016). However, annual climate data was unavailable at fine-scale resolutions for the study area of interest (see Section 6.2.3.1). Considerations

into how using 30-year climate summaries rather than annual climate data may have affected our results are discussed in Section 6.4.

Species distributions are limited in large part by abiotic conditions, biotic interactions, and dispersal ability (Simões & Peterson, 2018). While abiotic factors, such as temperature and precipitation, are incorporated into SDMs as predictor variables, it is not common to directly model biotic factors (Staniczenko et al., 2017). Instead, SDMs may incorporate biotic interactions by using specific information about interacting species, such as occurrences of these species, as predictor variables in the model (Araújo & Luoto, 2007; Franklin, 2010; Godsoe et al., 2016; Morueta-Holme et al., 2016). Biotic interactions, including competition, parasitism, and mutualism, can have large effects on the distribution of plant species (Dam, 2009). However, integrating biotic interactions with SDMs is still a developing field of study (Wisz et al., 2013). Furthermore, mapping species distributions across large macroecological scales makes it difficult to incorporate local species interactions, which are often studied at much smaller extents and finer resolutions (Staniczenko et al., 2017). It is also often difficult to predict the spatial extent and intensity at which biotic interactions will influence species distributions (Kadowaki et al., 2016). For instance, future management practices are unpredictable and have the potential to strongly influence interacting species. For these reasons, we chose to examine only how abiotic factors affect yellow pine distributions.

While survey data utilized for this study was in the form of presence/absence data (Section 6.2.3.2), we selected MaxEnt as our SDM of choice, which was designed to work with presence-only data (Elith et al. 2011; Guillera-Aroita et al., 2014). Biotic factors, such as canopy cover, likely influence yellow pine distributions. Yellow pine adults and seedlings are shade intolerant and are often replaced by more shade tolerant conifers, such as white fir and incense cedar, under shade conditions (Bigelow et al., 2011; Minnich et al., 1995). YPMC forest tree density and canopy cover have significantly increased in southern California (Section 5.1 and 5.5), suggesting that shade may be influencing yellow pine distributions. While a given region may be climatically suitable for yellow pine saplings, high canopy cover may prevent seedlings and saplings from germinating and surviving in the shaded conditions. Surveying across these areas could result in recorded yellow pine sapling absences that were more a factor of canopy cover, rather than the modeled abiotic environment. Additionally, surveying in recent fire scars would result in yellow pine saplings being recorded as absent from recently burned areas. However, in the absence of fire, the abiotic conditions across these locations may actually be suitable for yellow pine establishment and growth. By modeling presences only, we ensure that our models are not affected by absences that could have been influenced by biotic factors. Our predictions of suitable habitat represent areas that are predicted to be climatically suitable for yellow pine saplings. Results from our analysis may be considered along with information on local species presences and interactions to ensure a more holistic approach towards conservation planning.

Lastly, our method of requiring all cells to be considered suitable habitat when creating the summed future scenarios could result in future habitat suitability being underestimated. For example, if a cell was suitable in 7 of the 8 future scenarios, then the cell would not be considered suitable. Future analyses should explore different thresholds when determining future suitable habitat.

7. Prioritization

Our goal with this objective is to demonstrate one way our quantitative analysis and a NRV can be used in a management setting while tying together our results from the species distribution model. We identify YPMC forests in SBNF that are a priority for forest health projects using a multi-criteria decision analysis. Forest health projects aim to increase the resiliency of forested lands and provide watershed protection that maintain the ecosystem services provided by the forest. Some examples of management actions utilized in forest health projects include reintroducing fire into these landscapes through the use of prescribed burning or if prescribed fire is not possible, actions that mimic fire, like thinning may also be utilized.

While our NRV results are not used directly in this example to identify priority conservation areas, our NRV analysis can be used to create management goals and define desired conditions. For example, if a manager's goal is to protect future watersheds from runoff and erosion caused by high severity fire, an assessment of the current stand structure (tree density, canopy cover, etc.) can be compared to historical conditions to evaluate the need for action and define a target desired condition. Our NRV results can be used to set goals for tree density and size class distribution that will promote forest resilience. Additionally, our analysis comparing changes in historic and contemporary forest structure were not used in this analysis. However, our results can be used to create a spatial model of tree density or basal area to further determine where to focus forest health projects.

We acknowledge that managers will have to incorporate their own constraints and select their own criteria when determining where to do forest health projects. Thus, this analysis represents an exploratory case study to demonstrate how limited resources can be utilized towards conserving forests that will have the greatest impact on long-term ecosystem health.

7.1 Methods

To identify key conservation areas within YPMC forests, we first identified areas in which management actions are allowed. These areas are referred to as legal and administrative constraints (North et al., 2015). We identified three main legal and administrative constraints: wilderness, California spotted owl (*Strix occidentalis occidentalis*) habitat, and riparian zones. Forests within wilderness boundaries were excluded because activities within wilderness, even conservation activities, are harder to accomplish for several reasons. First, mechanical devices are not allowed within wilderness boundaries (e.g., no cars or chainsaws; hand tools only). This limitation prohibits forest health activities like mechanical thinning (North et al., 2015). Second, working in wilderness would require a minimum requirements decision guide to be completed (<https://wilderness.net/practitioners/minimum-requirements-analysis>). We excluded California spotted owl habitat because working within these areas is also highly restricted because they are a species of special concern (North et al., 2015). Last, we excluded areas within 100ft of a river, as recommended by current USFS guidelines (North et al., 2015). Any YPMC forest within these legal and administrative constraints was excluded from the prioritization model.

After identifying areas where conservation actions can legally take place, we overlapped three layers in ArcGIS to determine which of the remaining YPMC forests would be a priority for forest health projects based off of three considerations:

1. Ecosystem services: Underwood et al. (2018) created five layers at 30m resolution that were combined to represent ecosystem services in southern California: runoff, groundwater recharge, soil retention, biodiversity, and biomass. We did not use the biomass layer because the estimates had low accuracy in forested regions (Underwood per. comm.), making it unreliable to apply to

our study area. Marxan was used to estimate biodiversity across southern California. Biodiversity is an important underlying factor that influences ecosystem resilience (Peterson et al., 1998; Tilman, 1996). Runoff and groundwater recharge were extracted from the Basin Characterization Model. Water security and watershed management is an increasingly important issue as climate change is expected to alter precipitation patterns (Hayhoe et al., 2004). Soil retention (i.e., sediment erosion potential) was estimated using sediment delivery ratio model (SDR) from InVEST which required inputs like DEM, a rainfall erosivity index, soil erodibility, and normalized difference vegetation index (NDVI). Soil erosion, especially after wildfires which can strip the landscape of native vegetation, causes severe damage to human dominated and natural downstream communities and reduces water quality (Wohlgemuth & Beyers, 2012). This layer identifies areas across the landscape that have the best ability to retain sediment and thus avoid soil erosion.

The continuous values of each layer were converted to deciles. We utilized values that were in the top three deciles (top 30%) of each layer (adapted from Underwood et al. 2018) to represent cells that would be a priority for conservation (Figure 46A-D). Then we used Raster Calculator in ArcGIS to sum the layers to identify ecosystem hotspots. Part of the definition of “hotspots” by Underwood et al. (2018) included cells that contained the top deciles of all layers. However, we wanted to take a more flexible approach in identifying areas that would be a priority for forest health projects, so we defined ecosystem hotspots as cells that contain the top 30% of 3-4 ecosystem services.

2. Probability of high fire severity: High severity wildfire has severe repercussions on ecosystem health and human infrastructure (Bladon et al., 2014; Fraser et al., 2020; McCaffrey & Rhodes, 2009). Identifying areas that are at risk for high severity wildfire is the first step in risk reduction (Scott et al., 2013). Parks et al. (2018) used a machine learning model to determine the probability of a fire being a high severity fire at 30m resolution in ecoregions across the southwest U.S. SBNF fell within the South Coast Ecoregion of Parks et al.’s (2018) study (layers are available at <https://www.frames.gov/NextGen-FireSeverity>). Weather and live fuel variables best explained severe fire severity in this ecoregion. We used the layer that predicted high fire severity under extreme weather conditions and overlapped cells whose probability of fires ranged from 0.405-0.8097. 0.8097 is the maximum value of probability of high fire severity. Pixels with a value of 0.405 have half the probability of high fire severity occurring as the maximum value.
3. Future suitable habitat: Within YPMC forests, yellow pines are some of the most drought and fire tolerant conifers (Hilberg et al., 2016, US Forest Service, 2019). These characteristics are important for resilient forests as droughts and wildfires are projected to increase in the future (Liu et al., 2010, Fried et al., 2004, Diffenbaugh et al. 2015). Thus, identifying areas that will be suitable habitat for yellow pines in the future is a crucial step in selecting priority conservation areas. This layer is a product of our habitat suitability analysis in which we used 8 climate scenarios (4 wet and 4 dry) to predict suitable habitat for yellow pine saplings from 2010-2039. We conservatively defined cells that were a priority for forest health projects if habitat for yellow pine saplings was suitable under 6 of the 8 future climate scenarios.

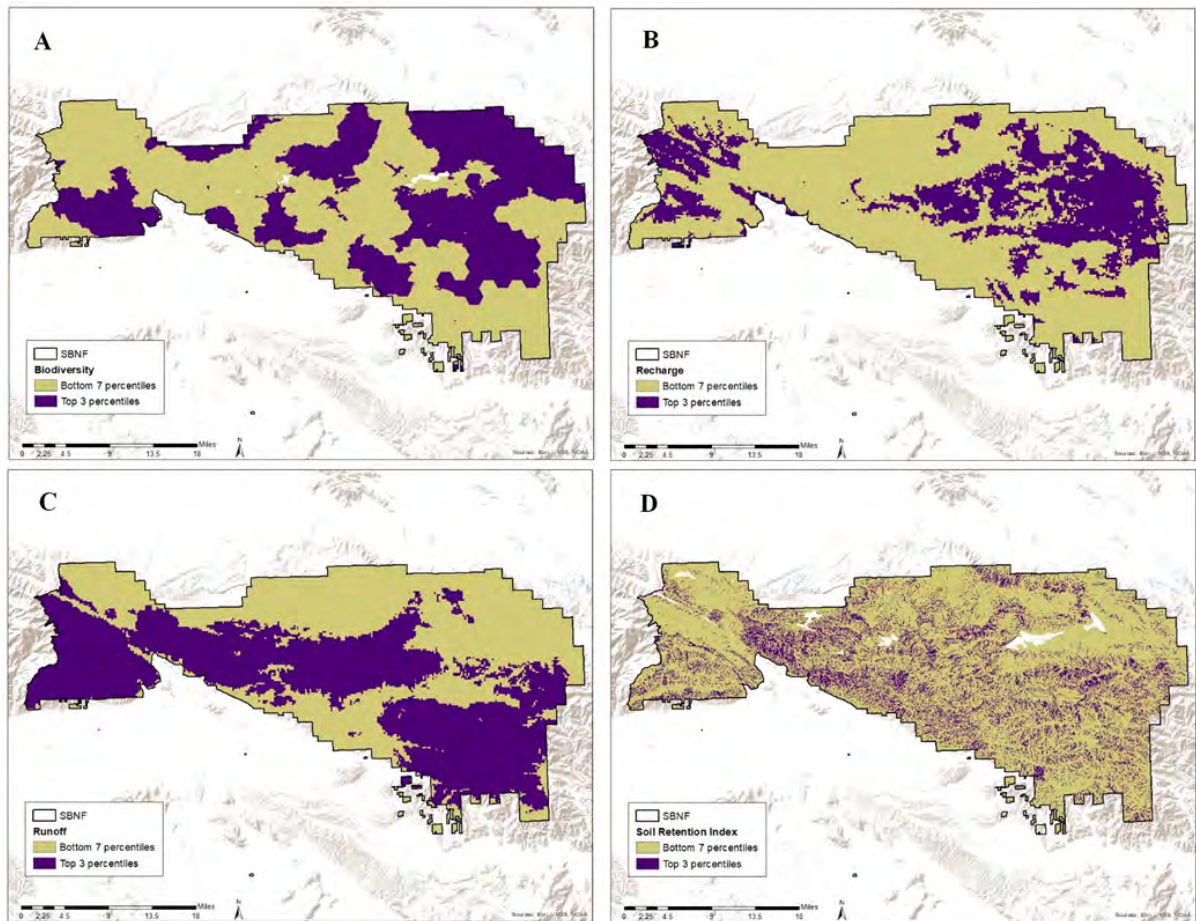


Figure 46. Top 3 percentiles of four ecosystem service layers (biodiversity (A), recharge (B), runoff (C), and soil retention index(D)) from Underwood et al. (2018). See Figure 48A for the sum map of these ecosystem services.

The final step in our analysis incorporated feasibility into the selection of areas that could be a priority for forest health projects. We used a 1,000m buffer around roads and trails to identify areas easiest to reach (adapted from North et al. 2015). Areas where there are existing roads and trails indicate areas where personnel can access conservation sites, and are therefore prioritized (i.e., ranked higher) in our model. Areas too far from roads are often too difficult to reach due to steep terrain or dense vegetation.

7.2 Results

There are a total of 113,900 acres of YPMC forests in SBNF. Of this, forest health projects can take place in 86,937 acres (76.2%) after excluding areas in which legal and administrative constraints make forest health projects infeasible (Figure 47). We used a binary approach in our multi-criteria decision analysis to select areas that would be a priority for conservation, meaning if a cell met one of the priority criteria it was assigned a value of 1. We only used cells that were a priority in all 3 criteria (ecosystem services, fire severity, and future habitat suitability of yellow pine saplings). After incorporating the priority criteria, only 9,280 acres (8.1%) of YPMC forest would be prioritized for forest health projects (Figure 48). Finally, after incorporating feasibility by only considering priority forests that are within 1,000m of a road or trail, only 6,749 acres of these priority areas would be feasible for forest health projects (Figure 49). After accounting for legal and administrative constraints, feasibility, and priority requirements a total of 5.9% of YPMC forests (6,749 acres) are a feasible priority for forest health projects (Figure 50).

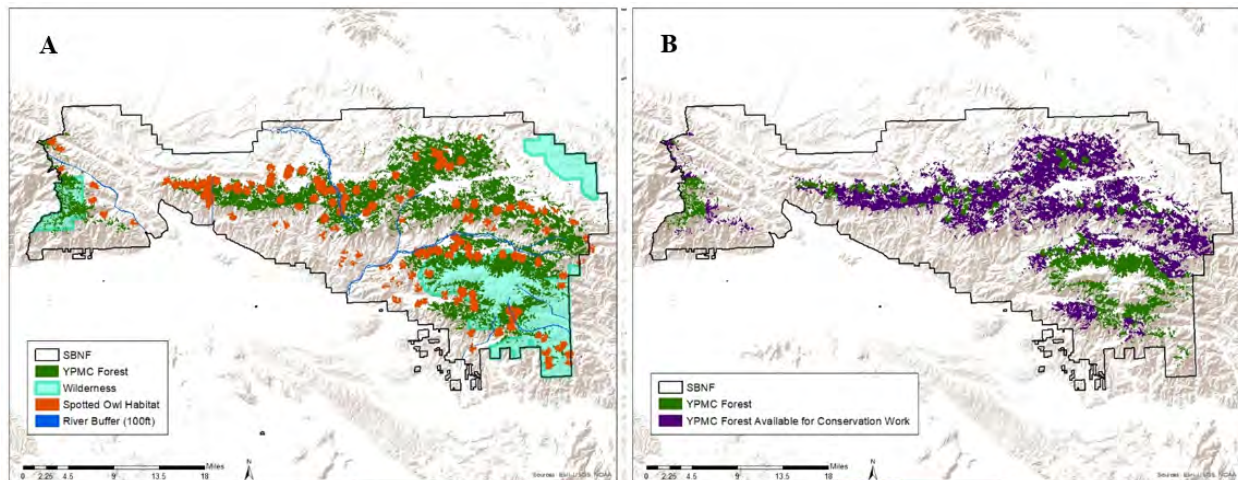


Figure 47. (A) Areas in SBNF where conservation would not be possible due to legal and administrative restrictions overlapped with YPMC forests. (B) YPMC forests where forest health projects can be conducted as they are not restricted by legal or administrative constraints (areas in purple).

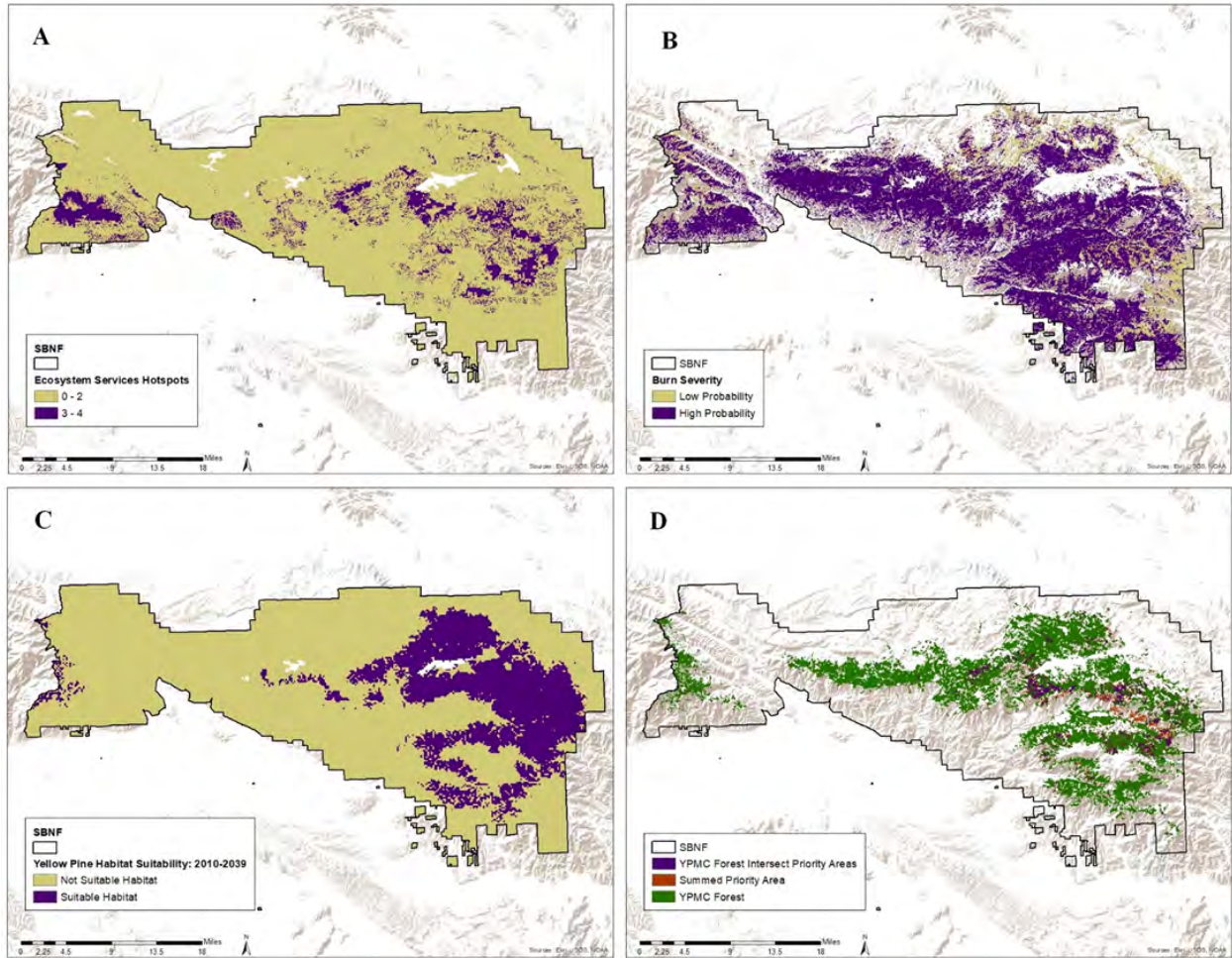


Figure 48. (A) Ecosystem services hotspots. We utilized cells that contained the top 3 deciles of 3-4 ecosystem services. (B) Probability of burn severity in extreme weather conditions if a fire were to occur (Parks et al., 2018). We utilized cells that had a 0.405-0.8097 probability of high severity fire if a fire were to occur. (C) Projected future suitable habitat of yellow pines from 2010-2039. We utilized cells that were suitable in 6 of 8 climate scenarios. (D) Cells that occurred in all 3 layers used to identify areas that would be a priority for forest health projects (orange). These areas were overlapped with YPMC forests that fall outside of legal and administrative constraints (see Figure 46B) (purple).

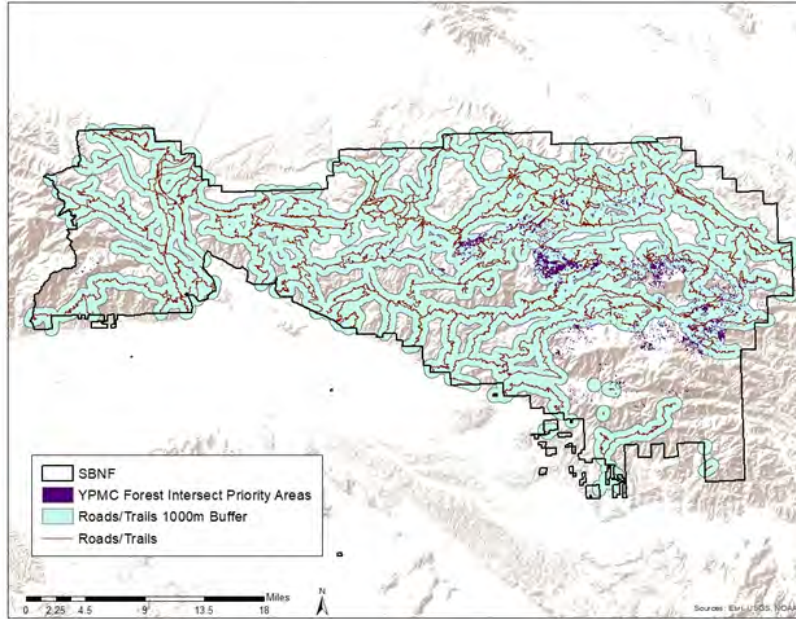


Figure 49. YPMC forests that are a priority for conservation and outside of legal and administrative constraints were intersected with a 1000m roads buffer.

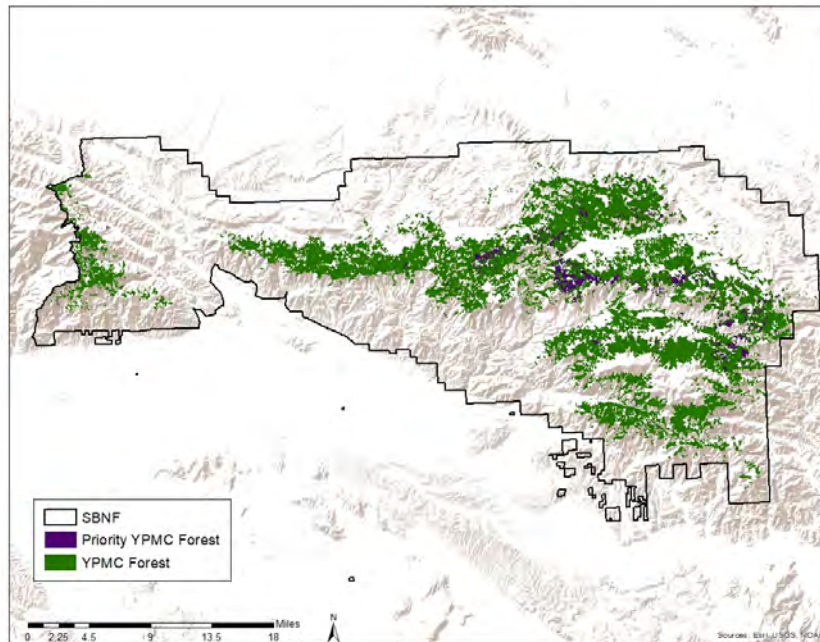


Figure 50. YPMC forests that are a priority for conservation after overlapping areas that are outside of legal and administration constraints feasible for conservation (Figure 47), contain priority attributes (Figure 48), and are feasible to access (Figure 49).

7.3 Discussion

Ultimately, identifying areas that should be a priority for forest health projects is a subjective task that may vary with the needs of stakeholders and or funding constraints. Selecting the criteria used to identify what values represent forests that would be a priority for conservation was the most subjective part of the analysis that will change depending on management goals, stakeholders, and the forest health activity.

Additionally, managers and stakeholders may opt for a different approach in their multi-criteria decision analysis. While we used a binary approach that applied equal weight to each of the three priority layers, others may choose to assign more or less weight to the layers depending on the management objectives.

Several parts of our analysis still remain relevant when planning for a non-theoretical forest health project. The most applicable part of this analysis for future projects was determining where forest health projects are allowed to take place due to legal and administrative constraints. All managers will be affected by these constraints when planning forest health projects. Feasibility will also be a critical component influencing where forest health projects are likely to occur. Our feasibility analysis likely overestimates the total acres of YPMC forests that we determined to be feasible for conservation projects. For one, it is very likely that not all the roads and trails used to create the feasibility buffer are actually passable. Local knowledge of the traversability of roads and trails would further narrow down the amount of YPMC forests feasible for conservation. Second, inclusion of a threshold for slope (North et al., 2015) would also narrow down forests that can be safely accessed. Additionally, a NRV will remain useful despite the situation, but it is up to the managers to decide how to utilize the NRV analysis. A NRV can be used to determine what conditions warrant intervention, create management goals, and inform the public on justifications for forest health projects.

While the variables managers use to define priority areas will change depending on the situation, we encourage prioritization efforts to incorporate, in some way, all the three topics used in this analysis to prioritize locations for forest health projects: ecosystem services, fire, and future climate change. Three of the four ecosystem services layers we used (runoff, recharge, and soil retention index) pertained to water quality and security. Since climate change is expected to alter precipitation patterns (Hayhoe et al., 2004), managing watersheds will be an increasingly important task to protect and preserve water resources. Future prioritization should also consider how fire will impact YPMC forests. Fire suppression has led to the densification of forests in southern California (see Section 5.2), which can result in high severity crown fires (Steel et al., 2015). Crown fires can have long lasting impacts on natural ecosystems and human environments (Bladon et al., 2014; McCaffrey & Rhodes, 2009; Fraser et al., 2020). Thus, preventing crown fires should be a priority for managers and can be achieved in part by considering fire risk when establishing priority criteria. Lastly, managers should incorporate climate change impacts into prioritization models. This can help direct limited resources to forests that will be the most likely to persist under future climate scenarios. For example, restoration may be prioritized in areas where the future climate will be most likely to support YPMC forests. Alternatively, if protecting current, mature YPMC forests was the management goal, one can make the argument that resources should be prioritized to forests that are least likely to be suitable for recruiting seedlings under future climates. Since adult conifers can continue to persist in climates no longer suitable for new recruits, managers may want to keep these forests on the landscape so they can continue to provide important ecosystem services for as long as possible. Thus, managers may want to conduct forest health projects, such as thinning, in these areas to reduce the likelihood of high fire severity since conifer seedlings would be unlikely to replace adult conifers after a wildfire.

In conclusion, the goal of this case study was not to determine definitively where forest health projects should be done. Rather, the goal was to conduct a thought exercise demonstrating how managers can integrate several criteria to help make educated decisions for conservation activities that prioritize ecosystem health with limited funding. Our approach exhibits one way forest managers can incorporate modern research when planning for resilient forests.

Citations

- Abella, S. R., Gering, L. R., & Shelburne, V. B. (2004). Slope Correction of Plot Dimensions for Vegetation Sampling in Mountainous Terrain. *Natural Areas Journal*, 24(4), 358–360.
- Adam, D. P., & West, G. J. (1983). Temperature and precipitation estimates through the last glacial cycle from Clear Lake, California, pollen data. *Science*, 219(4581), 168–170.
- Aguirre-Gutiérrez, J., Carvalheiro, L. G., Polce, C., Loon, E. E. van, Raes, N., Reemer, M., & Biesmeijer, J. C. (2013). Fit-for-Purpose: Species Distribution Model Performance Depends on Evaluation Criteria – Dutch Hoverflies as a Case Study. *PLOS ONE*, 8(5), e63708. <https://doi.org/10.1371/journal.pone.0063708>
- Alpert, H., & Loik, M. E. (2013). Pinus jeffreyi establishment along a forest-shrub ecotone in eastern California, USA. *Journal of Arid Environments*, 90, 12–21. <https://doi.org/10.1016/j.jaridenv.2012.09.017>
- Araújo, M. B., & Luoto, M. (2007). The importance of biotic interactions for modelling species distributions under climate change. *Global Ecology and Biogeography*, 16(6), 743–753. <https://doi.org/10.1111/j.1466-8238.2007.00359.x>
- Ault, T. R., Cole, J. E., Overpeck, J. T., Pederson, G. T., & Meko, D. M. (2014). Assessing the Risk of Persistent Drought Using Climate Model Simulations and Paleoclimate Data. *Journal of Climate*, 27(20), 7529–7549. <https://doi.org/10.1175/JCLI-D-12-00282.1>
- Austin, M. (2007). Species distribution models and ecological theory: A critical assessment and some possible new approaches. *Ecological Modelling*, 200(1), 1–19. <https://doi.org/10.1016/j.ecolmodel.2006.07.005>
- Barbour, M. (2007). *Terrestrial Vegetation of California* (3rd ed., Vol. 3rd). University of California Press.
- Barbour, M. G., & Minnich, R. A. (2000). Californian upland forests and woodlands. In *North American Terrestrial Vegetation*. Cambridge University Press.
- Bedsworth, L., Cayan, D., Franco, G., Fisher, L., & Ziaja, S. (2018). *Statewide Summary Report: California's Fourth Climate Change Assessment* (SUM-CCCA4-2018-013; p. 98).
- Bell, D. M., Bradford, J. B., & Lauenroth, W. K. (2014). Early indicators of change: Divergent climate envelopes between tree life stages imply range shifts in the western United States. *Global Ecology and Biogeography*, 23(2), 168–180. <https://doi.org/10.1111/geb.12109>
- Berg, N., & Hall, A. (2017). Anthropogenic warming impacts on California snowpack during drought. *Geophysical Research Letters*, 44, 2511–2518.
- Berg, Neil, Hall, A., Sun, F., Capps, S., Walton, D., Langenbrunner, B., & Neelin, D. (2015). Twenty-First-Century Precipitation Changes over the Los Angeles Region. *Journal of Climate*, 28(2), 401–421. <https://doi.org/10.1175/JCLI-D-14-00316.1>
- Bestelmeyer, B. T. (2012). Is the historical range of variation relevant to rangeland management? In J. A. Weins, G. D. Hayward, H. D. Safford, & C. M. Giffen (Eds.), *Historical Environmental Variation in Conservation and Natural Resource Management* (1st ed., pp. 289–296). Wiley-Blackwell.
- Beven, K. J., & Kirkby, M. J. (1979). A physically based, variable contributing area model of basin hydrology / Un modèle à base physique de zone d'appel variable de l'hydrologie du bassin versant. *Hydrological Sciences Bulletin*, 24(1), 43–69. <https://doi.org/10.1080/02626667909491834>
- Bigelow, S. W., North, M. P., & Salk, C. F. (2011). Using light to predict fuels-reduction and group-selection effects on succession in Sierran mixed-conifer forest. *Canadian Journal of Forest Research*, 41(10), 2051–2063. <https://doi.org/10.1139/x11-120>
- Birch, D. S., Morgan, P., Kolden, C. A., Abatzoglou, J. T., Dillon, G. K., Hudak, A. T., & Smith, A. M. S. (2015). Vegetation, topography and daily weather influenced burn severity in central Idaho and western Montana forests. *Ecosphere*, 6(1), art17. <https://doi.org/10.1890/ES14-00213.1>
- Bladon, K. D., Emelko, M. B., Silins, U., & Stone, M. (2014). Wildfire and the Future of Water Supply. *Environmental Science & Technology*, 48(16), 8936–8943. <https://doi.org/10.1021/es500130g>
- Blakley, E. R., & Barnette, K. (1985). *Historical Overview of the Los Padres National Forest*. https://lpfw.org/wp-content/uploads/2013/06/19850700_Blakley_HistoricalOverviewLPNF.pdf
- Bohlman, G. N., Safford, H. D., & Skinner, C. N. (n.d.). Natural range of variation for yellow pine and mixed conifer forests in northwestern California and southwestern Oregon, USA (in prep). *United State Department of Agriculture, Forest Service, Pacific Southwest Research Station*.

- Borchert, M. (1985). SEROTINY AND CONE-HABIT VARIATION IN POPULATIONS OF PINUS COULTERI (PINACEAE) IN THE SOUTHERN COAST RANGES OF CALIFORNIA. *Madroño*, 32(1), 29–48.
- Bouldin, J. (1999). *Twentieth-century changes in forests of the Sierra Nevada, California* [Ph.D thesis].
- Bouldin, Jim. (2009). Comment on “Has fire suppression increased the amount of carbon stored in western U.S. forests?” by A. W. Fellows and M. L. Goulden. *Geophysical Research Letters*, 36(21). <https://doi.org/10.1029/2009GL039391>
- Bourdo, E. A. (1956). A Review of the General Land Office Survey and of Its Use in Quantitative Studies of Former Forests. *Ecology*, 37(4), 754–768. <https://doi.org/10.2307/1933067>
- Bowen, B. J., & Pate, J. S. (1993). The Significance of Root Starch in Post-fire Shoot Recovery of the Resprouter *Stirlingia latifolia* R. Br. (Proteaceae). *Annals of Botany*, 72(1), 7–16. <https://doi.org/10.1006/anbo.1993.1075>
- Bradbury, D. (1974). *Vegetation history of Ramona Quadrangle* [Ph.D dissertation]. University of California, Los Angeles.
- Brown, J. K., & Smith, J. K. (2000). *Wildland fire in ecosystems: Effects of fire on flora* (RMRS-GTR-42-V2; p. RMRS-GTR-42-V2). U.S. Department of Agriculture, Forest Service, Rocky Mountain Research Station. <https://doi.org/10.2737/RMRS-GTR-42-V2>
- Brown, P. M., & Wu, R. (2005). Climate and Disturbance Forcing of Episodic Tree Recruitment in a Southwestern Ponderosa Pine Landscape. *Ecology*, 86(11), 3030–3038. <https://doi.org/10.1890/05-0034>
- Brown, T. C., Froemke, P., Mahat, V., & Ramirez, J. A. (2016). *Mean Annual Renewable Water Supply of the Contiguous United States* (p. 55). Rocky Mountain Research Station.
- California State Board Forestry. (1886). *First biennial report of the California State Board of Forestry for the years 1885-86*.
- CDF. (2018). *Total Population by County*. California Department of Finance. <https://www.dof.ca.gov/Forecasting/Demographics/Projections/>
- Chmura, D. J., Anderson, P. D., Howe, G. T., Harrington, C. A., Halofsky, J. E., Peterson, D. L., Shaw, D. C., & Brad St.Clair, J. (2011). Forest responses to climate change in the northwestern United States: Ecophysiological foundations for adaptive management. *Forest Ecology and Management*, 261(7), 1121–1142. <https://doi.org/10.1016/j.foreco.2010.12.040>
- Chou, Y. H., Minnich, R. A., & Chase, R. A. (1993). Mapping probability of fire occurrence in San Jacinto Mountains, California, USA. *Environmental Management*, 17, 129–140.
- Cocking, M. I., Varner, J. M., & Knapp, E. E. (2014). Long-term effects of fire severity on oak–conifer dynamics in the southern Cascades. *Ecological Applications*, 24(1), 94–107. <https://doi.org/10.1890/13-0473.1>
- Collins, B. M., Everett, R. G., & Stephens, S. L. (2011). Impacts of fire exclusion and recent managed fire on forest structure in old growth Sierra Nevada mixed-conifer forests. *Ecosphere*, 2(4), Art. 51.
- Comer, P., Keeler-Wolf, T., Kittel, G., & Schulz, K. A. (2018, May 24). *California Montane Jeffrey Pine-(Ponderosa Pine) Woodland*. NatureServe Explorer. [https://explorer.natureserve.org/Taxon/ELEMENT_GLOBAL.2.722763/California_Montane_Jeffrey_Pine-\(Ponderosa_Pine\)_Woodland](https://explorer.natureserve.org/Taxon/ELEMENT_GLOBAL.2.722763/California_Montane_Jeffrey_Pine-(Ponderosa_Pine)_Woodland)
- Conrad, S. G., Jaramillo, A. E., Cromack, K., & Rose, S. (1985). *The role of the genus Ceanothus in western forest ecosystems* (General Technical Report PNW-GTR-182). USDA Forest Service: Pacific Southwest Region.
- Cook, B. I., Ault, T. R., & Smerdon, J. E. (2015). Unprecedented 21st century drought risk in the American Southwest and Central Plains. *Science Advances*, 1(1). <https://doi.org/10.1126/sciadv.1400082>
- Cope, A. B. (1993). *Pinus coulteri*. Fire Effects Information System, [Online]. <https://www.fs.fed.us/database/feis/plants/tree/pincou/all.html>
- Cornwell, W. K., Stuart, S., Ramirez, A. R., Dolanc, C. R., Thorne, J. H., & Ackerly, D. D. (2012). *Climate Change Impacts on California Vegetation: Physiology, Life History, and Ecosystem Change*. (CEC-500-2012-023; p. 79). University of California, Berkeley.
- Cronmiller, F. P. (1959). The Life History of Deerbrush-A Fire Type. *Journal of Range Management*, 12(1), 21. <https://doi.org/10.2307/3895212>
- Crookston, N. L., & Stage, A. R. (1999). *Percent canopy cover and stand structure statistics from the Forest Vegetation Simulator* (RMRS-GTR-24; p. RMRS-GTR-24). U.S. Department of Agriculture, Forest Service, Rocky Mountain Research Station. <https://doi.org/10.2737/RMRS-GTR-24>
- Crotteau, J. S., Morgan Varner, J., & Ritchie, M. W. (2013). Post-fire regeneration across a fire severity gradient in the southern Cascades. *Forest Ecology and Management*, 287, 103–112. <https://doi.org/10.1016/j.foreco.2012.09.022>

- Dam, N. M. V. (2009). How plants cope with biotic interactions. *Plant Biology*, 11(1), 1–5. <https://doi.org/10.1111/j.1438-8677.2008.00179.x>
- Davis, F. W., Sweet, L. C., Serra-Diaz, J. M., Franklin, J., McCullough, I., Flint, A., Flint, L., Dingman, J. R., Regan, H. M., Syphard, A. D., Hannah, L., Redmond, K., & Moritz, M. A. (2016). Shrinking windows of opportunity for oak seedling establishment in southern California mountains. *Ecosphere*, 7(11). <https://doi.org/10.1002/ecs2.1573>
- Davis, K. T., Dobrowski, S. Z., Higuera, P. E., Holden, Z. A., Veblen, T. T., Rother, M. T., Parks, S. A., Sala, A., & Maneta, M. P. (2019). Wildfires and climate change push low-elevation forests across a critical climate threshold for tree regeneration. *Proceedings of the National Academy of Sciences*, 116(13), 6193–6198. <https://doi.org/10.1073/pnas.1815107116>
- Diffenbaugh, N. S., Swain, D. L., & Touma, D. (2015). Anthropogenic warming has increased drought risk in California. *Proceedings of the National Academy of Sciences*, 112(13), 3931–3936. <https://doi.org/10.1073/pnas.1422385112>
- Dilts, T. E. (2015). *Topography Tools for ArcGIS 10.1*. ArcGIS. <https://www.arcgis.com/home/item.html?id=b13b3b40fa3c43d4a23a1a09c5fe96b9>
- Dingman, J. R., Sweet, L. C., McCullough, I., Davis, F. W., Flint, A., Franklin, J., & Flint, L. E. (2013). Cross-scale modeling of surface temperature and tree seedling establishment in mountain landscapes. *Ecological Processes*, 2(1), 30. <https://doi.org/10.1186/2192-1709-2-30>
- Dolanc, C. R., Safford, H. D., Dobrowski, S. Z., & Thorne, J. H. (2013). Twentieth century shifts in abundance and composition of vegetation types of the Sierra Nevada, CA, US. *Applied Vegetation Science*, 17(3), 442–455. <https://doi.org/10.1111/avsc.12079>
- Dolanc, C. R., Safford, H. D., Thorne, J. H., & Dobrowski, S. Z. (2014). Changing forest structure across the landscape of the Sierra Nevada, CA, USA, since the 1930s. *Ecosphere*, 5(8), art101. <https://doi.org/10.1890/ES14-00103.1>
- Dolph, K. L., Mori, S. R., & Oliver, W. W. (1995). Long-Term Response of Old-Growth Stands to Varying Levels of Partial Cutting in the Eastside Pine Type. *Western Journal of Applied Forestry*, 10(3), 101–108. <https://doi.org/10.1093/wjaf/10.3.101>
- Donato, D. C., Fontaine, J. B., Campbell, J. L., Robinson, W. D., Kauffman, J. B., & Law, B. E. (2009). Conifer regeneration in stand-replacement portions of a large mixed-severity wildfire in the Klamath–Siskiyou Mountains. *Canadian Journal of Forest Research*, 39(4), 823–838. <https://doi.org/10.1139/X09-016>
- Dunbar-Irwin, M., & Safford, H. (2016). Climatic and structural comparison of yellow pine and mixed-conifer forests in northern Baja California (México) and the eastern Sierra Nevada (California, USA). *Forest Ecology and Management*, 363, 252–266. <https://doi.org/10.1016/j.foreco.2015.12.039>
- Elith, J., & Leathwick, J. R. (2009). Species Distribution Models: Ecological Explanation and Prediction Across Space and Time. *Annual Review of Ecology, Evolution, and Systematics*, 40(1), 677–697. <https://doi.org/10.1146/annurev.ecolsys.110308.120159>
- Elith, J., Graham, C. H., Anderson, R. P., Dudík, M., Ferrier, S., Guisan, A., Hijmans, R. J., Huettmann, F., Leathwick, J. R., Lehmann, A., Li, J., Lohmann, L. G., Loiselle, B. A., Manion, G., Moritz, C., Nakamura, M., Nakazawa, Y., Overton, J. M. M., Peterson, A. T., ... Zimmermann, N. E. (2006). Novel methods improve prediction of species' distributions from occurrence data. *Ecography*, 29(2), 129–151. <https://doi.org/10.1111/j.2006.0906-7590.04596.x>
- Elith, J., Phillips, S. J., Hastie, T., Dudík, M., Chee, Y. E., & Yates, C. J. (2011). A statistical explanation of MaxEnt for ecologists: Statistical explanation of MaxEnt. *Diversity and Distributions*, 17(1), 43–57. <https://doi.org/10.1111/j.1472-4642.2010.00725.x>
- Erickson, H. E., & White, R. (2008). *Soils Under Fire: Soils Research and the Joint Fire Science Program (PNW-GTR-759)*. U.S. Department of Agriculture, Forest Service, Pacific Northwest Research Station. https://www.fs.fed.us/pnw/pubs/pnw_gtr759.pdf
- Evans, A. M., Everett, R. G., Stephens, S. L., & Youtz, J. A. (2011). *Comprehensive Fuels Treatment Practices Guide for Mixed Conifer Forests: California, Central and Southern Rockies, and the Southwest* (p. 112). Forest Guild, US Forest Service.
- Fellows, A. W., & Goulden, M. L. (2008). Has fire suppression increased in the amount of carbon stored in western U.S. forests? *Geophysical Research Letters*, 35, L122404.
- Fellows, A. W., & Goulden, M. L. (2012). Rapid vegetation redistribution in Southern California during the early 2000s drought: Drought driven vegetation redistribution. *Journal of Geophysical Research: Biogeosciences*, 117(G3), n/a-n/a. <https://doi.org/10.1029/2012JG002044>
- Fisichelli, N., Wright, A., Rice, K., Mau, A., Buschena, C., & Reich, P. B. (2014). First-year seedlings and climate change: Species-specific responses of 15 North American tree species. *Oikos*, 123(11), 1331–1340. <https://doi.org/10.1111/oik.01349>
- Flint, L. E., & Flint, A. L. (2014). California Basin characterization model: A dataset of historical and future hydrologic response to climate change. *U.S. Geological Survey Dataset Release*. <https://doi.org/10.5066/F76T0JPB>
- Franklin, J. (2010). *Mapping species distributions: Spatial inference and prediction*. Cambridge University Press.

- Franklin, J., Davis, F. W., Ikegami, M., Syphard, A. D., Flint, L. E., Flint, A. L., & Hannah, L. (2013). Modeling plant species distributions under future climates: How fine scale do climate projections need to be? *Global Change Biology*, *19*(2), 473–483. <https://doi.org/10.1111/gcb.12051>
- Franklin, Janet, & Bergman, E. (2011). Patterns of pine regeneration following a large, severe wildfire in the mountains of southern California. *Canadian Journal of Forest Research*, *41*(4), 810–821. <https://doi.org/10.1139/x11-024>
- Franklin, Janet, Spears-Lebrun, L. A., Deutschman, D. H., & Marsden, K. (2006). Impact of a high-intensity fire on mixed evergreen and mixed conifer forests in the Peninsular Ranges of southern California, USA. *Forest Ecology and Management*, *235*(1–3), 18–29. <https://doi.org/10.1016/j.foreco.2006.07.023>
- Fraser, A. M., Chester, M. V., & Underwood, B. S. (2020). Wildfire risk, post-fire debris flows, and transportation infrastructure vulnerability. *Sustainable and Resilient Infrastructure*, *0*(0), 1–13. <https://doi.org/10.1080/23789689.2020.1737785>
- Freedman, J. R. (1984). *Uncontrolled fire and chaparral resilience in the Sierra Juarez, Baja California, Mexico* [M.S. Thesis]. University of California, Riverside.
- Fried, J. S., Torn, M. S., & Mills, E. (2004). The Impact of Climate Change on Wildfire Severity: A Regional Forecast for Northern California. *Climate Change*, *64*, 169–191.
- Gibson, J., Moisen, G., Frescino, T., & Edwards, T. C. (2014). Using Publicly Available Forest Inventory Data in Climate-Based Models of Tree Species Distribution: Examining Effects of True Versus Altered Location Coordinates. *Ecosystems*, *17*(1), 43–53. <https://doi.org/10.1007/s10021-013-9703-y>
- Giovanelli, J. G. R., de Siqueira, M. F., Haddad, C. F. B., & Alexandrino, J. (2010). Modeling a spatially restricted distribution in the Neotropics: How the size of calibration area affects the performance of five presence-only methods. *Ecological Modelling*, *221*(2), 215–224. <https://doi.org/10.1016/j.ecolmodel.2009.10.009>
- Godsoe, W., Franklin, J., & Blanchet, F. G. (2016). Effects of biotic interactions on modeled species' distribution can be masked by environmental gradients. *Ecology and Evolution*, *7*(2), 654–664. <https://doi.org/10.1002/ece3.2657>
- Goforth, B. R., & Minnich, R. A. (2008). Densification, stand-replacement wildfire, and extirpation of mixed conifer forest in Cuyamaca Rancho State Park, southern California. *Forest Ecology and Management*, *256*(1), 36–45. <https://doi.org/10.1016/j.foreco.2008.03.032>
- Grabs, T., Seibert, J., Bishop, K., & Laudon, H. (2009). Modeling spatial patterns of saturated areas: A comparison of the topographic wetness index and a dynamic distributed model. *Journal of Hydrology*, *373*(1), 15–23. <https://doi.org/10.1016/j.jhydrol.2009.03.031>
- Grubb, P. J. (1977). The Maintenance of Species-Richness in Plant Communities: The Importance of the Regeneration Niche. *Biological Reviews*, *52*(1), 107–145. <https://doi.org/10.1111/j.1469-185X.1977.tb01347.x>
- Grubb, P. J. (1977). The Maintenance of Species-Richness in Plant Communities: The Importance of the Regeneration Niche. *Biological Reviews*, *52*(1), 107–145. <https://doi.org/10.1111/j.1469-185X.1977.tb01347.x>
- Gucker, C. L. (n.d.). *Pinus jeffreyi* [Fire Effects Information System, [Online]]. U.S. Department of Agriculture, Forest Service, Rocky Mountain Research Station, Fire Sciences Laboratory (Producer). <https://www.fs.fed.us/database/feis/plants/tree/pinjef/all.html>
- Guillera-Arroita, G., Lahoz-Monfort, J. J., & Elith, J. (2014). Maxent is not a presence–absence method: A comment on Thibaud et al. *Methods in Ecology and Evolution*, *5*(11), 1192–1197. <https://doi.org/10.1111/2041-210X.12252>
- Guisan, A., Weiss, S. B., & Weiss, A. D. (1999). GLM versus CCA spatial modeling of plant species distribution. *Plant Ecology*, *143*(1), 107–122. <https://doi.org/10.1023/A:1009841519580>
- Gutiérrez, R. J., Tempel, D. J., & Peery, M. Z. (2017). The Spotted Owl in Southern and Central Coastal California. In *The California spotted owl: Current state of knowledge* (p. 294). U.S. Dept. of Agriculture, Forest Service, Pacific Southwest Region.
- Haffey, C., Sisk, T. D., Allen, C. D., Thode, A. E., & Margolis, E. Q. (2018). Limits to Ponderosa Pine Regeneration following Large High-Severity Forest Fires in the United States Southwest. *Fire Ecology*, *14*(1), 143–163. <https://doi.org/10.4996/fireecology.140114316>
- Hagmann, R. K., Franklin, J. F., & Johnson, K. N. (2013). Historical structure and composition of ponderosa pine and mixed-conifer forests in south-central Oregon. *Forest Ecology and Management*, *304*, 492–504. <https://doi.org/10.1016/j.foreco.2013.04.005>
- Hall, H. M. (1902). *A Botanical Survey of San Jacinto Mountain*. The University Press.

- Haller, J. R. (1959). FACTORS AFFECTING THE DISTRIBUTION OF PONDEROSA AND JEFFREY PINES IN CALIFORNIA. *Madroño*, 15(3), 65–71. JSTOR.
- Haller, J. R. (1959). FACTORS AFFECTING THE DISTRIBUTION OF PONDEROSA AND JEFFREY PINES IN CALIFORNIA. *Madroño*, 15(3), 65–71. JSTOR.
- Hallin, W. (1957). *Silvical Characteristics of Jeffrey Pine* (No. 17). U.S. Department of Agriculture, Forest Service.
- Hayhoe, K., Cayan, D., Field, C. B., Frumhoff, P. C., Maurer, E. P., Miller, N. L., Moser, S. C., Schneider, S. H., Cahill, K. N., Cleland, E. E., Dale, L., Drapek, R., Hanemann, R. M., Kalkstein, L. S., Lenihan, J., Lunch, C. K., Neilson, R. P., Sheridan, S. C., & Verville, J. H. (2004). Emissions pathways, climate change, and impacts on California. *Proceedings of the National Academy of Sciences*, 101(34), 12422–12427. <https://doi.org/10.1073/pnas.0404500101>
- Heusser, L. E. (1992). Pollen stratigraphy and paleoecologic interpretation of the 160-ky record from Santa Barbara Basin, Hole 893A1. *Proceedings of the Ocean Drilling Program Scientific Results*, 146(2), 265–279.
- Hilberg, L. E., Reynier, W. A., & Kershner, J. M. (2016). *Southern California Climate Change Vulnerability Assessment: Conifer Habitats*. EcoAdapt.
- Hobbs, R. J., Zavaleta, E. S., Cole, D. N., & White, P. S. (2010). Evolving ecological understandings: The implications of ecosystem dynamics. In D. N. Cole & L. Yung (Eds.), *Beyond Naturalness: Rethinking Park and Wilderness Stewardship in an Era of Rapid Change* (pp. 34–49). Island Press.
- Hohmann, M. G., & Wall, W. A. (2016). *A species distribution modeling informed conservation assessment of Bog Spicebush* [Technical Report]. Construction Engineering Research Laboratory (U.S.). <https://erdc-library.erd.c.dren.mil/jspui/handle/11681/20647>
- Holzman, B. A., & Allen-Diaz, B. H. (1991). Vegetation Change in Blue Oak Woodlands in California. In: Standiford, Richard B., Tech. Coord. 1991. *Proceedings of the Symposium on Oak Woodlands and Hardwood Rangeland Management; October 31 - November 2, 1990; Davis, California. Gen. Tech. Rep. PSW-GTR-126. Berkeley, CA: Pacific Southwest Research Station, Forest Service, U.S. Department of Agriculture; p. 189-193, 126.* <https://www.fs.usda.gov/treearch/pubs/28419>
- Holzman, B. A., & Allen-Diaz, B. H. (1991). Vegetation Change in Blue Oak Woodlands in California. In: Standiford, Richard B., Tech. Coord. 1991. *Proceedings of the Symposium on Oak Woodlands and Hardwood Rangeland Management; October 31 - November 2, 1990; Davis, California. Gen. Tech. Rep. PSW-GTR-126. Berkeley, CA: Pacific Southwest Research Station, Forest Service, U.S. Department of Agriculture; p. 189-193, 126.* <https://www.fs.usda.gov/treearch/pubs/28419>
- Howard, J. L. (1992). *Pseudotsuga macrocarpa*. Fire Effects Information System, [Online]. <https://www.fs.fed.us/database/feis/plants/tree/psemac/all.html>
- Indicators of Climate Change in California*. (2018). Office of Environmental Health Hazard Assessment, California Environmental Protection Agency.
- Jackson, S. T., Betancourt, J. L., Booth, R. K., & Gray, S. T. (2009). Ecology and the ratchet of events: Climate variability, niche dimensions, and species distributions. *Proceedings of the National Academy of Sciences*, 106(Supplement 2), 19685–19692. <https://doi.org/10.1073/pnas.0901644106>
- Jenkinson, J. L. (1990). *Pinus jeffreyi* Grev. & Balf. Jeffrey pine. In R. M. Burns & B. H. Honkala (Eds.), *Silvics of North America* (Vol. 1, pp. 359–369). U.S. Department of Agriculture, Forest Service.
- Jenness, J., Brost, B., Beier, P. 2011. Land facet corridor designer: extension for ArcGIS. Jenness enterprises. Available from: http://jennessent.com/arcgis/land_facets.htm.
- Jepson, R., Clegg, A., Forbes, C., & et al. (2000). *The determinants of screening uptake and interventions for increasing uptake: A systematic review*. Database of Abstracts of Reviews of Effects (DARE): Quality-Assessed Reviews. <https://www.ncbi.nlm.nih.gov/books/NBK68068/>
- Kadowaki, K., Barbera, C. G., Godsoe, W., Delsuc, F., & Mouquet, N. (2016). Predicting biotic interactions and their variability in a changing environment. *Biology Letters*, 12(5), 20151073. <https://doi.org/10.1098/rsbl.2015.1073>
- Kapnick, S., & Hall, A. (2012). Causes of recent changes in western North American snowpack. *Climate Dynamics*, 38(9), 1885–1899. <https://doi.org/10.1007/s00382-011-1089-y>
- Kapnick, S., & Hall, A. (2012). Causes of recent changes in western North American snowpack. *Climate Dynamics*, 38(9), 1885–1899. <https://doi.org/10.1007/s00382-011-1089-y>
- Keane, R. E., Hessburg, P. F., Landres, P. B., & Swanson, F. J. (2009). The use of historical range and variability (HRV) in landscape management. *Forest Ecology and Management*, 258(7), 1025–1037. <https://doi.org/10.1016/j.foreco.2009.05.035>

- Keeley, J. E. (2004). VTM plots as evidence of historical change: Goldmine or landmine? In *Madroño* (Vol. 51, Issue 4, p. 372378).
- Keeley, J. E. (2006). South Coast Bioregion. In N. Sugihara (Ed.), *Fire in California's Ecosystems* (pp. 350–390). University of California Press. <https://doi.org/10.1525/california/9780520246058.003.0015>
- Keeley, J. E., & Fotheringham, C. J. (2001). Historic Fire Regime in Southern California Shrublands. *Conservation Biology*, *15*(6), 1536–1548. <https://doi.org/10.1046/j.1523-1739.2001.00097.x>
- Kelly, M., & Allen-Diaz, B. (2009). Digitization of a historic dataset: The Wieslander California Vegetation Type Mapping Project. *Madroño*, *52*(3), 191–201.
- Kelly, M., Easterday, K., Rapacciuolo, G., Koo, M., McIntyre, P., & Thorne, J. (2016). Rescuing and Sharing Historical Vegetation Data for Ecological Analysis: The California Vegetation Type Mapping Project. *Biodiversity Informatics*, *11*, 40–62. <https://doi.org/10.17161/bi.v11i0.5886>
- Keyser, C. E., & Dixon, G. E. (2012). *Western Sierra Nevada (WS) Variant Overview—Forest Vegetation Simulator* (p. 58). U.S. Department of Agriculture, Forest Service, Forest Management Service Center.
- Kirby, K. J. (2012). A view from the past to the future. In John A. Wiens, G. D. Hayward, H. D. Safford, & C. M. Giffen (Eds.), *Historical Environmental Variation in Conservation and Natural Resource Management* (1st ed., pp. 281–288). Wiley-Blackwell.
- Knapp, E. E., Weatherspoon, C. P., & Skinner, C. N. (2012). Shrub Seed Banks in Mixed Conifer Forests of Northern California and the Role of Fire in Regulating Abundance. *Fire Ecology*, *8*(1), 32–48. <https://doi.org/10.4996/fireecology.0801032>
- Krantz, T. P. (1994). *A phytogeography of San Bernardino mountains, San Bernardino County, California*. University of California, Berkeley.
- LaHaye, W. S., Gutiérrez, R. J., & Call, D. R. (1997). Nest-site selection and reproductive success of California spotted owls. *Wilson Bulletin*, *109*, 42–51.
- Landres, P. B., Morgan, P., & Swanson, F. J. (1999). OVERVIEW OF THE USE OF NATURAL VARIABILITY CONCEPTS IN MANAGING ECOLOGICAL SYSTEMS. *Ecological Applications*, *9*(4), 1179–1188. [https://doi.org/10.1890/1051-0761\(1999\)009\[1179:OOTUON\]2.0.CO;2](https://doi.org/10.1890/1051-0761(1999)009[1179:OOTUON]2.0.CO;2)
- League, K. R. (2005). *Ceanothus cuneatus*. Fire Effects Information Systems (FEIS). <https://www.fs.fed.us/database/feis/plants/shrub/ceacun/all.html>
- Legras, E. C., Vander Wall, S. B., & Board, D. I. (2010). The role of germination microsite in the establishment of sugar pine and Jeffrey pine seedlings. *Forest Ecology and Management*, *260*(5), 806–813. <https://doi.org/10.1016/j.foreco.2010.05.039>
- Leiberg, J. B. (1899a). The San Bernardino Forest Reserve. In *Twentieth Annual report of the United States Geological Survey, 1898-1899: Part V - Forest reserves* (pp. 429–454). https://doi.org/10.3133/ar20_5
- Leiberg, J. B. (1899b). The San Jacinto Forest Reserve. In *Twentieth Annual report of the United States Geological Survey, 1898-1899: Part V - Forest reserves* (pp. 455–478). https://doi.org/10.3133/ar20_5
- Lenihan, J. M., Drapek, R., Bachelet, D., & Neilson, R. P. (2003). Climate Change Effects on Vegetation Distribution, Carbon, and Fire in California. *Ecological Applications*, *13*(6), 1667–1681. <https://doi.org/10.1890/025295>
- Lenoir, J., Gégout, J.-C., Pierrat, J.-C., Bontemps, J.-D., & Dhôte, J.-F. (2009). Differences between tree species seedling and adult altitudinal distribution in mountain forests during the recent warm period (1986–2006). *Ecography*, *32*(5), 765–777. <https://doi.org/10.1111/j.1600-0587.2009.05791.x>
- Lindsey, R., & Dahlman, L. (n.d.). *Climate Change: Global Temperature*. NOAA Climate.Gov. Retrieved March 15, 2021, from <https://www.climate.gov/news-features/understanding-climate/climate-change-global-temperature>
- Littell, J. S., McKenzie, D., Kerns, B. K., Cushman, S., & Shaw, C. G. (2011). Managing uncertainty in climate-driven ecological models to inform adaptation to climate change. *Ecosphere*, *2*(9), art102. <https://doi.org/10.1890/ES11-00114.1>
- Liu, C., Berry, P. M., Dawson, T. P., & Pearson, R. G. (2005). Selecting thresholds of occurrence in the prediction of species distributions. *Ecography*, *28*(3), 385–393. <https://doi.org/10.1111/j.0906-7590.2005.03957.x>
- Liu, C., Newell, G., & White, M. (2015). On the selection of thresholds for predicting species occurrence with presence-only data. *Ecology and Evolution*, *6*(1), 337–348. <https://doi.org/10.1002/ece3.1878>
- Liu, Y., Stanturf, J., & Goodrick, S. (2010). Trends in global wildfire potential in a changing climate. *Forest Ecology and Management*, *259*(4), 685–697. <https://doi.org/10.1016/j.foreco.2009.09.002>

- Loarie, S. R., Carter, B. E., Hayhoe, K., McMahon, S., Moe, R., Knight, C. A., & Ackerly, D. D. (2008). Climate Change and the Future of California's Endemic Flora. *PLoS ONE*, 3(6), e2502. <https://doi.org/10.1371/journal.pone.0002502>
- Lutz, J. A., van Wagtenonk, J. W., & Franklin, J. F. (2009). Twentieth-century decline of large-diameter trees in Yosemite National Park, California, USA. *Forest Ecology and Management*, 257(11), 2296–2307. <https://doi.org/10.1016/j.foreco.2009.03.009>
- Martin, B. D. (1981). *Vegetation Responses to Prescribed Burning in a Mixed-conifer Woodland, Cuyamaca Rancho State Park, California* [Loma Linda University]. <https://scholarsrepository.llu.edu/etd/716/>
- McCaffrey, S. M., & Rhodes, A. (2009). Public Response to Wildfire: Is the Australian “Stay and Defend or Leave Early” Approach an Option for Wildfire Management in the United States? *Journal of Forestry*, 107(1), 9–15. <https://doi.org/10.1093/jof/107.1.9>
- McCann, E. (n.d.). [Manuscript about conifer sapling and adult suitable habitat in Western U.S.] (in prep.).
- McCann, E., & Spasojevic, M. (2020, August 3). *Dispersal traits mediate range shifts in western US tree species*. 2020 ESA Annual Meeting. <https://eco.confex.com/eco/2020/meetingapp.cgi/Paper/87404>
- McComb, S., Powers, C., Uy, J., Winchell, A., & Wolf, L. (2019). *Climate Change Vulnerability Assessment of Quercus Tomentella* [Bren school group project report, University of California, Santa Barbara]. [http://bren.ucsb.edu/research/2019Group_Projects/documents/OAKOLOGY/Oakology_Final_Report%20\(unsigned\).pdf](http://bren.ucsb.edu/research/2019Group_Projects/documents/OAKOLOGY/Oakology_Final_Report%20(unsigned).pdf)
- McCormack, J. E., Huateng, H., & Knowles, L. L. (2009). *Sky Islands*. <http://sites.oxy.edu/mccormack/McCormack/picks/McCormack>
- McCullough, I. M., Davis, F. W., Dingman, J. R., Flint, L. E., Flint, A. L., Serra-Diaz, J. M., Syphard, A. D., Moritz, M. A., Hannah, L., & Franklin, J. (2016). High and dry: High elevations disproportionately exposed to regional climate change in Mediterranean-climate landscapes. *Landscape Ecology*, 31(5), 1063–1075. <https://doi.org/10.1007/s10980-015-0318-x>
- McDonald, P. M., & Tappeiner, J. C. (2002). *California's Hardwood Resource: Seeds, Seedlings, and Sprouts of Three Important Forest-zone Species* (General Technical Report PSW-GTR-185; p. 39). Pacific Southwest Research Station, Forest Service, U.S. Department of Agriculture.
- McIntyre, P. J., Thorne, J. H., Dolanc, C. R., Flint, A. L., Flint, L. E., Kelly, M., & Ackerly, D. D. (2015). Twentieth-century shifts in forest structure in California: Denser forests, smaller trees, and increased dominance of oaks. *Proceedings of the National Academy of Sciences*, 112(5), 1458–1463. <https://doi.org/10.1073/pnas.1410186112>
- McKelvey, K. S., & Johnston, J. D. (1992). Historical Perspectives on Forests of the Sierra Nevada and the Transverse Ranges of Southern California: Forest Conditions at the Turn of the Century. In *The California spotted owl: A technical assessment of its current status* (pp. 225–246). U.S. Department of Agriculture, Forest Service, Pacific Southwest Research Station. <https://www.fs.usda.gov/treearch/pubs/3536>
- McKenzie, D., Peterson, D. W., & Peterson, D. L. (2003). Modelling conifer species distributions in mountain forests of Washington State, USA. *The Forestry Chronicle*, 79(2), 253–258. <https://doi.org/10.5558/tfc79253-2>
- Merckx, B., Steyaert, M., Vanreusel, A., Vincx, M., & Vanaverbeke, J. (2011). Null models reveal preferential sampling, spatial autocorrelation and overfitting in habitat suitability modelling. *Ecological Modelling*, 222(3), 588–597. <https://doi.org/10.1016/j.ecolmodel.2010.11.016>
- Merow, C., Smith, M. J., & Silander, J. A. (2013). A practical guide to MaxEnt for modeling species' distributions: What it does, and why inputs and settings matter. *Ecography*, 36(10), 1058–1069. <https://doi.org/10.1111/j.1600-0587.2013.07872.x>
- Meyer, R. (2011). *Ceanothus leucodermis*. Fire Effects Information Systems (FEIS). <https://www.fs.fed.us/database/feis/plants/shrub/cealeu/all.html>
- Millar, C. I., Stephenson, N. L., & Stephens, S. L. (2007). Climate Change and Forests of the Future: Managing in the Face of Uncertainty. *Ecological Applications*, 17(8), 2145–2151. <https://doi.org/10.1890/06-1715.1>
- Miller, J. D., Safford, H. D., Crimmins, M., & Thode, A. E. (2009). Quantitative Evidence for Increasing Forest Fire Severity in the Sierra Nevada and Southern Cascade Mountains, California and Nevada, USA. *Ecosystems*, 12(1), 16–32. <https://doi.org/10.1007/s10021-008-9201-9>
- Miller, Jay D., & Safford, H. (2012). Trends in Wildfire Severity: 1984 to 2010 in the Sierra Nevada, Modoc Plateau, and Southern Cascades, California, USA. *Fire Ecology*, 8(3), 41–57. <https://doi.org/10.4996/fireecology.0803041>
- Minnich, R. A. (1978). *The geography of fire and conifer forests in the eastern Transverse Ranges, California* [Ph.D dissertation]. University of California, Los Angeles.

- Minnich, R. A. (1987). *The Distribution of Forest Trees in Northern Baja California, Mexico*. <http://archive.org/details/biostor-163067>
- Minnich, R. A., & Bahre, C. J. (1995). Wildland fire and chaparral succession along the California-Baja California boundary. *International Journal of Wildland Fire*, 5, 13–24.
- Minnich, R. A., & Chou, Y. H. (1997). Wildland Fire Patch Dynamics in the Chaparral of Southern California and Northern Baja California. *International Journal of Wildland Fire*, 7(3), 221–248.
- Minnich, R. A., & Dezzani, R. J. (1998). Historical Decline of Coastal Sage Scrub in the Riverside-Perris Plain, California. *Western Birds*, 29(4), 366–391.
- Minnich, R. A., Barbour, M. G., Burk, J. H., & Sosa-Ramírez, J. (2000). Californian mixed-conifer forests under unmanaged fire regimes in the Sierra San Pedro Mártir, Baja California, Mexico. *Journal of Biogeography*, 27(1), 105–129. <https://doi.org/10.1046/j.1365-2699.2000.00368.x>
- Minnich, Richard A. (1988). *The Biogeography of Fire in the San Bernardino Mountains of California: A Historical Study* (Vol. 28). University of California Press.
- Minnich, RICHARD A. (2007). Southern California Conifer Forests. In MICHAEL G. Barbour, T. Keeler-Wolf, & A. A. Shoemaker (Eds.), *Terrestrial Vegetation of California, 3rd Edition* (1st ed., pp. 502–538). University of California Press; JSTOR. <http://www.jstor.org/stable/10.1525/j.ctt1pnqfd.22>
- Minnich, Richard A., & Dezzani, R. J. (1998). Historical Decline of Coastal Sage Scrub in the Riverside-Perris Plain, California. *Western Birds*, 29(4), 366–391.
- Minnich, Richard A., & Everett, R. G. (2001). Conifer Tree Distributions in Southern California. *Madrono (USA)*, 48(3), 177–197.
- Minnich, Richard A., & Vizcaino, E. F. (1998). *Land of Chamise and Pines: Historical Accounts and Current Status of Northern Baja California's Vegetation* (Vol. 80). University of California Publications in Botany.
- Minnich, Richard A., Barbour, M. G., Burk, J. H., & Fernau, R. F. (1995). Sixty Years of Change in Californian Conifer Forests of the San Bernardino Mountains. *Conservation Biology*, 9(4), 902–914. <https://doi.org/10.1046/j.1523-1739.1995.09040902.x>
- Minnich, Richard A., Goforth, B. R., & Paine, T. D. (2016). Follow the Water: Extreme Drought and the Conifer Forest Pandemic of 2002–2003 Along the California Borderland. In T. D. Paine & F. Lieutier (Eds.), *Insects and Diseases of Mediterranean Forest Systems* (pp. 859–890). Springer International Publishing. https://doi.org/10.1007/978-3-319-24744-1_29
- Monleon, V. J., & Lintz, H. E. (2015). Evidence of Tree Species' Range Shifts in a Complex Landscape. *PLOS ONE*, 10(1), e0118069. <https://doi.org/10.1371/journal.pone.0118069>
- Mooney, H., Larigauderie, A., Cesario, M., Elmquist, T., Hoegh-Guldberg, O., Lavorel, S., Mace, G. M., Palmer, M., Scholes, R., & Yahara, T. (2009). Biodiversity, climate change, and ecosystem services. *Current Opinion in Environmental Sustainability*, 1(1), 46–54. <https://doi.org/10.1016/j.cosust.2009.07.006>
- Mooney, H., Larigauderie, A., Cesario, M., Elmquist, T., Hoegh-Guldberg, O., Lavorel, S., Mace, G. M., Palmer, M., Scholes, R., & Yahara, T. (2009). Biodiversity, climate change, and ecosystem services. *Current Opinion in Environmental Sustainability*, 1(1), 46–54. <https://doi.org/10.1016/j.cosust.2009.07.006>
- Moore, D. S., Notz, W. I., & Flinger, M. A. (2013). *The Basic Practice of Statistics* (6th ed.). W.H. Freeman & Company.
- Moore, J., Pope, J., Woods, M., & Ellis, A. (2019). *2018 Aerial Survey Results: California* (No. R5-PR-034; Forest Health Monitoring Program, pp. 1–9). U.S. Department of Agriculture, Forest Service.
- Moore, L. M. (2006). *Plant Guide: Jeffrey Pine*. USDA NRCS National Plant Data Center.
- Morueta-Holme, N., Blonder, B., Sandel, B., McGill, B. J., Peet, R. K., Ott, J. E., Violle, C., Enquist, B. J., Jørgensen, P. M., & Svenning, J.-C. (2016). A network approach for inferring species associations from co-occurrence data. *Ecography*, 39(12), 1139–1150. <https://doi.org/10.1111/ecog.01892>
- Murphy, A., Abrams, J., Daniel, T., & Yazzie, V. (2007). Living among Frequent-fire Forests: Human History and Cultural Perspectives. *Ecology and Society*, 12(2). <https://doi.org/10.5751/ES-02167-120217>
- Nigro, K., & Molinari, N. (2019). Status and trends of fire activity in southern California yellow pine and mixed conifer forests. *Forest Ecology and Management*, 441, 20–31. <https://doi.org/10.1016/j.foreco.2019.01.020>
- Niinemets, Ü. (2010). Responses of forest trees to single and multiple environmental stresses from seedlings to mature plants: Past stress history, stress interactions, tolerance and acclimation. *Forest Ecology and Management*, 260(10), 1623–1639. <https://doi.org/10.1016/j.foreco.2010.07.054>

- North, M., Brough, A., Long, J., & et al. (2015). Constraints on mechanized treatment significantly limit mechanical fuels reduced extent in the Sierra Nevada. *Journal of Forestry*, *113*, 40–48.
- North, M., Innes, J., & Zald, H. (2007). Comparison of thinning and prescribed fire restoration treatments to Sierran mixed-conifer historic conditions. *Canadian Journal of Forest Research*, *32*(2), 331–342.
- O’Connell, B. M., LaPoint, E. B., Turner, J. A., Ridley, T., Pugh, S. A., Wilson, A. M., Waddell, K. L., & Conkling, B. L. (2015). *The Forest Inventory and Analysis Database: Database description and user guide version 6.0.2 for Phase 2*. U.S. Department of Agriculture, Forest Service. <https://www.fia.fs.fed.us/library/database-documentation/>
- Oliver, W. W. (1972). *Growth after thinning ponderosa and Jeffrey pine pole stands in northeastern California*. 14.
- Opedal, Ø. H., Armbruster, W. S., & Graae, B. J. (2015). Linking small-scale topography with microclimate, plant species diversity and intra-specific trait variation in an alpine landscape. *Plant Ecology & Diversity*, *8*(3), 305–315. <https://doi.org/10.1080/17550874.2014.987330>
- Parks, S. A., Holsinger, L. M., Panunto, M. H., Jolly, W. M., Dobrowski, S. Z., & Dillon, G. K. (2018). High-severity fire: Evaluating its key drivers and mapping its probability across western US forests. *Environmental Research Letters*, *13*(4), 044037. <https://doi.org/10.1088/1748-9326/aab791>
- Passini, J. F., Delgadillo, J., & Salazar, M. (1989). L’ecosystème forestier de Basse-Californie: Composition floristique, variables écologiques principales, dynamique. *Acta Oecologica*, *10*, 275–293.
- Pausas, J. G., & Keeley, J. E. (2017). Epicormic Resprouting in Fire-Prone Ecosystems. *Trends in Plant Science*, *22*(12), 1008–1015. <https://doi.org/10.1016/j.tplants.2017.08.010>
- Pearson, R. (2010). Species’ Distribution Modeling for Conservation Educators and Practitioners. *Lessons in Conservation*, *3*, 54–89.
- Peterson, G., Allen, C. R., & Holling, C. S. (1998). Ecological Resilience, Biodiversity, and Scale. *Ecosystems*, *1*, 6–18.
- Phillips, S. J., & Dudík, M. (2008). Modeling of species distributions with Maxent: New extensions and a comprehensive evaluation. *Ecography*, *31*(2), 161–175. <https://doi.org/10.1111/j.0906-7590.2008.5203.x>
- Phillips, S. J., Anderson, R. P., & Schapire, R. E. (2006). Maximum entropy modeling of species geographic distributions. *Ecological Modelling*, *190*(3), 231–259. <https://doi.org/10.1016/j.ecolmodel.2005.03.026>
- Plummer, F. G., & Gowsell, M. G. (1905). *Forest Conditions in the Santa Barbara Forest Reserve, California*.
- Qin, A., Liu, B., Guo, Q., Bussmann, R. W., Ma, F., Jian, Z., Xu, G., & Pei, S. (2017). Maxent modeling for predicting impacts of climate change on the potential distribution of *Thuja sutchuenensis* Franch., an extremely endangered conifer from southwestern China. *Global Ecology and Conservation*, *10*, 139–146. <https://doi.org/10.1016/j.gecco.2017.02.004>
- Radosavljevic, A., & Anderson, R. P. (2014). Making better Maxent models of species distributions: Complexity, overfitting and evaluation. *Journal of Biogeography*, *41*(4), 629–643. <https://doi.org/10.1111/jbi.12227>
- Riordan, E. C., Montalvo, A. M., & Beyers. (2018). Using species distribution models with climate change scenarios to aid ecological restoration decisionmaking for southern California shrublands. *U.S. Department of Agriculture, Forest Service, Pacific Southwest Research Station, Pacific Southwest Research Station*, 130.
- Ritchie, M. W., Wing, B. M., & Hamilton, T. A. (2008). Stability of the large tree component in treated and untreated late-seral interior ponderosa pine stands This article is one of a selection of papers from the Special Forum on Ecological Studies in Interior Ponderosa Pine—First Findings from Blacks Mountain Interdisciplinary Research. *Canadian Journal of Forest Research*, *38*(5), 919–923. <https://doi.org/10.1139/x07-242>
- Rivera-Huerta, H., Safford, H. D., & Miller, J. D. (2016). Patterns and Trends in Burned Area and Fire Severity from 1984 to 2010 in the Sierra de San Pedro Mártir, Baja California, Mexico. *Fire Ecology*, *12*(1), 52–72. <https://doi.org/10.4996/fireecology.1201052>
- Robinson, J. W. (1991). *The San Gabriels: The mountain country from Soledad Canyon to Lytle Creek*. Big Santa Anita Historical Society.
- Romme, W. H., Wiens, J. A., & Safford, H. D. (2012). Setting the Stage: Theoretical and Conceptual Background of Historical Range of Variation. In John A. Wiens, G. D. Hayward, H. D. Safford, & C. M. Giffen (Eds.), *Historical Environmental Variation in Conservation and Natural Resource Management* (1st ed.). Wiley-Blackwell.
- Rundel, P. W. (2005). *Introduction to the Planet Life of Southern California*. University of California Press.
- Rundel, P. W., Parsons, D. J., & Gordon, D. T. (1988). Montane and Subalpine Vegetation of the Sierra Nevada and Cascade Ranges. In *Terrestrial Vegetation of California* (2nd ed., pp. 559–600).

- Russell, W. H., McBride, J., & Rowntree, R. (1998). Revegetation after four stand-replacing fires in the Lake Tahoe basin. *Madrono (USA)*. <https://agris.fao.org/agris-search/search.do?recordID=US1999004807>
- Saarimaa, M., Aapala, K., Tuominen, S., Karhu, J., Parkkari, M., & Tolvanen, A. (2019). Predicting hotspots for threatened plant species in boreal peatlands. *Biodiversity and Conservation*, 28(5), 1173–1204. <https://doi.org/10.1007/s10531-019-01717-8>
- Safford, H. D., Stevens, J. T., Merriam, K., Meyer, M. D., & Latimer, A. M. (2012b). Fuel treatment effectiveness in California yellow pine and mixed conifer forests. *Forest Ecology and Management*, 274, 17–28. <https://doi.org/10.1016/j.foreco.2012.02.013>
- Safford, H.D., Wiens, J. A., & Hayward, G. D. (2012a). The Growing Importance of the Past in Managing Ecosystems of the Future. In *Historical Environmental Variation in Conservation and Natural Resource Management* (pp. 319–328). Wiley-Blackwell.
- Safford, Hugh D. & Stevens, J. T. (2017). *Natural Range of Variation for Yellow Pine and Mixed-Conifer Forests in the Sierra Nevada, Southern Cascades, and Modoc and Inyo National Forests, California, USA* (p. 241).
- Saunders, C. F. (1923). *The Southern Sierras of California*.
- Savage, M., Nystrom, M., & J, F. (2013). Double whammy: High-severity fire and drought in ponderosa pine forests of the Southwest. *Canadian Journal of Forest Research*. <https://doi.org/10.1139/cjfr-2012-0404>
- Scholl, A. E., & Taylor, A. H. (2010). Fire regimes, forest change, and self-organization in an old-growth mixed-conifer forest, Yosemite National Park, USA. *Ecological Applications*, 20(2), 362–380.
- Scott, J. H., Thompson, M. P., & Calkin, D. E. (2013). *A wildfire risk assessment framework for land and resource management* (RMRS-GTR-315; p. RMRS-GTR-315). U.S. Department of Agriculture, Forest Service, Rocky Mountain Research Station. <https://doi.org/10.2737/RMRS-GTR-315>
- Serra-Diaz, J. M., Franklin, J., Sweet, L. C., McCullough, I. M., Syphard, A. D., Regan, H. M., Flint, L. E., Flint, A. L., Dingman, J. R., Moritz, M. A., Redmond, K., Hannah, L., & Davis, F. W. (2016). Averaged 30 year climate change projections mask opportunities for species establishment. *Ecography*, 39(9), 844–845. <https://doi.org/10.1111/ecog.02074>
- Serra-Diaz, J. M., Scheller, R. M., Syphard, A. D., & Franklin, J. (2015). Disturbance and climate microrefugia mediate tree range shifts during climate change. *Landscape Ecology*, 30(6), 1039–1053. <https://doi.org/10.1007/s10980-015-0173-9>
- Shafteel, H., Jackson, R., Callery, S., & Bailey, D. (2021, March 8). *The Effects of Climate Change*. NASA Global Climate Change. <https://climate.nasa.gov/effects>
- Shedd, M., Gallagher, J., Jimenez, M., & Lula, D. (2012). Incorporating HRV in Minnesota National Forest Land and Resource Management Plans: A Practitioner’s Story. In *Historical Environmental Variation in Conservation and Natural Resource Management* (p. 337). Wiley-Blackwell.
- Shirk, A. J., Cushman, S. A., Waring, K. M., Wehenkel, C. A., Leal-Sáenz, A., Toney, C., & Lopez-Sanchez, C. A. (2018). Southwestern white pine (*Pinus strobiformis*) species distribution models project a large range shift and contraction due to regional climatic changes. *Forest Ecology and Management*, 411, 176–186. <https://doi.org/10.1016/j.foreco.2018.01.025>
- Simões, M. V. P., & Peterson, A. T. (2018). Importance of biotic predictors in estimation of potential invasive areas: The example of the tortoise beetle *Eurypedus nigrosignatus*, in Hispaniola. *PeerJ*, 6. <https://doi.org/10.7717/peerj.6052>
- Skinner, C. N., Burk, J. H., Barbour, M. G., Franco-Vizcaíno, E., & Stephens, S. L. (2008). Influences of climate on fire regimes in montane forests of north-western Mexico. *Journal of Biogeography*, 35, 1436–1451.
- Smith, R. B., LaHaye, W. S., Gutiérrez, R. J., & Zimmerman, G. S. (2002). Spatial habitat characteristics of an insular spotted owl (*Strix occidentalis*) population in southern California. In *Ecology and conservation of owls* (pp. 137–147). CSIRO Publishing.
- Smith, T. F., Rizzo, D. M., & North, M. (2005). Patterns of mortality in an old-growth mixed-conifer forest of the southern Sierra Nevada, California. *Forest Science*, 51, 266–275.
- Society of American Foresters. (1980). *Forest cover types of the United States and Canada* (F. Howlett Eyre, Ed.). Society of American Foresters.
- Solbrig, O., & Harper, J. (1979). Population Biology of Plants. *The Journal of Ecology*, 67, 386. <https://doi.org/10.2307/2259359>
- Staniczenko, P. P. A., Sivasubramaniam, P., Suttle, K. B., & Pearson, R. G. (2017). Linking macroecology and community ecology: Refining predictions of species distributions using biotic interaction networks. *Ecology Letters*, 20(6), 693–707. <https://doi.org/10.1111/ele.12770>
- State of the Climate: Global Climate Report for Annual 2019*. (2020). NOAA National Centers for Environmental Information. <https://www.ncdc.noaa.gov/sotc/global/201913>.

- Staudinger, M. D., Carter, S. L., Cross, M. S., Dubois, N. S., Duffy, J. E., Enquist, C., Griffis, R., Hellmann, J. J., Lawler, J. J., O'Leary, J., Morrison, S. A., Sneddon, L., Stein, B. A., Thompson, L. M., & Turner, W. (2013). Biodiversity in a changing climate: A synthesis of current and projected trends in the US. *Frontiers in Ecology and the Environment*, 11(9), 465–473. <https://doi.org/10.1890/120272>
- Steel, Z. L., Safford, H. D., & Viers, J. H. (2015). The fire frequency-severity relationship and the legacy of fire suppression in California forests. *Ecosphere*, 6(1), art8. <https://doi.org/10.1890/ES14-00224.1>
- Stephens, S. L., & Fulé, P. Z. (2005). Western Pine Forests with Continuing Frequent Fire Regimes: Possible Reference Sites for Management. *Journal of Forestry*, 103(7), 357–362. <https://doi.org/10.1093/jof/103.7.357>
- Stephens, S. L., & Gill, S. J. (2005). Forest structure and mortality in an old-growth Jeffrey pine-mixed conifer forest in north-western Mexico. *Forest Ecology and Management*, 205(1–3), 15–28. <https://doi.org/10.1016/j.foreco.2004.10.003>
- Stephens, S. L., Collins, B. M., Fetting, C. J., Finney, M. A., Hoffman, C. M., Knapp, E. E., North, M. P., Safford, H., & Wayman, R. B. (2018). Drought, Tree Mortality, and Wildfire in Forests Adapted to Frequent Fire. *BioScience*, 68(2), 77–88. <https://doi.org/10.1093/biosci/bix146>
- Stephens, S. L., Fry, D. L., Franco-Vizcaíno, E., Collins, B. M., & Moghaddas, J. M. (2007). Coarse woody debris and canopy cover in an old-growth Jeffrey pine-mixed conifer forest from the Sierra San Pedro Martir, Mexico. *Forest Ecology and Management*, 240(1–3), 87–95. <https://doi.org/10.1016/j.foreco.2006.12.012>
- Stephens, S. L., Lydersen, J. M., Collins, B. M., Fry, D. L., & Meyer, M. D. (2015). Historical and current landscape-scale ponderosa pine and mixed conifer forest structure in the Southern Sierra Nevada. *Ecosphere*, 6(5), art79. <https://doi.org/10.1890/ES14-00379.1>
- Stephens, S. L., Skinner, C. N., & Gill, S. J. (2003). Dendrochronology-based fire history of Jeffrey pine—Mixed conifer forests in the Sierra San Pedro Martir, Mexico. *Canadian Journal of Forest Research*, 33(6), 1090–1101. <https://doi.org/10.1139/x03-031>
- Stephenson, J. R., & Calcarone, G. M. (1999). *Southern California mountains and foothills assessment: Habitat and species conservation issues*. (General Technical Report GTR-PSW-175; p. 402). Pacific Southwest Research Station, Forest Service, U.S. Department of Agriculture.
- Stephenson, N. L. (1990). Climatic Control of Vegetation Distribution: The Role of the Water Balance. *The American Naturalist*, 135(5), 649–670. <https://doi.org/10.1086/285067>
- Stephenson, N. L., Millar, C. I., & Cole, D. N. (2010). Shifting Environmental Foundations: The Unprecedented and Unpredictable Future. In D. N. Cole & L. Yung (Eds.), *Beyond Naturalness: Rethinking Park and Wilderness Stewardship in an Era of Rapid Change* (pp. 50–66). Island Press.
- Stewart, J. A. E., Thorne, J. H., Gogol-Prokurat, M., & Osborn, S. D. (2016). A climate change vulnerability assessment for twenty California mammal taxa. *Information Center for the Environment, University of California, Davis, CA*.
- Stocker, T. F., Qin, D., Plattner, G.-K., Tignor, M. M. B., Allen, S. K., Boschung, J., Nauels, A., Xia, Y., Bex, V., & Midgley, P. M. (2013). *Climate Change 2013: The Physical Science Basis. Contribution of Working Group I to the Fifth Assessment Report of the Intergovernmental Panel on Climate Change* (p. 1535). Cambridge University Press, Cambridge United Kingdom and New York, NY, USA.
- Stohlgren, K. M., Spear, S. F., & Stevenson, D. J. (2015). *A Status Assessment and Distribution Model for the Eastern Diamondback Rattlesnake (Crotalus adamanteus) in Georgia*. 26.
- Sullivan, G. M., & Feinn, R. (2012). Using Effect Size—Or Why the P Value Is Not Enough. *Journal of Graduate Medical Education*, 4(3), 279–282. <https://doi.org/10.4300/JGME-D-12-00156.1>
- Swetnam, T. W., & Baisan, C. H. (1996). *Historical Fire Regime Patterns in the Southwestern United States Since AD 1700* (General Technical Report RM-GTR-286; Fire Effects in Southwestern Forests: Proceedings of the 2nd La Mesa Fire Symposium, pp. 11–32). U.S. Department of Agriculture, Forest Service, Rocky Mountain Research Station. <https://digitalcommons.usu.edu/cgi/viewcontent.cgi?article=1085&context=barkbeetles>
- Swetnam, T. W., Allen, C. D., & Betancourt, J. L. (1999). Applied Historical Ecology: Using the Past to Manage for the Future. *Ecological Applications*, 9(4), 1189–1206. [https://doi.org/10.1890/1051-0761\(1999\)009\[1189:AHEUTP\]2.0.CO;2](https://doi.org/10.1890/1051-0761(1999)009[1189:AHEUTP]2.0.CO;2)
- Tappeiner, J. C., & Helms, J. A. (1971). Natural Regeneration of Douglas Fir and White Fir on Exposed Sites in the Sierra Nevada of California. *The American Midland Naturalist*, 86(2), 358–370. <https://doi.org/10.2307/2423629>
- Taylor, A.H. (2004). Identifying forest reference conditions on early cut-over lands, Lake Tahoe Basin, USA. *Ecological Applications*, 14, 1903–1920.

- Taylor, A.H., Vandervluugt, A. M., Maxwell, R. S., Beaty, R. M., Airey, C., & Skinner, C. N. (2014). Changes in forest structure, fuels and potential fire behavior since 1873 in the Lake Tahoe Basin, USA. *Applied Vegetation Science*, 17(1), 17–31.
- Taylor, Alan H. (2010). Fire disturbance and forest structure in an old-growth *Pinus ponderosa* forest, southern Cascades, USA. *Journal of Vegetation Science*, 21(3), 561–572. JSTOR.
- Thorne, J. H., & Le, T. N. (2016). California's Historic Legacy For Landscape Change, the Wieslander Vegetation Type Maps. *Madroño*, 63(4), 293–328. <https://doi.org/10.3120/0024-9637-63.4.293>
- Thorne, J. H., Morgan, B. J., & Kennedy, J. A. (2008). Vegetation Change Over Sixty Years In the Central Sierra Nevada, California, USA. *Madroño*, 55(3), 223–237. <https://doi.org/10.3120/0024-9637-55.3.223>
- Thrasher, B., Xiong, J., Wang, W., Melton, F., Michaelis, A., & Nemani, R. (2013). Downscaled Climate Projections Suitable for Resource Management. *Eos, Transactions American Geophysical Union*, 94(37), 321–323. <https://doi.org/10.1002/2013EO370002>
- Tilman, D. (1996). Biodiversity: Population Versus Ecosystem Stability. *Ecology*, 77(2), 350–363. <https://doi.org/10.2307/2265614>
- Tollefson, J. E. (2008). *Quercus chrysolepis*. Fire Effects Information Systems (FEIS). <https://www.fs.fed.us/database/feis/plants/tree/quechr/all.html>
- Touchan, R., Swetnam, T., & Grissino-Mayer, H. D. (1995, January 1). Effects of livestock grazing on pre-settlement fire regimes in New Mexico. *Symposium on Fire in Wilderness and Park Management*.
- Tree Mortality*. (n.d.). PSW Research Station | Forest Service. Retrieved June 1, 2020, from https://www.fs.fed.us/psw/topics/tree_mortality/california/bark-beetles.shtml
- U.S. Geological Survey. (1902). *Annual report to the Director of the United States Geological Survey to the Secretary of the Interior*.
- Ullrich, P. A., Xu, Z., Rhoades, A. M., Dettinger, M. D., Mount, J. F., Jones, A. D., & Vahmani, P. (2018). California's Drought of the Future: A Midcentury Recreation of the Exceptional Conditions of 2012–2017. *Earth's Future*, 6(11), 1568–1587. <https://doi.org/10.1029/2018EF001007>
- Underwood, E. C., Hollander, A. D., Huber, P. R., & Schrader-Patton, C. (2018). Mapping the Value of National Forest Landscapes for Ecosystem Service Provision. In E. C. Underwood, H. D. Safford, N. A. Molinari, & J. E. Keeley (Eds.), *Valuing Chaparral: Ecological, Socio-Economic, and Management Perspectives* (pp. 245–270). Springer International Publishing. https://doi.org/10.1007/978-3-319-68303-4_9
- USDA. (1905). *California Forest Reserves and Other Lands: Field Reports, 1902-1906*. (Volume 4) [Field Report]. United States Forest Service.
- USDA. (2012). *USDA Forest Planning Rule: National Forest System Land and Resource Management Planning*. U.S. Department of Agriculture, Forest Service.
- USDA. (2019). *California's National Forest Fact Sheets*. U.S. Forest Service. <https://www.fs.usda.gov/detailfull/r5/landmanagement/?cid=FSEPRD596345&width=full>
- USDA. (2019). *California's National Forest Fact Sheets*. U.S. Forest Service. <https://www.fs.usda.gov/detailfull/r5/landmanagement/?cid=FSEPRD596345&width=full>
- USDA. (2021). *Forest Inventory and Analysis National Program*. About Us. https://www.fia.fs.fed.us/about/about_us/index.php
- USGS. (1899). *Nineteenth Annual Report of the United States Geological Survey to the Secretary of the Interior 1897–1898*. <https://doi.org/10.3133/ar19>
- Valladares, F., Matesanz, S., Guilhaumon, F., Araújo, M. B., Balaguer, L., Benito-Garzón, M., Cornwell, W., Gianoli, E., Kleunen, M. van, Naya, D. E., Nicotra, A. B., Poorter, H., & Zavala, M. A. (2014). The effects of phenotypic plasticity and local adaptation on forecasts of species range shifts under climate change. *Ecology Letters*, 17(11), 1351–1364. <https://doi.org/10.1111/ele.12348>
- Van de Water, K. M., & Safford, H. D. (2011). A Summary of Fire Frequency Estimates for California Vegetation before Euro-American Settlement. *Fire Ecology*, 7(3), 26–58. <https://doi.org/10.4996/fireecology.0703026>
- van Mantgem, P. J., Stephenson, N. L., Byrne, J. C., Daniels, L. D., Franklin, J. F., Fule, P. Z., Harmon, M. E., Larson, A. J., Smith, J. M., Taylor, A. H., & Veblen, T. T. (2009). Widespread Increase of Tree Mortality Rates in the Western United States. *Science*, 323(5913), 521–524. <https://doi.org/10.1126/science.1165000>
- Veblen, T. T., Romme, W. H., & Regan, C. (2012). Regional application of historical ecology at ecologically defined scales: Forest ecosystems in the Colorado Front Range. In John A. Wiens, G. D. Hayward, H. D. Safford, & C. M. Giffen (Eds.), *Historical Environmental Variation in Conservation and Natural Resource Management* (1st ed., pp. 149–165). Wiley-Blackwell.

- Vizcaino Palomar, N. (2016). *Conifer responses to environment at local and regional scales: The role of intraspecific phenotypic variation*. <https://doi.org/10.13140/RG.2.2.25642.62405>
- W T Adams, Campbell, R. K., & Kitzmiller, J. H. (n.d.). *Genetic considerations in reforestation* (pp. 284–308).
- Walck, J. L., Hidayati, S. N., Dixon, K. W., Thompson, K., & Poschlod, P. (2011). Climate change and plant regeneration from seed. *Global Change Biology*, 17(6), 2145–2161. <https://doi.org/10.1111/j.1365-2486.2010.02368.x>
- Wayman, R. B., & Safford, H. D. (n.d.). Recent bark beetle outbreaks influence wildfire severity in mixed-conifer forests of the Sierra Nevada, California, USA. *Ecological Applications*, n/a(n/a), e02287. <https://doi.org/10.1002/eap.2287>
- Wayman, R. B., & Safford, H. D. (n.d.). Recent bark beetle outbreaks influence wildfire severity in mixed-conifer forests of the Sierra Nevada, California, USA. *Ecological Applications*, n/a(n/a), e02287. <https://doi.org/10.1002/eap.2287>
- Weatherspoon, C. P., Husari, S. J., & Van Wagtenonk, J. W. (1992). Fire and fuels management in relation to owl habitat in forests of the Sierra Nevada and southern California. In *The California Spotted Owl: A technical assessment of its current status* (pp. 247–260). U.S. Forest Service.
- Weeks, D., Wieslander, A. E., Josephson, H. R., & Hill, C. L. (1942). *Land utilization statistics for the northern Sierra Nevada*. U.S. Forest Service.
- Weislander, A. E. (1935). First steps of the forest survey in California. *Journal of Forestry*, 33, 877–884.
- Welch, K. R., Safford, H. D., & Young, T. P. (2016). Predicting conifer establishment post wildfire in mixed conifer forests of the North American Mediterranean-climate zone. *Ecosphere*, 7(12). <https://doi.org/10.1002/ecs2.1609>
- Wiens, J.A., Hayward, G. D., Safford, H. D., & Giffen, C. M. (Eds.). (2012). *Historical environmental variation in conservation and natural resource management*. John Wiley & Sons.
- Wiens, John A., Stralberg, D., Jongsomjit, D., Howell, C. A., & Snyder, M. A. (2009). Niches, models, and climate change: Assessing the assumptions and uncertainties. *Proceedings of the National Academy of Sciences*, 106(Supplement 2), 19729–19736. <https://doi.org/10.1073/pnas.0901639106>
- Williams, A. P., Abatzoglou, J. T., Gershunov, A., Guzman-Morales, J., Bishop, D. A., Balch, J. K., & Lettenmaier, D. P. (2019). Observed Impacts of Anthropogenic Climate Change on Wildfire in California. *Earth's Future*, 7(8), 892–910. <https://doi.org/10.1029/2019EF001210>
- Williams, A. P., Seager, R., Abatzoglou, J. T., Cook, B. I., Smerdon, J. E., & Cook, E. R. (2015). Contribution of anthropogenic warming to California drought during 2012–2014. *Geophysical Research Letters*, 42(16), 6819–6828. <https://doi.org/10.1002/2015GL064924>
- Williams, J. W., Jackson, S. T., & Kutzbach, J. E. (2007). Projected distributions of novel and disappearing climates by 2100 AD. *Proceedings of the National Academy of Sciences*, 104(14), 5738–5742. <https://doi.org/10.1073/pnas.0606292104>
- Wis, M.S., Hijmans, R. J., Li, J., Peterson, A. T., Graham, C. H., & Guisan, A. (2008). Effects of sample size on the performance of species distribution models. *Diversity and Distribution: A Journal of Conservation Biogeography*, 14(5), 763–773. <https://doi.org/10.1111/j.1472-4642.2008.00482.x>
- Wis, Mary Susanne, Pottier, J., Kissling, W. D., Pellissier, L., Lenoir, J., Damgaard, C. F., Dormann, C. F., Forchhammer, M. C., Grytnes, J.-A., Guisan, A., Heikkinen, R. K., Høye, T. T., Kühn, I., Luoto, M., Maiorano, L., Nilsson, M.-C., Normand, S., Öckinger, E., Schmidt, N. M., ... Svenning, J.-C. (2013). The role of biotic interactions in shaping distributions and realised assemblages of species: Implications for species distribution modelling. *Biological Reviews of the Cambridge Philosophical Society*, 88(1), 15–30. <https://doi.org/10.1111/j.1469-185X.2012.00235.x>
- Wohlgemuth, P., & Beyers, J. (2012). *Postfire Hillslope Erosion in Southern California Chaparral: A Case Study of Prescribed Fire as a Sediment Management Tool*.
- Wright, A., Schnitzer, S. A., Dickie, I. A., Gunderson, A. R., Pinter, G. A., Mangan, S. A., & Reich, P. B. (2013). Complex facilitation and competition in a temperate grassland: Loss of plant diversity and elevated CO₂ have divergent and opposite effects on oak establishment. *Oecologia*, 171(2), 449–458. <https://doi.org/10.1007/s00442-012-2420-y>
- Wright, H. A., & Bailey, W. A. (1982). *Fire Ecology*.
- Yiwen, Z., Low, B. W., & Yeo, D. (2016). Novel methods to select environmental variables in MaxEnt: A case study using invasive crayfish. *Ecological Modelling*, 341, 5–13. <https://doi.org/10.1016/j.ecolmodel.2016.09.019>

- Young, D. J. N., Meyer, M., Estes, B., Gross, S., Wuenschel, A., Restaino, C., & Safford, H. D. (2019). Forest recovery following extreme drought in California, USA: Natural patterns and effects of pre-drought management. *Ecological Applications*, 30(1). <https://doi.org/10.1002/eap.2002>
- Young, D. J. N., Stevens, J. T., Earles, J. M., Moore, J., Ellis, A., Jirka, A. L., & Latimer, A. M. (2017). Long-term climate and competition explain forest mortality patterns under extreme drought. *Ecology Letters*, 20(1), 78–86. <https://doi.org/10.1111/ele.12711>
- Zhu, K., Woodall, C. W., & Clark, J. S. (2012). Failure to migrate: Lack of tree range expansion in response to climate change. *Global Change Biology*, 18(3), 1042–1052. <https://doi.org/10.1111/j.1365-2486.2011.02571.x>
- Zhu, K., Woodall, C. W., Ghosh, S., Gelfand, A. E., & Clark, J. S. (2014). Dual impacts of climate change: Forest migration and turnover through life history. *Global Change Biology*, 20(1), 251–264. <https://doi.org/10.1111/gcb.12382>

Appendix

Appendix A: Literature review

Our client, Nicole Molinari, contacted USFS librarian, Julie Blankenburg, on April 2, 2020. Her search was as follows:

- California montane conifer forest search strategies
 - Google Scholar: “montane conifer” AND (“Southern California” OR Baja) AND (paleoclimate OR paleoclimatology).
 - Google: “montane conifer” AND (“Southern California” OR Baja) AND (paleoclimate OR paleoclimatology).
- Flora
 - Hathitrust: “montane conifer” AND (“Southern California” OR Baja) AND (flora OR survey); Title(plants OR flora) AND title(California); “montane forest” AND California; (“Southern California” OR baja) AND ("pinus jeffreyi"OR "pinus lambertiana" OR "pseudotsuga macrocarpa" OR "pinus flexilis" OR "pinus coulteri"); Montane AND (“Southern California” OR baja) AND ("pinus jeffreyi"OR "pinus lambertiana" OR "pseudotsuga macrocarpa" OR "pinus flexilis" OR "pinus coulteri")
 - Google Scholar: Montane AND (“Southern California” OR baja) AND ("pinus jeffreyi"OR "pinus lambertiana" OR "pseudotsuga macrocarpa" OR "pinus flexilis" OR "pinus coulteri"); “montane conifer forest” (“Southern California” OR baja) history; early exploration of Southern California; botanical exploration of Southern California and Baja; flora and fauna Baja conifer
- Fire
 - Google Scholar: Fire AND “montane conifer” AND (California OR Baja); "Fire history" “montane conifer” (California OR Baja)
- Locations
 - Google Scholar: “sierra Juarez” OR “sierra san Pedro Mártir” OR idyllwild OR “san Jacinto mountains” OR “big bear” OR “Cuyamaca State Park” OR “Mount Pinos” OR “Reyes Peak” OR “Frazier Mountain” OR “Laguna Mountain” OR “Palomar Mountains”
 - HathiTrust: “sierra Juarez” OR “sierra san Pedro Mártir” OR idyllwild OR “san Jacinto mountains” OR “big bear” OR “Cuyamaca State Park” OR “Mount Pinos” OR “Reyes Peak” OR “Frazier Mountain” OR “Laguna Mountain” OR “Palomar Mountains”; (“sierra Juarez” OR “sierra san Pedro Mártir”) AND (“montane conifer”); (idyllwild OR “san Jacinto mountains”) AND (“montane conifer”); (“big bear” OR “Cuyamaca State Park”) AND (“montane conifer”); (“Mount Pinos” OR “Reyes Peak”) AND (“montane conifer”); (“Frazier Mountain” OR “Laguna Mountain”) AND (“montane conifer”); “Palomar Mountains” AND “montane conifer”; Southern California conifer mountain
- Dendrochronology
 - Google Scholar: dendrochronology "Southern California"

We had an initial consultation with UCSB Research and Engagement Librarian, Kristen LaBonte, on April 28, 2020. GotF members conducted their own literature search to find additional sources.

- Key terms included a combination of the following:
 - Location: Southern California; Baja California/Baja, Mexico; San Bernardino National Forest, Los Padres National Forest, Cleveland National Forest, Angeles National Forest

- Time periods: current; future; historic; pre-european; 16th-19th Century; holocene; early 1900s; pre-historic
- Fire: Wildfire; Wildland urban interface (WUI); Prescribed burns; Fuels management/reduction; forest resilience; regeneration; tree rings/dendroecology; Forest thinning; Native American burning; fire suppression
- Forest Structure and Composition: d.b.h. (diameter at breast height); Yellow Pine; Mixed Conifer; Jeffrey Pine; Ponderosa Pine; Ecosystem services; snags; Weislander
- Natural Range of Variability: NRV; Historic/natural range of variation
- Spotted Owls/Wildlife: Endangered species; Species of concern; Southern spotted owl; Policy; Listed species
- Climate & Mortality: Climate modeling; Drought Predictions; Mitigation; Business as usual (BAU); Increased temperatures; Habitat shift/regime shift; Tree mortality; Dieback; Bark Beetles
- Databases searched: Melvyl, Hathi Trust Digital Library, LA Times historic newspapers, Google Scholar, Web of Science, National Emergency Library, and ProQuest Dissertations and Theses.
- Searched reference sections of key articles primarily from Dr. Richard Minnich.

Appendix B: Tree density code example

```
##### slope corrected area #####

#### VTM data ####
vtm_slope <- vtm_tidy %>%
  dplyr::select(plotkey, slope_percent) %>%
  distinct(.keep_all=T) %>% # remove duplicates to get 1 row per plot
  mutate(slope_decimal = slope_percent/100,
         slope_corrected_area = 0.0809*cos(atan(slope_decimal))) %>% # vtm plot size units = hectare
  dplyr::select(plotkey, slope_corrected_area) %>%
  mutate(slope_corrected_area = replace_na(slope_corrected_area, 809))

#### FIA data ####
fia_slope <- fia_tidy %>%
  group_by(join_plot) %>%
  mutate(slope_avg = mean(slope)) %>% # some plots had different slopes recorded***
  mutate(slope_decimal = slope_avg/100,
         slope_corrected_area = 0.067245*cos(atan(slope_decimal))) %>%
  dplyr::select(join_plot, slope_corrected_area) %>%
  distinct(.keep_all=T)

##### calculate tree density #####

#### VTM data ####
vtm_shade2 <- vtm_data | %>%
  group_by(plotkey, shade_tolerance2) %>%
  tally() %>%
  inner_join(vtm_slope, by = "plotkey") %>%
  mutate(stem_density = as.numeric(n)/slope_corrected_area) %>%
  dplyr::select(-n) %>%
  pivot_wider(names_from = shade_tolerance2,
             values_from = stem_density) %>%
  clean_names() %>%
  mutate(shade_tolerant_fire_intolerant = replace_na(shade_tolerant_fire_intolerant, 0),
         shade_intolerant_fire_tolerant = replace_na(shade_intolerant_fire_tolerant, 0)) %>%
  pivot_longer(3:4,
              names_to = 'shade_tolerance2',
              values_to = 'stem_density') %>%
  group_by(shade_tolerance2) %>%
  summarise(quantile_25 = quantile(stem_density, probs = 0.25),
           avg_stem_density = mean(stem_density),
           median = median(stem_density),
           quantile_75 = quantile(stem_density, probs = 0.75),
           sd = sd(stem_density),
           se = sd((stem_density) / sqrt(n())),
           var = var(stem_density),
           sample_size = n())
```

```

#### FIA data ####
fia_shade <- fia_data %>%
  group_by(join_plot, shade_tolerance2) %>%
  tally() %>%
  inner_join(fia_slope, by = "join_plot") %>%
  mutate(stem_density = as.numeric(n)/slope_corrected_area) %>%
  dplyr::select(-n) %>%
  pivot_wider(names_from = shade_tolerance2,
              values_from = stem_density) %>%
  clean_names() %>%
  mutate(shade_tolerant_fire_intolerant = replace_na(shade_tolerant_fire_intolerant, 0),
         shade_intolerant_fire_tolerant = replace_na(shade_intolerant_fire_tolerant, 0)) %>%
  pivot_longer(3:4,
              names_to = 'shade_tolerance2',
              values_to = 'stem_density') %>%
  group_by(shade_tolerance2) %>%
  summarise(quantile_25 = quantile(stem_density, probs = 0.25),
            avg_stem_density = mean(stem_density),
            median = median(stem_density),
            quantile_75 = quantile(stem_density, probs = 0.75),
            sd = sd(stem_density),
            se = sd((stem_density) / sqrt(n())),
            var = var(stem_density),
            sample_size = n())

```

Figure B1. Sample code of how we calculated tree density using a landscape approach and slope calculated area.

Appendix C: Additional tree density analysis

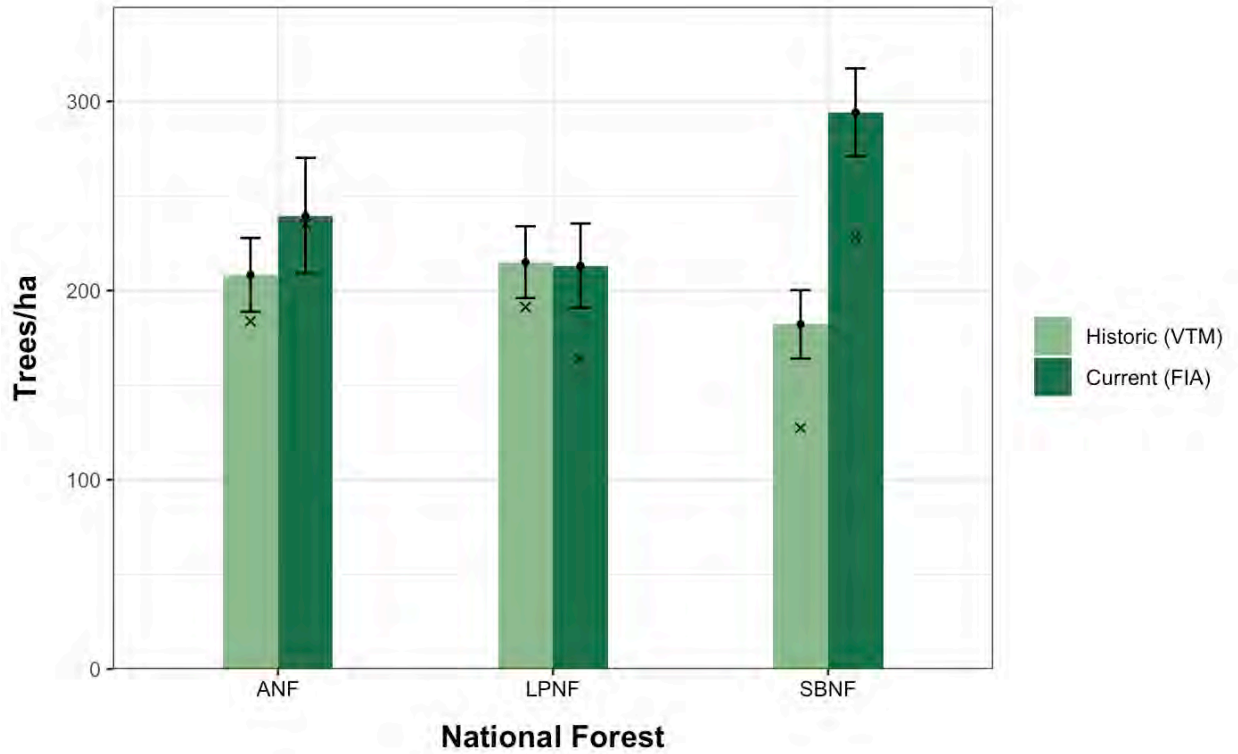


Figure C1. Mean tree density by National Forest excluding oak species (*Q. chrysolepis* and *Q. kelloggii*). Xs represent the median, black circles represent the mean, and the bars represent the standard error.

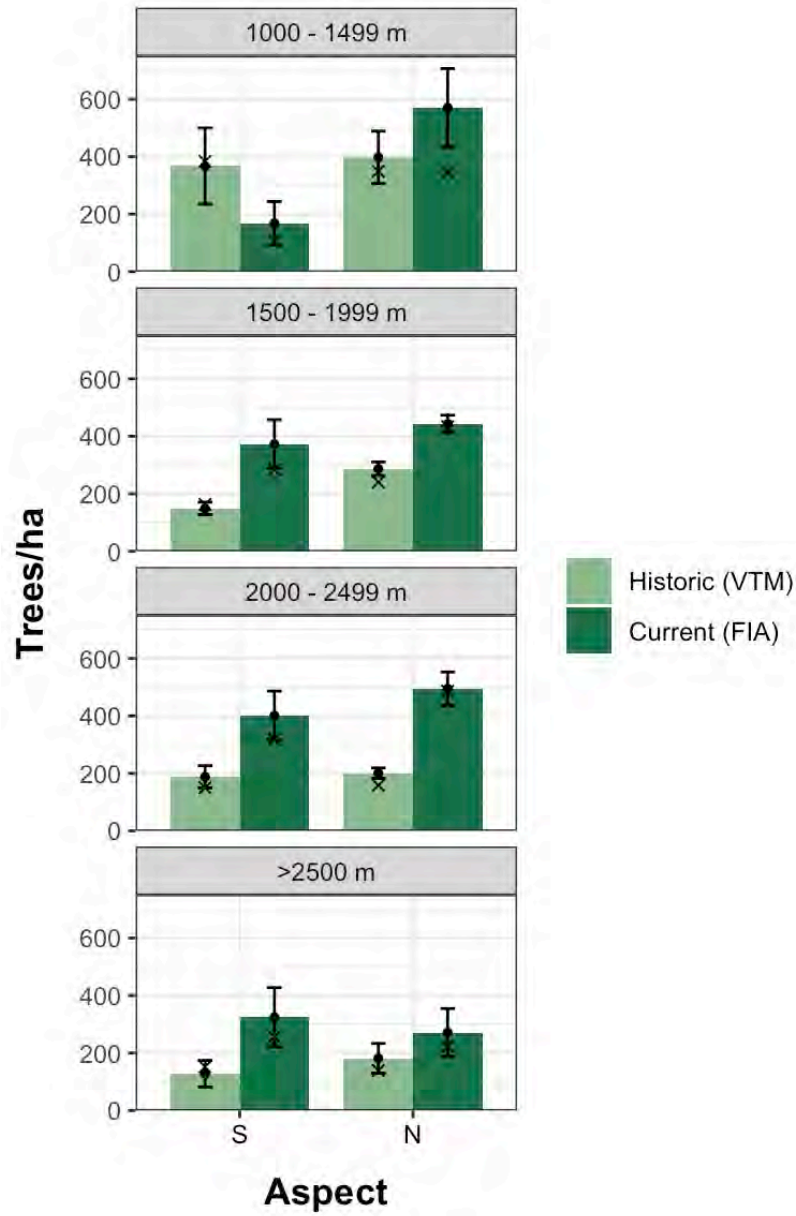


Figure C2. Mean tree density by elevation and aspect between VTM and FIA data. Xs represent the median, black circles represent the mean, and the bars represent the standard error.

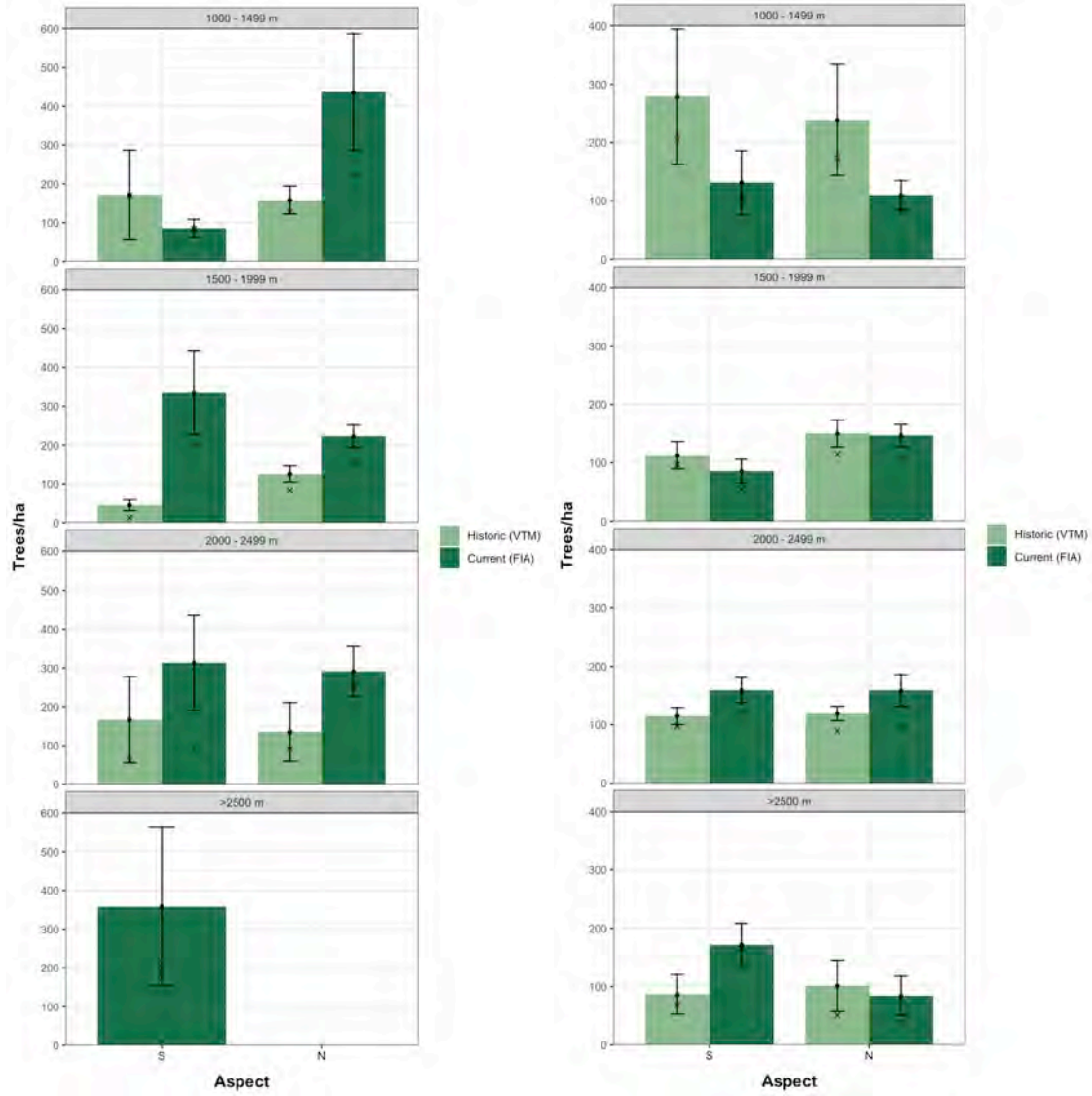


Figure C3. Mean tree density by elevation and aspect for oaks only (left). Mean tree density by elevation and aspect for conifers only (right). Note, all data was used even if it had a small sample size. Xs represent the median, black circles represent the mean, and the bars represent the standard error.

Appendix D: Tree density metrics of variance

Table D1. Means, quantiles, and other measures of distribution for tree density by functional group (oaks & conifers), shade and fire tolerance, and shade and fire tolerance excluding oaks. Means were calculated across all plots in the landscape (VTM: n=195, FIA: n=210).

	25 th Quantile	Mean	Median	75 th Quantile	Standard Deviation	Standard Error	Variance	No. of plots observed in	Dataset
Total	125.1 183.9	242.7 414.5	193.6 355.9	305.9 555.0	190.8 311.7	13.7 21.5	36411.1 97178.9	195 210	VTM FIA
Functional Group									
Conifers	86.7 92.7	194.1 257.0	152.0 204.2	256.5 372.6	167.6 209.9	12.0 14.5	28079.3 44047.2	195 210	VTM FIA
Oaks	0.0 0.0	48.7 157.6	0.0 47.0	52.9 209.1	109.6 257.9	7.8 17.8	12013.7 66486.9	78 125	VTM FIA
Shade/Fire Tolerant (including oaks)									
Shade Intolerant/Fire Tolerant	70.6 62.3	161.0 178.4	123.8 152.2	209.3 260.5	140.2 144.0	10.0 9.9	19654.4 20743.4	189 201	VTM FIA
Shade Tolerant/Fire Intolerant	0.0 21.2	81.7 236.1	37.1 151.8	123.2 339.4	127.0 286.6	9.1 19.8	16122.2 82133.2	126 168	VTM FIA
Shade/Fire Tolerant (excluding oaks)									
Shade Intolerant/Fire Tolerant	50.5 59.9	133.6 150.2	100.0 116.4	178.6 215.7	127.1 128.4	9.1 8.9	16146.1 16491.6	184 201	VTM FIA
Shade Tolerant/Fire Intolerant	0.0 0.0	60.5 106.8	12.6 31.2	91.5 144.1	101.8 166.9	7.3 11.5	10370.9 27852.1	102 128	VTM FIA

Table D2. Means, quantiles, and other measures of distribution for tree density by species. Means were calculated across all plots in the landscape (VTM: n=195, FIA: n=210).

Species	25 th Quantile	Mean	Median	75 th Quantile	Standard Deviation	Standard Error	Variance	No. of plots observed in	Dataset
<i>A. concolor</i>	0.0	46.6	0.0	66.2	89.4	6.4	7984.7	92	VTM
	0.0	87.8	15.2	105.6	154.0	10.6	23707.4	110	FIA
<i>C. decurrens</i>	0.0	13.9	0.0	0.0	45.4	3.3	2060.5	37	VTM
	0.0	19.0	0.0	0.0	63.9	4.4	4082.6	43	FIA
<i>P. coulteri</i>	0.0	10.8	0.0	0.0	38.2	2.7	1459.7	24	VTM
	0.0	8.6	0.0	0.0	29.5	2.0	868.7	25	FIA
<i>P. lambertiana</i>	0.0	23.5	0.0	26.9	46.9	3.4	2200.4	70	VTM
	0.0	24.2	0.0	18.6	50.8	3.5	2582.3	77	FIA
<i>P. macrocarpa</i>	0.0	4.7	0.0	0.0	21.1	1.5	444.0	14	VTM
	0.0	10.0	0.0	0.0	36.1	2.5	1304.3	24	FIA
Yellow Pine	0.0	94.7	55.3	133.2	127.2	9.1	16173.4	145	VTM
	16.1	107.4	62.1	164.4	126.5	8.7	16002.0	169	FIA
<i>Q. chrysolepis</i>	0.0	21.2	0.0	0.0	84.6	6.1	7153.7	38	VTM
	0.0	129.3	0.0	155.4	254.6	17.6	64807.9	102	FIA
<i>Q. kelloggii</i>	0.0	27.4	0.0	12.8	72.7	5.2	5289.5	54	VTM
	0.0	28.3	0.0	0.0	74.0	5.1	5482.2	44	FIA

Table D3. Means, quantiles, and other measures of distribution for tree density by elevation and elevation and aspect.

	25 th Quantile	Mean	Median	75 th Quantile	Standard Deviation	Standard Error	Variance	No. of plots observed in	Dataset
Elevation (m)									
1000 – 1499	157.5	372.7	248.8	510.5	325.4	72.8	105855.2	20	VTM
	159.7	381.3	229.6	528.0	346.7	68.0	120218.4	26	FIA
1500 – 1999	161.5	264.3	219.0	342.2	174.2	19.0	30346.8	84	VTM
	246.9	407.8	363.5	541.5	257.1	28.7	66105.3	80	FIA
2000 – 2499	100.8	199.7	154.5	271.6	147.9	16.9	21877.2	77	VTM
	190.5	465.4	389.5	640.7	360.5	40.8	129991.4	78	FIA
>2500	82.9	169.2	152.0	198.8	147.4	40.9	21732.3	13	VTM
	127.9	316.1	278.9	434.9	252.0	49.4	63500.0	26	FIA
Elevation (m) and Aspect									
1000 – 1499 N	194.9	397.5	349.1	506.0	316.5	91.4	100199.1	12	VTM
	244.6	570.3	345.9	1028.7	408.5	136.2	166905.2	9	FIA
1000 – 1499 S	159.7	367.3	383.5	591.1	264.8	132.4	70115.0	4	VTM
	60.3	168.2	107.3	167.8	200.1	75.6	40045.6	7	FIA
1500 – 1999 N	172.2	286.6	240.6	342.2	179.5	24.0	32212.0	56	VTM
	322.2	442.9	433.6	551.8	201.3	30.7	40505.4	43	FIA
1500 – 1999 S	77.5	149.1	163.3	186.2	91.7	21.6	8401.1	18	VTM
	107.1	373.1	284.0	525.2	367.1	84.2	134764.6	19	FIA
2000 – 2499 N	100.9	200.9	158.3	291.9	130.9	18.1	17128.9	52	VTM
	190.4	494.4	485.6	691.7	354.4	58.3	125608.7	37	FIA
2000 – 2499 S	83.4	188.1	150.0	219.5	186.4	38.9	34753.3	23	VTM
	148.7	401.1	318.5	439.8	426.7	85.3	182079.7	25	FIA
>2500 N	87.7	181.6	139.0	226.6	163.8	51.8	26816.0	10	VTM
	70.7	271.4	222.2	455.8	234.9	83.1	55194.9	8	FIA
>2500 S	95.4	128.1	152.0	172.7	80.1	46.3	6418.1	3	VTM
	130.5	324.6	256.3	398.9	309.4	103.1	95700.6	9	FIA

Table D4. Means, quantiles, and other measures of distribution for tree density by elevation and aspect for oaks.

Elevation (m) and Aspect - Oaks	25 th Quantile	Mean	Median	75 th Quantile	Standard Deviation	Standard Error	Variance	No. of plots observed in	Dataset
1000 – 1499 N	90.8	158.4	127.3	184.9	102.6	36.3	10523.6	8	VTM
	136.8	435.9	223.8	685.8	426.5	150.8	181903.2	8	FIA
1000 – 1499 S	113.2	171.1	171.1	228.9	163.7	115.8	26805.6	2	VTM
	65.1	85.4	84.1	105.1	40.0	23.1	1603.5	3	FIA
1500 – 1999 N	31.0	125.2	83.8	138.9	126.7	20.6	16063.4	38	VTM
	117.7	222.5	156.1	296.5	171.7	29.0	29486.6	35	FIA
1500 – 1999 S	12.5	44.5	12.9	61.2	46.2	13.9	2134.6	11	VTM
	61.3	334.6	199.7	382.4	387.0	107.3	149731.1	13	FIA
2000 – 2499 N	31.5	135.0	91.0	194.5	151.5	75.7	22948.1	4	VTM
	67.9	291.5	251.7	476.5	239.3	64.0	57257.2	14	FIA
2000 – 2499 S	41.0	166.6	61.1	84.7	314.7	111.3	99030.3	8	VTM
	36.2	313.8	93.2	397.1	487.5	121.9	237626.9	16	FIA
>2500 S	154.0	357.6	186.7	475.7	354.1	204.5	125410.5	3	FIA

Table D5. Means, quantiles, and other measures of distribution for tree density by elevation and aspect for conifers.

Elevation (m) and Aspect - Conifers	25th Quantile	Mean	Median	75th Quantile	Standard Deviation	Standard Error	Variance	No. of plots observed in	Dataset
1000 – 1499 N	54.2	238.9	173.0	236.5	285.7	95.2	81616.0	9	VTM
	66.1	110.0	81.5	156.0	65.9	24.9	4345.3	7	FIA
1000 – 1499 S	118.3	278.4	205.6	365.7	231.4	115.7	53537.9	4	VTM
	27.0	131.7	106.5	175.9	132.9	54.3	17674.1	6	FIA
1500 – 1999 N	56.4	150.2	115.3	180.7	147.6	23.1	21794.5	41	VTM
	68.0	146.7	108.9	178.3	123.0	19.0	15122.5	42	FIA
1500 – 1999 S	52.9	113.0	96.7	148.5	90.7	23.4	8223.9	15	VTM
	16.6	85.7	55.8	133.0	83.2	20.2	6919.8	17	FIA
2000 – 2499 N	62.2	119.2	89.2	144.2	88.6	12.4	7857.6	51	VTM
	58.5	158.9	96.1	208.1	161.5	27.3	26074.3	35	FIA
2000 – 2499 S	71.7	114.9	96.7	149.3	70.0	14.6	4898.9	23	VTM
	67.9	159.2	121.4	232.9	107.7	21.5	11590.3	25	FIA
>2500 N	27.6	101.4	51.0	198.8	98.3	44.0	9670.7	5	VTM
	34.8	84.5	39.0	109.2	88.6	33.5	7841.8	7	FIA
>2500 S	53.9	86.6	69.1	110.6	58.6	33.9	3439.4	3	VTM
	130.5	171.5	164.4	182.9	111.3	37.1	12379.0	9	FIA

Table D6. Means, quantiles, and other measures of distribution for tree density by national forest, including and excluding oaks.

National Forest	25th Quantile	Mean	Median	75th Quantile	Standard Deviation	Standard Error	Variance	No. of plots observed in	Dataset
<i>Including Oaks</i>									
ANF	162.9	222.6	207.0	268.9	76.2	17.0	5798.9	20	VTM
	141.2	351.4	342.7	455.3	268.9	52.7	72306.4	26	FIA
LPNF	148.9	243.4	230.8	300.3	145.5	19.8	21179.9	54	VTM
	186.5	380.0	341.6	538.7	258.6	32.8	66875.4	62	FIA
SBNF	100.8	245.1	165.8	317.9	222.4	20.9	49480.8	113	VTM
	195.5	451.5	380.0	624.4	324.9	31.4	105561.5	107	FIA
<i>Excluding Oaks</i>									
ANF	151.3	208.3	183.8	268.9	87.2	19.5	7597.0	20	VTM
	103.4	239.6	235.1	345.0	155.9	30.6	24295.4	26	FIA
LPNF	126.2	215.0	191.3	273.9	139.3	19.0	19392.5	54	VTM
	65.5	213.2	163.9	337.4	175.4	22.3	30761.3	62	FIA
SBNF	74.3	182.2	127.4	223.6	192.4	18.1	37003.5	113	VTM
	109.6	294.3	228.5	438.9	239.8	23.2	57497.8	107	FIA

Appendix E: Additional tree size class density analysis and metrics of variance

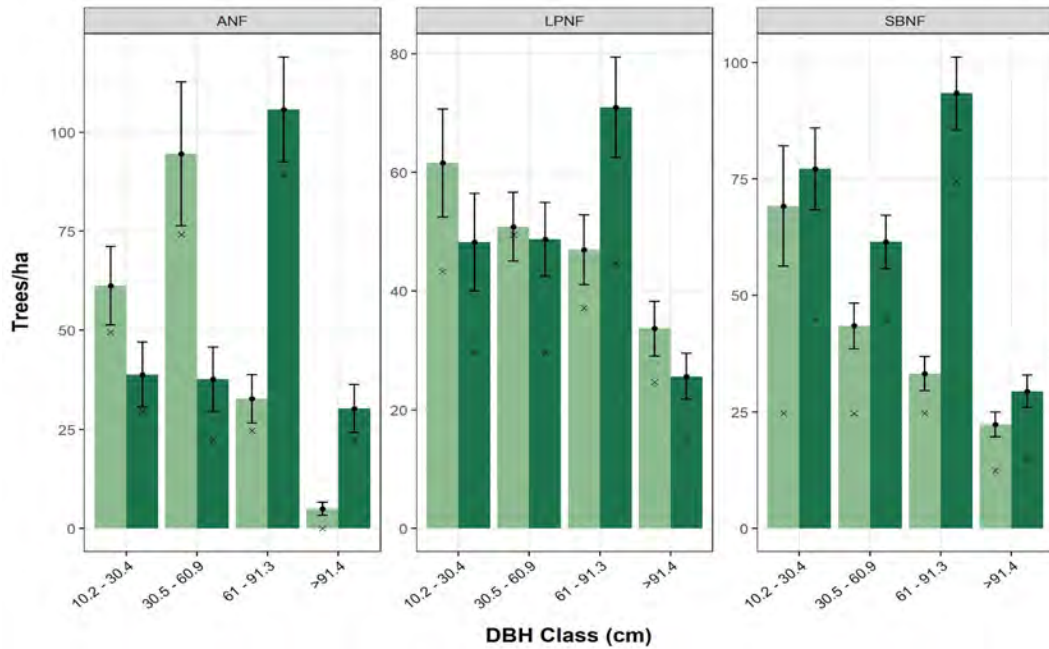


Figure E1. Tree density by size class by National Forest excluding oaks.

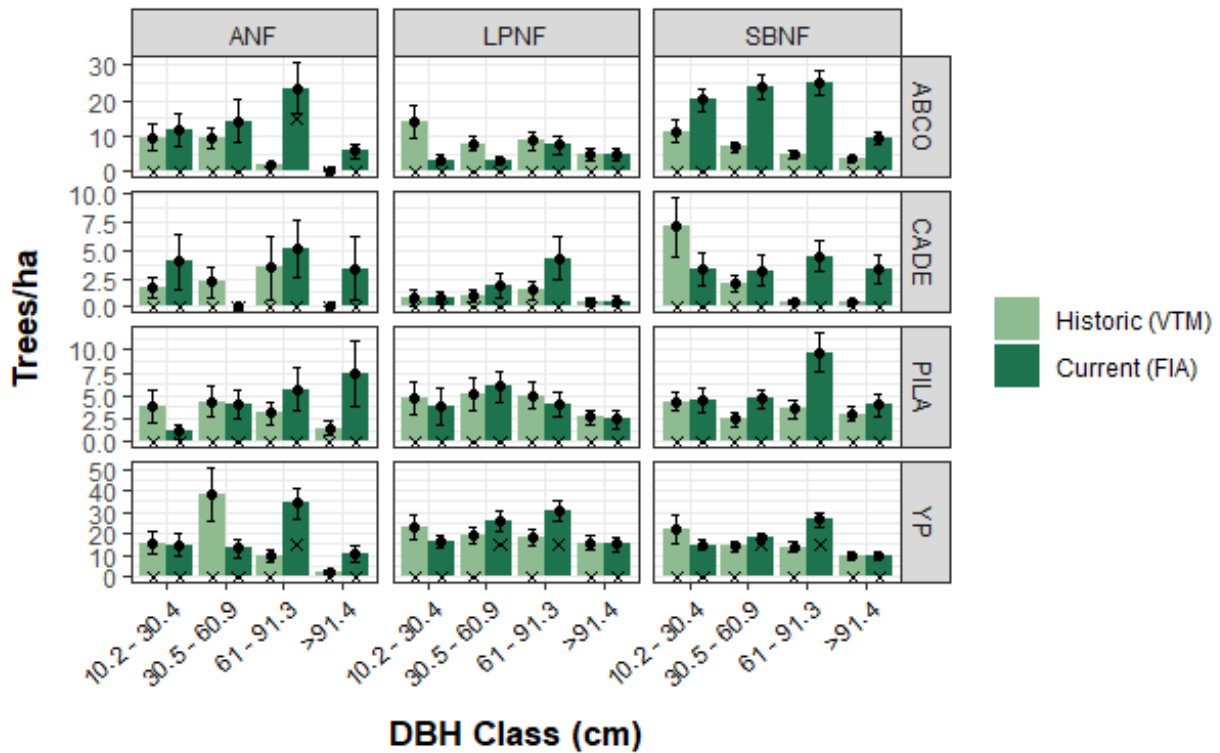


Figure E2: Comparison of the average tree density of *A. concolor*, *C. decurrens*, *P. lambertiana*, and yellow pine by size class and National Forests across all southern California plots using VTM and FIA data using a landscape approach. Sample sizes for ANF: n=20 (VTM) and n=26 (FIA); LPNF: n=54 (VTM) and n=62 (FIA); and SBNF: n=113 (VTM) and n=107 (FIA). Interpretations from this graph should be made with caution. Most groupings had very small sample sizes (n<10).

Table E1. Means, quantiles, and other measures of distribution of tree size class distribution for all plots in the landscape. Means were calculated across all plots in the landscape (VTM: n=195, FIA: n=210).

	Tree Size Class (cm)	25 th Quantile	Mean	Median	75 th Quantile	Standard Deviation	Standard Error	Variance	No. of plots observed in	Dataset
Total	10.2 – 30.4	24.8	110.4	62.1	137.3	154.5	11.1	23881.2	175	VTM
		32.8	201.9	121.4	285.0	248.1	17.1	61554.6	187	FIA
	30.5 – 60.9	13.8	62.1	49.7	88.3	61.7	4.4	3806.1	165	VTM
		18.4	76.9	60.7	113.7	70.4	4.9	4952.3	183	FIA
	61.0 – 91.3	12.4	42.9	29.5	61.9	43.7	3.1	1910.6	148	VTM
		34.1	103.6	78.4	158.2	89.1	6.2	7945.2	198	FIA
	>91.4	0.0	27.4	13.6	47.4	32.4	2.3	1046.6	118	VTM
		0.0	32.1	16.5	50.7	38.9	2.7	1511.2	134	FIA

Table E2. Means, quantiles, and other measures of distribution of tree size class distribution by functional group. Means were calculated across all plots in the landscape (VTM: n=195, FIA: n=210).

Functional Group	Tree Size Class (cm)	25 th Quantile	Mean	Median	75 th Quantile	Standard Deviation	Standard Error	Variance	No. of plots observed in	Dataset
Conifers	10.2 – 30.4	12.6	73.9	39.9	82.9	122.7	8.8	15043.5	159	VTM
		14.9	68.2	32.3	96.7	85.4	5.9	7300.9	159	FIA
	30.5 – 60.9	12.8	54.3	37.8	74.8	57.7	4.1	3333.7	159	VTM
		15.5	59.5	37.2	88.9	59.4	4.1	3533.8	170	FIA
	61.0 – 91.3	0.0	39.9	27.6	60.4	42.6	3.1	1814.9	141	VTM
		32.2	97.8	75.2	145.0	86.2	6.0	7438.7	198	FIA
	>91.4	0.0	25.9	13.3	42.4	32.1	2.3	1028.4	113	VTM
		0.0	31.5	16.4	50.7	38.7	2.7	1497.4	131	FIA
Oaks	10.2 – 30.4	0.0	36.5	0.0	19.9	98.3	7.0	9671.8	64	VTM
		0.0	133.7	24.6	165.5	243.2	16.8	59126.2	116	FIA
	30.5 – 60.9	0.0	7.8	0.0	0.0	21.9	1.6	478.6	42	VTM
		0.0	17.4	0.0	17.2	37.3	2.6	1388.3	71	FIA
	61.0 – 91.3	0.0	2.9	0.0	0.0	9.6	0.7	92.9	23	VTM
		0.0	5.9	0.0	0.0	17.1	1.2	292.8	32	FIA

Table E3. Means, quantiles, and other measures of distribution of tree size class distribution by species. Means were calculated across all plots in the landscape (VTM: n=195, FIA: n=210).

Species	Tree Size Class (cm)	25 th Quantile	Mean	Median	75 th Quantile	Standard Deviation	Standard Error	Variance	No. of plots observed in	Dataset	
<i>A. concolor</i>	10.2 – 30.4	0.0	20.2	0.0	15.1	47.7	3.4	2271.7	67	VTM	
		0.0	28.7	0.0	18.8	63.6	4.4	4047.1	74	FIA	
	30.5 – 60.9	0.0	12.3	0.0	14.3	25.2	1.8	634.0	63	VTM	
		0.0	21.2	0.0	19.0	43.9	3.0	1930.3	72	FIA	
	61.0 – 91.3	0.0	8.7	0.0	6.3	19.9	1.4	396.5	49	VTM	
		0.0	29.0	0.0	44.6	53.9	3.7	2910.2	88	FIA	
	>91.4	0.0	5.4	0.0	0.0	13.8	1.0	189.4	38	VTM	
		0.0	8.9	0.0	15.1	19.7	1.4	387.7	56	FIA	
	<i>C. decurrens</i>	10.2 – 30.4	0.0	8.9	0.0	0.0	37.7	2.7	1421.8	27	VTM
			0.0	5.0	0.0	0.0	24.2	1.7	585.1	18	FIA
30.5 – 60.9		0.0	2.8	0.0	0.0	10.0	0.7	100.7	22	VTM	
		0.0	4.2	0.0	0.0	18.6	1.3	344.6	22	FIA	
61.0 – 91.3		0.0	1.7	0.0	0.0	8.8	0.6	77.3	14	VTM	
		0.0	6.9	0.0	0.0	23.1	1.6	533.8	32	FIA	
>91.4		0.0	0.5	0.0	0.0	3.2	0.2	10.2	5	VTM	
		0.0	2.9	0.0	0.0	13.5	0.9	183.0	15	FIA	
<i>P. coulteri</i>		10.2 – 30.4	0.0	3.8	0.0	0.0	14.1	1.0	197.9	18	VTM
			0.0	2.6	0.0	0.0	12.8	0.9	164.9	14	FIA
	30.5 – 60.9	0.0	4.7	0.0	0.0	19.0	1.4	359.3	19	VTM	
		0.0	2.7	0.0	0.0	10.4	0.7	109.2	17	FIA	
	61.0 – 91.3	0.0	1.8	0.0	0.0	7.8	0.6	60.7	13	VTM	
		0.0	3.1	0.0	0.0	12.2	0.8	149.1	15	FIA	
	<i>P. lambertiana</i>	10.2 – 30.4	0.0	8.0	0.0	0.0	21.8	1.6	477.3	40	VTM
			0.0	4.3	0.0	0.0	15.9	1.1	253.6	27	FIA
		30.5 – 60.9	0.0	5.58	0.0	0.0	16.3	1.2	264.5	34	VTM
			0.0	5.60	0.0	0.0	12.5	0.9	156.3	47	FIA
61.0 – 91.3		0.0	5.8	0.0	0.0	14.8	1.1	218.0	41	VTM	
		0.0	9.6	0.0	0.0	25.4	1.8	645.8	48	FIA	
>91.4		0.0	4.1	0.0	0.0	10.7	0.8	113.6	37	VTM	
		0.0	4.6	0.0	0.0	14.7	1.0	216.1	26	FIA	

Table E4. Means, quantiles, and other measures of distribution of tree size class distribution by species (continued). Means were calculated across all plots in the landscape (VTM: n=195, FIA: n=210).

Species	Tree Size Class (cm)	25 th Quantile	Mean	Median	75 th Quantile	Standard Deviation	Standard Error	Variance	No. of plots observed in	Dataset
<i>P. macrocarpa</i>	30.5 – 60.9	0.0	1.3	0.0	0.0	7.4	0.5	55.5	10	VTM
		0.0	1.7	0.0	0.0	9.6	0.7	93.0	10	FIA
	61.0 – 91.3	0.0	1.6	0.0	0.0	9.4	0.7	89.0	7	VTM
		0.0	4.4	0.0	0.0	20.3	1.4	410.4	19	FIA
Yellow Pine	10.2 – 30.4	0.0	32.2	0.0	28.5	85.5	6.1	7304.6	90	VTM
		0.0	25.9	0.0	30.6	49.6	3.4	2461.9	92	FIA
	30.5 – 60.9	0.0	27.6	12.4	38.0	45.5	3.3	2071.1	99	VTM
		0.0	24.1	15.1	31.9	36.1	2.5	1306.4	111	FIA
	61.0 – 91.3	0.0	20.3	0.0	28.2	32.2	2.3	1037.9	94	VTM
		0.0	44.8	19.0	65.2	58.4	4.0	3407.7	144	FIA
>91.4	0.0	14.6	0.0	24.8	23.4	1.7	549.7	84	VTM	
	0.0	12.6	0.0	17.2	21.5	1.5	462.8	77	FIA	
<i>Q. chrysolepis</i>	10.2 – 30.4	0.0	16.8	0.0	0.0	77.9	5.6	6069.2	33	VTM
		0.0	113.5	0.0	131.8	239.8	16.5	57510.0	95	FIA
	30.5 – 60.9	0.0	3.4	0.0	0.0	17.1	1.2	291.9	17	VTM
		0.0	11.9	0.0	0.0	32.7	2.3	1070.8	46	FIA
<i>Q. kelloggii</i>	10.2 – 30.4	0.0	19.7	0.0	0.0	62.5	4.5	3906.0	42	VTM
		0.0	20.1	0.0	0.0	62.9	4.3	3950.3	39	FIA
	30.5 – 60.9	0.0	4.4	0.0	0.0	13.1	0.9	172.5	30	VTM
		0.0	5.5	0.0	0.0	18.0	1.2	325.4	32	FIA
	61.0 – 91.3	0.0	2.1	0.0	0.0	7.0	0.5	48.4	18	VTM
		0.0	2.6	0.0	0.0	11.8	0.8	138.2	15	FIA

Table E5. Means, quantiles, and other measures of distribution of tree size class distribution by shade and fire tolerance including oaks. Means were calculated across all plots in the landscape (VTM: n=195, FIA: n=210).

Shade/Fire Tolerant - Including Oaks	Tree Size Class (cm)	25 th Quantile	Mean	Median	75 th Quantile	Standard Deviation	Standard Error	Variance	No. of plots observed in	Dataset
Shade Intolerant/Fire Tolerant	10.2 – 30.4	0.0	64.5	27.6	86.5	103.8	7.4	10774.0	106	VTM
		0.0	54.7	19.3	69.4	80.8	5.6	6525.5	150	FIA
	30.5 – 60.9	0.0	43.5	27.6	63.4	51.9	3.7	2695.5	89	VTM
		14.9	39.6	30.2	55.4	42.6	2.9	1812.9	115	FIA
	61.0 – 91.3	0.0	31.6	24.8	45.3	37.5	2.7	1406.0	61	VTM
		17.1	64.4	49.9	89.4	63.1	4.4	3982.5	110	FIA
	>91.4	0.0	21.4	12.7	37.1	27.4	2.0	748.2	43	VTM
		0.0	19.8	0.0	32.5	27.5	1.9	757.6	71	FIA
Shade Tolerant/Fire Intolerant	10.2 – 30.4	0.0	45.9	12.6	53.3	99.4	7.1	9881.2	145	VTM
		0.0	147.2	52.0	186.7	240.4	16.6	57810.7	140	FIA
	30.5 – 60.9	0.0	18.6	0.0	27.4	31.3	2.2	982.1	144	VTM
		0.0	37.3	15.8	46.2	55.1	3.8	3041.3	158	FIA
	61.0 – 91.3	0.0	11.2	0.0	13.3	22.7	1.6	516.7	136	VTM
		0.0	39.2	15.2	52.0	61.5	4.2	3786.8	181	FIA
	>91.4	0.0	6.0	0.0	0.0	14.2	1.0	201.1	109	VTM
		0.0	12.4	0.0	16.3	25.7	1.8	658.3	104	FIA

Table E6. Means, quantiles, and other measures of distribution of tree size class distribution by shade and fire tolerance excluding oaks. Means were calculated across all plots in the landscape (VTM: n=195, FIA: n=210).

Shade/Fire Tolerant - Excluding Oaks	Tree Size Class (cm)	25 th Quantile	Mean	Median	75 th Quantile	Standard Deviation	Standard Error	Variance	No. of plots observed in	Dataset
Shade Intolerant/Fire Tolerant	10.2 – 30.4	0.0	44.9	14.7	50.4	87.9	6.3	7731.3	130	VTM
		0.0	34.5	16.5	44.8	51.8	3.6	2679.1	127	FIA
	30.5 – 60.9	0.0	39.1	25.0	58.4	49.8	3.6	2477.6	135	VTM
		0.0	34.1	18.8	48.0	37.7	2.6	1420.1	151	FIA
	61.0 – 91.3	0.0	29.6	14.4	43.9	36.6	2.6	1336.9	127	VTM
		16.6	61.8	45.9	83.9	62.8	4.3	3949.1	179	FIA
	>91.4	0.0	20.0	12.5	28.8	26.9	1.9	725.9	104	VTM
		0.0	19.7	0.0	32.5	27.6	1.9	759.4	103	FIA
Shade Tolerant/Fire Intolerant	10.2 – 30.4	0.0	29.1	0.0	27.9	63.7	4.6	4060.8	81	VTM
		0.0	33.7	0.0	31.1	68.9	4.8	4752.4	83	FIA
	30.5 – 60.9	0.0	15.1	0.0	15.6	27.6	2.0	763.2	76	VTM
		0.0	25.4	0.0	32.9	47.1	3.3	2220.9	85	FIA
	61.0 – 91.3	0.0	10.4	0.0	12.8	21.9	1.6	480.8	57	VTM
		0.0	35.9	7.5	49.9	58.0	4.0	3360.9	105	FIA
	>91.4	0.0	5.9	0.0	0.0	14.1	1.0	198.9	42	VTM
		0.0	11.8	0.0	16.0	25.3	1.7	639.2	66	FIA

Table E7. Means, quantiles, and other measures of distribution of tree size class distribution by elevation classes.

Elevation (m)	Tree Size Class (cm)	25 th Quantile	Mean	Median	75 th Quantile	Standard Deviation	Standard Error	Variance	No. of plots observed in	Dataset	
1000 – 1499	10.2 – 30.4	49.9	218.4	126.4	333.8	264.0	59.0	69690.3	19	VTM	
		29.8	214.4	136.2	240.0	281.7	55.2	79335.3	22	FIA	
	30.5 – 60.9	24.0	89.3	62.2	119.8	93.8	21.0	8790.6	18	VTM	
		29.8	75.8	44.0	95.0	86.0	16.9	7396.5	23	FIA	
	61.0 – 91.3	9.6	39.7	25.5	52.9	43.7	9.8	1910.5	15	VTM	
		23.4	71.5	64.1	91.4	64.9	12.7	4213.8	24	FIA	
	>91.4	0.0	25.4	6.2	42.9	34.7	7.8	1205.8	10	VTM	
		0.0	19.6	15.4	30.6	23.6	4.6	555.7	15	FIA	
	1500 – 1999	10.2 – 30.4	35.5	127.8	87.1	163.9	141.6	15.4	20049.5	82	VTM
			59.7	206.8	150.6	295.4	219.1	24.5	48021.6	73	FIA
30.5 – 60.9		24.9	65.0	55.3	87.7	57.2	6.2	3272.7	71	VTM	
		31.0	83.8	72.6	124.3	66.6	7.4	4435.3	71	FIA	
61.0 – 91.3		9.3	48.7	37.7	73.7	49.6	5.4	2461.2	63	VTM	
		32.0	94.0	62.8	137.7	80.0	8.9	6395.3	75	FIA	
>91.4		0.0	22.7	12.9	32.5	28.2	3.1	795.0	49	VTM	
		0.0	23.2	15.1	36.1	31.0	3.5	961.7	43	FIA	
2000 – 2499		10.2 – 30.4	12.4	72.3	43.2	88.2	124.7	14.2	15539.3	58	VTM
			45.3	221.8	110.4	299.3	281.9	31.9	79485.7	74	FIA
	30.5 – 60.9	12.6	55.2	37.8	87.3	58.1	6.6	3372.0	65	VTM	
		29.8	78.4	54.9	112.9	69.2	7.8	4781.9	72	FIA	
	61.0 – 91.3	12.5	37.7	27.6	53.3	37.6	4.3	1412.0	59	VTM	
		46.4	122.3	101.9	180.0	104.8	11.9	10984.6	73	FIA	
	>91.4	0.0	34.5	27.1	57.7	35.2	4.0	1237.2	53	VTM	
		0.0	42.8	18.6	68.7	48.0	5.4	2302.2	55	FIA	
	>2500	10.2 – 30.4	25.8	62.7	38.2	69.1	70.5	19.6	4975.4	11	VTM
			0.0	114.6	31.3	196.1	171.2	33.6	29302.1	18	FIA
30.5 – 60.9		12.9	43.5	37.3	69.1	40.0	11.1	1599.9	10	VTM	
		0.0	52.3	23.9	74.8	66.8	13.1	4466.9	17	FIA	
61.0 – 91.3		25.2	42.4	38.7	59.0	37.3	10.3	1392.0	10	VTM	
		50.0	109.0	98.2	164.7	75.3	14.8	5677.2	26	FIA	
>91.4		0.0	20.7	0.0	14.7	32.9	9.1	1083.8	6	VTM	
		16.0	40.2	32.1	70.6	33.2	6.5	1104.4	21	FIA	

Table E8. Means, quantiles, and other measures of distribution of tree size class distribution by elevation classes for oaks only.

Elevation (m) - Oaks	Tree Size Class (cm)	25 th Quantile	Mean	Median	75 th Quantile	Standard Deviation	Standard Error	Variance	Sample Size	Dataset
1000 – 1499	10.2 – 30.4	47.1	104.8	78.0	123.0	100.6	29.0	10125.3	10	VTM
		46.6	246.8	130.5	271.5	312.9	75.9	97894.6	15	FIA
	30.5 – 60.9	13.4	28.1	26.5	38.2	19.8	5.7	390.4	11	VTM
		16.0	41.5	30.7	46.6	52.0	12.6	2704.8	13	FIA
1500 – 1999	10.2 – 30.4	12.5	76.1	35.2	95.9	100.7	13.7	10134.3	43	VTM
		47.3	201.3	133.0	285.3	232.6	29.3	54084.0	58	FIA
	30.5 – 60.9	0.0	20.1	6.2	25.6	35.1	4.8	1230.5	27	VTM
		0.0	34.5	15.9	47.7	46.1	5.8	2127.0	41	FIA
	61.0 – 91.3	0.0	8.5	0.0	13.7	15.7	2.1	247.0	18	VTM
		0.0	12.5	0.0	15.4	25.1	3.2	629.8	19	FIA
2000 – 2499	10.2 – 30.4	15.1	145.2	53.9	91.7	267.9	77.3	71753.1	11	VTM
		37.3	241.1	134.7	308.8	332.3	51.3	110432.8	40	FIA

Table E9. Means, quantiles, and other measures of distribution of tree size class distribution by elevation classes for conifers only. Means were calculated across all plots in the landscape (sample sizes here).

Elevation (m) - Conifers	Tree Size Class (cm)	25 th Quantile	Mean	Median	75 th Quantile	Standard Deviation	Standard Error	Variance	No. of plots observed in	Dataset
1000 – 1499	10.2 – 30.4	22.1	155.5	47.0	137.5	268.7	60.1	72216.6	17	VTM
		0.0	53.0	29.8	58.3	77.9	15.3	6063.3	16	FIA
	30.5 – 60.9	13.6	72.4	39.0	97.6	81.4	18.2	6618.0	18	VTM
		15.1	48.7	29.8	74.1	56.1	11.0	3149.8	20	FIA
	61.0 – 91.3	0.0	35.6	19.9	52.9	42.0	9.4	1760.5	13	VTM
		23.3	59.5	42.5	80.6	57.0	11.2	3249.0	24	FIA
	>91.4	0.0	19.8	0.0	27.4	31.5	7.0	991.3	9	VTM
		0.0	17.8	7.7	30.2	24.0	4.7	577.5	13	FIA
1500 – 1999	10.2 – 30.4	14.4	78.9	42.4	88.2	112.8	12.3	12721.7	73	VTM
		11.2	48.3	30.8	62.6	57.0	6.4	3245.3	60	FIA
	30.5 – 60.9	12.7	52.1	38.7	72.5	53.2	5.8	2835.3	66	VTM
		15.4	56.7	42.1	87.5	50.9	5.7	2592.8	63	FIA
	61.0 – 91.3	0.0	43.3	33.0	65.0	48.3	5.3	2329.4	58	VTM
		31.6	84.2	60.4	111.4	72.9	8.2	5320.3	75	FIA
	>91.4	0.0	20.7	12.6	29.0	27.7	3.0	769.8	45	VTM
		0.0	22.1	15.1	33.3	29.7	3.3	882.7	42	FIA
2000 – 2499	10.2 – 30.4	0.0	49.6	37.1	72.1	57.1	6.5	3262.1	57	VTM
		16.6	92.0	67.9	114.3	101.2	11.5	10240.5	65	FIA
	30.5 – 60.9	12.6	53.9	37.1	79.9	58.2	6.6	3390.5	64	VTM
		17.5	68.4	48.0	102.9	65.7	7.4	4313.1	70	FIA
	61.0 – 91.3	12.5	37.4	27.6	50.4	37.3	4.3	1393.9	59	VTM
		40.2	120.7	101.9	171.4	102.8	11.6	10576.0	73	FIA
	>91.4	0.0	34.5	27.1	57.7	35.2	4.0	1237.2	53	VTM
		0.0	42.8	18.6	68.7	48.0	5.4	2302.2	55	FIA
>2500	10.2 – 30.4	25.8	62.7	38.2	69.1	70.5	19.6	4975.4	11	VTM
		0.0	73.4	16.8	113.3	99.4	19.5	9876.0	18	FIA
	30.5 – 60.9	12.9	43.5	37.3	69.1	40.0	11.1	1599.9	10	VTM
		0.0	52.3	23.9	74.8	66.8	13.1	4466.9	17	FIA
	61.0 – 91.3	25.2	42.4	38.7	59.0	37.3	10.3	1392.0	10	VTM
		50.0	109.0	98.2	164.7	75.3	14.8	5677.2	26	FIA

Table E10. Means, quantiles, and other measures of distribution of tree size class distribution by National Forest. Sample sizes for ANF: n=20 (VTM) and n=26 (FIA); LPNF: n=54 (VTM) and n=62 (FIA); and SBNF: n=113 (VTM) and n=107 (FIA).

National Forest	Tree Size Class (cm)	25 th Quantile	Mean	Median	75 th Quantile	Standard Deviation	Standard Error	Variance	No. of plots observed in	Dataset
ANF	10.2 – 30.4	37.9	78.3	66.2	97.9	56.5	12.6	3188.7	19	VTM
		21.5	130.8	59.9	153.1	190.1	37.3	36141.7	22	FIA
	30.5 – 60.9	62.1	103.6	87.4	125.0	77.2	17.3	5955.6	19	VTM
		17.3	60.4	36.9	91.4	61.4	12.1	3775.3	21	FIA
	61.0 – 91.3	15.1	35.2	35.0	42.7	27.4	6.1	753.1	17	VTM
		61.8	124.2	98.5	183.7	79.1	15.5	6249.8	25	FIA
	>91.4	0.0	5.5	0.0	12.7	8.5	1.9	72.9	7	VTM
		0.0	36.0	24.9	63.3	38.1	7.5	1448.6	18	FIA
LPNF	10.2 – 30.4	24.9	85.2	57.7	115.5	77.4	10.5	5992.9	51	VTM
		45.1	194.8	153.5	246.8	217.9	27.7	47475.4	54	FIA
	30.5 – 60.9	17.9	66.3	59.3	102.1	52.6	7.2	2771.8	47	VTM
		15.9	72.6	66.2	111.3	63.0	8.0	3973.5	52	FIA
	61.0 – 91.3	12.6	54.4	48.0	94.3	50.1	6.8	2507.1	41	VTM
		19.7	83.3	61.1	122.3	74.4	9.5	5541.0	57	FIA
	>91.4	0.0	37.6	28.5	73.7	37.1	5.0	1375.1	37	VTM
		0.0	29.2	16.6	49.9	34.5	4.4	1193.0	38	FIA
SBNF	10.2 – 30.4	12.6	124.1	67.8	141.1	186.2	17.5	34655.5	93	VTM
		43.6	222.7	136.5	318.6	232.0	22.4	53805.8	98	FIA
	30.5 – 60.9	13.3	54.7	37.8	74.3	61.7	5.8	3808.9	92	VTM
		29.8	84.4	64.0	133.8	78.1	7.5	6093.8	96	FIA
	61.0 – 91.3	0.0	39.6	27.6	57.7	43.2	4.1	1867.8	84	VTM
		35.5	110.7	78.8	166.3	100.3	9.7	10052.4	101	FIA
	>91.4	0.0	26.8	13.6	45.3	31.5	3.0	994.9	67	VTM
		0.0	33.7	16.6	57.1	42.1	4.1	1769.0	68	FIA

Appendix F: Basal area code example

```
##### vtm data #####
vtm_dbh <- vtm %>%
  pivot_longer('dbh_4_11':'dbh_36',
              names_to = "dbh_class",
              values_to = "dbh_count") %>%
  filter(dbh_count != 0) %>% # get error when use uncount() and there are rows with a value of
  0
  tidyr::uncount(dbh_count) %>%
  mutate(dbh_class = case_when(
    dbh_class == "dbh_4_11" ~ "10.2-30.4",
    dbh_class == "dbh_12_23" ~ "30.5-60.9",
    dbh_class == "dbh_24_35" ~ "61.0-91.3",
    dbh_class == "dbh_36" ~ "91.4+"
  )) %>%
  mutate(dbh_class = as.factor(dbh_class),
         dbh_class = fct_relevel(dbh_class, levels=c("10.2-30.4", "30.5-60.9", "61.0-91.3",
"91.4+")))
##### FIA #####
fia_dbh <- fia %>%
  filter(!is.na(dbh)) %>%
  mutate(dbh_class = case_when(
    dbh < 10.2 ~ "0-10.2",
    dbh <= 30.4 ~ "10.2-30.4",
    dbh <= 60.9 ~ "30.5-60.9",
    dbh < 91.44 ~ "61.0-91.3",
    dbh >= 91.44 ~ "91.4+"
  )) %>%
  filter(dbh_class != "0-10.2")
```

Figure F1. R code for classifying tree size classes for VTM and combined FIA data.

```
##### sub data #####
# calc avg stem density/ size class
vtm_basic_df <- vtm_dbh %>%
  group_by(plotkey, dbh_class) %>% tally() %>%
  mutate(stem_density = n/0.0809) %>% # trees/ha (stem density) in each size class
  #filter(plotkey%in% c("154B14", "154B117", "154D13")) %>%
  group_by(dbh_class) %>%
  summarize(avg_stem_density = mean(stem_density),
            median = median(stem_density),
            sd = sd(stem_density),
            se = sd((stem_density) / sqrt(n())),
            sample_size = n()) %>%
  mutate(data = "VTM")

fia_basic_df <- fia_dbh %>%
  group_by(join_plot, dbh_class) %>%
  tally() %>%
  mutate(stem_density = n/0.067245) %>%
  group_by(dbh_class) %>%
  summarize(avg_stem_density = mean(stem_density),
            median = median(stem_density),
            sd = sd(stem_density),
            se = sd((stem_density) / sqrt(n())),
            sample_size = n()) %>%
  mutate(data = "FIA")

dbh_basic_df <- rbind(vtm_basic_df, fia_basic_df)
```

Figure F2. R code for calculating tree density per size class for VTM and FIA data.

Appendix G: Basal area histograms and one-to-one graphs

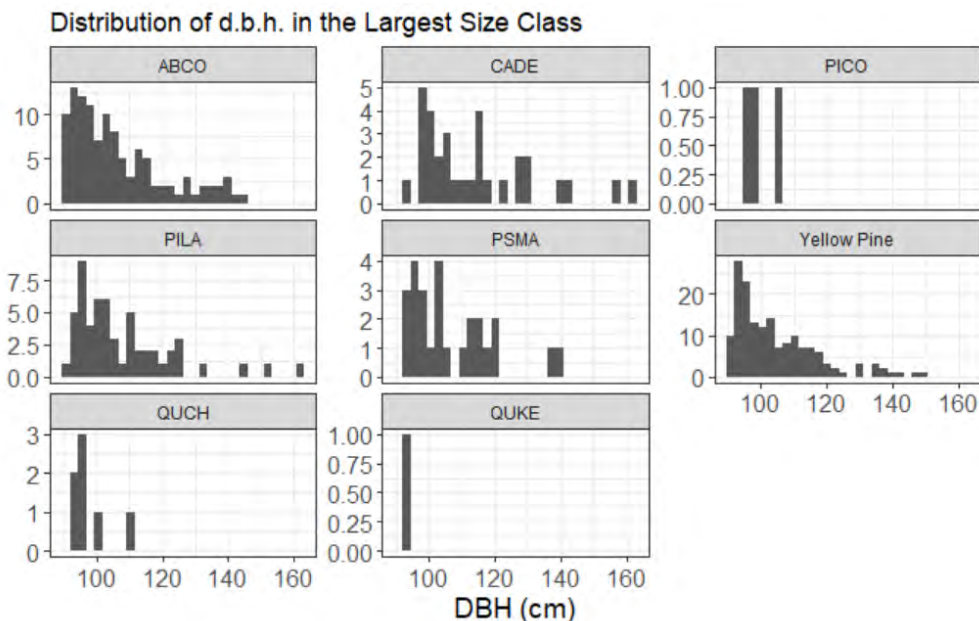


Figure G1. Distribution of trees in the largest size class (>91.4cm) by species. Not shown in graph is cade with the largest d.b.h. of 228.

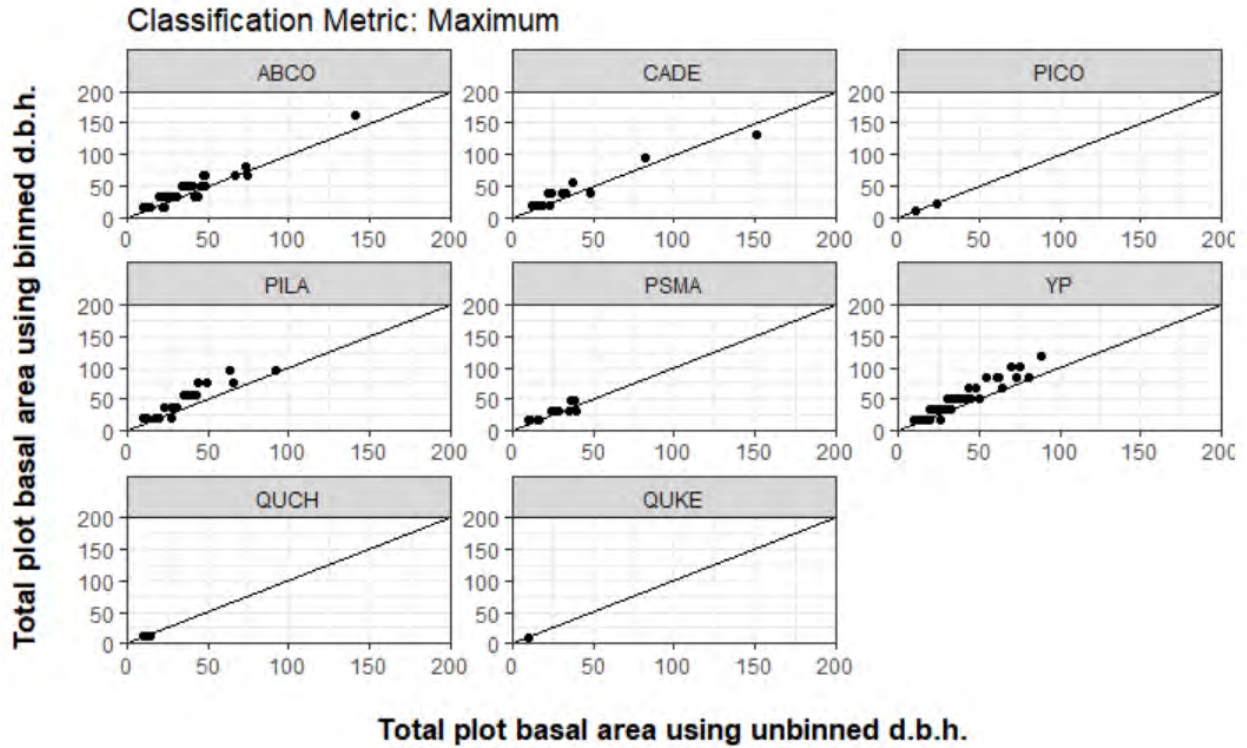


Figure G2. One-to-one line with total plot basal area using unboxed FIA and binned FIA data.

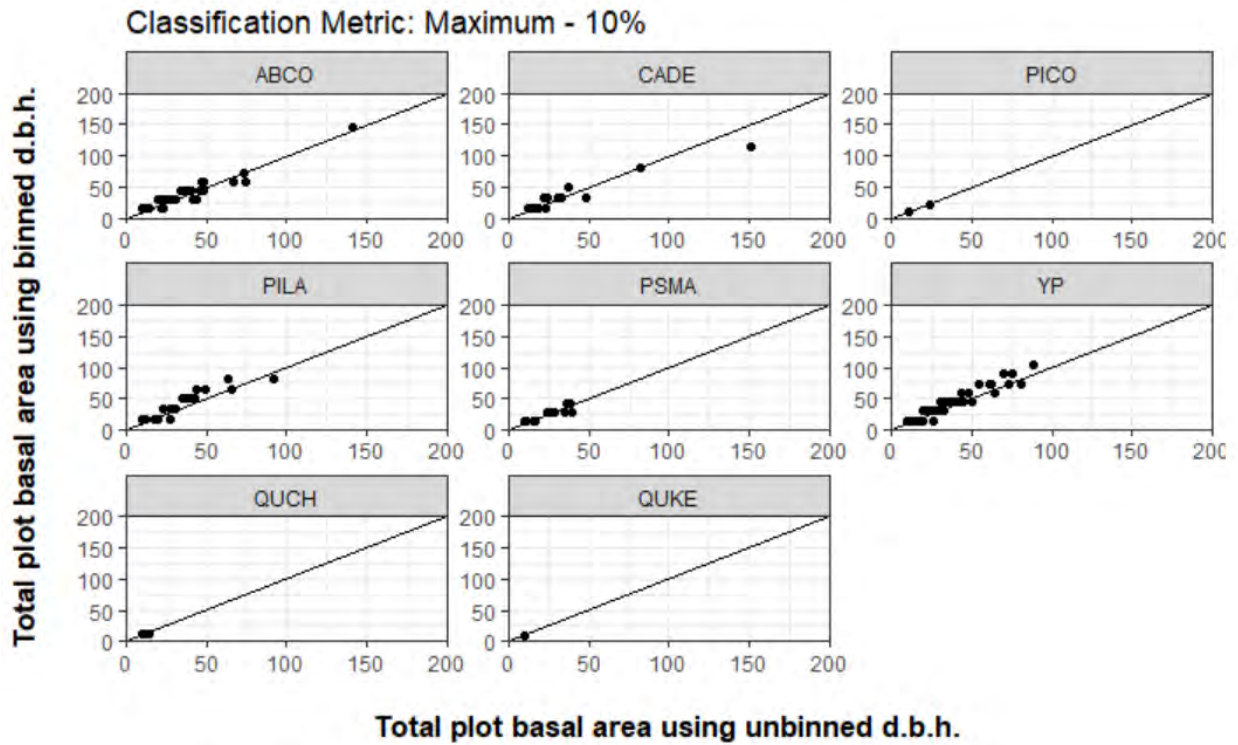


Figure G2. One-to-one line with total plot basal area using unboxed FIA and binned FIA data.

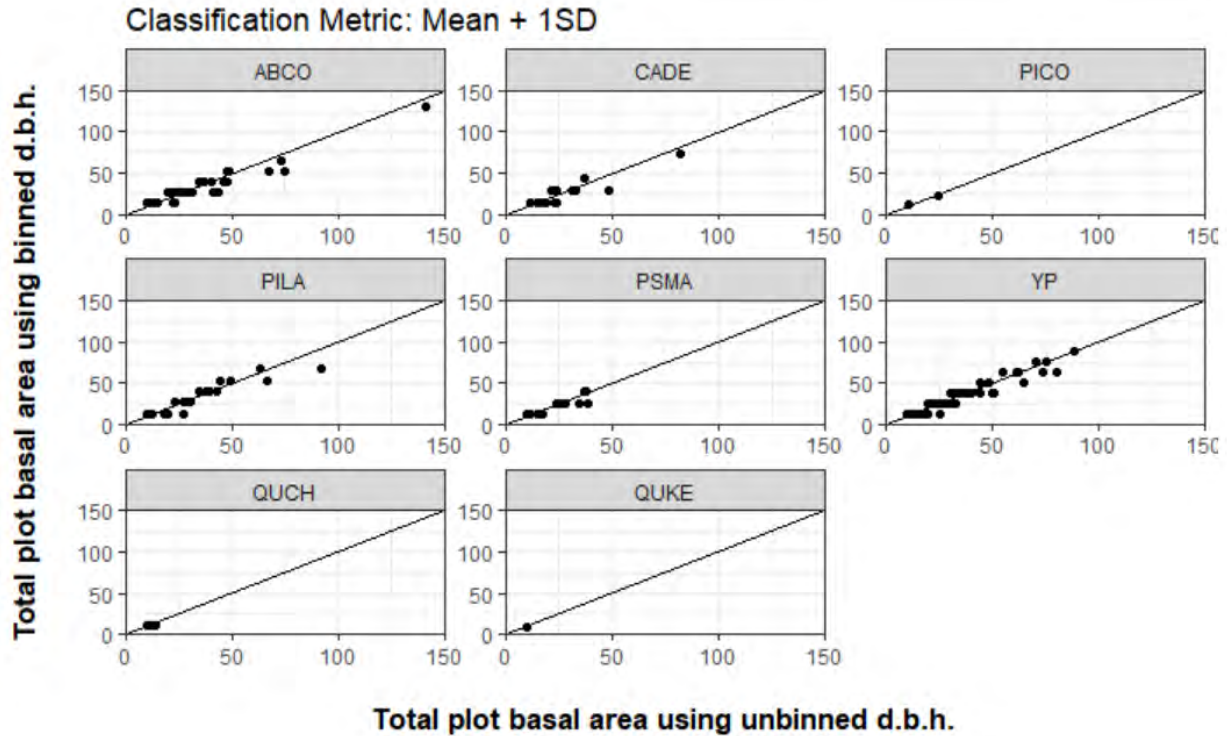


Figure G3. One-to-one line with total plot basal area using unboxed FIA and binned FIA data.

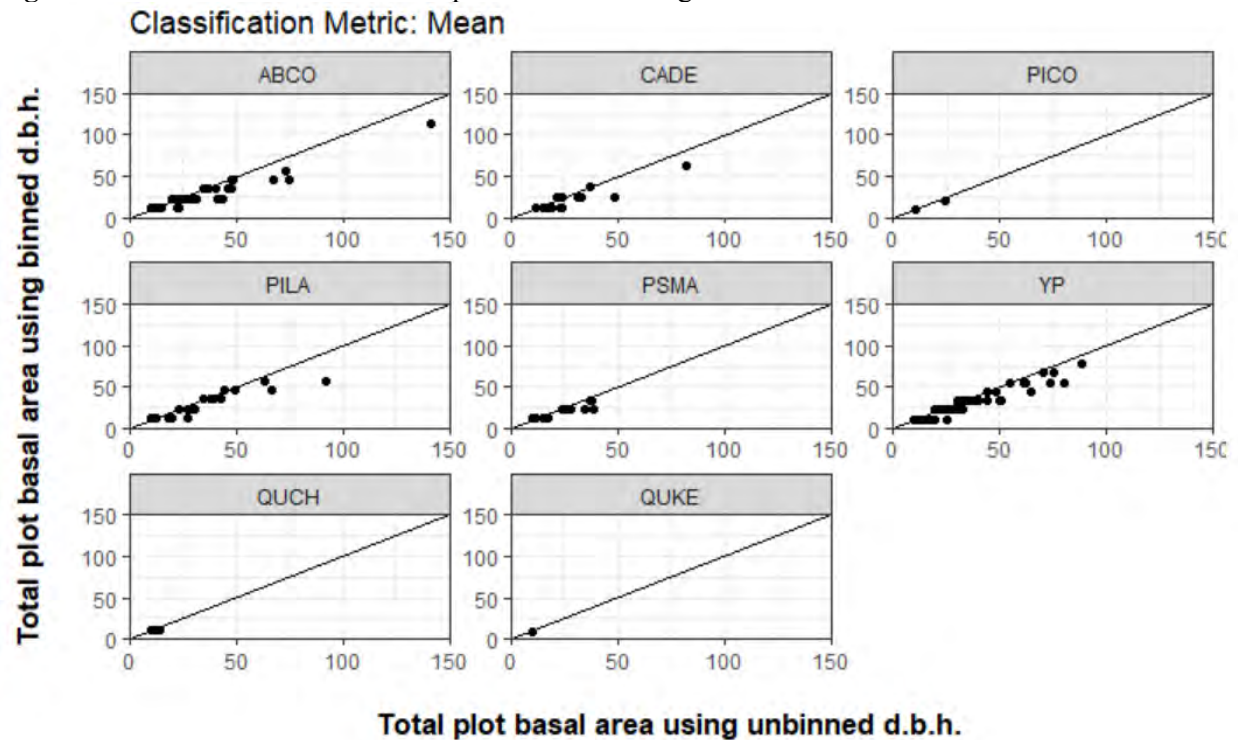


Figure G4. One-to-one line with total plot basal area using unboxed FIA and binned FIA data.

Appendix H: Additional basal area analysis and metrics of variance

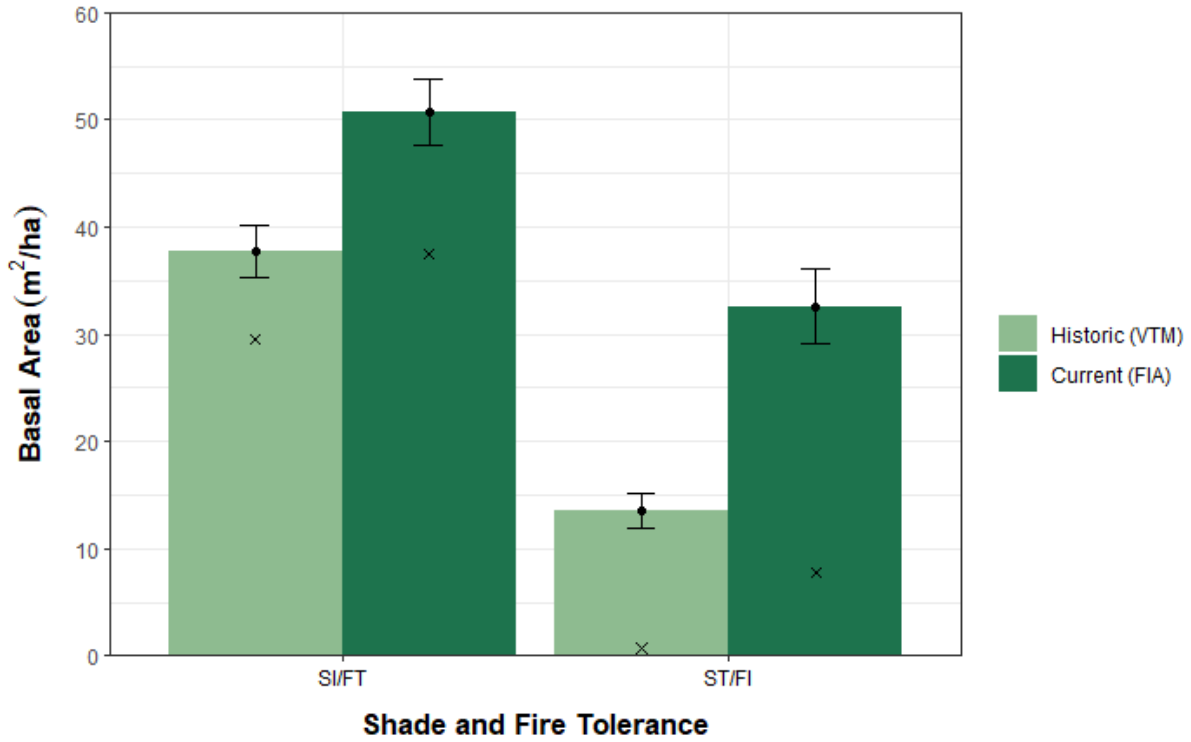


Figure H1. Change in mean basal area by shade and fire tolerance across all YPMC species and excluding oaks.

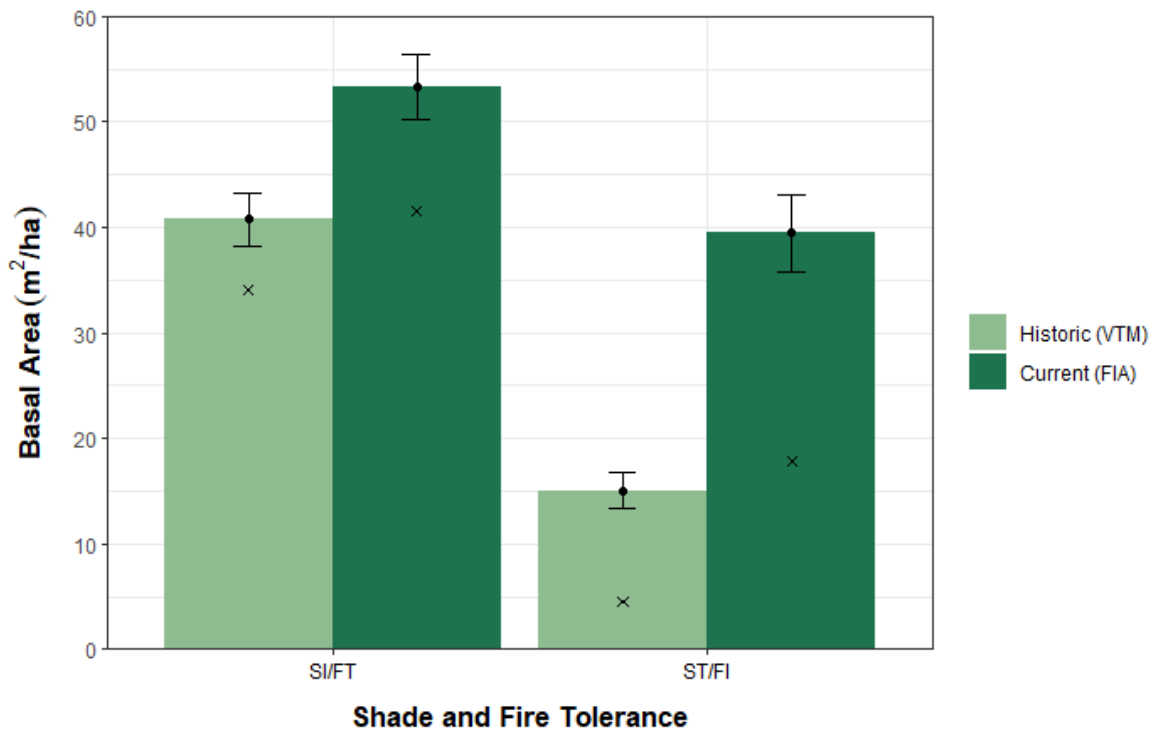


Figure H2. Change in mean basal area by shade and fire tolerance across all YPMC species and including oaks.

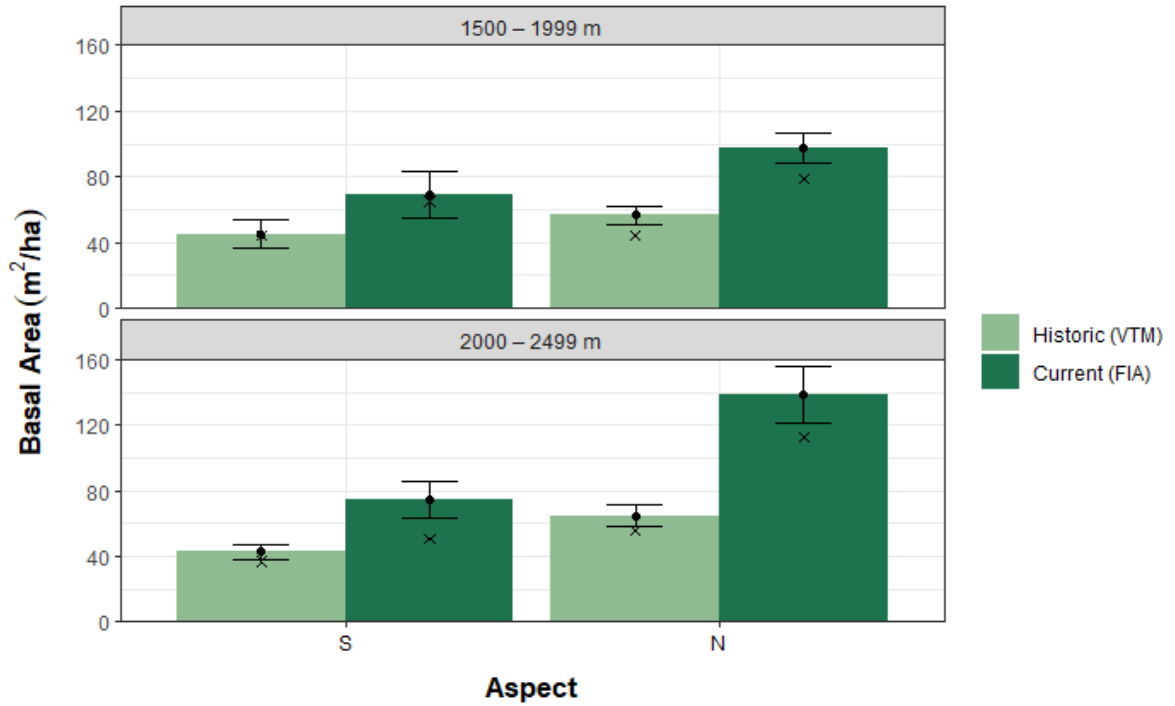


Figure H3. Changes in mean basal area by elevation class and aspect across all YPMC species. Only the 1500–1999m and 2000–2499m classes are shown here as the other classes were removed due to small sample sizes.

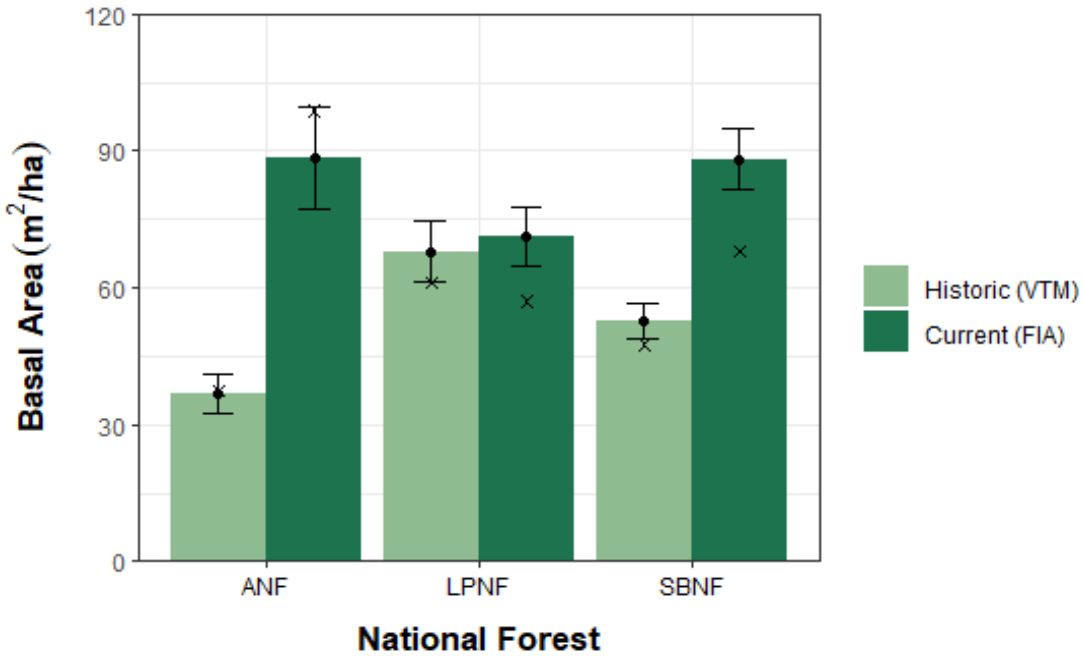


Figure H4. Changes in mean basal area by National Forest across all plots in the landscape. CNF is not shown here due to small sample sizes. Sample sizes for ANF: n=20 (VTM) and n=26 (FIA); LPNF: n=54 (VTM) and n=62 (FIA); and SBNF: n=113 (VTM) and n=107 (FIA).

Table H5. Means, quantiles, and other measures of distribution for basal area (m²/ha) by total number of plots, classification, and shade/fire tolerance. Means were calculated across the entire landscape.

	25 th Quantile	Mean	Median	75 th Quantile	Standard Deviation	Standard Error	Variance	No. of plots observed in	Dataset
Total	26.6 39.6	55.7 92.8	45.4 75.1	70.7 133.8	42.2 72.0	3.0 5.0	1780.9 5178.3	195 210	VTM FIA
Functional Group									
Conifers	21.9 30.3	51.2 83.3	42.9 60.4	67.6 125.3	41.6 71.0	3.0 4.9	1731.0 5039.9	195 210	VTM FIA
Oaks	0.0 0.0	4.5 9.5	0.0 3.6	3.8 11.7	9.9 14.7	0.7 1.0	97.3 217.3	78 125	VTM FIA
Shade/Fire Tolerance (including Oaks)									
Shade Intolerant/Fire Tolerant	16.5 18.0	40.7 53.3	34.1 41.5	52.6 79.4	34.6 45.1	2.5 3.1	1198.5 2031.2	189 201	VTM FIA
Shade Tolerant/Fire Intolerant	0.0 1.7	15.0 39.5	4.6 17.9	21.8 57.9	24.0 53.1	1.7 3.7	577.9 2822.3	126 168	VTM FIA
Shade/Fire Tolerance (excluding Oaks)									
Shade Intolerant/Fire Tolerant	13.7 16.4	37.7 50.7	29.5 37.4	49.3 75.0	34.1 45.4	2.4 3.1	1165.7 2062.1	184 201	VTM FIA
Shade Tolerant/Fire Intolerant	0.0 0.0	13.5 32.6	0.7 7.7	19.8 49.9	23.6 50.8	1.7 3.5	558.5 2581.0	102 128	VTM FIA

Table H6. Means, quantiles, and other measures of distribution for basal area (m²/ha) by species. Means were calculated across the entire landscape.

Species	25 th Quantile	Mean	Median	75 th Quantile	Standard Deviation	Standard Error	Variance	No. of plots observed in	Dataset
<i>A. concolor</i>	0.0 0.0	11.6 25.6	0.0 2.3	17.5 36.1	22.9 44.1	1.6 3.0	526.3 1944.7	90 110	VTM FIA
<i>C. decurrens</i>	0.0 0.0	2.0 7.0	0.0 0.0	0.0 0.0	6.3 23.4	0.5 1.6	39.5 548.0	36 43	VTM FIA
<i>P. coulteri</i>	0.0 0.0	2.03 2.01	0.0 0.0	0.0 0.0	8.8 7.2	0.6 0.5	77.8 51.5	23 25	VTM FIA
<i>P. lambertiana</i>	0.0 0.0	7.3 9.4	0.0 0.0	8.3 7.3	15.9 23.7	1.1 1.6	253.9 560.8	69 77	VTM FIA
<i>P. macrocarpa</i>	0.0 0.0	1.7 4.3	0.0 0.0	0.0 0.0	9.2 15.6	0.7 1.1	84.0 243.4	14 24	VTM FIA
Yellow Pine	0.0 4.0	26.6 35.0	18.3 21.4	39.1 52.3	31.3 40.4	2.2 2.8	977.2 1635.1	145 169	VTM FIA
<i>Q. chrysolepis</i>	0.0 0.0	1.5 6.9	0.0 0.0	0.0 8.5	6.4 13.1	0.5 0.9	40.4 172.2	38 102	VTM FIA
<i>Q. kelloggii</i>	0.0 0.0	3.0 2.6	0.0 0.0	0.4 0.0	7.4 7.6	0.5 0.5	55.1 57.8	54 44	VTM FIA

Table H7. Means, quantiles, and other measures of distribution for basal area (m²/ha) by National Forest. Means are calculated across the entire landscape.

National Forest	25 th Quantile	Mean	Median	75 th Quantile	Standard Deviation	Standard Error	Variance	No. of plots observed in	Dataset
ANF	24.8	38.7	38.4	45.9	18.9	4.2	357.6	20	VTM
	43.9	100.6	104.9	135.8	67.6	13.3	4575.2	26	FIA
LPNF	26.2	69.8	65.1	98.8	50.9	6.9	2595.1	54	VTM
	33.7	79.6	63.6	125.9	57.0	7.2	3251.1	62	FIA
SBNF	26.7	52.9	45.2	66.0	40.1	3.8	1607.9	113	VTM
	38.6	99.8	74.9	139.9	82.4	8.0	6794.6	107	FIA

Table H8. Means, quantiles, and other measures of distribution for basal area (m²/ha) by elevation classes. Means are calculated across the entire landscape.

Elevation (m)	25 th Quantile	Mean	Median	75 th Quantile	Standard Deviation	Standard Error	Variance	No. of plots observed in	Dataset
1000 – 1499	23.5	58.1	53.6	74.0	44.1	9.9	1941.5	20	VTM
	30.6	66.8	54.6	91.9	48.0	9.4	2304.9	26	FIA
1500 – 1999	26.1	55.1	43.7	70.6	42.6	4.6	1811.4	84	VTM
	35.9	81.6	69.8	121.9	59.0	6.6	3481.7	80	FIA
2000 – 2499	34.2	58.0	49.3	71.3	40.9	4.7	1676.7	77	VTM
	43.8	112.0	97.1	166.6	89.4	10.1	7987.6	78	FIA
>2500	17.3	46.2	41.6	56.7	47.7	13.2	2271.5	13	VTM
	56.9	95.7	88.4	142.0	55.8	11.0	3117.7	26	FIA

Appendix I: Canopy cover FVS equations and code example

Table 4.4.2.1 Coefficients and equation reference for crown width equations {4.4.2.1} – {4.4.2.5} in the WS variant. *Equation refers to the species-specific equation used when $DBH > DBH_T$

{4.4.2.1} $CW = a_1 + a_2 * DBH$	$DBH \geq DBH_T$
{4.4.2.2} $CW = a_1 * DBH^{a_2}$	$DBH \geq DBH_T$
{4.4.1.4} $CW = HT * s_1$	$HT < 4.5'$ and $DBH < DBH_T$
{4.4.1.5} $CW = d_1 + d_2 * DBH$	$HT > 4.5'$ and $DBH < DBH_T$

CW is maximum tree crown width

DBH is tree diameter at breast height

DBH_T is threshold diameter shown in table 4.4.2.1

d_{1-2} , a_{1-2} , s_1 are species-specific coefficients shown in table 4.4.2.1

FVA Alpha Code	Species Name	Equation Used*	DBH_T	d_1	d_2	a_1	a_2	s_1
SP	Sugar Pine	{4.4.2.1}	7.4	3.5	0.338	-1.476	1.01	0.7778
WH	White Fir	{4.4.2.1}	5	3.26	1.103	5.82	0.591	0.7778
IC	Incense Cedar	{4.4.2.1}	5	3.5	1.192	7.11	0.47	0.7778
JP	Jeffrey Pine	{4.4.2.2}	5	3.5	0.5754	1.52	0.891	0.7778
PP	Ponderosa Pine	{4.4.2.2}	5	3.77	0.7756	2.24	0.763	0.7778
CP	Coulter Pine	{4.4.2.2}	5	3.5	1.7618	3.9347	0.7086	0.7778
BD	Big-Cone Douglas Fir	{4.4.2.1}	5	3.5	5.5672	27.030	0.8612	0.7778
CY	Canyon Live Oak	{4.4.2.1}	5	2.5	2.19	5	1.69	0.5556
BO	Black Oak	{4.4.2.1}	5	2.5	2.7	10	1.2	0.5556

After applying the FVS equations to each tree species, we calculated crown area. To calculate crown area, we used πr^2 (ft²). Crown with measured the diameter of the canopy, so we multiplied the radius (r) by 0.5. Crown areas were summed for all species for each plot and then converted to square meters (m²). To find the total percent cover per plot, we divided each total plot crown area by the size of their plot (for VTM, plots are 809 m²; for FIA, plots are 672.45m²).

```

{r}
## VTM PIP0
# Use Equation 4.4.2.2: CW = a1 * DBH^a2 (DBH>=DBHT)
# DBH(subT) = 5

vtm_pipo <- vtm_data %>%
  filter(abbreviation == "PIP0") %>% # select only Pinus ponderosa
  select(plotkey, abbreviation, n,
         dbh_4_11, dbh_12_23, dbh_24_35, dbh_36,
         national_forest_name,
         elevation, exposure, slope_percent) %>%
  pivot_longer('dbh_4_11':'dbh_36',
              names_to = "dbh_class",
              values_to = "dbh_count") %>%
  filter(dbh_count != 0) %>% # get rid of zeroes
  uncount(dbh_count) %>%
  mutate(dbh_class = case_when(
    dbh_class == "dbh_4_11" ~ "7.5",
    dbh_class == "dbh_12_23" ~ "17.5",
    dbh_class == "dbh_24_35" ~ "29.5",
    dbh_class == "dbh_36" ~ "36")) # assign midpoint values for each size class

## -----

# change dbh_class & canopy_cover to numeric
vtm_pipo$dbh_class <- as.numeric(vtm_pipo$dbh_class)

# calculate canopy width with above equation using species-specific constants from
# Keyser (2010) table 4.4.2.1
vtm_pipo <- mutate(vtm_pipo, canopy_width = (pipo_a1 * (dbh_class^(pipo_a2))))
vtm_pipo$canopy_width <- as.numeric(vtm_pipo$canopy_width)

## -----

# calculate canopy area
vtm_pipo_canopy <- vtm_pipo %>%
  mutate(canopy_area = (pi) * ((0.5 * canopy_width)^2))

# sum canopy cover across all size classes for each plot
vtm_pipo_sum <- vtm_pipo_canopy %>%
  group_by(plotkey, dbh_class, abbreviation, national_forest_name) %>%
  tally(canopy_area)

```

Figure 11. An example of our canopy cover code, assigning the FVS equation and species-specific constants to *P. ponderosa* trees.

```

####{r}
# combine all species dataframes to sum the species per plots
vtm_total_canopy <- do.call("rbind", list(vtm_pipo_sum,
                                         vtm_pije_sum,
                                         vtm_pico_sum,
                                         vtm_pila_sum,
                                         vtm_psmo_sum,
                                         vtm_abco_sum,
                                         vtm_cade_sum,
                                         vtm_quch_sum,
                                         vtm_quke_sum))

## -----

# Sum the total canopy cover of all trees from all size classes per plot
vtm_total_canopy_plot <- vtm_total_canopy %>%
  group_by(plotkey, national_forest_name) %>%
  tally(n) %>%
  rename("total_canopy_area" = "n" )
# n = the area (ft^2) covered by the canopies of all the trees in that size class/species/plot

## -----

# Conver total_canopy_area from ft^2 to m^2

# create a column that converts feet squared to meters squared
vtm_total_canopy_plot <- vtm_total_canopy_plot %>%
  mutate(total_canopy_area_meters = (total_canopy_area *0.092903))

# Divide the total canopy area per plot (m^2) by the size of the plot
# Note: A vtm plot is 809 m^2. Then multiply by 100 to obtain a percent canopy cover.
vtm_total_canopy_plot <- vtm_total_canopy_plot %>%
  mutate(percent_canopy_cover = ((total_canopy_area_meters/809) * 100))

####{r}
# Apply Crookston and Stage (1999) equation to account for overlapping canopies
# C = 100 [1 - exp ( - .01 C' )]
# C = percent canopy cover that accounts for overlap,
# C' = equation 1-percent canopy cover without accounting for overlap,
# exp = e^

vtm_total_canopy_plot <- vtm_total_canopy_plot %>%
  mutate(percent_canopy_cover_nonoverlap = (100*(1-(e^(-.01*percent_canopy_cover))))))

```

Figure 12. An example of our code combining all of our calculations into one data frame, finding the percent cover per plot, and then applying the Crookston and Stage (1999) equation to account for overlap.

Appendix J: FIA Canopy cover using d.b.h. midpoints and actual d.b.h. measurements

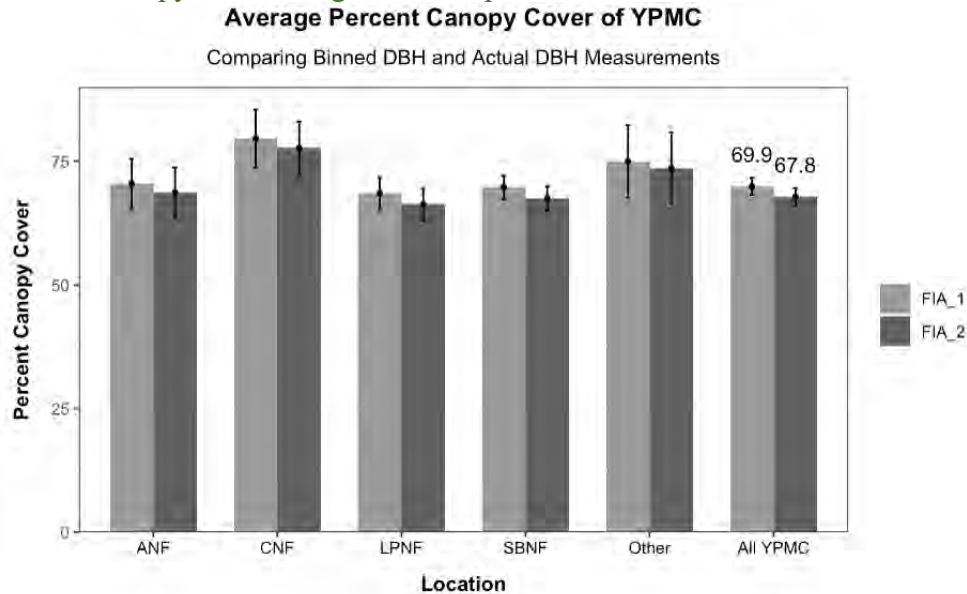


Figure J1. The above graph shows the difference between using binned d.b.h. midpoint values in the FVS equations (FIA_1) and actual d.b.h. measurements in the FVS equations (FIA_2). Mean values between the two were relatively similar.

Table J2. Two-sided t-test between using binned d.b.h. measurements and actual d.b.h. measurements in the FVS equations. There was no statistical difference between the two.

	Actual	Midpoint			
Mean diff	d.b.h. mean	d.b.h. mean	t statistic	p-value	Method
0.183503	67.8215	67.638	0.07545	0.9398961	Welch two sample t-test

Appendix K: Canopy cover metrics of variance

Table K1. Means, quantiles, and other measures of distribution for total canopy cover including and excluding oaks.

Total	25th Quantile	Mean	Median	75th Quantile	Standard Deviation	Standard Error	Variance	No. of plots observed in	Dataset
Including Oaks	38.5	53.4	50.6	71.5	23.0	1.7	531.0	195	VTM
	54.9	70.2	76.1	90.8	24.6	1.7	607.2	210	FIA
Excluding Oaks	29.5	45.2	45.5	60.4	23.2	1.7	540.2	195	VTM
	36.9	57.1	59.2	81.2	27.0	1.9	726.4	210	FIA

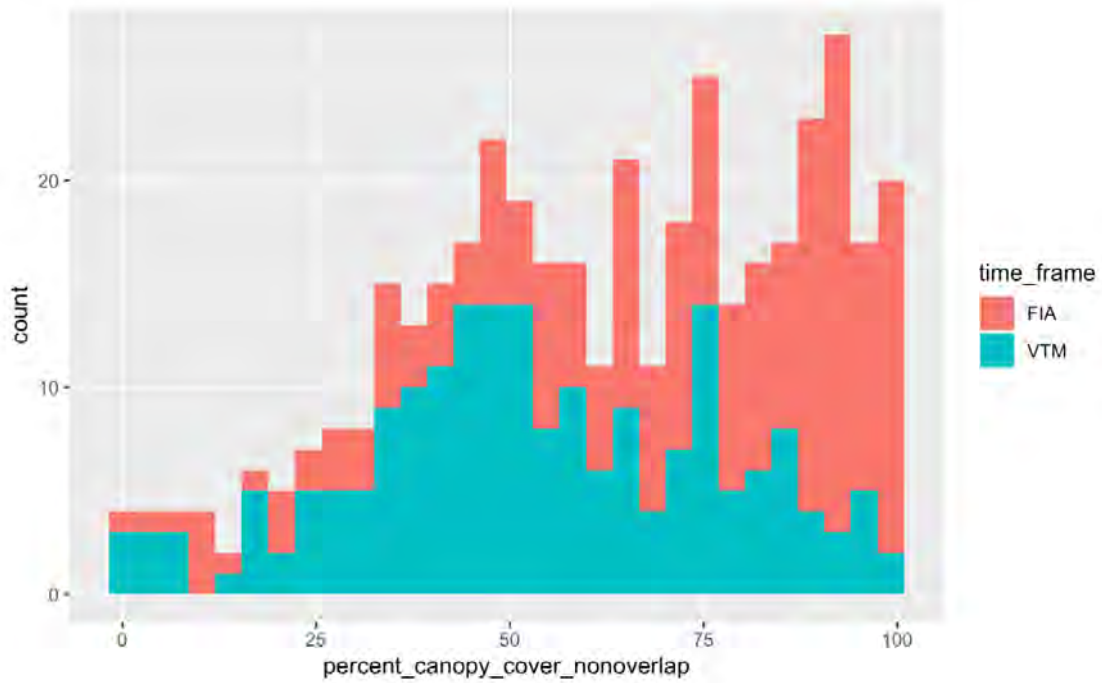
Table K2. Means, quantiles, and other measures of distribution for canopy cover by National Forest, including and excluding oaks.

National Forest	25th Quantile	Mean	Median	75th Quantile	Standard Deviation	Standard Error	Variance	No. of plots observed in	Dataset
<i>Including Oaks</i>									
ANF	36.9	46.3	41.7	61.4	15.3	3.4	235.3	20	VTM
	48.3	70.7	76.2	91.9	24.6	4.8	605.3	26	FIA
CNF	26.2	38.7	38.7	51.3	35.5	25.1	1260.1	2	VTM
	73.9	80.5	82.3	88.9	11.4	5.7	130.8	4	FIA
LPNF	34.7	56.0	59.3	76.3	26.5	3.6	699.7	54	VTM
	51.5	68.7	74.8	89.4	25.5	3.2	648.7	62	FIA
SBNF	41.2	53.6	50.5	70.5	22.6	2.1	509.9	113	VTM
	55.4	70.1	76.3	90.6	24.8	2.4	613.4	107	FIA
Other	42.9	52.8	49.2	55.0	15.9	6.5	253.2	6	VTM
	67.4	74.0	75.7	89.6	24.6	7.4	604.3	11	FIA
<i>Excluding Oaks</i>									
ANF	35.3	43.8	39.2	56.2	15.2	3.4	229.7	20	VTM
	40.8	62.6	69.6	87.2	29.5	5.8	870.0	26	FIA
CNF	21.9	30.2	30.2	38.4	23.4	16.6	548.3	2	VTM
	44.2	46.4	45.5	47.7	4.0	2.0	15.7	4	FIA
LPNF	29.5	52.8	55.0	76.1	26.1	3.5	680.2	54	VTM
	30.1	53.8	56.3	81.8	28.5	3.6	813.5	62	FIA
SBNF	29.2	42.4	44.7	54.4	22.9	2.2	522.8	113	VTM
	41.7	58.3	62.9	80.4	26.0	2.5	678.3	107	FIA
Other	30.4	40.0	39.5	48.7	11.0	4.5	120.0	6	VTM
	37.1	54.8	58.1	73.3	25.2	7.6	634.6	11	FIA

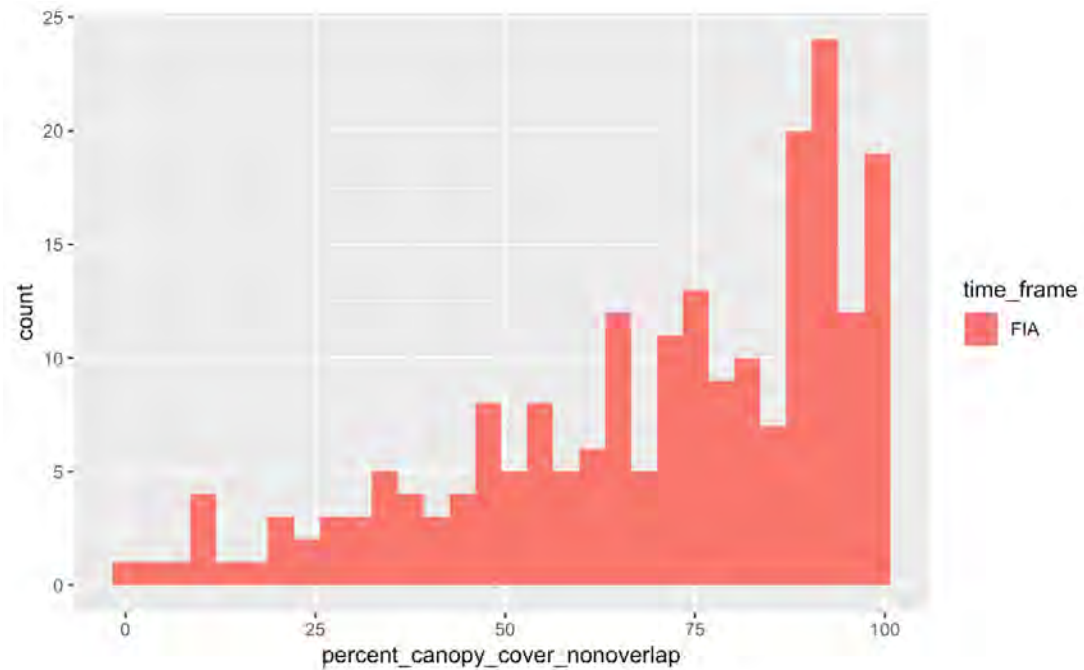
Table K3. Means, quantiles, and other measures of distribution for canopy cover by elevation

Elevation (m)	25th Quantile	Mean	Median	75th Quantile	Standard Deviation	Standard Error	Variance	No. of plots observed in	Dataset
1000 – 1499	47.4	63.0	70.4	90.4	29.0	6.5	842.2	20	VTM
	49.4	67.7	72.2	91.7	27.1	5.3	733.8	26	FIA
1500 – 1999	44.3	58.4	56.9	76.4	22.3	2.4	498.5	84	VTM
	62.6	74.1	82.1	92.9	24.0	2.7	577.1	80	FIA
2000 – 2499	37.6	48.7	47.7	59.8	19.0	2.2	362.5	77	VTM
	53.7	69.9	76.1	89.9	23.7	2.7	563.9	78	FIA
>2500	20.4	35.8	35.3	47.1	24.3	6.8	592.6	13	VTM
	55.0	61.4	70.3	77.1	25.4	5.0	647.1	26	FIA

Appendix L: Canopy cover histograms



Appendix L1. Histogram of the canopy cover for VTM and FIA plots. VTM data has a normal distribution and FIA is left skewed.



Appendix L2. Histogram of the canopy cover for FIA plots. As you can see, it is left skewed, which is why many of our medians were higher than our means for FIA canopy cover estimates.

Appendix M: VTM logging map in southern California

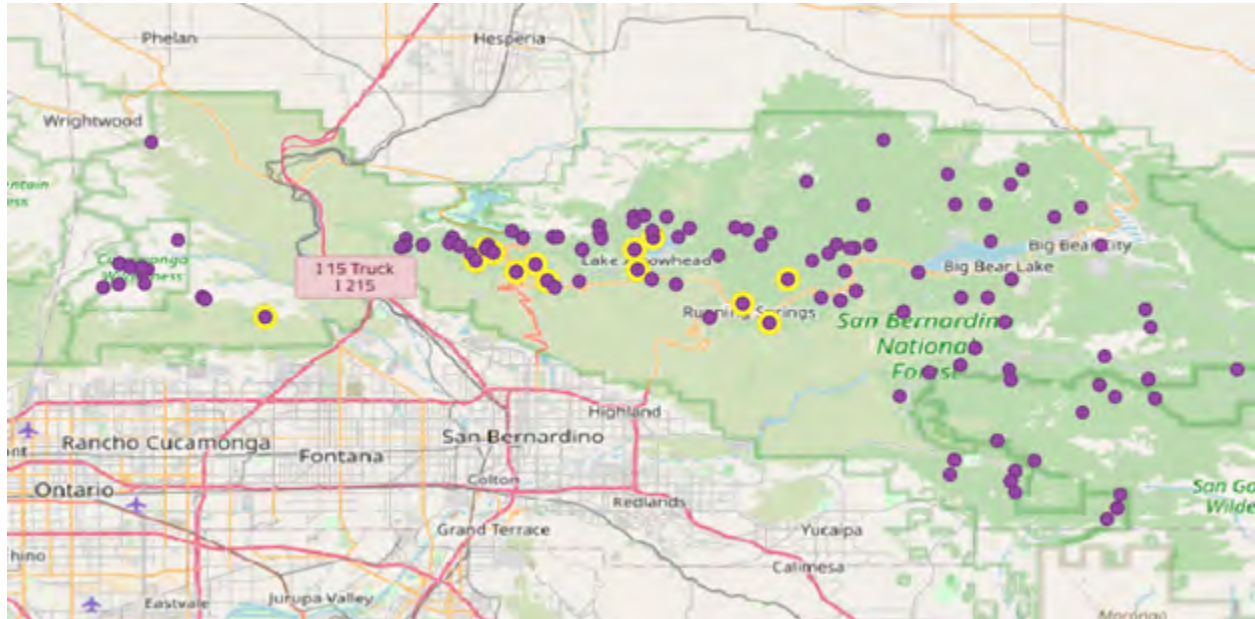


Figure M1. VTM Plots: 13 VTM plots (out of 195) had notes about being "cut/logged" or "second growth" and they were all from SBNF. Logged plots (in yellow) as compared to all plots used in our analysis (purple).

Appendix N: TWI Calculations

Process: see <https://www.youtube.com/watch?v=kVJPYnwq04k>. Default parameters were used unless otherwise noted.

- 1) Fill (Hydrology tool): Make sure DEM is in the projected coordinate system. WGS 1984 UTM 11N was used. This is to fill in any missing data in the DEM.
- 2) Flow direction (Hydrology tool): Use filled DEM.
- 3) Flow accumulation (Hydrology tool): use flow direction layer.
- 4) Slope (Surface tool): use filled DEM. Units must be in degrees.
- 5) Raster calculator:
 - a. $\text{Raster_calc_slope} = (\text{"Slope"} * 1.570796) / 90$
 - b. $\text{Tanslope} = \text{Con}(\text{"Raster_calc_slope"} > 0, \text{Tan}(\text{"Raster_calc_slope"}), 0.001)$
 - c. $\text{Raster_calc_flow_acc} = (\text{"Flow accumulation"} + 1) * \text{cell size of dem}$
 - d. $\text{Twi} = \text{Ln}(\text{"Raster_calc_flow_acc"} / \text{"Tanslope"})$

Appendix O: Environmental data processing

Creating the extent:

We used ArcGIS ModelBuilder to create an extent mask raster of our study area. This mask was used in the final preparation of all environmental data layers to ensure that all layers were clipped to the same extent. This raster was already in our desired projection, NAD 1983 California Teale Albers, but was resampled to 270 m resolution. ArcGIS tools utilized:

- Extract by mask: use one of the BCM layers and mask to the extent of our study area, the Transverse Ranges
- Resample: Resampled extent raster to 270 x 270 meters

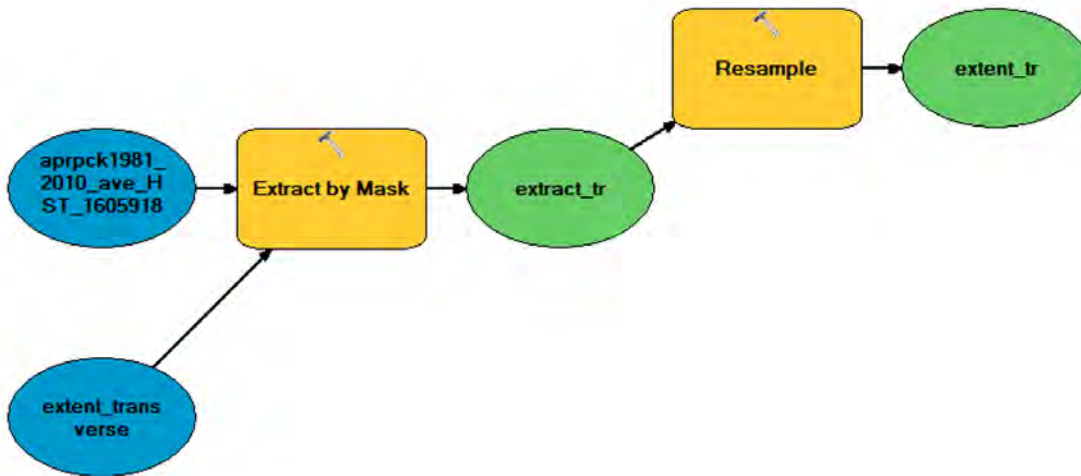


Figure O1. ArcGIS Model to create an extent mask raster of the study area, the Transverse Ranges

Setting model parameters:

ModelBuilder properties were set to the parameters displayed below. This window can be accessed in ModelBuilder under 'Environments'. Select the boxes for 'Processing Extent', 'Raster Analysis', and 'Output Coordinates', and then select 'Value' to set parameters.

- Processing extent:
 - “Extent” = “same as variable extent”
 - “Snap raster” = “extent”
- Raster analysis:
 - “Cell size” = “same as variable extent”

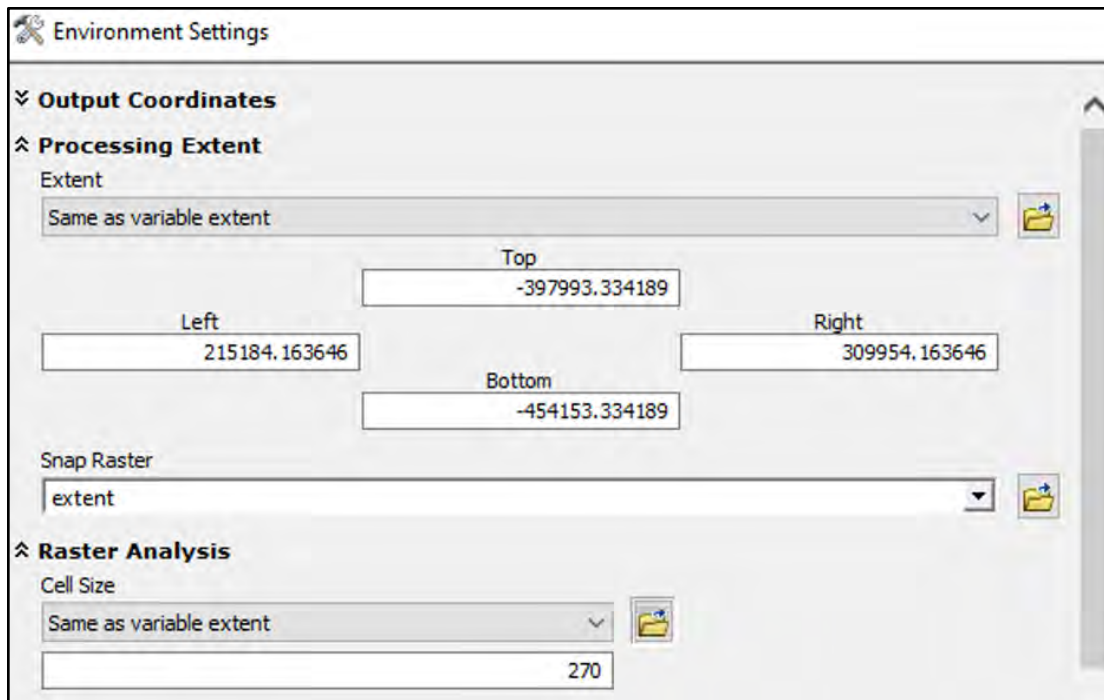


Figure O2. ModelBuilder parameter settings.

ModelBuilder was used to iterate through all raw environmental rasters and transform soil data from polygon to raster data, projected into NAD 1983 California Teale albers. All rasters were clipped to the desired extent and converted to ASCII file format for input into MaxEnt.

Appendix P: MaxEnt model parameter settings

Maximum Entropy Species Distribution Modeling, Version 3.3.3k

Samples

File:

Adult

Sapling

Environmental layers

Directory/File:

<input checked="" type="checkbox"/> apr	Continuous	▼
<input checked="" type="checkbox"/> cwd	Continuous	▼
<input checked="" type="checkbox"/> ppt	Continuous	▼
<input checked="" type="checkbox"/> tmx	Continuous	▼
<input checked="" type="checkbox"/> tpi2	Continuous	▼

Linear features

Quadratic features

Product features

Threshold features

Hinge features

Auto features

Create response curves

Make pictures of predictions

Do jackknife to measure variable importance

Output format: ▼

Output file type: ▼

Output directory:

Projection layers directory/file:

Figure P1. MaxEnt parameter settings.

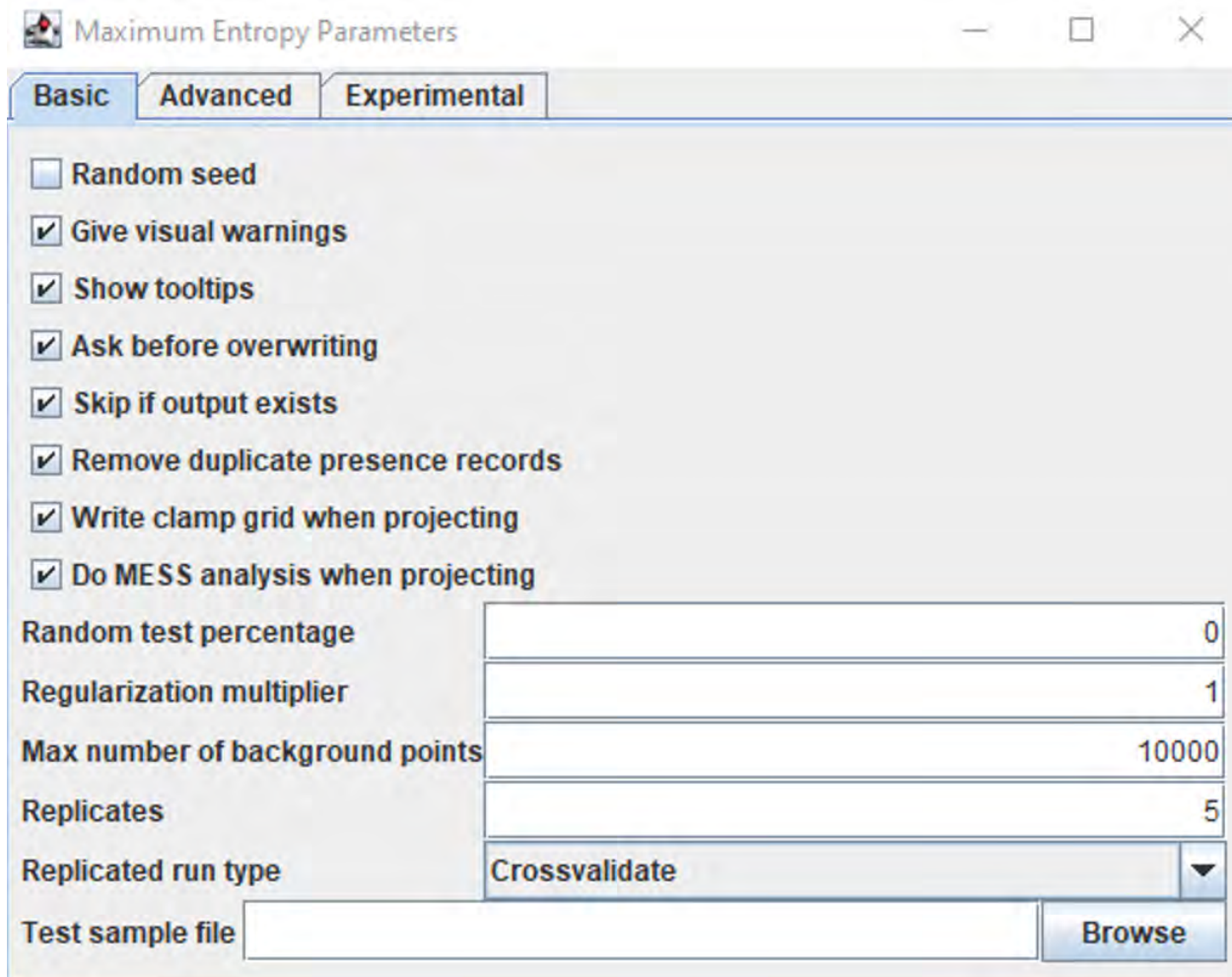


Figure P2. Basic MaxEnt parameter settings.

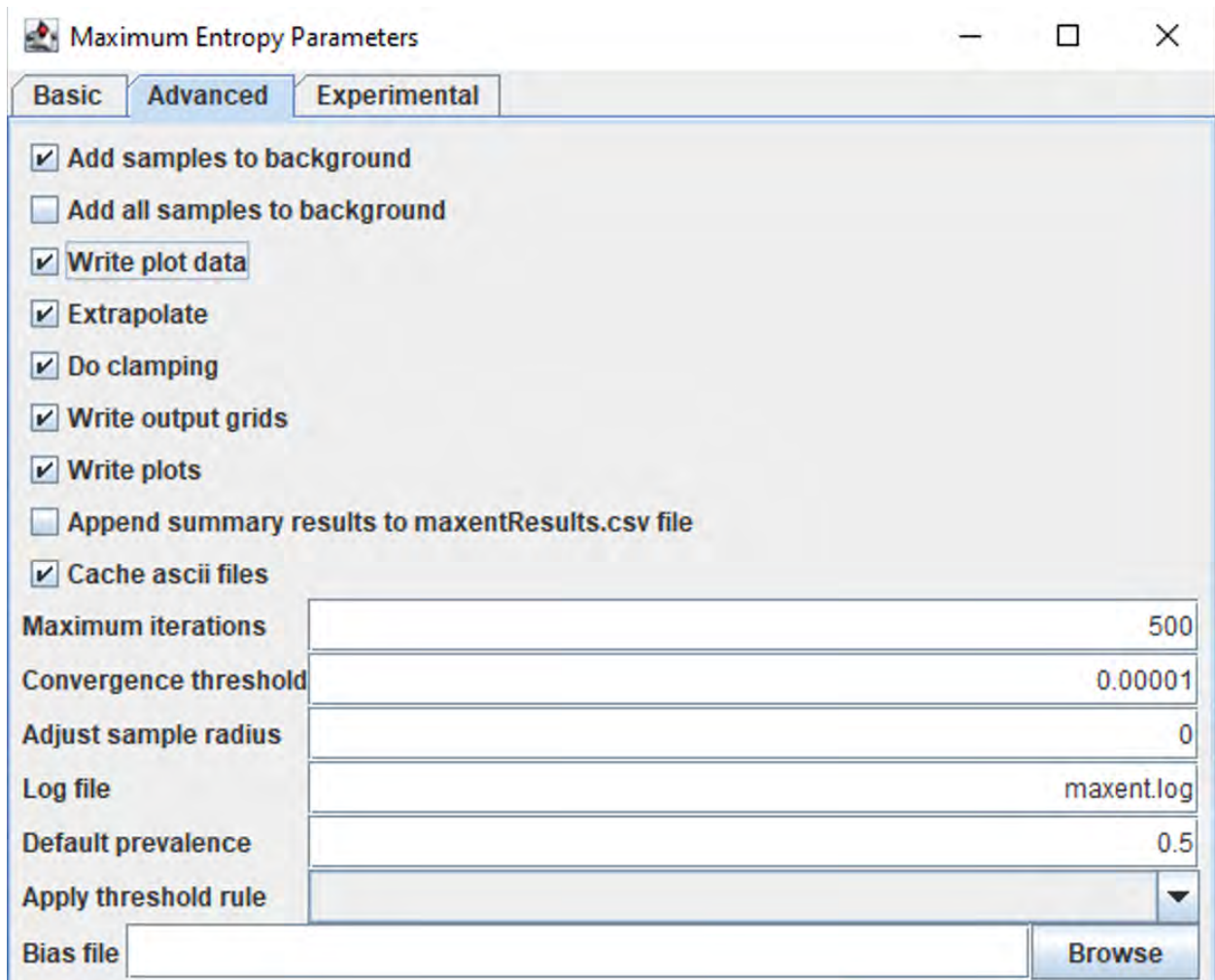


Figure P3. Advanced MaxEnt parameter settings.

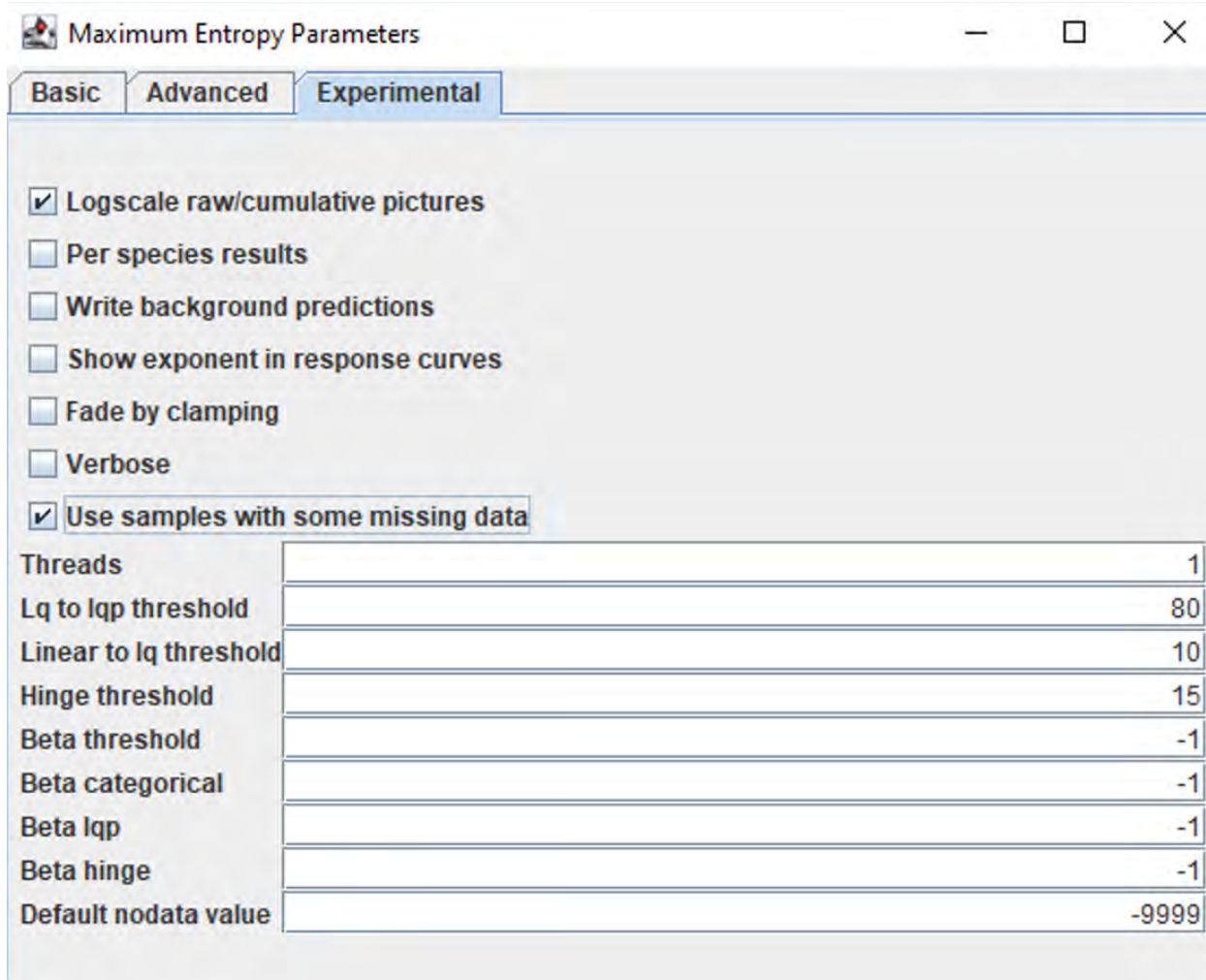


Figure P4. Experimental MaxEnt parameter settings.

Appendix Q: Environmental histograms for SDM

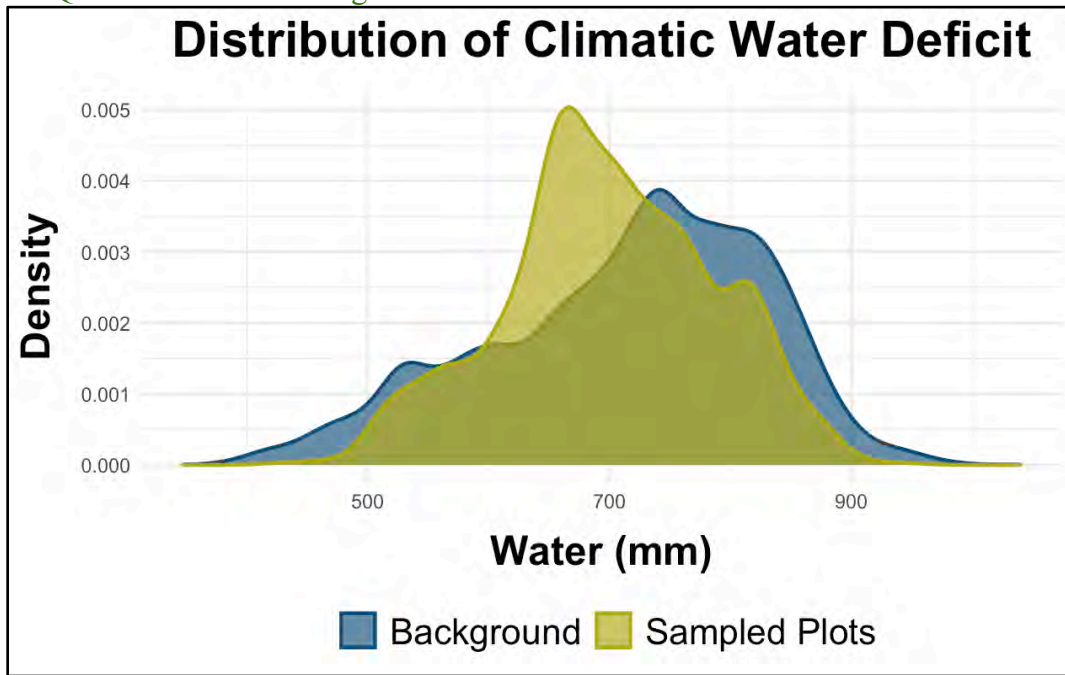


Figure Q1. Distribution of climatic water deficit (CWD). The distribution of CWD (mm) at sampled plots is displayed in yellow and is compared to the distribution of CWD across a random background sample taken from YPMC forest in the sample area, as displayed in blue.

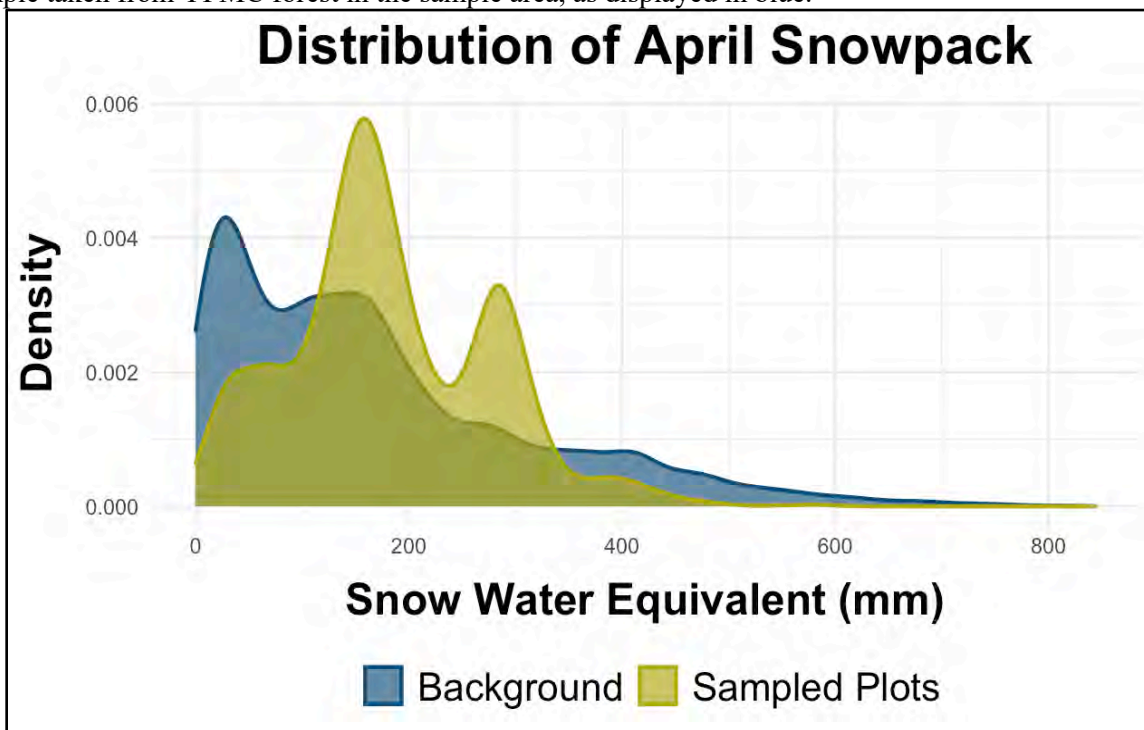


Figure Q2. Distribution of April snowpack. The distribution of April snowpack (mm) at sampled plots is displayed in yellow and is compared to the distribution of April snowpack across a random background sample taken from YPMC forest in the sample area, as displayed in blue.

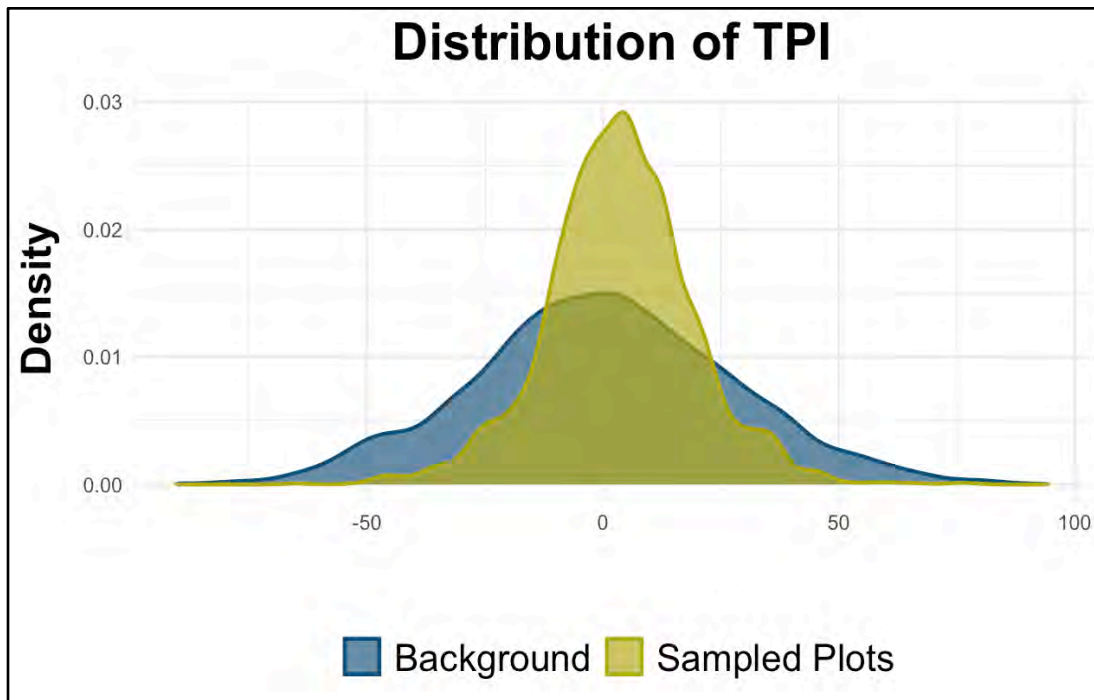


Figure Q3. Distribution of topographic position index (TPI). The distribution of TPI at sampled plots is displayed in yellow and is compared to the distribution of TPI across a random background sample taken from YPMC forest in the sample area, as displayed in blue.

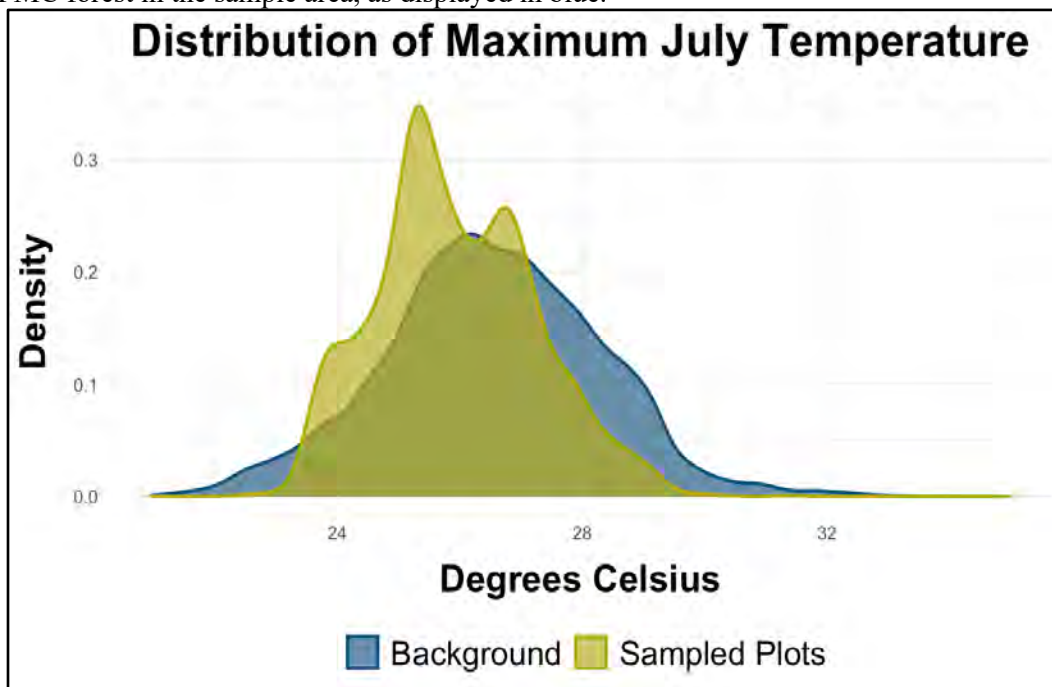


Figure Q4. Distribution of maximum July temperature. The distribution of maximum July temperature (degrees Celsius) at sampled plots is displayed in yellow and is compared to the distribution of maximum July temperature across a random background sample taken from YPMC forest in the sample area, as displayed in blue.

Appendix R: SDM results - Current suitable habitat of yellow pine saplings and adults

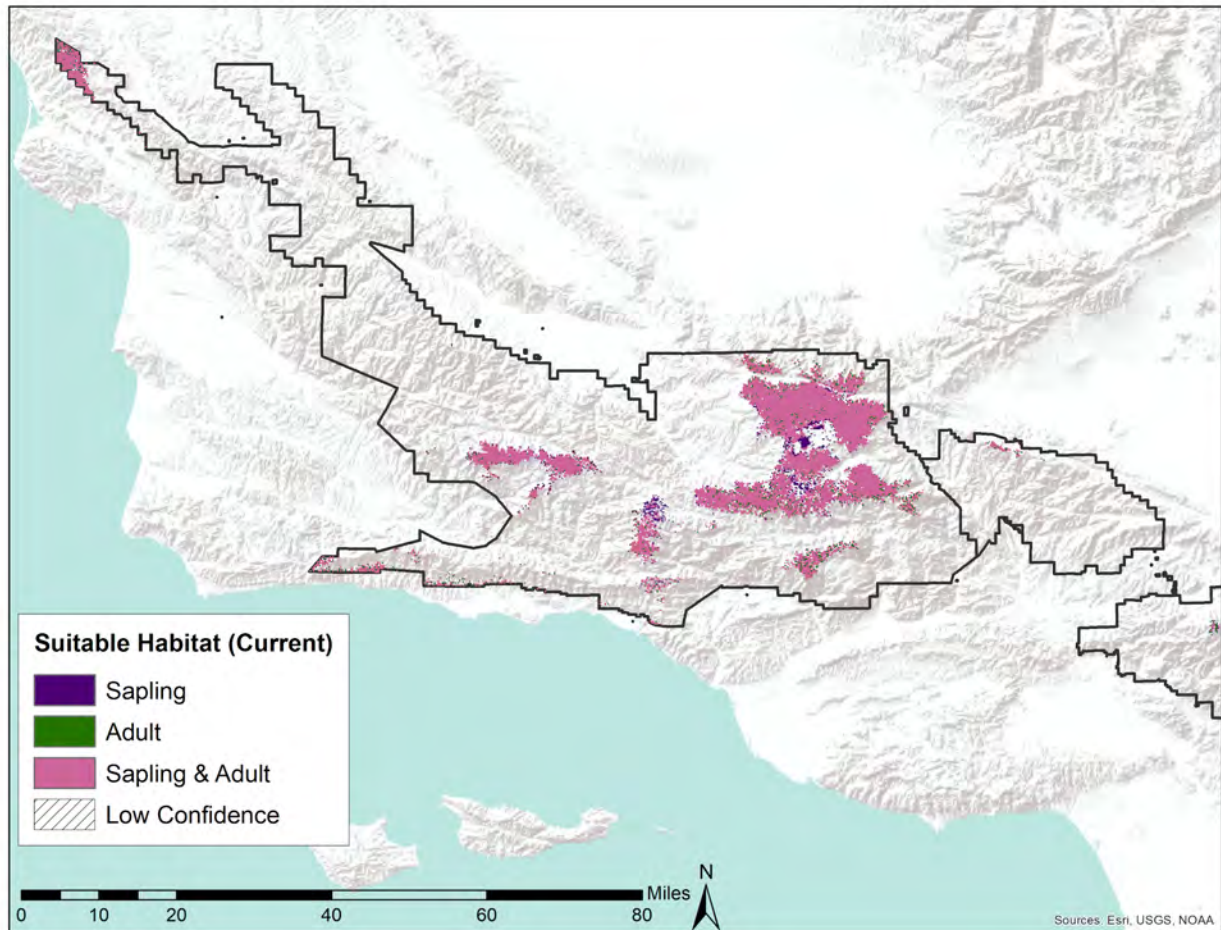


Figure R1. Current (1981-2010) projected yellow pine sapling and adult suitable habitat across the western Transverse Ranges. Pink regions depict habitat projected to be suitable for both saplings and adults, while purple regions depict habitat projected to be suitable for only saplings and green regions depict habitat projected to be suitable for only adults. We have high confidence in our models' abilities to project habitat suitability across the entire western Transverse Ranges.

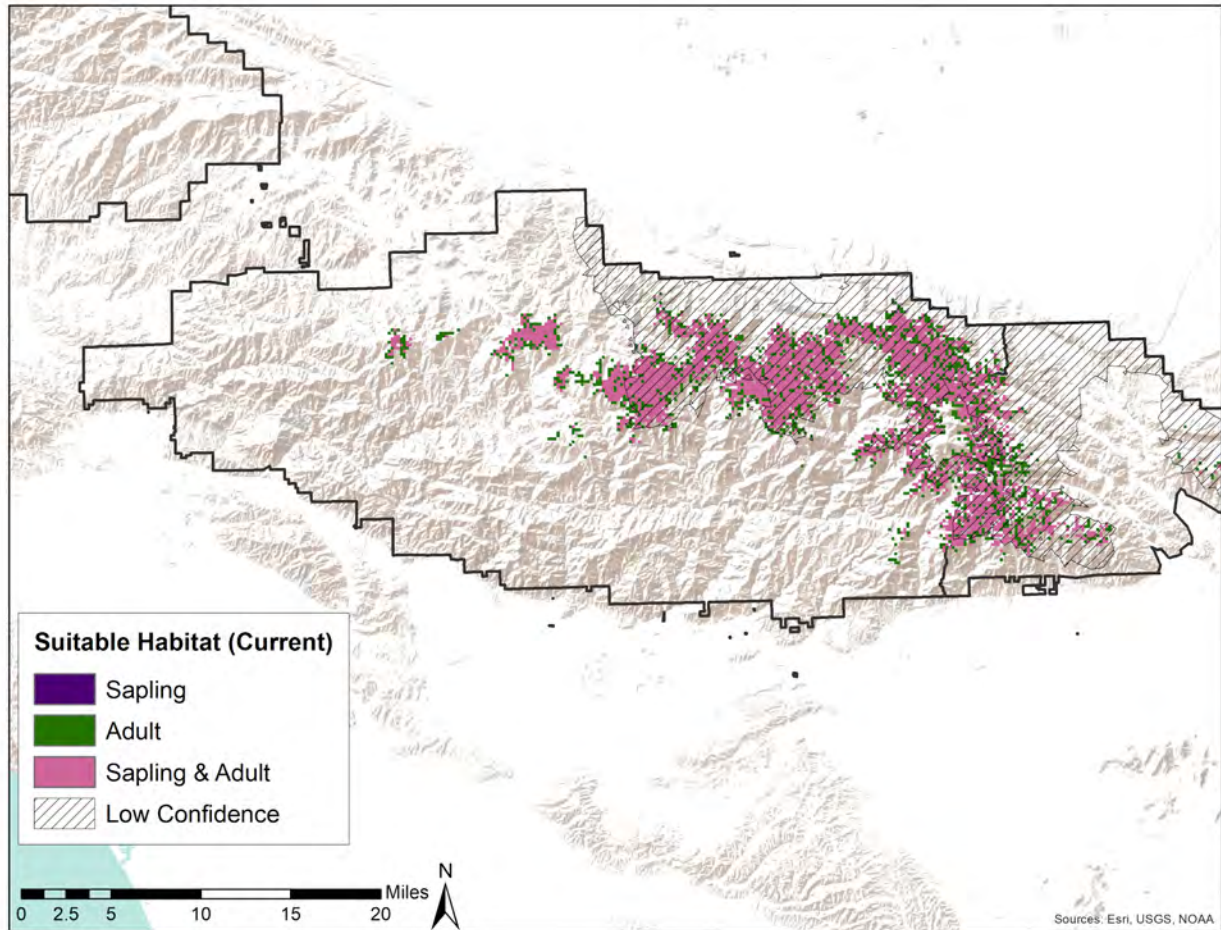


Figure R2. Current (1981-2010) projected yellow pine sapling and adult suitable habitat across the central Transverse Ranges. Pink regions depict habitat projected to be suitable for both saplings and adults, while purple regions depict habitat projected to be suitable for only saplings and green regions depict habitat projected to be suitable for only adults. Low confidence areas are represented by hash marks.

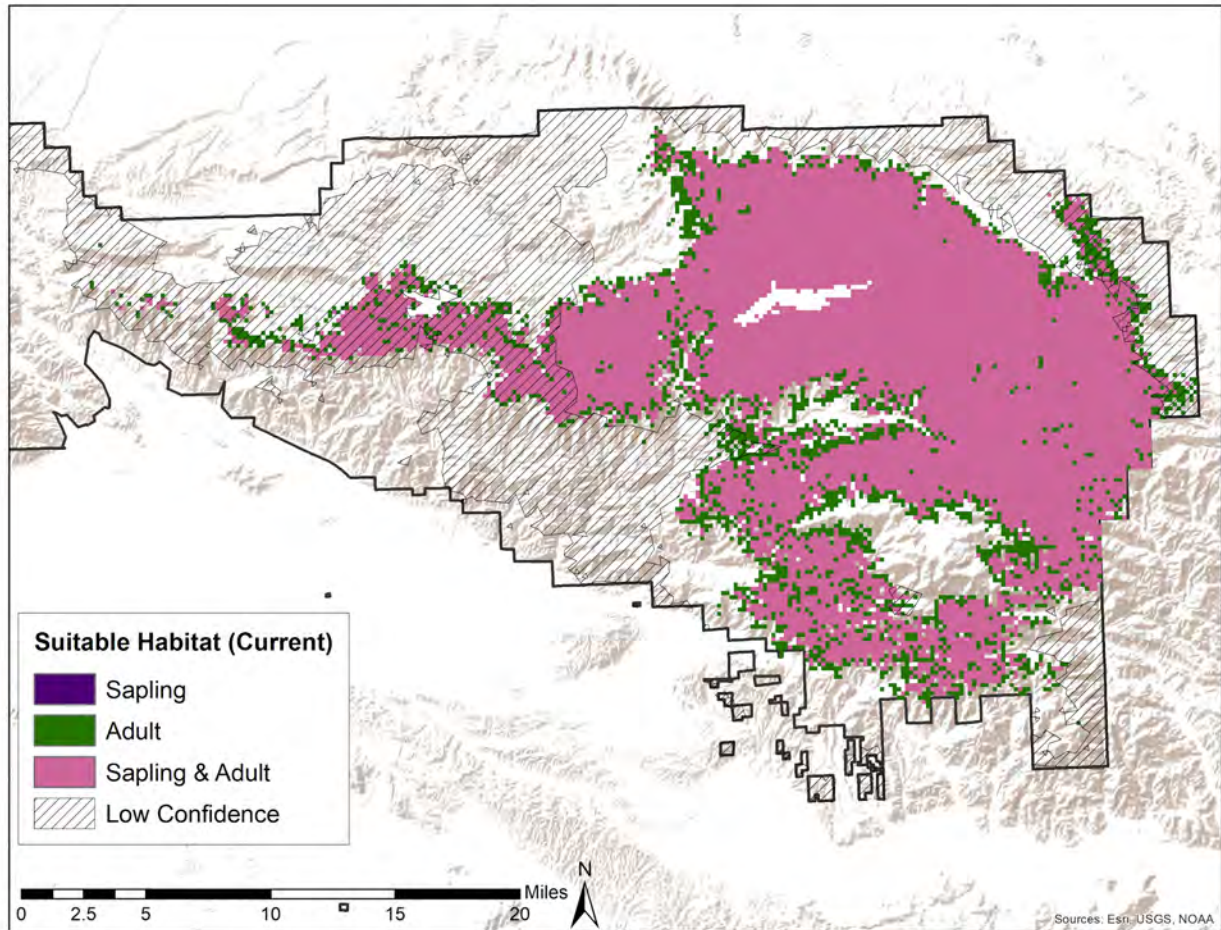


Figure R3. Current (1981-2010) projected yellow pine sapling and adult suitable habitat across the eastern Transverse Ranges. Pink regions depict habitat projected to be suitable for both saplings and adults, while purple regions depict habitat projected to be suitable for only saplings and green regions depict habitat projected to be suitable for only adults. Low confidence areas are represented by hash marks.

Table R1. Current (1981-2010) projected yellow pine sapling and adult suitable habitat by region.

Lifeform Current	Acres Suitable Habitat <i>High Confidence</i>	Acres Suitable Habitat <i>Low Confidence</i>
Western Transverse Ranges		
Sapling	190,768.07	0
Adult	195,127.45	0
Central Transverse Ranges		
Sapling	10,898.46	40,729.61
Adult	19,058.79	56,383.76
Eastern Transverse Ranges		
Sapling	161,657.47	15,492.02
Adult	191,488.63	24,661.14

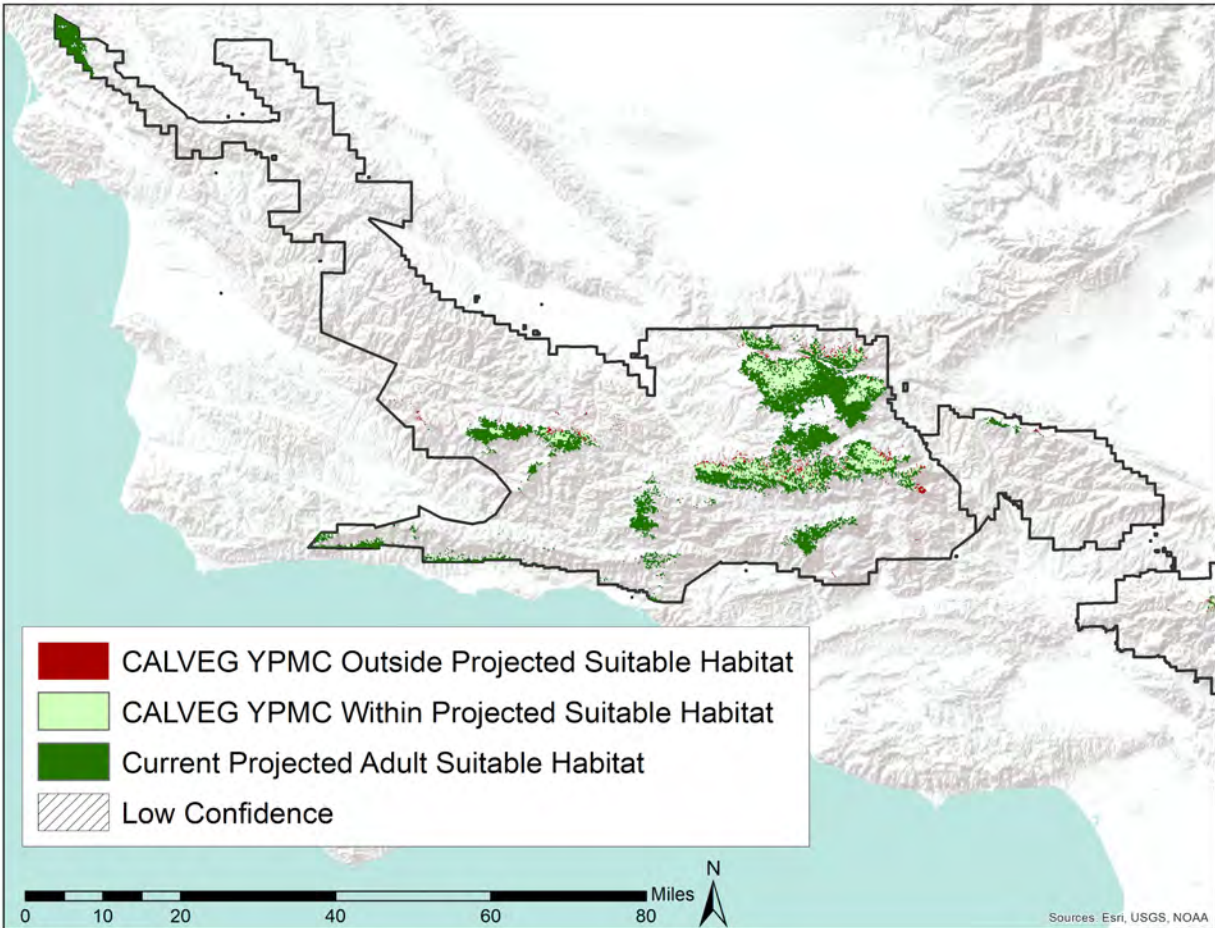


Figure R4. Current CALVEG classified Ponderosa pine, Jeffrey pine, and mixed conifer forests as compared to current projected adult suitable habitat in the western Transverse Ranges. Light green regions represent regions where current YPMC forests overlap with projected suitable habitat for adult yellow pines, while red regions represent regions where current YPMC forests do not fall within regions of projected suitable habitat. Dark green regions depict projected suitable habitat not currently dominated by YPMC forest. We have high confidence in our models' abilities to project habitat suitability across the entire western Transverse Ranges.

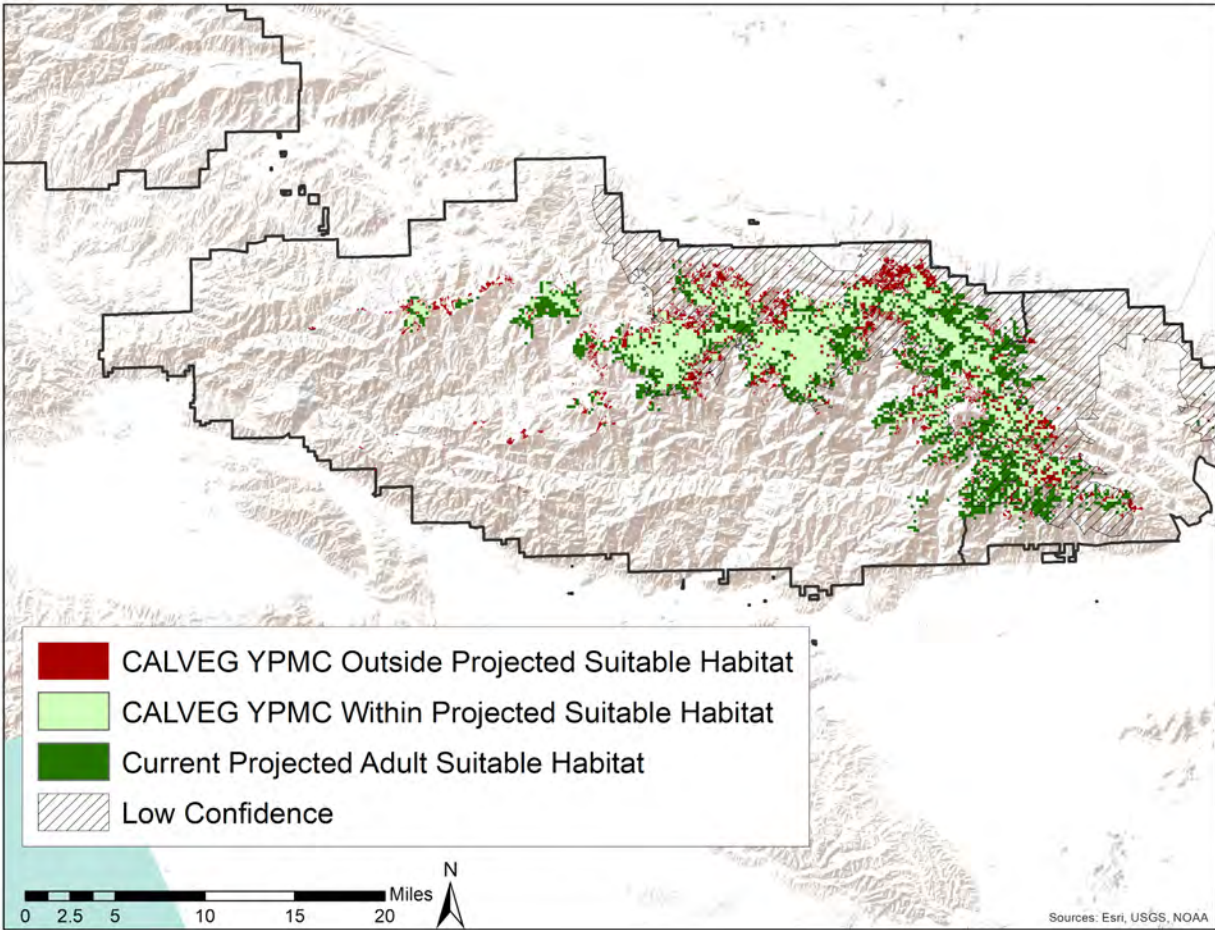


Figure R5. Current CALVEG classified Ponderosa pine, Jeffrey pine, and mixed conifer forests as compared to current projected adult suitable habitat in the central Transverse Ranges. Light green regions represent regions where current YPMC forests overlap with projected suitable habitat for adult yellow pines, while red regions represent regions where current YPMC forests do not fall within regions of projected suitable habitat. Dark green regions depict projected suitable habitat not currently dominated by YPMC forest. Low confidence areas are represented by hash marks.

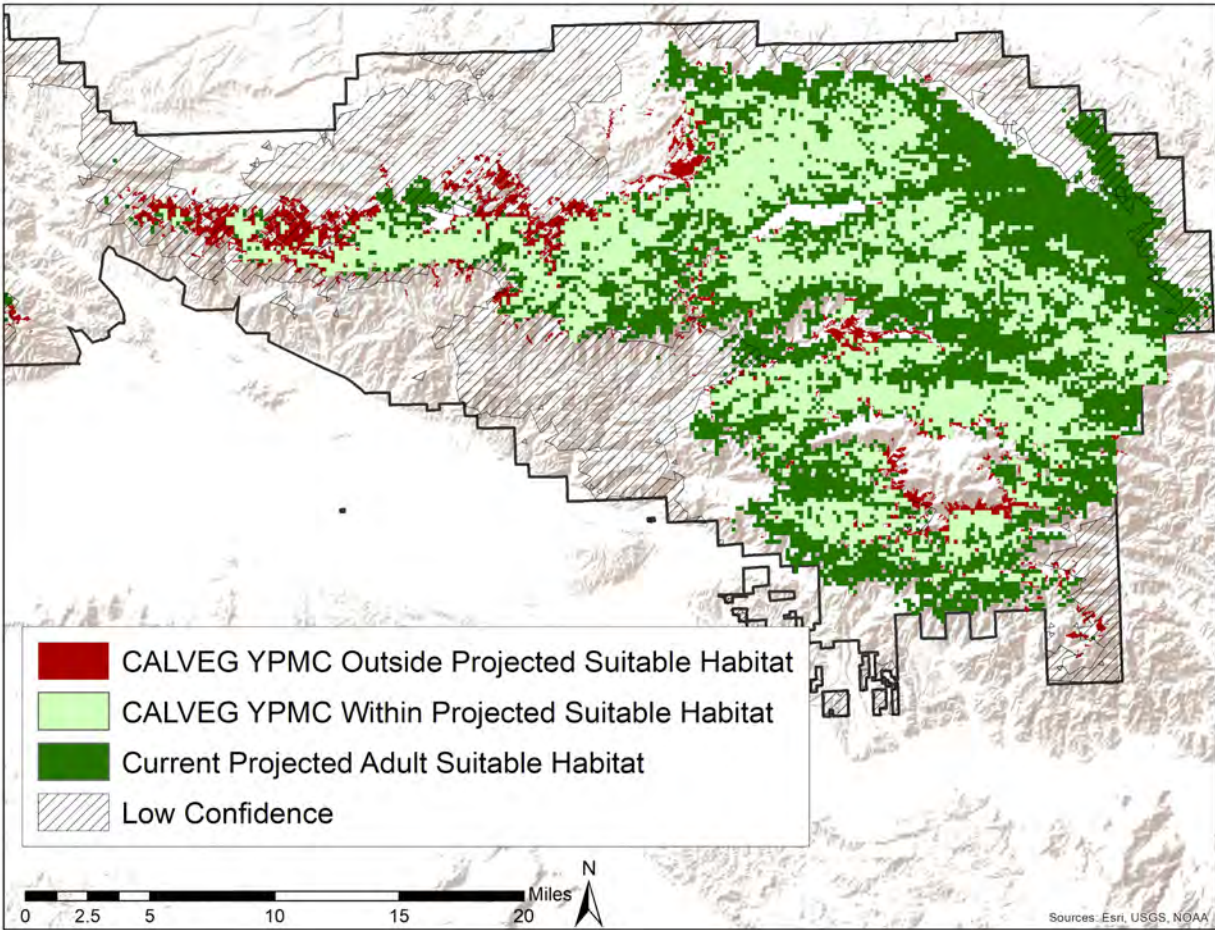


Figure R6. Current CALVEG classified Ponderosa pine, Jeffrey pine, and mixed conifer forests as compared to current projected adult suitable habitat in the eastern Transverse Ranges. Light green regions represent regions where current YPMC forests overlap with projected suitable habitat for adult yellow pines, while red regions represent regions where current YPMC forests do not fall within regions of projected suitable habitat. Dark green regions depict projected suitable habitat not currently dominated by YPMC forest. Low confidence areas are represented by hash marks.

Appendix S: SDM results - Past suitable habitat of yellow pine saplings

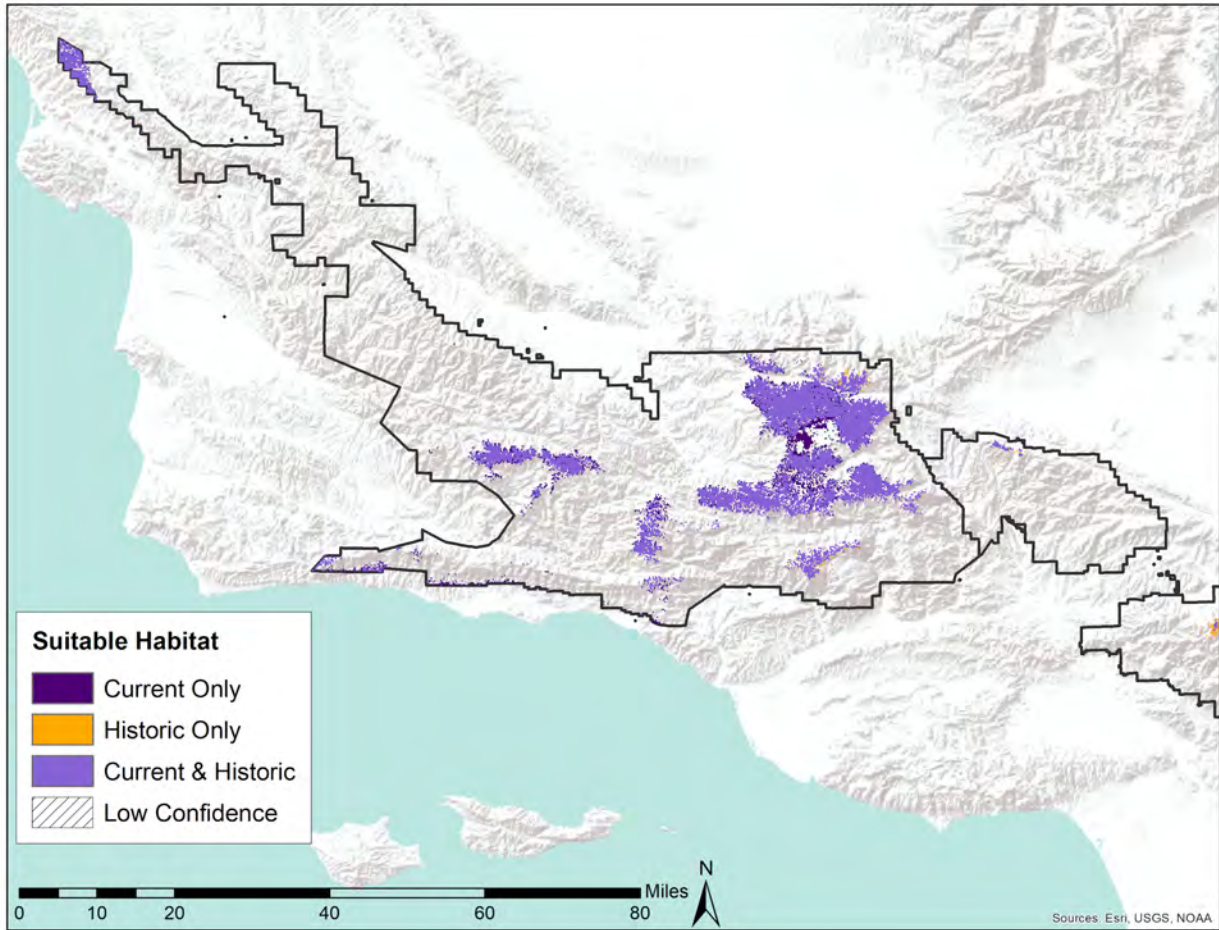


Figure S1. Historic (1921-1950) postdicted and current (1981-2010) projected yellow pine sapling suitable habitat in the western Transverse Ranges. Light purple regions depict habitat that is predicted to be suitable under both time periods. Orange regions depict habitat only predicted to be suitable under historic conditions, while dark purple regions depict habitat only predicted to be suitable under current conditions. We have high confidence in our models' abilities to project habitat suitability across the entire western Transverse Ranges.

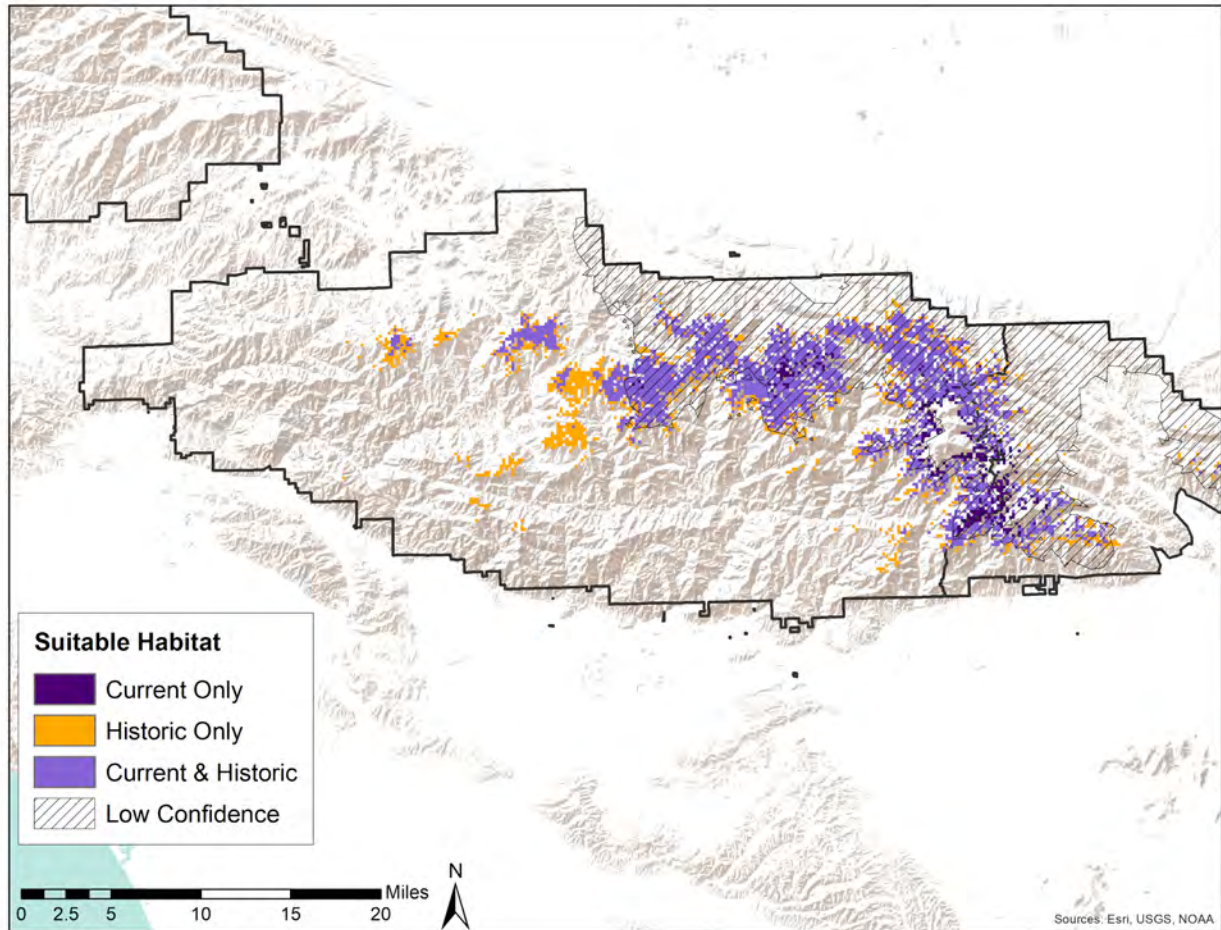


Figure S2. Historic (1921-1950) postdicted and current (1981-2010) projected yellow pine sapling suitable habitat in the central Transverse Ranges. Light purple regions depict habitat that is predicted to be suitable under both time periods. Orange regions depict habitat only predicted to be suitable under historic conditions, while dark purple regions depict habitat only predicted to be suitable under current conditions. Low confidence areas are represented by hash marks.

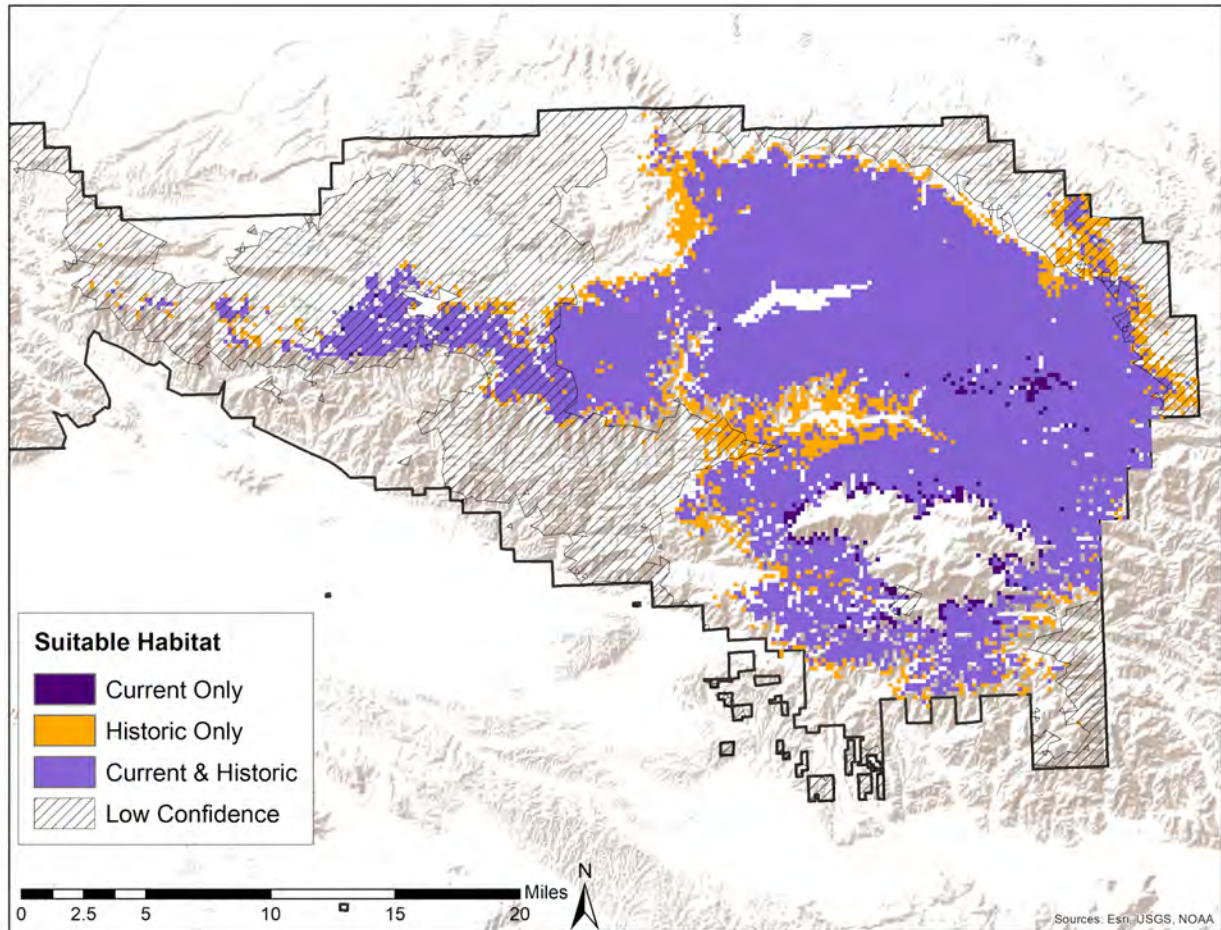


Figure S3. Historic (1921-1950) postdicted and current (1981-2010) projected yellow pine sapling suitable habitat in the eastern Transverse Ranges. Light purple regions depict habitat that is predicted suitable under both time periods. Orange regions depict habitat only predicted suitable under historic conditions, while dark purple regions depict habitat only predicted to be suitable under current conditions. Low confidence areas are represented by hash marks.

Table S1. Historic (1921-1950) postdicted and current (1981-2010) projected yellow pine sapling suitable habitat by region.

Time Period	Acres Suitable Habitat <i>High Confidence</i>	Acres Suitable Habitat <i>Low Confidence</i>
Western Transverse Ranges		
Historic (VTM)	163,548.94	0
Current (FIA)	190,768.07	0
Central Transverse Ranges		
Historic (VTM)	22,409.39	43,593.84
Current (FIA)	10,898.46	40,729.61
Eastern Transverse Ranges		
Historic (VTM)	176,122.7	23,652.36
Current (FIA)	161,657.47	15,492.02

Appendix T: SDM results - Future suitable habitat of yellow pine saplings

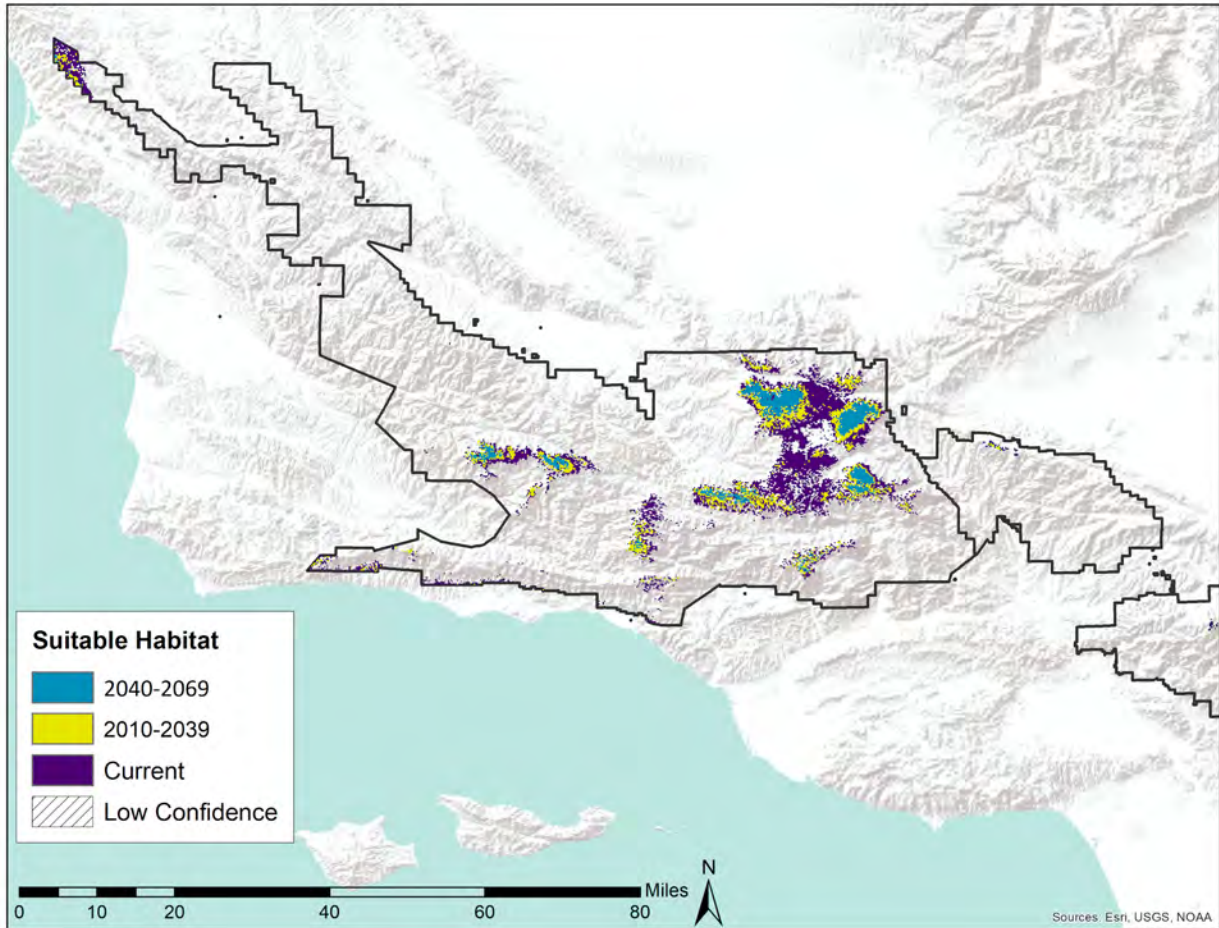


Figure T1. Current and future projected yellow pine sapling suitable habitat across the western Transverse Ranges. Dark purple regions depict projected suitable habitat under current climate, yellow regions represent projected suitable habitat under the summed 2010-2039 scenario and blue regions represent projected suitable habitat under the summed 2040-2069 scenario. We have high confidence in our models' abilities to project habitat suitability across the entire western Transverse Ranges.

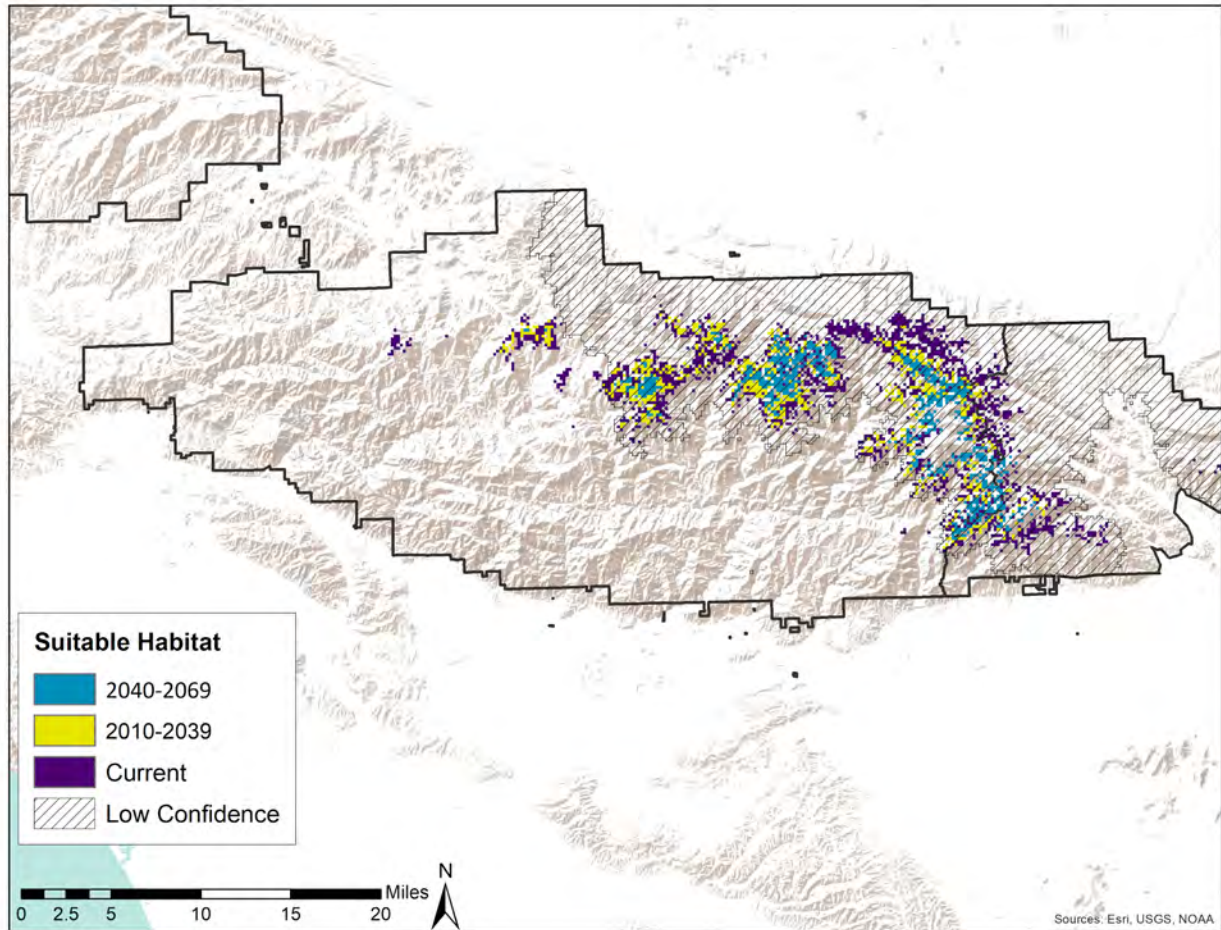


Figure T2. Current and future projected yellow pine sapling suitable habitat across the central Transverse Ranges. Dark purple regions depict projected suitable habitat under current climate, yellow regions represent projected suitable habitat under the summed 2010-2039 scenario and blue regions represent projected suitable habitat under the summed 2040-2069 scenario. Low confidence areas are represented by hash marks.

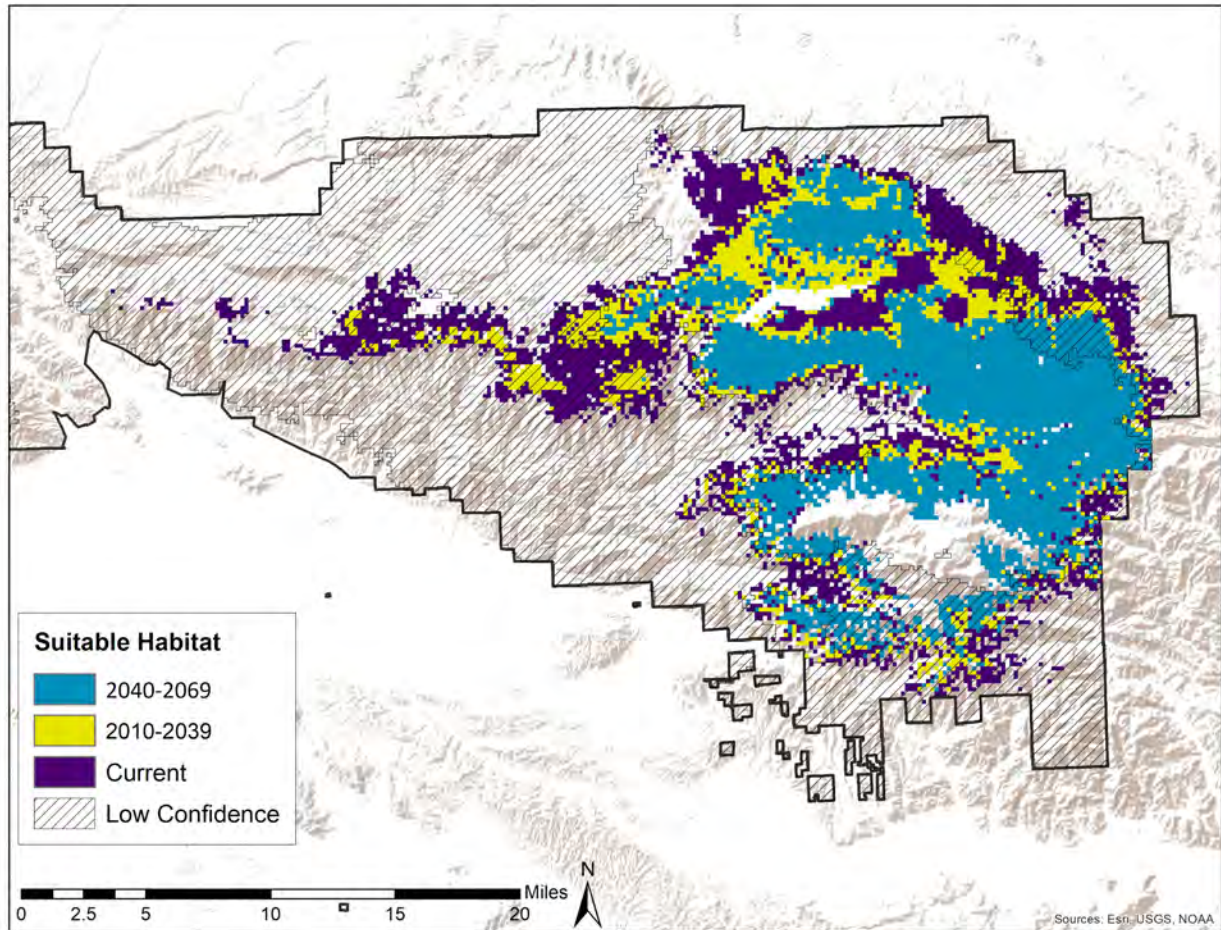


Figure T3. Current and future projected yellow pine sapling suitable habitat across the eastern Transverse Ranges. Dark purple regions depict projected suitable habitat under current climate, yellow regions represent projected suitable habitat under the summed 2010-2039 scenario and blue regions represent projected suitable habitat under the summed 2040-2069 scenario. Low confidence areas are represented by hash marks.

Table T1. Projected yellow pine sapling suitable habitat under current, 2010-2039, and 2040-2069 climates by region.

Time Period	Acres Suitable Habitat <i>High Confidence</i>	Percent Change in Suitable Habitat <i>High Confidence</i>	Acres Suitable Habitat <i>Low Confidence</i>	Percent Change in Suitable Habitat <i>Low Confidence</i>
Western Transverse Ranges				
Current	190,768.07	N/A	0	N/A
2010-2039 <i>Summed Scenario</i>	73,064.71	-61.70%	0	0
2040-2069 <i>Summed Scenario</i>	31,038.09	-83.73%	0	0
Central Transverse Ranges				
Current	3,278.54	N/A	48349.53	N/A
2010-2039 <i>All Scenarios</i>	774.60	-76.37%	20103.6	-58.42%
2040-2069 <i>All Scenarios</i>	54.04	-98.35%	12699.86	-73.73%
Eastern Transverse Ranges				
Current	110,281.60	N/A	66867.9	N/A
2010-2039 <i>Summed Scenario</i>	77,027.79	-30.15%	20427.86	-69.45%
2040-2069 <i>Summed Scenario</i>	68,993.55	-37.44%	10970.52	-83.59%

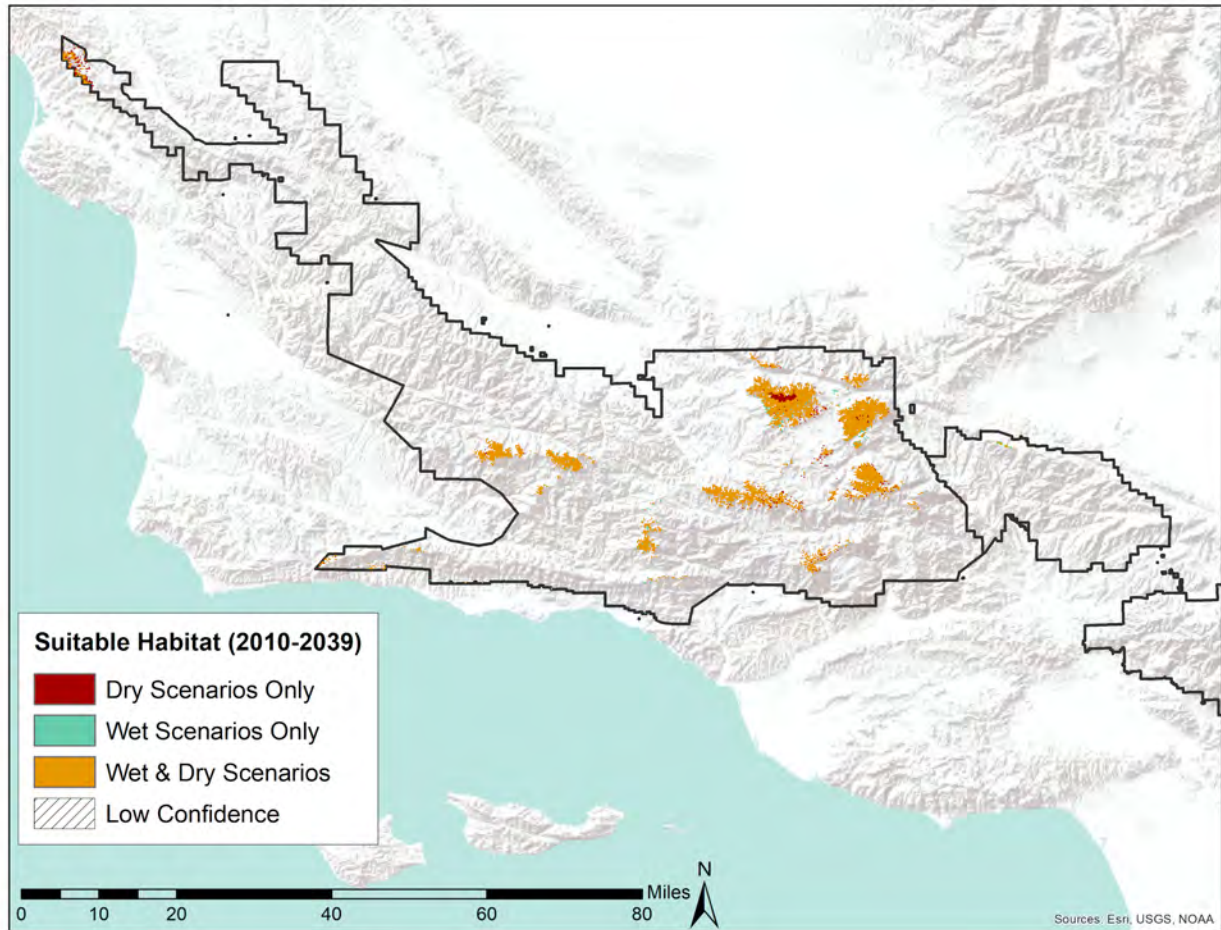


Figure T4. 2010-2039 projected yellow pine sapling suitable habitat across the western Transverse Ranges. Orange regions depict habitat projected to be suitable under both the 2010-2039 summed dry scenario and the 2010-2039 summed wet scenario. Aqua regions represent habitat projected to be suitable only under the summed wet scenario, and red regions represent habitat projected to be suitable only under the summed dry scenario. We have high confidence in our models' abilities to project habitat suitability across the entire western Transverse Ranges.

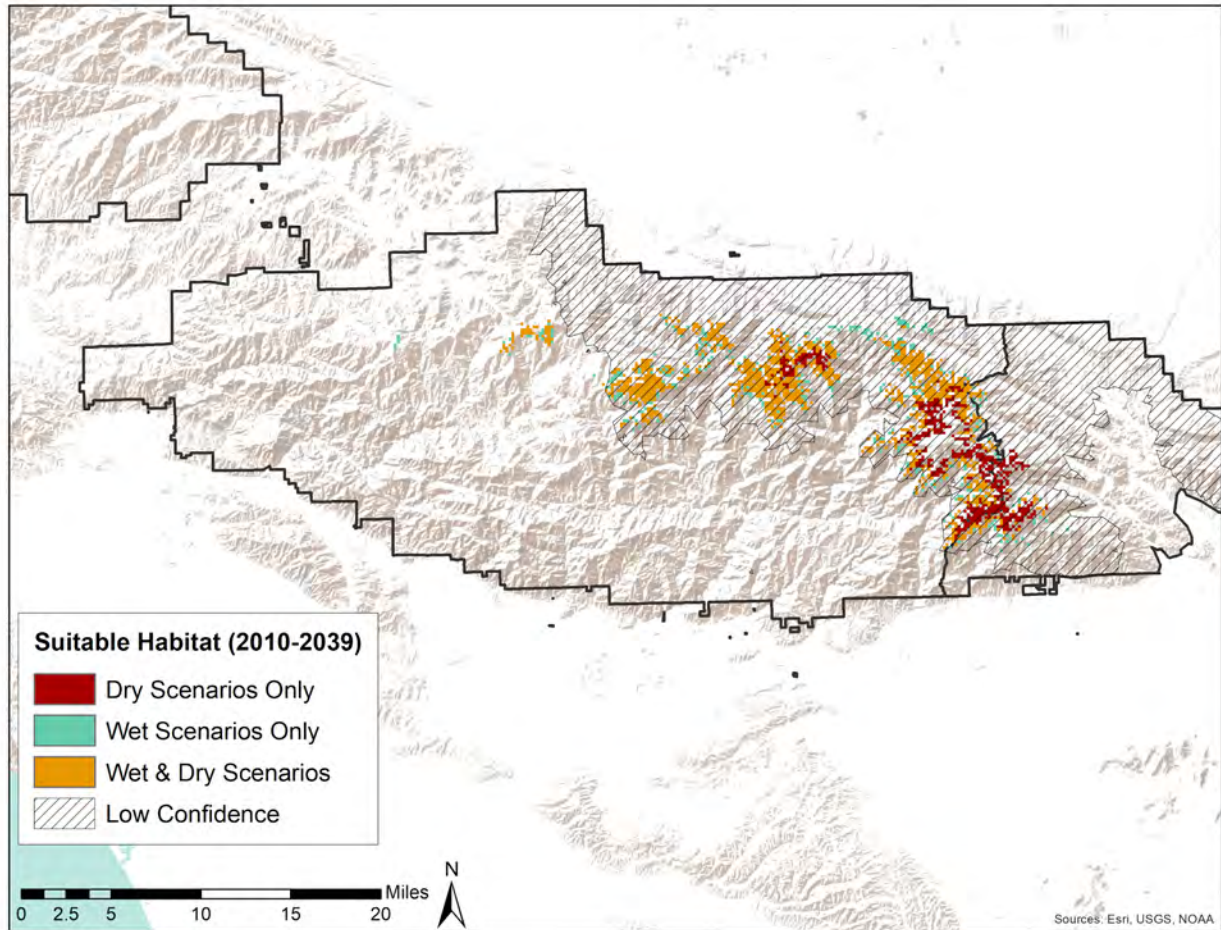


Figure T5. 2010-2039 projected yellow pine sapling suitable habitat across the central Transverse Ranges. Orange regions depict habitat projected to be suitable under both the 2010-2039 summed dry scenario and the 2010-2039 summed wet scenario. Aqua regions represent habitat projected to be suitable only under the summed wet scenario, and red regions represent habitat projected to be suitable only under the summed dry scenario. Low confidence areas are represented by hash marks.

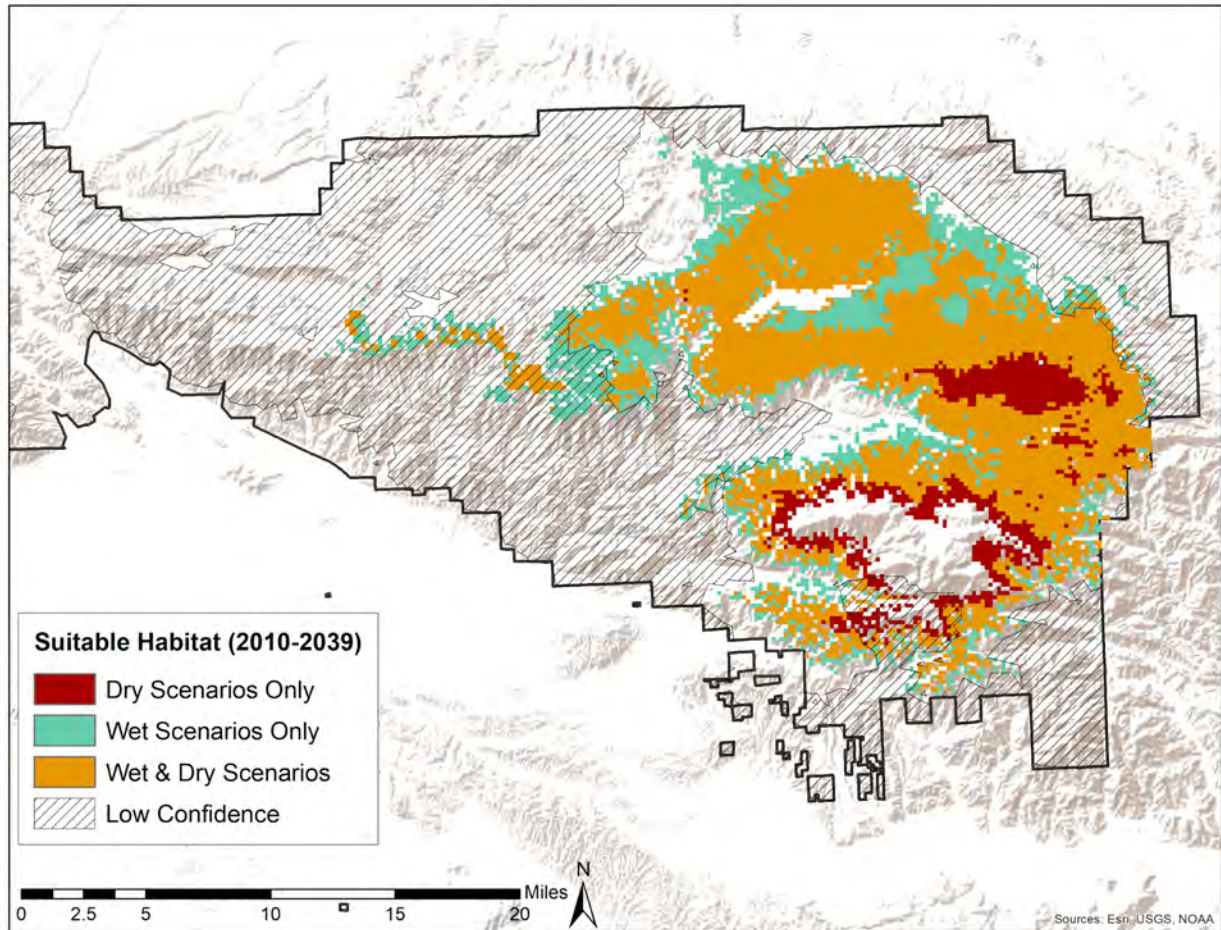


Figure T6. 2010-2039 projected yellow pine sapling suitable habitat across the eastern Transverse Ranges. Orange regions depict habitat projected to be suitable under both the 2010-2039 summed dry scenario and the 2010-2039 summed wet scenario. Aqua regions represent habitat projected to be suitable only under the summed wet scenario, and red regions represent habitat projected to be suitable only under the summed dry scenario. Low confidence areas are represented by hash marks.

Table T2. Projected yellow pine sapling suitable habitat under 2010-2039 wet and dry futures by region.

Time Period	Acres Suitable Habitat <i>High Confidence</i>	Percent Change in Suitable Habitat <i>High Confidence</i>	Acres Suitable Habitat <i>Low Confidence</i>	Percent Change in Suitable Habitat <i>Low Confidence</i>
Western Transverse Ranges				
Current	190,768.07	NA	0	NA
2010-2039 <i>Summed Dry Scenario</i>	78,973.30	-58.60%	0	0
2010-2039 <i>Summed Wet Scenario</i>	75,982.98	-60.17%	0	0
Central Transverse Ranges				
Current	3,440.67	NA	48,187.4	NA
2010-2039 <i>Summed Dry Scenario</i>	792.62	-76.96%	28,624.22	-40.6%
2010-2039 <i>Summed Wet Scenario</i>	1,170.91	-65.97%	25,814.04	-46.43%
Eastern Transverse Ranges				
Current	146,381.62	NA	30,767.88	NA
2010-2039 <i>Summed Dry Scenario</i>	108,984.59	-25.55%	7,079.49	-76.99%
2010-2039 <i>Summed Wet Scenario</i>	124,890.94	-14.68%	14,158.99	-53.98%

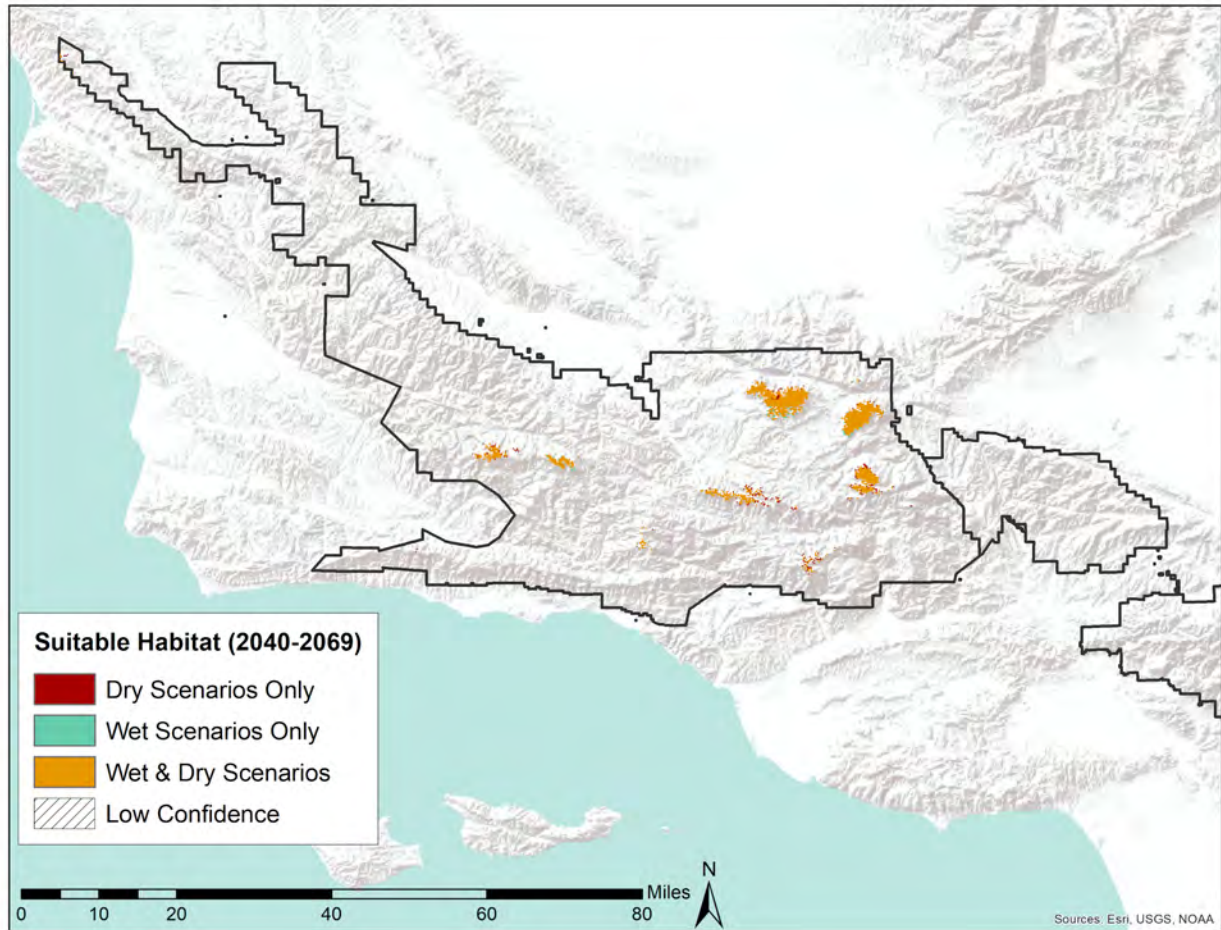


Figure T7. 2040-2069 projected yellow pine sapling suitable habitat across the western Transverse Ranges. Orange regions depict habitat projected to be suitable under both the 2040-2069 summed dry scenario and the 2040-2069 summed wet scenario. Aqua regions represent habitat projected to be suitable only under the summed wet scenario, and red regions represent habitat projected to be suitable only under the summed dry scenario. We have high confidence in our models' abilities to project habitat suitability across the entire western Transverse Ranges.

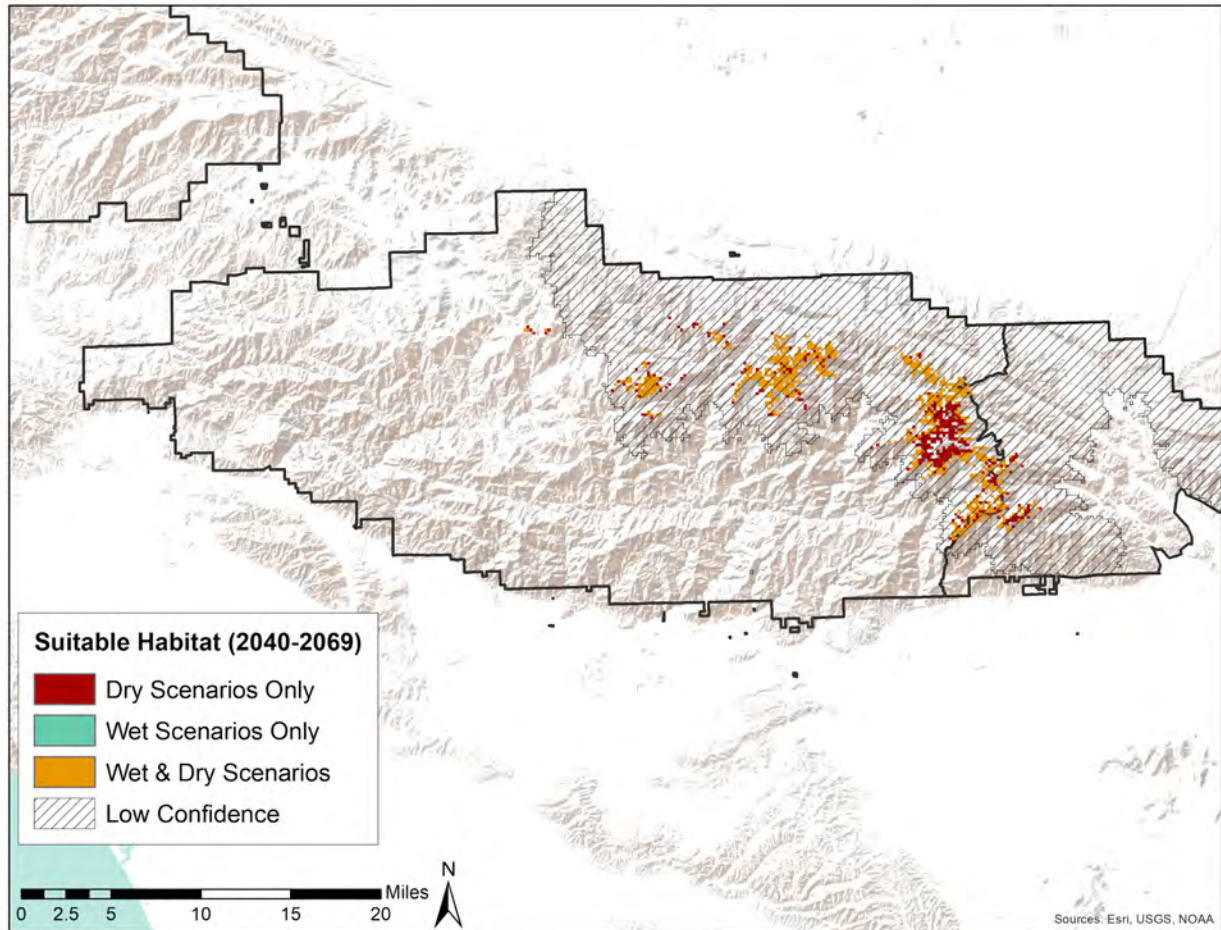


Figure T8. 2040-2069 projected yellow pine sapling suitable habitat across the central Transverse Ranges. Orange regions depict habitat projected to be suitable under both the 2040-2069 summed dry scenario and the 2040-2069 summed wet scenario. Aqua regions represent habitat projected to be suitable only under the summed wet scenario, and red regions represent habitat projected to be suitable only under the summed dry scenario. Low confidence areas are represented by hash marks.

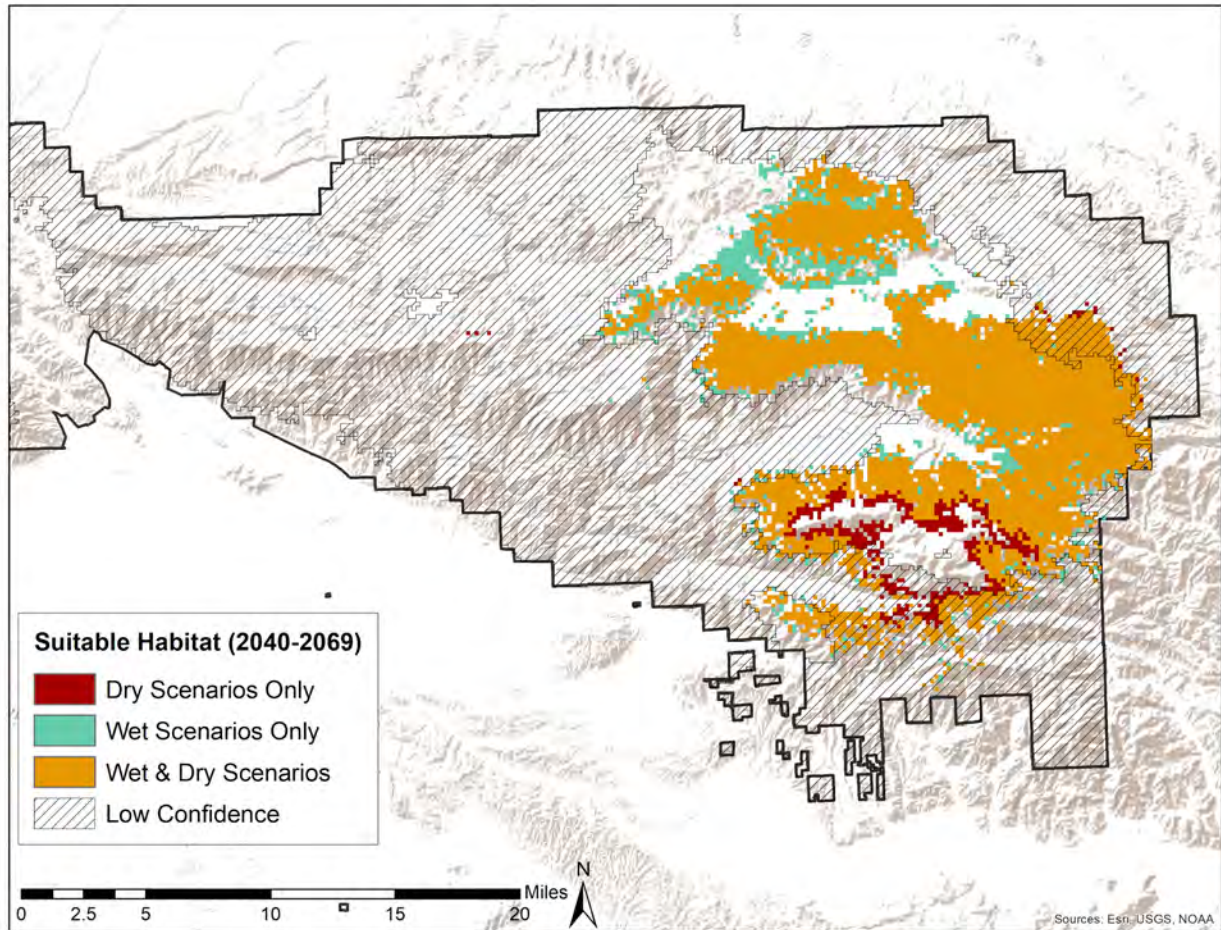


Figure T9. 2040-2069 projected yellow pine sapling suitable habitat across the eastern Transverse Ranges. Orange regions depict habitat projected to be suitable under both the 2040-2069 summed dry scenario and the 2040-2069 summed wet scenario. Aqua regions represent habitat projected to be suitable only under the summed wet scenario, and red regions represent habitat projected to be suitable only under the summed dry scenario. Low confidence areas are represented by hash marks.

Table T3. Projected yellow pine sapling suitable habitat under 2040-2069 wet and dry futures by region.

Time period	Acres Suitable Habitat <i>High Confidence</i>	Percent Change in Suitable Habitat <i>High Confidence</i>	Acres Suitable Habitat <i>Low Confidence</i>	Percent Change in Suitable Habitat <i>Low Confidence</i>
Western Transverse Ranges				
Current	190,768.07	NA	0	NA
2040-2069 <i>Summed Dry Scenario</i>	34,334.65	-82.00%	0	0
2040-2069 <i>Summed Wet Scenario</i>	32,154.96	-83.14%	0	0
Central Transverse Ranges				
Current	3,278.54	NA	48,349.53	NA
2040-2069 <i>Summed Dry Scenario</i>	144.11	-95.60%	18,356.25	-62.03%
2040-2069 <i>Summed Wet Scenario</i>	54.04	-98.35%	12,771.91	-73.58%
Eastern Transverse Ranges				
Current	110,281.60	NA	66,867.9	NA
2040-2069 <i>Summed Dry Scenario</i>	74,235.62	-32.69%	13,114.18	-80.39%
2040-2069 <i>Summed Wet Scenario</i>	82,323.90	-25.35%	12,159.44	-81.82%

